



UNIVERSITAT DE BARCELONA

New modalities to evaluate cardiovascular remodeling in fetuses with congenital heart defects

Laura Nogué i Garrigolas

ADVERTIMENT. La consulta d'aquesta tesi queda condicionada a l'acceptació de les següents condicions d'ús: La difusió d'aquesta tesi per mitjà del servei TDX (www.tdx.cat) i a través del Dipòsit Digital de la UB (diposit.ub.edu) ha estat autoritzada pels titulars dels drets de propietat intel·lectual únicament per a usos privats emmarcats en activitats d'investigació i docència. No s'autoritza la seva reproducció amb finalitats de lucre ni la seva difusió i posada a disposició des d'un lloc aliè al servei TDX ni al Dipòsit Digital de la UB. No s'autoritza la presentació del seu contingut en una finestra o marc aliè a TDX o al Dipòsit Digital de la UB (framing). Aquesta reserva de drets afecta tant al resum de presentació de la tesi com als seus continguts. En la utilització o cita de parts de la tesi és obligat indicar el nom de la persona autora.

ADVERTENCIA. La consulta de esta tesis queda condicionada a la aceptación de las siguientes condiciones de uso: La difusión de esta tesis por medio del servicio TDR (www.tdx.cat) y a través del Repositorio Digital de la UB (diposit.ub.edu) ha sido autorizada por los titulares de los derechos de propiedad intelectual únicamente para usos privados enmarcados en actividades de investigación y docencia. No se autoriza su reproducción con finalidades de lucro ni su difusión y puesta a disposición desde un sitio ajeno al servicio TDR o al Repositorio Digital de la UB. No se autoriza la presentación de su contenido en una ventana o marco ajeno a TDR o al Repositorio Digital de la UB (framing). Esta reserva de derechos afecta tanto al resumen de presentación de la tesis como a sus contenidos. En la utilización o cita de partes de la tesis es obligado indicar el nombre de la persona autora.

WARNING. On having consulted this thesis you're accepting the following use conditions: Spreading this thesis by the TDX (www.tdx.cat) service and by the UB Digital Repository (diposit.ub.edu) has been authorized by the titular of the intellectual property rights only for private uses placed in investigation and teaching activities. Reproduction with lucrative aims is not authorized nor its spreading and availability from a site foreign to the TDX service or to the UB Digital Repository. Introducing its content in a window or frame foreign to the TDX service or to the UB Digital Repository is not authorized (framing). Those rights affect to the presentation summary of the thesis as well as to its contents. In the using or citation of parts of the thesis it's obliged to indicate the name of the author.

NEW MODALITIES TO EVALUATE CARDIOVASCULAR REMODELING IN FETUSES WITH CONGENITAL HEART DEFECTS

Doctoral thesis dissertation presented by

LAURA NOGUÉ I GARRIGOLAS

To apply for the degree of

Doctor at the University of Barcelona

Directed by

MAR BENNASAR SANS, BCNatal | center for Maternal, Fetal and Neonatal Medicine,
Hospital Clínic de Barcelona and Hospital Sant Joan de Déu

OLGA GÓMEZ DEL RINCÓN, BCNatal | center for Maternal, Fetal and Neonatal Medicine,
Hospital Clínic de Barcelona and Hospital Sant Joan de Déu and associate professor of the
University of Barcelona

Doctoral Program Medicine and Translational Research
School of Medicine and Health Sciences. University of Barcelona

October 2023



AUTORIZATION FOR THE PRESENTATION OF THE THESIS

Dr. Olga Gómez del Rincón, BCNatal | center for Maternal, Fetal and Neonatal Medicine, Hospital Clínic de Barcelona and Hospital Sant Joan de Déu and associate professor of the University of Barcelona, and **Dr. Mar Bennasar Sans**, BCNatal | center for Maternal, Fetal and Neonatal Medicine, Hospital Clínic de Barcelona and Hospital Sant Joan de Déu

DECLARE THAT:

The thesis memory presented by Laura Nogué i Garrigolas with title “**New modalities to evaluate cardiovascular remodeling in fetuses with congenital heart defects**” has been developed under our supervision and we authorize the deposit for being defended and judged by a tribunal.

Signed on the day 16th October 2023



Mar Bennasar Sans

Thesis director



Olga Gómez del Rincón

Thesis director and tutor

**STATEMENT OF THE DOCTORAL CANDIDATE AND DIRECTORS OF ORIGINALITY AND
GOOD PRACTICES OF THE THESIS**

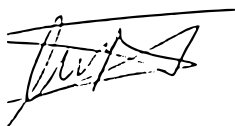
Dr. Olga Gómez del Rincón, BCNatal | center for Maternal, Fetal and Neonatal Medicine, Hospital Clínic de Barcelona and Hospital Sant Joan de Deu and associate professor of the University of Barcelona, and **Dr. Mar Bennasar Sans**, BCNatal | center for Maternal, Fetal and Neonatal Medicine, Hospital Clínic de Barcelona and Hospital Sant Joan de Deu

DECLARE THAT

The doctoral thesis entitled “**New modalities to evaluate cardiovascular remodeling in fetuses with congenital heart defects**”, is original, containing own results and information, without plagiarism from other thesis, publications or research from other authors. They also confirm that ethical codes and good practices have been followed for its preparation.

They declare that they consent that the thesis may be submitted to procedures to verify its originality.

Signed on the day 16th October 2023



Mar Bennasar Sans

Directora



Olga Gómez del Rincón

Directora



Laura Nogué i Garrigolas

Doctoranda

DECLARATION OF AUTHORSHIP OF THE THESIS

The doctoral candidate Laura Nogué i Garrigolas with DNI 43633187W

DECLARE THAT

Is the author of the doctoral thesis entitled “**New modalities to evaluate cardiovascular remodeling in fetuses with congenital heart defects**”



Laura Nogué i Garrigolas

Signed on the day 16th October 2023

Acknowledgements

En el transcurs d'aquest llarg camí que m'ha portat a poder fer realitat aquest somni, volia dedicar unes paraules d'agraïment a tots aquells que heu sigut uns pilars fonamentals en aquest viatge:

En primer lloc agraeixo de tot cor a les pacients la seva participació en la meva investigació, sense elles no hagués sigut possible. També a tots aquells residents que han dedicat hores infinites a omplir bases de dades amb paràmetres indesxifrables.

Als meus apreciats companys de l'hospital, la seva col·laboració i ensenyança. Per fer-me descobrir l'apassionant món de la cardiologia i la medicina fetal. Gràcies per les oportunitats que m'heu donat i per creure en mi.

A tots els amics que m'heu acompanyat i donat suport i estima durant tots aquests anys, que han sigut dels més durs de la meva vida.

També vull agrair a la Glòria, l'Àlvaro, l'Àlex i l'Edu, gràcies per tot el suport i ajuda i fer-me sentir una més de la família.

A les meves directores de tesi, a les quals dec un reconeixement especial. Gràcies per la vostra dedicació i paciència. Han sigut molts anys en el que m'heu ensenyat des de zero com agafar un transductor i com escriure un "paper". Sembla mentida tot el que he après, ni tan sols jo m'ho podia imaginar. He après també el perfeccionisme, l'amor a la recerca i tantes altres coses, tant a nivell professional com personal. Heu fet donar el millor de mi. No hagués arribat fins aquí sense el vostre suport.

Vull agrair de forma molt especial a en Crístian, que ha cregut en mi en tot moment, en el alts i baixos que he tingut, els llargs caps de setmana tancats a casa treballant. Està clar que sense tu aquest i la resta de somnis haguessin sigut incomplets. Gràcies per ser-hi sempre.

I finalment vull agrair als meus pares tot el que m'han ensenyat al llarg dels anys, sobretot l'esforç i la constància. M'heu recordat sempre que era el pilar per poder aconseguir tot el que em proposi. I així ha sigut. Perdoneu les "bronques" quan cada dia al telèfon em preguntàveu si havia estudiat pels exàmens de la carrera, pel MIR i ara també per la tesi. Malauradament persones molt importants a la meva vida m'han anat

deixat durant el camí, però estic segura que sigueu on sigueu sou les persones més orgulloses al veure el que he aconseguit.

Gràcies de tot cor.

Funding

The investigation that conducted to the following results has received funding from Hospital Clinic de Barcelona (Ajut Josep Font 2015 y Premi Emili Letang 2019, Barcelona, España), Instituto de Salud Carlos III (ISCIII) (PI15/00263, PI17/00675, PI20/00246, INT21/00027) co-funded by the European Union, Cerebra Foundation for the Brain Injured Child (Carmarthen, Gales, Reino Unido), Fundació La Marató de TV3 (Ref 202016-30-31), and Red de Salud y Desarrollo Materno-Infantil (SAMID), RD16/0022/0015.

Table of contents

| | |
|---|-----|
| ACKNOWLEDGEMENTS | 4 |
| FUNDING | 6 |
| TABLE OF CONTENTS..... | 7 |
| FIGURES INDEX..... | 9 |
| ABBREVIATIONS | 10 |
| LIST OF ARTICLES IN THE THESIS | 11 |
| RESUM DE LA TESI | 13 |
| INTRODUCTION | 17 |
| 1. CONGENITAL HEART DEFECTS..... | 17 |
| 2. NEW MODALITIES TO STUDY FETAL CARDIOVASCULAR REMODELING | 18 |
| 2.1. Patterns of cardiovascular remodeling | 19 |
| 2.2. Imaging techniques for the study of cardiovascular remodeling | 21 |
| 2.3. Cardiovascular plasmatic biomarkers in CHD..... | 30 |
| 3. APLICACION OF NEW MODALITIES TO CONGENITAL HEART DEFECTS..... | 35 |
| 3.1. Pulmonary stenosis | 36 |
| 3.2. Tetralogy of Fallot | 38 |
| 3.3. D-Transposition of the great arteries | 41 |
| 3. RATIONALE OF THE DOCTORAL THESIS | 43 |
| HYPOTHESIS | 45 |
| OBJECTIVES | 46 |
| MATERIAL, METHODS AND RESULTS | 47 |
| STUDY 1..... | 48 |
| STUDY 2..... | 77 |
| STUDY 3..... | 128 |
| STUDY 4..... | 139 |

| | |
|--|-----|
| DISCUSSION..... | 157 |
| 1. Study of cardiac morphometry and function using 4D-STIC speckle tracking echocardiography..... | 157 |
| 2. STE to evaluate cardiovascular remodeling and function in PS fetuses and neonatal valvuloplasty prediction..... | 160 |
| 3. Cord blood cardiovascular biomarkers in conotruncal CHD..... | 163 |
| 4. STE to evaluate cardiovascular remodeling and function in ToF fetuses..... | 167 |
| 5. Limitations..... | 172 |
| 6. Future clinical perspectives..... | 173 |
| CONCLUSIONS..... | 175 |
| REFERENCES..... | 176 |

Figures index

- Figure 1.** Fetal cardiac 4-chamber views showing patterns of fetal cardiac remodeling..... Page 21
- Figure 2:** Diagram showing the different types of Lagrangian strain..... Page 24
- Figure 3:** Left ventricle segmental strain curves display in a normal fetus..... Page 27
- Figure 4:** Multiplanar display of a 4D-Spatio Temporal Image Correlation (STIC) volume..... Page 29
- Figure 5:** Three vessel view of a fetus with pulmonary stenosis..... Page 37
- Figure 6:** Fetal cardiac characteristics of pulmonary stenosis..... Page 37
- Figure 7.** Tetralogy of Fallot with pulmonary stenosis..... Page 39
- Figure 8.** D-Transposition of the great arteries..... Page 41
- Figure 9.** Receiver-operating characteristic (ROC) curves for neonatal valvuloplasty prediction..... Page 163
- Figure 10.** Correlation of transforming growth factor β (TGF β) and echocardiographic parameters..... Page 166

Abbreviations

CHD: congenital heart defects

STE: speckle tracking echocardiography

4D-STIC: 4 dimension – spatio-temporal image correlation

PS: pulmonary stenosis

D-TGA: D – transposition of the great arteries

NT-proBNP: N-terminal pro B-type natriuretic peptide

TGF β : Transforming growth factor β

PLGF: Placental growth factor

Sflt-1: soluble fms-like tyrosine kinase 1

RV: right ventricle

2D: 2-dimensional

SF: shortening fraction

LV: left ventricle

TAPSE: tricuspid annular plane systolic excursion

MAPSE: mitral annular plane systolic excursion

FAC: fractional area change

GLS: global longitudinal strain

SI: sphericity index

ToF: Tetralogy of Fallot

DA: ductus arteriosus

VSD: ventricular septal defect

List of articles in the thesis

Thesis in compendium of publications format. The thesis consists of 4 objectives and 4 articles:

Article 1:

Nogué L, Gómez O, Izquierdo N, Mula C, Masoller N, Martínez JM, Gratacós E, Devore G, Crispi F, Bennasar M. **Feasibility of 4D-Spatio Temporal Image Correlation (STIC) in the Comprehensive Assessment of the Fetal Heart using FetalHQ®**. Journal of Clinical Medicine. 2022, Mar 4;11(5):1414.

Impact factor: 4.96. **1st quartile**

Article 2:

Nogué L, Bennasar M, Guirado L, Dall'Asta A, Ghi T, Masoller N, Escobar-Diaz MC, Bijmens B, Martínez JM, Crispi F, Gómez O. **Incremental value of 2D strain fetal echocardiography in the prediction of neonatal valvuloplasty in isolated mild to critical pulmonary valve stenosis.**

Status: under 3rd review in Ultrasound in Obstetrics and Gynecology

Article 3:

Gómez O, **Nogué L**, Soveral I, Guirado L, Izquierdo N, Pérez-Cruz M, Masoller N, Escobar MC, Sánchez de Toledo J, Martínez JM, Bennasar M*, Crispi F*. **Cord blood cardiovascular biomarkers in Tetralogy of Fallot and D-transposition of the great arteries.** Frontiers in pediatrics. 2023, Apr 28;11:1151814

*These authors have contributed equally to this article.

Impact factor: 3.569. **1st quartile**

Article 4:

Biventricular remodeling and dysfunction in fetuses with Tetralogy of Fallot. A speckle tracking echocardiography study.

Status: draft

Noves modalitats per avaluar el remodelat cardiovascular en fetus amb cardiopaties congènites

Introducció

Les cardiopaties congènites són les malformacions congènites severes més freqüents. Donat que el diagnòstic prenatal és òptim, la investigació actual estudia el remodelat cardiovascular per millorar l'avaluació pronòstica abans de néixer. El remodelat parteix de canvis subtils difícils d'identificar mitjançant ecocardiografia estàndard, pel que l'ús de tècniques avançades, com l'ecocardiografia *speckle tracking*, permet estudiar paràmetres més sensibles com l'*strain* (deformació miocàrdica). Existeixen biomarcadors de remodelat cardiovascular: pèptid natriurètic tipus-B (marcador de disfunció cardíaca), Troponina I (marcador de lesió miocàrdica), *transforming growth factor β* (citoquina segregada en resposta a una sobrecarrega de pressió o volum), factor de creixement placentari i el seu receptor soluble (sFlt-1) (factors de creixement endotelial vascular), que poden ser estudiats en sang umbilical i podrien aportar informació complementària a l'ecocardiografia.

Hipòtesi

1. L'ecocardiografia "*speckle tracking*" és una eina aplicable per avaluar el remodelat cardiovascular (canvis morfomètrics i funcionals cardíacs) en el cor fetal normal.
2. L'ecocardiografia "*speckle tracking*" en combinació amb l'ecocardiografia convencional permet l'avaluació acurada dels patrons de remodelat cardiovascular associats amb les cardiopaties congènites a l'etapa prenatal.
3. Les cardiopaties congènites estan associades a patrons específics de biomarcadors cardiovasculars i factors angiogènics en sang de cordó i es correlacionen amb paràmetres ecocardiogràfics.
4. La incorporació de l'ecocardiografia "*speckle tracking*" a la vida fetal millora l'avaluació pronòstica de les cardiopaties congènites.

Objectius

1. Demostrar l'aplicabilitat de l'ecocardiografia "*speckle tracking*" per l'avaluació de paràmetres morfomètrics i funcionals en vida fetal en una cohort de fetus sans. **Estudi 1.**
2. Validar l'aplicabilitat de l'avaluació morfomètrica i funcional de l'ecocardiografia "*speckle tracking*" en fetus amb cardiopaties congènites severes. **Estudi 2 i 4.**
3. Definir el patró de biomarcadors cardiovasculars i factors angiogènics en sang de cordó en diferents cardiopaties congènites i avaluar la seva potencial correlació amb paràmetres ecocardiogràfics. **Estudi 3.**
4. Validar l'aplicabilitat clínica i utilitat pronòstica de l'ecocardiografia "*speckle tracking*" en fetus amb cardiopaties congènites. **Estudi 2 i 4.**

Mètodes

Es van dissenyar 4 estudis de cohorts prospectius amb la inclusió de gestants en seguiment a BCNatal (Hospital Clínic de Barcelona i Hospital Sant Joan de Déu).

Estudi 1: 31 gestants de baix risc. Es van obtenir clips en 2 dimensions i volums 4 dimensions-STIC (*spatio temporal image correlation*) del pla de 4 càmeres. Es va realitzar una ecocardiografia "*speckle tracking*" per tal d'avaluar-ne la reproductibilitat mitjançant el coeficient de correlació intraclasse.

Estudi 2: 24 fetus amb estenosi pulmonar i 48 controls. Al diagnòstic de l'estenosi pulmonar es va realitzar una ecocardiografia i una ecocardiografia "*speckle tracking*". Es van analitzar paràmetres ecocardiogràfics en funció de la necessitat de valvuloplastia neonatal per identificar predictors d'intervenció precoç.

Estudi 3: 22 complex Fallot, 12 D-transposició de grans artèries i 36 controls. Es va realitzar una ecocardiografia al tercer trimestre de gestació. Al naixement es va obtenir sang de cordó umbilical per determinar-ne les concentracions dels biomarcadors de remodelat cardiovascular.

Estudi 4: 63 fetus amb Fallot i 66 controls. Es va realitzar una ecocardiografia en 2 dimensions i una ecocardiografia “speckle tracking” al tercer trimestre de gestació. Es van avaluar paràmetres morfomètrics i funcionals per definir el patró de remodelat cardiovascular.

Principals resultats

En l'**estudi 1** es va demostrar una reproductibilitat excel·lent per l'avaluació cardíaca morfomètrica global, així com una bona reproductibilitat per l'avaluació funcional. L'avaluació cardíaca segmentaria va demostrar una reproductibilitat pobre.

A l'**estudi 2** els fetus amb estenosi pulmonar crítica van mostrar un deteriorament de la funció ventricular dreta. Els fetus amb valvuloplàstia neonatal (50%) van mostrar una pitjor funció del ventricle dret. Es va descriure un sistema de puntuació multiparamètric per la predicció de valvuloplàstia neonatal combinant el percentil de l'índex de pulsatilitat del ductus venós, el *strain* global longitudinal del ventricle dret, la presència de flux revers al ductus arteriós i insuficiència tricuspídea significativa, amb una sensibilitat del 91.7% i especificitat del 100%.

L'**estudi 3** va demostrar un increment del *transforming growth factor* β en sang de cordó de fetus amb complex Fallot (24.9 ng/mL (15.6-45.3) vs. Cor normal 15.7 ng/mL (7.2-24.3) vs. D- transposició de grans artèries 12.6 ng/ml (8.7-37.9); $p = 0.012$). Els nivells de *transforming growth factor* β van demostrar una correlació negativa amb el z-score del diàmetre valvular pulmonar ($r=-0.576$, $p=0.039$).

L'**estudi 4** va mostrar signes de remodelat cardíac en els fetus amb complex Fallot amb una disminució de la funció cardíaca diastòlica (augment fracció de temps d'ompliment) i sistòlica (*strain* global del ventricle dret (complex Fallot: 17.25 ± 3.76 vs controls: 19.33 ± 3.09 ; $p= 0.001$) i del ventricle esquerre (complex Fallot: -17.96 ± 3.78 vs controls: -20.87 ± 3.45 ; $p= 0<.001$)). Aquest descens en la funció biventricular es correlaciona amb la disincronia mecànica.

Conclusions

L'ecocardiografia *speckle tracking* en volums en 4 dimensions - *spatio temporal image correlation* és factible, reproduïble i comparable a l'ecocardiografia amb 2 dimensions per l'avaluació de la morfometria i funció cardíaca en fetus sans (**Estudi 1**).

Els fetus amb estenosi pulmonar crítica presenten una menor deformació del ventricle dret, que es correlaciona amb una disincronia mecànica entre els diferents segments ventriculars. La combinació multiparamètrica amb l'*strain* global longitudinal del ventricle dret, el percentil de l'índex de pulsilitat del ductus venós, la presència de flux revers al ductus arteriós i d'insuficiència tricuspídea significativa, permet identificar aquells fetus amb risc de valvuloplàstia neonatal que es beneficiaran d'un assessorament precoç per part de cardiólegs pediàtrics (**Estudi 2**).

El fetus amb complex Fallot presenten concentracions de *transforming growth factor β* incrementades en comparació amb fetus amb D-transposició de les grans artèries i amb fetus sans, que a més a més es correlacionen amb la severitat de l'obstrucció del tracte de sortida del ventricle dret (**Estudi 3**).

Els fetus amb complex Fallot presenten signes de remodelat cardiovascular des de la vida fetal caracteritzat per un cor més esfèric amb hipertròfia concèntrica. A més, els canvis morfomètrics s'associen tant amb una disfunció diastòlica i menor contractilitat biventricular, que es correlaciona amb la presència de disincronia mecànica (**Study 4**).

Introduction

1. CONGENITAL HEART DEFECTS

Congenital heart defects (CHD) are the most frequent severe congenital malformations, affecting approximately 0.8-1% of newborns(1,2). Its etiology is not clearly defined, but it is believed to be caused by a combination of genetic and environmental factors(3,4). CHD are responsible for 50% of infant mortality in relation to congenital defects(5). However, advances in the field of cardiovascular surgery and neonatal care in recent years have significantly improved the prognosis of CHD and currently 80-85% of children with CHD will survive to adulthood(2). The decrease in mortality and the increase in life expectancy of these patients has led current interest in fetal cardiology to focus on improving the prognostic evaluation of the different groups of CHD.

Prenatal diagnosis of CHD, which currently averages more than 50% worldwide(6) and almost 90% in developed countries(6,7), is crucial to optimize perinatal management(8). Thus, diagnosis during fetal life has improved the prognosis of many CHD, especially ductus-dependent CHD, in which numerous studies have demonstrated a decrease in postoperative mortality and the risk of serious complications related to hypoxemia and acidosis, including necrotizing enterocolitis. However, CHD remains an important cause of neurodevelopmental abnormalities in children, which is one of the major adverse outcomes associated with CHD. Many efforts are currently directed to better understand the prenatal origin of these disorders. It has been demonstrated that children with CHD already present brain changes from fetal life. These prenatal findings may be attributed to cerebral hypoperfusion present in some CHD or chronic deficient oxygenation of certain brain areas(9,10). However, it is still necessary to define which CHD groups are at higher risk of neurodevelopmental abnormalities and whether potential prophylactic measures can be established from fetal life.

It is also known that fetal spectrum of CHD is worse than in the postnatal scenario due to its association with genetic syndromes and fetal death in the most severe CHD. Moreover, CHD are associated with pregnancy complications related to placental

dysfunction. In fact, recent studies have demonstrated that pregnancies complicated with fetal CHD have a 7-fold increase in the incidence of early preeclampsia and fetal growth retardation(11), which are also contributors to worse perinatal outcome in CHD. It is therefore of particular importance to apply new genetic tests to improve the detection of genetic anomalies and to better redefine CHD classification from prenatal life, taking into account prognostic factors such as the presence of placental dysfunction.

CHD have a complex 3D anatomy, which makes it difficult to evaluate cardiac morphometry and function, particularly in fetal life. Recently, there have been significant advances in imaging technologies that allow the evaluation of myocardial deformation and 3D structure in the fetal stage, with promising results. Additionally, the study of different biomarkers of cardiovascular remodeling and dysfunction has been described to improve prognostic evaluation of CHD. All these advances provide earlier and more comprehensive information compared to conventional echocardiography, as they allow the exploration of the direct impact of CHD on myocardial development and function, which will determine the medium to long-term prognosis in CHD from a cardiovascular point of view.

2. NEW MODALITIES TO STUDY FETAL CARDIOVASCULAR REMODELING

Cardiovascular remodeling refers to changes in the structure and shape of the heart (morphometric changes) to maintain optimal function in a pathological environment(12). The study of fetal cardiovascular remodeling is relevant in predicting long-term outcomes, as insults suffered in fetal life may determine persistent changes in adulthood, a concept known as fetal cardiovascular programming(13). Cardiovascular remodeling in its initial stage starts from subtle and subclinical changes and therefore it is difficult to identify by conventional echocardiography.

Fetal echocardiography has greatly advanced since the development of M-Mode in the 1970s and is now the main tool for diagnosing CHD and studying cardiovascular function in fetuses(2). Technical improvements have allowed for earlier diagnosis of CHD in fetuses with risk factors, and normality curves and z-score have been developed for

studying cardiovascular remodeling in both CHD and extracardiac conditions(14–17). New ultrasound modalities, such as tissue Doppler and speckle tracking echocardiography (STE), have allowed to define more sensitive parameters for studying cardiac function such as strain, but their clinical use in fetal cardiology is still limited(18). On the other hand, the acquisition of 4 dimension-spatio temporal image correlation (4D-STIC) volumes with improved quality may be useful for the study of cardiovascular remodeling in CHD, since it allows the improvement of the different cardiac planes obtained through volume navigation(19). However, the evaluation of cardiovascular remodeling in fetal life is complex due to the small size of the heart, the high heart rate and the differences in fetal circulation.

The information available on cardiovascular remodeling associated with different groups of CHD in the fetal stage is still very limited and in fetal life has only been studied in some CHD such as pulmonary stenosis (PS)(20), transposition of great arteries(D-TGA)(21), coarctation of the aorta(22)and hypoplastic left heart(23) and focuses mainly on the study of different parameters evaluated by conventional echocardiography.

Cord blood plasma biomarkers, such as B-type natriuretic peptide (NT-proBNP), Troponin I, transforming growth factor β (TGF β), and angiogenic factors (placental growth factor (PlGF) and soluble fms-like tyrosine kinase 1 (Sflt-1)), have also been proposed to assess cardiovascular remodeling in fetal CHD. However, their role in diagnosis and prognosis has been poorly studied, and their correlation with different echocardiographic modalities including STE has not yet been evaluated.

The incorporation of these new diagnostic modalities could help to better define the patterns of cardiovascular remodeling associated with different types of CHD, which would allow the establishment of cardiovascular risk from the fetal stage, assessing whether these changes persist after postnatal cardiovascular surgery.

2.1. Patterns of cardiovascular remodeling

The fetal heart achieves its function of ejecting blood for tissue perfusion due to intrinsic properties of myocytes, fiber orientation, cardiac shape and depends on factors such as

electrical activation, myocardial perfusion and peripheral circulation; and can therefore adapt to different conditions to maintain its maximum efficiency. However, prolonged insult can lead to diastolic dysfunction (less capacity for relaxation and ventricular filling) and decreased systolic function (less capacity to eject blood), which can conduct to heart failure.

Cardiac remodeling can occur in different patterns in postnatal life, including pressure overload, volume overload, and direct myocardial damage. The main difference with the remodeling produced in fetal life is that the fetal heart still has the capacity to change its microstructure and adapt to conditions present at that stage, but these changes may not be optimal for adult circulation and can make the heart more susceptible to insults (fetal cardiovascular programming)(12). Thus, a better definition of main patterns of fetal cardiac remodeling from the fetal stage would be essential to improve the individual's mid- and long-term follow-up.

Main patterns of fetal cardiac remodeling are detailed as follows (**Figure 1**):

Pressure overload: The right ventricle (RV) in fetal life is the systemic ventricle as it perfuses the placenta and it is very sensitive to pressure overload. The heart adapts to pressure overload by changing its shape to better tolerate the vascular stress (more globular) and developing concentric cardiac hypertrophy to increase contractility. Examples of pressure overload include placental insufficiency, PS, and aortic stenosis.

Volume overload: Fetal or placental tumors and fetal anemia cause volume overload. Dilatation of the cardiac chambers and cardiomegaly occur to increase ejection volume and better manage volume overload. Eccentric hypertrophy may occur due to cardiomyocyte dilatation.

Direct myocardial damage: Myocardial damage can be caused by toxins such as antiretroviral drugs, ischemia, or genetic cardiomyopathy. Toxins can lead to myocyte loss and compensatory cardiac hypertrophy to increase contractility.

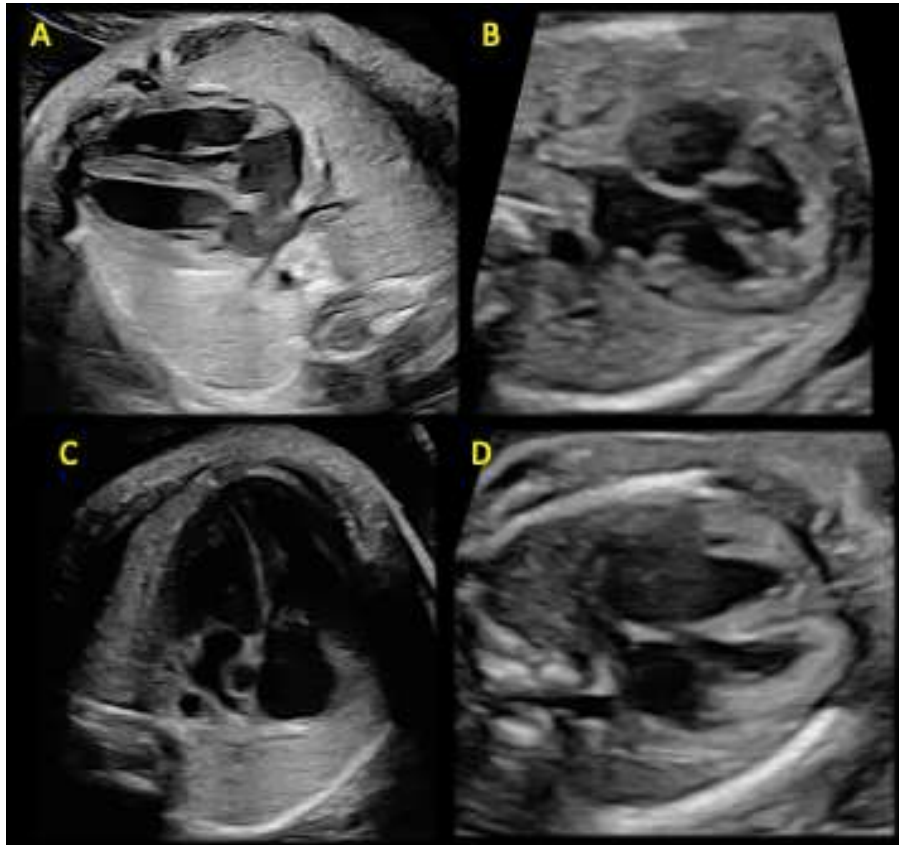


Figure 1. Fetal cardiac 4-chamber views showing patterns of fetal cardiac remodeling. **A** Normal fetal heart. **B** Cardiomegaly, globular shape and myocardial hypertrophy in fetal growth restriction. **C** Cardiomegaly secondary to volume overload in Galen's vein aneurysm **D** Myocardial hypertrophy and cardiomegaly in a fetus with a genetic cardiomyopathy. (Original figure).

2.2. Imaging techniques for the study of cardiovascular remodeling

2.2.1. Comprehensive 2-dimensional fetal echocardiography

Fetal echocardiography consists of the measurement of morphometric and functional parameters for the study of cardiovascular remodeling and fetal cardiac function in different clinical situations. Traditionally, heart function in fetal life was inferred from indirect signs such as the presence of hydrops, tricuspid insufficiency or cardiomegaly. However, the development and sophistication of new ultrasound equipment has allowed the emergence of new echocardiographic parameters for the evaluation of fetal

cardiac function, but limited access and the small size of the fetal heart make it a difficult technique requiring specific training.

The establishment of fetal nomograms for these new echocardiographic parameters, constructed with strict methodological criteria, allow us to evaluate in detail cardiac morphometry and function:

Morphometric evaluation: It includes the evaluation the transverse and longitudinal sizes, as well as the cardiac, atrial, and ventricular areas(14), valve size(24), and thickness of the ventricular walls and interventricular septum using 2-dimensional (2D) imaging. These measurements vary throughout gestation, so calculating z-score for each parameter is essential.

Functional evaluation: It comprises the examination of transverse cardiac contractility (shortening fraction (SF) and left ventricle (LV) ejection fraction), longitudinal contractility (longitudinal displacement at the level of the right (TAPSE) and left lateral (MAPSE) valvular annulus), and global contractility (fractional area change (FAC) of the RV)(15). Pulsed Doppler enables the assessment of diastolic function (timing parameters (filling time fraction)), systolic function (ejection velocities (aortic and pulmonary) and timing parameters (ejection time fraction))(17), or both simultaneously (Tei index), as well as flow at the level of the DA and aortic isthmus. Lastly, cardiac output can be also calculated by combining 2D and Doppler parameters.

Nowadays, 2D echocardiography is the basis for studying cardiovascular remodeling. When well-implemented with the use of strict nomograms and appropriate parameters, it can detect morphometric and functional changes, particularly in extracardiac conditions such as fetal growth restriction(13,25,26), maternal diabetes(27), fetuses of mothers under retroviral treatment(28) and pregnancies by assisted reproduction techniques(29,30). However, the studies on cardiovascular remodeling in fetal CHD are currently limited and have the inherent limitation of the applicability of conventional echocardiography to evaluate the complex three-dimensional structural changes that result in severe CHD. Therefore, new techniques that enable the assessment of 3D

changes of the heart and direct myocardial changes are crucial and specific validation is required for each CHD group(31).

2.2.2. Strain imaging by speckle tracking echocardiography

The assessment of ventricular function is complex due to the structure of myocardial fibers, which are organized in different layers. The LV has three layers: the subendocardial layer consists of fibers arranged in a counterclockwise oblique manner, the middle layer consists of fibers arranged circumferentially, and the subepicardial layer consists of fibers arranged in a clockwise oblique manner(32). This oblique orientation causes LV to torsion around its long axis in systole(33). The RV has an epicardial layer of circumferential fibers and a longitudinally oriented endocardial layer. Classical parameters for assessing left ventricular function, such as ejection fraction, do not consider the multidirectionality of myocardial deformation and may remain normal in the presence of subclinical dysfunction. However, new myocardial deformation parameters, such as strain, have shown to be superior to classical measurements as ejection fraction in detecting subclinical dysfunction. Additionally, it allows the assessment of myocardial deformation in the three directions of myocardial fibers, as well as segmental assessment.

Lagrangian Strain

Lagrangian Strain is defined as the relative change in myocardial length between systole and diastole ($Strain = (L-L_0)/L_0$, where L is the final length and L_0 is the initial length (32)). Negative strain represents the shortening of cardiac fibers, while positive strain represents their lengthening. However, the absolute value is usually used to avoid confusion. Due to the layered orientation of cardiac fibers, longitudinal, circumferential, and radial strain can be calculated (**Figure 3**).

The most commonly used is longitudinal strain, also known as global longitudinal strain (GLS), which has been validated as an index of global LV function. Circumferential strain assesses myocyte shortening in the circular perimeter in a short-axis plane, while radial strain measures myocardial deformation toward the ventricular cavity or thickening that

occurs at the myocardial level during systole (positive deformation). Although GLS has been validated for clinical use in adult cardiology due to its reproducibility, ease of obtainment, and good predictive value(33), circumferential and radial strain analysis have demonstrated their usefulness in research but have not yet been applied to daily clinical practice.

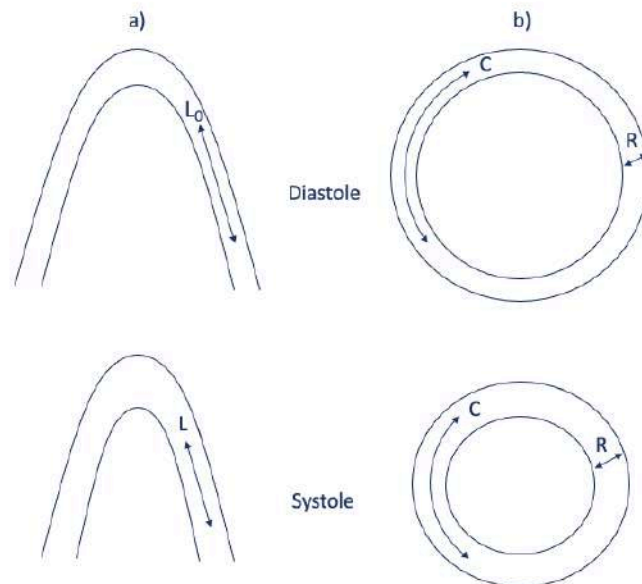


Figure 2: Diagram showing the different types of Lagrangian strain. a) longitudinal plane in systole and diastole. b) circumferential and radial strain in systole and diastole. (Original figure).

Speckle tracking technique

Myocardial strain can be assessed by tissue Doppler and STE. Tissue Doppler, that uses Doppler principles to measure the velocity of myocardial motion, is less commonly applied because it only allows calculation of longitudinal strain and is dependent on the angle of insonation. STE is a more popular alternative that allows for the assessment of global and regional myocardial function. STE consists on tracking the speckles in sequential images, where speckle refers to a segment of myocardial tissue in an ultrasound image represented by different shades and intensities of gray distributed in space. Each tissue segment has a unique gray pattern, behaving like a fingerprint(18). The software semi-automatically identifies the endocardium from a clip of a cardiac four-chamber view and follows the different speckles in all the frames of a cardiac cycle,

obtaining a trace of the endocardium during the entire cardiac cycle(34). STE allows the study of myocardial deformation in the circumferential, radial, and longitudinal planes by calculating strain and strain rate (change of strain over time). Additionally, the software automatically divides the myocardium into six segments for regional analysis. Its application is simple and independent of the acquisition angle(35), but it can be affected by afterload and requires a minimum of 60 frames per second for optimal tracing(32,36).

In recent years, there has been an increasing application of this technology to fetal cardiology, which has overcome the limitations of using software designed for adult or pediatric patients. Recently, new software have been developed specifically for the fetal heart, such as *2D STRAIN (Fetal)* developed by TomTec® and *Fetal Heart Quantification (FetalHQ®)*, which is an adaptation of 2D STRAIN Tomtec® to be included in the latest generation of ultrasound machines(37). This software semi-automatically identifies the endocardium of the fetal heart and divides the tracing into 49 equidistant points for the delineation of 24 segments from the base to the cardiac apex of both ventricles, allowing the measurement of functional and morphometric parameters, such as the size of the ventricles (longitudinal and transverse diameter of the 24 segments, biventricular area, LV volume) and ventricular shape (sphericity index (SI) of the 24 segments (longitudinal diameter/transverse diameter)) (37,38). Regarding functional parameters, it assesses global function with by right and left FAC (39), ejection volume, cardiac output and LV ejection fraction by means of Simpson's formula(40). Transverse function is assessed by transverse SF, and longitudinal function by GLS(41), valvular annular systolic excursion , and longitudinal SF(42). The great advantage of this methodology is its off-line applicability, since a single cardiac clip in a 4-chamber plane allows in a relatively simple way to obtain global and segmental information on cardiac morphometry and function.

Speckle tracking echocardiography applications

Nowadays, STE is a validated technique that is increasingly available. GLS is a sensitive parameter to identify patients with subclinical LV dysfunction, so it is now used in daily clinical practice in multiple settings in adult cardiology. For example, it is used to assess chemotherapy-related cardiotoxicity, for differential diagnosis of hypertrophic

cardiomyopathies, to risk stratify in valvular disease, and to improve prognostic utility in patients with heart failure. RV GLS measurement is no longer just a research tool, but a reliable parameter that adds value for decision making in RV dysfunction, mainly secondary to pulmonary hypertension(43). In pediatric cardiology, it has proven usefulness in detecting preclinical myocardial dysfunction in patients undergoing chemotherapy, in children at risk for ischemic heart disease, heart transplantation, CHD, cardiomyopathies, and systemic diseases(44). In relation to CHD, there are reports of the use of STE in adults with tetralogy of Fallot (ToF) and systemic RV CHD for risk stratification of future adverse cardiac events. STE has also been used in patients with palliative Fontan surgery to evaluate the presence of subclinical myocardial dysfunction(33).

Speckle tracking echocardiography in fetuses and CHD

The use of STE and strain in fetal life is becoming more frequent since 2008, when Barker et al. first described the feasibility of STE in fetal echocardiography(45). In recent years, the feasibility of its use from the first trimester of gestation(46) and its usefulness for the study of cardiovascular remodeling in small for gestational age fetuses(47), fetuses of diabetic mothers(48), fetuses of monochorionic gestations complicated with twin to twin transfusion syndrome(49) and fetuses conceived with assisted reproduction techniques(50) have also been described.

Recently, STE's usefulness in fetal life has been described to improve prenatal diagnosis of CHD, including coarctation of the aorta(51), Shone syndrome(52), ToF, and D-TGA(53,54). It has also been used for the prediction of urgent atrioseptostomy in D-TGA fetuses(55,56) and postnatal management in fetuses with pulmonary atresia(57). The use of STE and GLS for the evaluation of cardiac function in fetuses with restricted ductus arteriosus (DA)(58), hypoplastic LV(59), and ToF(60), has led to the conclusion that it is a more sensitive tool than conventional echocardiography for the study of fetal cardiac function in CHD.

Segmental STE and mechanical dyssynchrony

Moreover, STE allows the study of mechanical dyssynchrony between both ventricles or ventricular segments. The presence of mechanical dyssynchrony may result from an electrical disturbance, such as bundle branch block, associated with to mechanical alteration as in myocardial infarction or structural remodeling, for example, due to CHD. The assessment of dyssynchrony can be qualitative, by identifying anomalous movement of the interventricular septum, or quantitative, by measuring *time-to-peak strain* (time from the onset of myocardial shortening to maximum myocardial deformation) and *mechanical dispersion index* (standard deviation of the time-to-peak of the different ventricular segments)(44) (**Figure 3**). Dyssynchrony evaluation in children with repaired ToF has shown a good correlation with ventricular function parameters and could explain at least part of the RV dysfunction they present. It is also useful for the study of heart failure, for the selection of patients for cardiac resynchronization therapy, and for measuring its response. To date, few studies have evaluated dyssynchrony in fetuses with CHD. Drop et al. describe the presence of dyssynchrony between the two walls of the same ventricle and between the two ventricles in a cohort of fetuses with CHD(61), but the correlation between dyssynchrony and ventricular function, as well as the presence of mechanical dyssynchrony in the different CHD groups, remains to be explored.

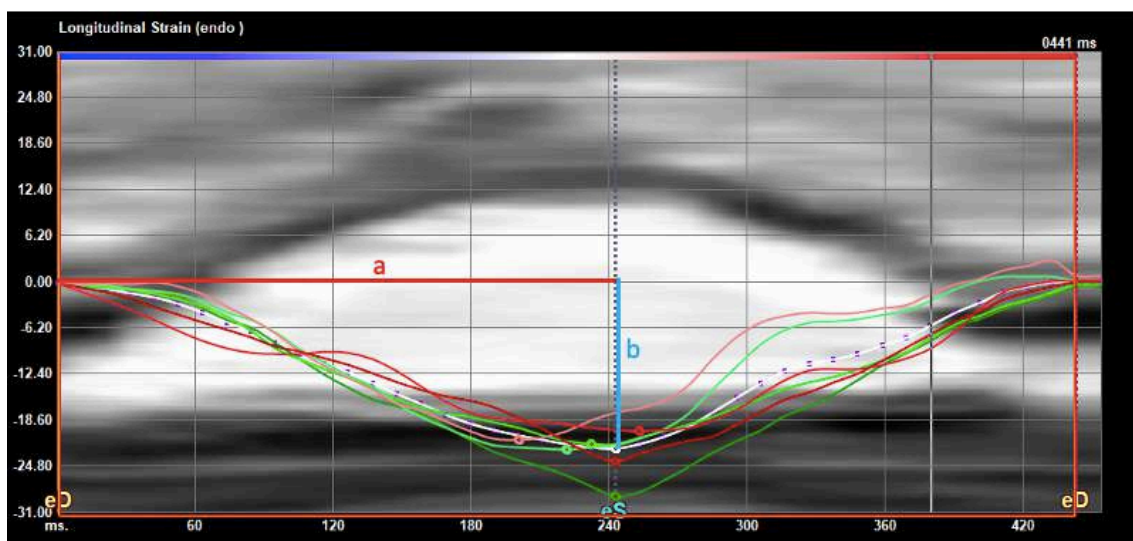


Figure 3: Left ventricle segmental strain curves display in a normal fetus. Segment 1 (free-wall basal) corresponds to dark green curve, segment 2 (free-wall mid-ventricle)

medium green curve, segment 3 (free-wall apical) light green curve, segment 4 (septum basal) dark red curve, segment 5 (septum mid-ventricular) light red curve, segment 6 (septum apical) pink curve. White curve represents global strain. (a) Time-to-peak shortening (ms) of global strain and segments 1, 2, 3. (b) Peak systolic strain (%) (global strain and segment 1, 4). eD is end diastolic frame and eS end systolic frame. (Original figure).

Speckle tracking echocardiography limitations

The use of STE is a promising tool for the assessment of fetal cardiac remodeling and function, but has limitations due to the small size and high heart rate of the fetal heart, as well as the challenges of fetal ultrasound (fetal movements and position) and require a learning curve. The quality of the 4-chamber clip and frame rate are crucial for successful use of STE. While the acquisition angle is not a limitation for STE, the apical acquisition of the 4-chamber clip may result in lost echo of the endocardial borders of the septal and lateral walls, making it difficult for the software to follow the speckles. Additionally, the inability to record the fetal electrocardiogram makes it difficult to determine different phases of the cardiac cycle. Moreover, the existence of different software on the market has led to different normality curves for each vendor, limiting the application of strain in clinical practice(62). A single software designed for fetal cardiology has helped with this limitation. To overcome these limitations, the use of 4D-STIC is a promising tool to address the problem of out-of-plane speckles inherent to 2D imaging.

In summary, STE is a sensitive technique that allows the study of myocardial deformation. Its use in some groups of CHD has already been proven, and it is able to detect preclinical functional changes, which will improve the prognostic evaluation from fetal stage.

2.2.3. 4D-Spatio Temporal Image correlation

4D-STIC echocardiography combines temporal and spatial information of a volume captured by an ultrasound transducer to obtain multiplanar and dynamic images of the fetal heart that can be viewed simultaneously in 3 orthogonal planes (axial, coronal, and

sagittal)(19) (**Figure 4**). During the scan, rhythmic changes occurring in the fetal heart are detected, determining the fetal heart rate, which is synchronized with the images. Each structure and plane are represented by multiple frames (images) of different cardiac cycles, resulting in a high-resolution reconstructed image. Offline volume analysis allows modification of the angle, the cardiac plane, and the frame analyzed so that an optimized and perfectly aligned 4-chamber plane can be obtained, which is especially useful in CHD where anatomical changes may make it difficult to obtain.

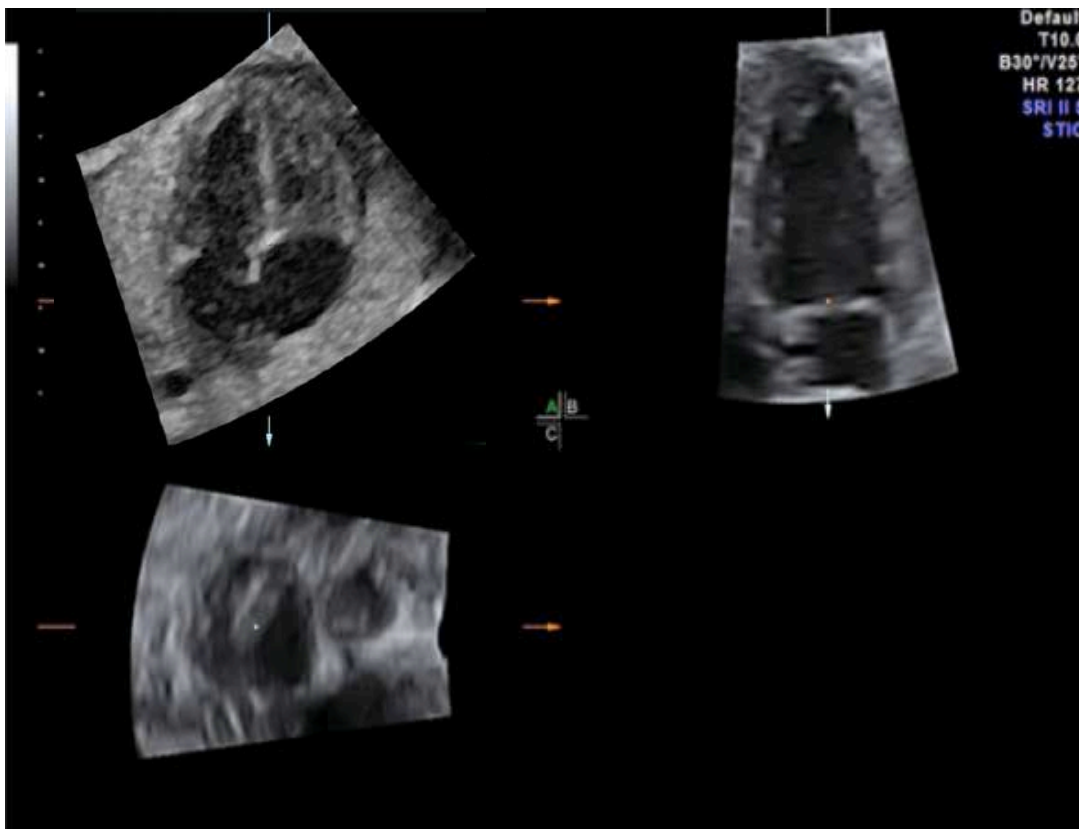


Figure 4: Multiplanar display of a 4D-Spatio Temporal Image Correlation (STIC) volume. Plane A: four chamber view. Plane B: two chamber view. Place C: short axis view. (Original figure).

The use of 4D-STIC technology has advantages over 2D echocardiography, such as the reconstruction of anatomical planes not available during real-time two-dimensional examination. This has proven useful in the prenatal diagnosis of CHD(63). Likewise, 4D-STIC allows functional assessment of the fetal heart using M-mode. This allows the analysis line to be precisely positioned at the level of the valvular annulus and at the

appropriate angle for more accurate measurement of annular systolic excursion (TAPSE and MAPSE)(64). In addition, it allows for a more accurate calculation of LV ejection fraction by Simpson's technique, the formula of choice in adult cardiology, thanks to the 2-chamber plane reconstruction(19). Quantification of LV volume can also be obtained by 4D-STIC (65). However, it has limitations such as poorer resolution in certain planes and artifacts from fetal movements or maternal breathing.

The role of 4D-STIC echocardiography in evaluating cardiovascular remodeling in CHD is also promising. Similar to the postnatal period, 4D assessment of the fetal heart in CHD would enable a more precise estimation of cardiac morphometric and volumetric changes, and consequently, a more accurate functional assessment.

2.3. Cardiovascular plasmatic biomarkers in CHD

Cardiovascular plasma biomarkers are proteins released in myocardial cells in response to an insult and are used in clinical practice in adult and pediatric populations for diagnosis, monitoring, and prognostic assessment of diseases such as heart failure and acute myocardial infarction. The study of plasma biomarkers in cord blood has been useful in detecting signs of cardiac dysfunction and myocardial cell in fetuses with intrauterine growth retardation(66)(67,68). More recently, it has shown prognostic utility in fetuses with left CHD by identifying a different biomarker profile depending on their prognosis(69).

Cardiovascular biomarkers provide a window of opportunity to be applied in combination with other modalities, or applied alone as the first step in settings with lower technological resources. The relationship between cardiac remodeling by STE and plasma biomarkers has not been evaluated so far, and could improve prognostic assessment in the prenatal period. Moreover, if cardiovascular biomarkers assed in umbilical cord blood demonstrate a clinical applicability, their potential clinical application in amniotic fluid could be evaluated as it would provide valuable prognostic information starting from the fetal stage.

2.3.1. *N-terminal B-type natriuretic peptide (NT-proBNP)*

There are several types of natriuretic peptides: atrial (atrial natriuretic peptide) and ventricular (BNP, C-type natriuretic peptide, and urodilatin). BNP is produced in response to myocardial distension due to volume overload, pressure overload, and hypoxia, and is cleaved into NT-proBNP (biologically inactive) and the active hormone (BNP)(70).

NT-proBNP has a longer half-life and fewer level fluctuations, making it a better biomarker(71). Increased BNP induces diuresis, natriuresis, inhibition of the renin-angiotensin-aldosterone system, vasodilatation, and decrease in plasma volume by passage of intravascular fluid to the extravascular space(72). Elevated values indicate cardiac dysfunction from subclinical periods, so it is widely used for the diagnosis and monitoring of heart failure in adult and pediatric populations(73). NT-proBNP values in umbilical cord blood are physiologically increased due to pronounced neonatal circulatory changes, but decrease during the first days of life (71).

NT-proBNP has shown to be a useful prognostic tool in neonates and children with univentricular CHD. It is associated with neonatal death, when increased in umbilical cord blood; and it is also an early marker of heart failure, when it elevates after the first palliative surgery(74–76). Children with systemic RV also have increased NT-proBNP values, which correlate with tricuspid regurgitation, RV functional parameters, and *New York Heart Association* NYHA functional class(75). Moreover, NT-proBNP is a good marker to identify RV ventricular dysfunction in children with ToF, showing a good correlation with cardiac dysfunction and the presence of pulmonary insufficiency(75,77).

The use of NT-proBNP in umbilical cord blood has been studied in fetuses with sacrococcygeal teratoma (increased levels indicate a higher risk of neonatal death) (78) and non-immune fetal (useful to determine a cardiac cause of non-immune fetal hydrops)(79,80), but studies in CHD are scarce. There are few studies evaluating the value of NT-proBNP in amniotic fluid in the context of CHD and they seem promising. These studies have shown increasing levels of NT-proBNP in amniotic fluid depending

on the severity of the CHD, and higher level than healthy fetuses(81,82). Moreover, a cut-off value for predicting biventricular outcome in fetal aortic stenosis has been proposed(83). Thus, further studies in this area may provide additional information to improve prenatal counseling for CHD.

2.3.2. Troponin I

Troponin is a protein found in cardiomyocytes and skeletal muscle that regulates muscle contraction, that is released into the bloodstream when there is reversible or non-reversible damage of the heart, often due to decreased oxygen supply or increased cardiac oxygen requirements (tachycardia or strenuous physical exercise) (84). Troponin has three subunits, including Troponin I, which is used to detect myocardial injury as it is specific of myocardial cells(85,86).

Troponin I has been found increased in pressure overload CHD such as PS, aortic stenosis, and aortic coarctation, and its value has been correlated with the lesion pressure gradient in these CHD. Interestingly, after surgery or catheterization, Troponin I value returned to normal. It is hypothesized that pressure overload induces myocardial hypertrophy and subendocardial hypoxia leading to a decrease in coronary microcirculation thus causing myocardial damage(84,87). Volume overload may also cause Troponin I elevation, causing a distension of cardiac chambers associated with increased oxygen demand (87), which has been shown to be a good predictor of neonatal mortality in fetuses with univentricular heart(76). Moreover, Troponin I is also a reliable indicator of myocardial injury and short-term complications after neonatal cardiac surgery as it correlates with the duration of the intervention and cardiopulmonary bypass(85,88).

Finally, cord blood Troponin I has been proposed to be a good biomarker for fetal myocardial injury since its high molecular weight prevents placental passage. Healthy fetuses and neonates have higher baseline Troponin I values compared to adults, possibly due to decreased placental and renal excretion during this period(89). Different studies have shown that cord blood troponin I levels are elevated in intrauterine growth retardation, and neonates with hypoxic-ischemic disease secondary to myocardial

ischemia due to neonatal acidosis, correlating with early neonatal mortality(67,85,90–92).

2.3.3. Transforming growth factor β (TGF β)

TGF β is a family of cytokines that play a role in various physiological (trophoblastic invasion and embryonic development, cell differentiation and growth) and pathological (inflammation, angiogenesis and fibrosis) responses. TGF β -1 is the most expressed subunit in the cardiovascular system and it is responsible for maintaining cardiovascular homeostasis. TGF β is activated in response to different stressors such as vascular shear stress secondary to turbulent flow through blood vessels, pressure overload and cardiac hypertrophy and fibrosis(93,94). In pulmonary hypertension, pressure overload increases TGF β levels to achieve a compensatory RV hypertrophy. However, progressive pressure overload will lead to excessive TGF β activation, conducting to diastolic dysfunction by increased collagen deposition in the myocardial extracellular matrix, thus making the myocardium stiffer(95). On the other hand, turbulent flow and increased pressure on vascular endothelial cells can also stimulate the production of TGF β , leading to an increase extracellular matrix production and hyperplasia of intimal and medial arterial layers(96,97). This phenomenon has been associated with the development of aortic aneurysms in patients with bicuspid aorta and in Marfan syndrome and it correlates with aortic dissection and the need for aortic root replacement(98). Mutations affecting TGF β signaling and elevated TGF β levels associated with aortic dilatation and stiffness have also been found in patients with ToF(99,100).

In fetal life, TGF β has been poorly studied, but increased umbilical cord blood concentrations have been demonstrated in growth-restricted fetuses due to abnormal vascular flow redistribution(101). A recent novel study, has preliminary shown that fetuses with left-CHD associated with pressure overload and turbulent vascular flow (coarctation of aorta and aortic stenosis), present increased umbilical cord blood TGF β levels, while TGF β was not increased in univentricular left-CHD, in which cardiac output was managed by the right heart and laminar flow through the pulmonary artery(69).

2.1.1. Angiogenic factors and congenital heart defects

There is an association between CHD and pregnancy complications related to placental dysfunction. Pregnancies with CHD have a 7-fold increase in the incidence of early preeclampsia and fetal growth retardation and in the opposite direction, pregnant women with increased risk of early preeclampsia also have a higher risk of fetal CHD(11). Although this association is still not completely understood, it could be explained from the concept of the “placenta-heart axis”, which refers to the simultaneous development of the placenta and the heart during early embryonic stages. These organs share genes and molecular pathways that promote their coordinated growth(3,102). Defective development of either organ can have a synergistic effect. Moreover, both the cardiovascular and placental systems are vulnerable to external agents such as teratogens or micronutrient deficiencies(103). Furthermore, hemodynamic disturbances resulting from abnormal placentation may influence cardiac morphogenesis(104) by altering the genes responsible for cardiomyocyte differentiation. Conversely, hemodynamic changes and hypoxia resulting from cardiac defects can induce placental dysfunction and growth retardation by altering vascular developmental pathways(105).

However, it is currently unknown whether placental disruption contributes to the development of CHD or CHD affects placental development, or whether it is a mutually altered pathway affecting both cardiac and placental development (106). The study of different biomarkers implicated in the pathophysiology of preeclampsia and growth retardation could provide relevant information to better understand the significance of the placenta-heart axis and to identify the groups of CHD with a higher risk of placental complications and thus with a worse prognosis.

2.1.2. Placental growth factor (PlGF)

PlGF is a glycoprotein that belongs to the vascular endothelial growth factor (VEGF) family. It is secreted by the placenta and plays an important role in regulating trophoblastic endothelial growth and vascular differentiation and development. PlGF promotes angiogenesis by binding to VEGF receptor-1 or VEGF receptor-2, which enhances the effect of VEGF(107).

PlGF expression in the heart promotes angiogenesis and helps with healing and preservation of LV function after acute myocardial infarction and heart failure(108,109). Previous studies have shown that fetuses with left CHD have lower cord blood levels of PlGF and in maternal plasma(69). This suggests the presence of an anti-angiogenic environment that may be linked to the development of CHD.

2.1.3. Soluble fms-like tyrosine kinase 1 (sFlt-1)

sFlt-1 is the soluble receptor of PlGF and prevents PlGF from interacting with its cellular receptor (Flt-1). Hypoxia decrease its production, leading to increased angiogenesis and cardiac remodeling(110). However, high levels of sFlt-1 have been linked to endothelial dysfunction in preeclampsia. Increased production of sFlt-1 has also been found in adults with acute myocardial infarction. High levels of sFlt-1 and the sFlt/PlGF ratio may predict progression to heart failure and mortality(111).

The sFlt-1/PlGF ratio has been studied in children with CHD and it is correlated with volume overload and hypoxia. Increased levels are found before surgery of volume overload CHD and decrease after surgical correction(112).

Moreover, increased umbilical cord and maternal plasma sFlt-1 levels have been found in a mixed CHD group(113). On the contrary, very decreased umbilical cord levels have been recently found in fetuses with univentricular left-sided CHD, possibly due to presence of severe hypoxic damage in the LV endocardium in fetal life (69).

3. APPLICATION OF NEW MODALITIES TO CONGENITAL HEART DEFECTS

The application of these new modalities in different groups of CHD in the fetal stage could help to improve specific aspects of perinatal management. For this, it necessary to conduct correctly designed studies including sufficient number of cases for each type of CHD.

PS is the most frequent right outflow tract obstruction CHD with overall good prognosis and postnatal corrective surgery. However, its spectrum is very broad and it is currently necessary to expand the prognostic evaluation from the fetal stage.

Conotruncal anomalies are also a common group of CHD, which share similar embryological origins. Within this group, the most frequent are ToF and D-TGA. ToF is a CHD with a broad spectrum of severity and a high risk of genetic or extracardiac malformation associations. On the other hand, D-TGA is usually isolated but the risk lies in the fact that, due to the anatomical structure, less oxygenated blood reaches the coronary and brain territory. Though, the study of cardiovascular biomarkers may offer clues to better understand its physiology and provide prognostic information.

Thus, the aforementioned anomalies constitute some of the CHDs that would benefit from applying new diagnostic modalities to improve their evaluation and prognostic evaluation in fetal life.

3.1. Pulmonary stenosis

PS is characterized by a partial obstruction of the RV outflow tract. It is an evolving pathology and it can shift from mild-moderate to severe forms or even to pulmonary atresia. The incidence of PS is high, accounting for 8% of postnatal CHD, but only 1% of CHD in fetal life. This discrepancy is due to the difficulty in the prenatal identification of mild forms due to their low ultrasound expressivity at the level of the four chamber view(114).

The presence of valvular dysplasia signs (thickened or dome-shaped pulmonary valve with fused leaflets) combined with an acceleration of the pulmonary transvalvular flow are the clues for its diagnosis (**Figure 5**).

In addition, to enhance PS diagnosis, it is also necessary to improve its prenatal classification to better define which cases are at higher risk of in utero evolution and/or will require fetal and/or neonatal treatment. The presence of significant tricuspid insufficiency and DA reversed flow are the classical parameters to establish the PS severity, differentiating mild/moderate from severe/critical forms (**Figure 6**).

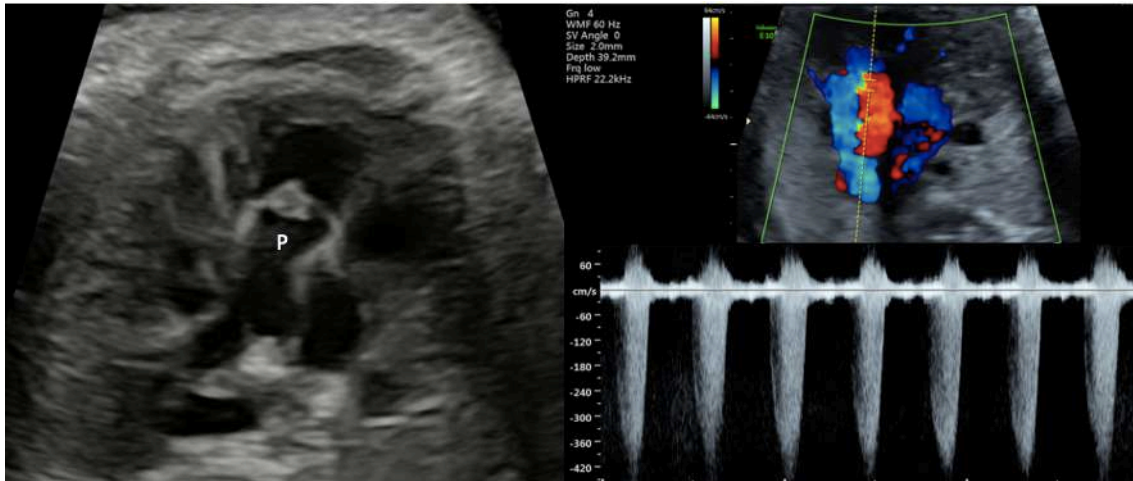


Figure 5: Three vessel view of a fetus with pulmonary stenosis. Left: Hyperechoic and thickened pulmonary valve (P) in a fetus with pulmonary stenosis. Right: Color Doppler three vessel and trachea view with aliasing at the pulmonary valve flow with high peak systolic velocities. (Original figure).

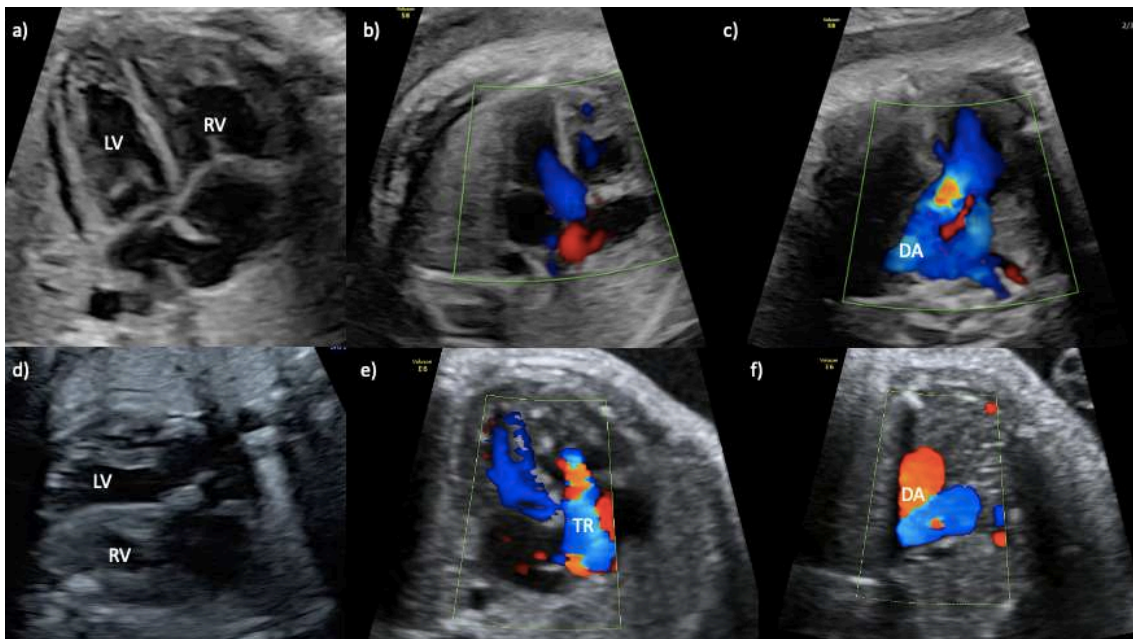


Figure 6: Fetal cardiac characteristics of pulmonary stenosis. Upper row: fetus with mild pulmonary stenosis. a) normal four-chamber view (RV: right ventricle, LV: left ventricle), b) color Doppler normal four-chamber view with no signs of tricuspid regurgitation (TR), c) color Doppler three vessel view showing aliasing at the level of the pulmonary valve and antegrade flow at the ductus arteriosus (DA) level. Lower row: fetus with critical pulmonary stenosis. D) four-chamber view showing a RV with

concentric hypertrophy, e) color Doppler four-chamber view with a significant TR reaching the atrial roof, f) color Doppler three vessel and trachea with reversed Flow at the ductus arteriosus. (Original figure).

3.1.1. Prenatal prognostic evaluation

The available current information is focused on the prognostic evaluation of the most severe forms. Several studies have defined prenatal predictors of progression to hypoplastic RV (such as tricuspid/mitral ratio, RV/LV length ratio and tricuspid filling time fraction)(115–121) and hydrops.

With the increasing prenatal diagnosis of milder forms of PS, the current interest is also focus is on identifying prenatal predictors of early neonatal valvuloplasty. This would help to coordinate the delivery in a tertiary care center with pediatric cardiology. Historically, reversed flow in the DA was considered a reliable parameter to predict postnatal ductus dependence. However, recent studies have shown that about 50% of newborns who require intervention or prostaglandin infusion had antegrade DA flow in prenatal echocardiography(20,118). To date, several parameters have been proposed to predict the need for postnatal valvuloplasty, including TAPSE, peak mitral E' velocity, LV cardiac output(20), as well as the presence of pulmonary insufficiency on second trimester ultrasound and the RV/LV length ratio for predicting neonatal prostaglandin requirement(118). Further studies, incorporating new echocardiographic modalities, are required to improve the results obtained so far.

3.2. Tetralogy of Fallot

ToF is a conotruncal CHD that combines an outlet ventricular septal defect (VSD), dextroposition of the aorta overriding the interventricular septum, RV outflow obstruction and RV hypertrophy, which in fetal life is not usually present, so at this stage ToF is called Fallot Complex (**Figure 7**).

ToF is the most frequent conotruncal CHD with an incidence of 1/1000-2000 newborns and is the most common cause of cyanosis due to CHD. Its etiology is unknown, but it is highly associated with genetic anomalies, extracardiac malformations and fetal growth

restriction. Prenatal echocardiography allows the correct characterization of different ToF phenotypes, based on the degree of RV outflow obstruction. ToF with PS is the most common type. It consists of a mild obstruction of the RV outflow tract, leading to a decrease in the size of the pulmonary artery and its branches but maintaining an antegrade flow through the pulmonary artery. Although it can evolve to more severe forms, it is a CHD with overall good prognosis.

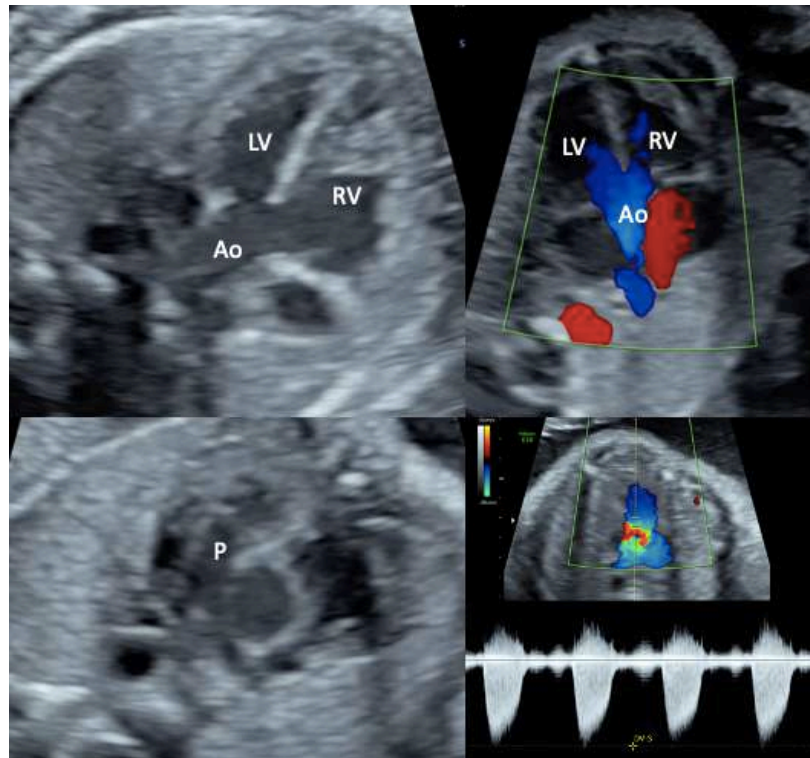


Figure 7. Tetralogy of Fallot with pulmonary stenosis. Upper left: five chamber view showing outlet ventricular septal defect with overriding aorta (Ao). Upper right: five chamber view in color Doppler showing outlet ventricular septal defect and left (LV) and right ventricle (RV) flow towards the aorta (“Y” sign). Down left: three vessel view showing hypoplastic pulmonary trunk (P) and arteries. Down right: three vessel view in color Doppler with aliasing at the pulmonary valve flow with high peak systolic velocities. (Original figure).

Classically, it was believed that RV hypertrophy and dysfunction were not present in fetal life due to the differences in fetal circulation. However, recent studies have

demonstrated that RV hypertrophy (122) and decreased biventricular function(60,123) are already present in fetal life.

Progressive aortic root dilation is also described in young adulthood long after corrective surgery for ToF. Interestingly, some studies have shown that dilation of the aortic valve and ascending aorta(122), as well as decreased aortic compliance(124), are already present during fetal life. The exact cause of aortic dilation is not fully understood but it is believed to be the consequence of the combination of hemodynamic changes and intrinsic histological changes (intrinsic aorthopathy) (124,125)

Another relevant prognostic factor in ToF during fetal life, is its association with placental dysfunction and lower birthweight(126). Its incidence is the higher among all CHD. The causes that lead to this placental dysfunction in ToF fetuses are not known. This association is relevant since placental dysfunction can lead to induced prematurity and low birthweight, two conditions that difficult postnatal management and surgical correction and is a cause of increased mortality among this newborns(127).

3.2.1. Prenatal prognostic evaluation

Fetal echocardiography has been shown to be useful in predicting the postnatal prognosis of fetuses with ToF. A study found that a pulmonary valve z-score <-3.2 , right pulmonary artery <-0.5 z-score, as well as low pulmonary valve/aortic valve ratio, were associated with a higher likelihood of needing a systemic pulmonary shunt and reintervention before corrective surgery(128), as well as a peak systolic velocity through the pulmonary valve higher than 87.5cm/s(129). Likewise, another study revealed that pulmonary valve z-score and pulmonary to aortic valve ratio <0.697 can predict the need for transannular patch in corrective surgery instead of valve-sparing surgery. This information can be useful for providing better prenatal advice to parents(130).

The evaluation of biventricular myocardial impact in varying degrees of right outflow tract obstruction with more precise echocardiographic techniques would enable the establishment of new predictor variables. These variables would help predict the progression of this CC in the fetal stage and the ventricular response to postnatal

surgery. In addition, the study of biomarkers in umbilical cord blood, which are widely used in postnatal setting, and their correlation with fetal echocardiography can also help define cardiovascular remodeling patterns in this disease. Furthermore, they may also help in understanding the degree of aortic involvement in the fetal stage and understand its potential usefulness in long-term prognosis. Additionally, the study of angiogenic factors in cord blood and feto-placental doppler may help elucidate the causes of the association between ToF and placental dysfunction.

3.3. D-Transposition of the great arteries

D-TGA is a conotruncal CHD with an incidence of 1 in 3000-5000 newborns. It consists of a ventriculo-arterial discordance, where the pulmonary artery arises from the LV and the aorta from the RV and have a parallel course (**Figure 8**). Contrary to ToF, the association of simple D-TGA with genetic or extracardiac anomalies and placental dysfunction is very rare.

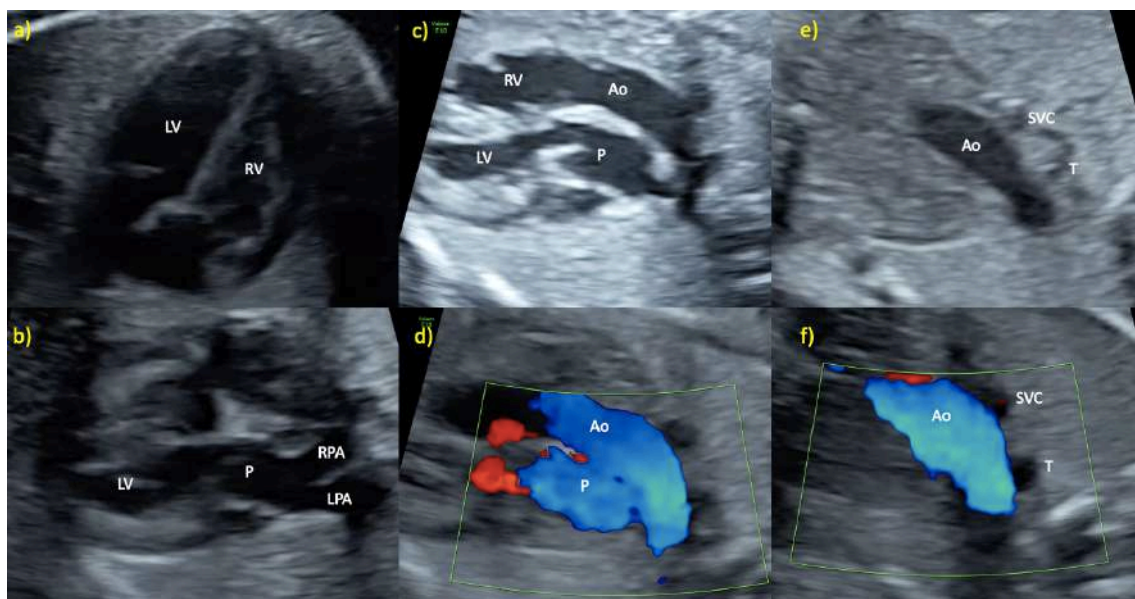


Figure 8. D-Transposition of the great arteries. a) normal four chamber view. LV: left ventricle, RV: right ventricle. b) Left ventricle outflow tract shows the pulmonary artery (P) arising from the left ventricle and its bifurcation in right pulmonary artery (RPA) and left pulmonary artery (LPA). c-d) Oblique view in 2-D (c) and in color Doppler (d) showing the parallel course of the great vessels. The RV connects with the aorta (Ao) and the LV with the pulmonary artery (P). e-f) Typical three vessel and trachea view in a D-

transposition of the great arteries showing only one great vessel (aorta) and the superior vena cava (SVC) and trachea (T). (Original figure).

The overall prognosis of simple D-TGA is good and importance of its prenatal diagnosis relies in optimizing the neonatal management to avoid the early postnatal severe and adverse consequences of two separate circulations: one involving the systemic territory (RV and aortic artery) and the other involving the pulmonary territory (LV and pulmonary artery).

3.3.2 Prenatal prognostic evaluation

Prenatal diagnosis of D-TGA is essential as approximately 50% of infants will require urgent postnatal intervention due to premature closure of the fossa ovalis leading to refractory hypoxia. Identifying infants who will present with hypoxia and need urgent atrioseptostomy before birth is of vital importance to prevent severe neurological sequelae resulting from hypoxemia, or death of the newborn.

Several studies have tried to identify echocardiographic parameters in fetal life to predict the need for urgent atrioseptostomy with good specificity but low sensitivity. A recent meta-analysis proposes the development of multi-parametric models combining several factors may help improve prenatal detection(131). Furthermore, the heterogeneity of studies in terms of the time considered as urgent atrioseptostomy (1 hour, 24 hours, etc.) and the different gestational ages at echocardiography (from 20 weeks to 40 weeks) does not allow robust conclusions.

Recent studies have used new STE techniques to study cardiovascular remodeling and function in D-TGA. The combination of several echocardiographic parameters, including GLS, as a marker of subendocardial dysfunction, has demonstrated improvement in atrioseptostomy prediction(55,56). The use of STE may also help the prediction of long-term ventricular function in D-TGA.

The study of cord blood biomarkers in fetuses with D-TGA has not been studied to date, but might help to identify those fetuses with preclinical changes of pressure or volume

overload and might have prognostic value for postnatal management. In addition, the study of biomarkers of myocardial ischemia in cord blood could help understand the myocardial changes caused by reduced coronary oxygen delivery in these infants.

3. RATIONALE OF THE DOCTORAL THESIS

CHD are the most common severe congenital malformations, with an annual incidence of over 1.000.000 newborns worldwide. They are the leading cause of mortality in the first year of life, even in developed countries. In recent years, the prognosis of CHD has significantly improved due to advancements in prenatal diagnosis, neonatal care, cardiovascular surgery and catheterization techniques. Most CHD cases require at least one surgery or catheterization, resulting in a hospital cost associated with treatment and follow-up estimated at \$1.8 billion per year. Additionally, the psychological and emotional impact of CHD on the individual and family must be considered. CHD also damages the heart muscle as early as fetal life, leading to greater cardiovascular risk in the long term, even after complete surgical correction.

The technical advances of recent years, including the development of STE and other echocardiographic modalities, have made it possible to perform a detailed study of cardiovascular remodeling in the context of CHD. This project aims to assess the applicability of STE combined with a comprehensive 2D echocardiography in some common CHD subgroups to evaluate cardiovascular remodeling, and their correlation with cord blood cardiovascular biomarkers. This will contribute to a better understanding of the pathophysiology of CHD and the mechanisms of cardiovascular adaptation in fetal life which may allow to identify new prognostic parameters to optimize the follow-up of children with CHD from fetal life. Early identification of cardiac remodeling associated with the CHD with worse prognosis would have a significant impact on the health of these children. If the hypothesis of this project is confirmed, STE could be incorporated into the systematic evaluation of fetuses with CHD and included in clinical guidelines for advanced fetal echocardiography, similar to the postnatal period.

In this thesis, we hypothesize that STE and plasma biomarkers can be used to assess cardiovascular remodeling associated with severe CHD in the prenatal period, and that incorporating them in fetal life would improve the prognostic assessment of CHD. To test these hypotheses, four studies were designed in four different prenatal cohorts that included both CHD cases and controls. First, the feasibility and reproducibility of STE was assessed using 4D echocardiography, a technique that improves the acquisition of a four-chamber cardiac plane (Study 1). In Study 2 the pattern of cardiovascular remodeling was studied by conventional echocardiography and STE in the longest prenatal PS cohort, and predictive parameters for neonatal valvuloplasty were identified. Next, the pattern of umbilical cord cardiovascular biomarkers and angiogenic factors in ToF and simple D-TGA and their potential prognostic value were evaluated. Finally, the pattern of cardiovascular remodeling by STE was evaluated in a long cohort of fetuses with TOF (Study 4).

Hypothesis

1. Speckle tracking echocardiography is an applicable tool to evaluate cardiovascular remodeling (cardiac morphometric and functional changes) in normal fetal heart.
2. Speckle tracking echocardiography in combination with conventional echocardiography allows to accurately evaluate the cardiovascular remodeling pattern associated with congenital heart defects in the prenatal stage.
3. Congenital heart defects are associated to specific patterns of blood cord cardiovascular biomarkers and angiogenic factors which correlate with echocardiographic parameters.
4. The incorporation of speckle tracking echocardiography in fetal life improves the prognostic evaluation of congenital heart defects.

Objectives

1. To demonstrate the applicability of speckle tracking echocardiography for the evaluation of morphometric and functional parameters in fetal life in a cohort of healthy fetuses.
2. To validate the applicability of morphometric and functional evaluation by speckle tracking echocardiography in fetuses with severe congenital heart defects.
3. To define the pattern of umbilical cord blood cardiovascular biomarkers and angiogenic factors in different congenital heart defects and to evaluate its potential correlation with echocardiographic parameters.
4. To validate the clinical applicability and prognostic utility of speckle tracking echocardiography in fetuses with congenital heart defects.

Material, methods and results

The design of the study, the study population, as well as the methodology used are detailed in the 'Material and Methods' sections of each of the articles that constitute the body of this Doctoral Thesis.

These articles are included below as they have been accepted and published in the scientific literature.

Study 1

Nogué L, Gómez O, Izquierdo N, Mula C, Masoller N, Martínez JM, Gratacós E, Devore G, Crispi F, Bennasar M. Feasibility of 4D-Spatio Temporal Image Correlation (STIC) in the Comprehensive Assessment of the Fetal Heart using FetalHQ®. *Journal of Clinical Medicine*. 2022, Mar 4;11(5):1414.

Impact factor: 4.96. **1st quartile**



Article

Feasibility of 4D-Spatio Temporal Image Correlation (STIC) in the Comprehensive Assessment of the Fetal Heart Using FetalHQ[®]

Laura Nogué ^{1,*}, Olga Gómez ^{1,*}, Nora Izquierdo ¹, Cristina Mula ¹, Narcís Masoller ¹, Josep M. Martínez ¹, Eduard Gratacós ¹, Gregory Devore ^{2,3}, Fàtima Crispi ¹ and Mar Bennasar ¹

¹ BCNatal-Barcelona Center for Maternal-Fetal and Neonatal Medicine, Hospital Clínic and Hospital Sant Joan de Déu, 08950 Barcelona, Spain; nogue@clinic.cat (L.N.); nizquierdo@clinic.cat (N.I.); mula@clinic.cat (C.M.); masoller@clinic.cat (N.M.); jmmarti@clinic.cat (J.M.M.); gratacos@clinic.cat (E.G.); fcrispi@clinic.cat (F.C.); bennasar@clinic.cat (M.B.)

² Fetal Diagnostic Centers, Pasadena, CA 91105, USA; grdevore@gmail.com

³ Department of Obstetrics and Gynecology, David Geffen School of Medicine, University of California, Los Angeles, Los Angeles, CA 90095, USA

* Correspondence: ogomez@clinic.cat; Tel.: +34-93-227-9904



Citation: Nogué, L.; Gómez, O.; Izquierdo, N.; Mula, C.; Masoller, N.; Martínez, J.M.; Gratacós, E.; Devore, G.; Crispi, F.; Bennasar, M. Feasibility of 4D-Spatio Temporal Image Correlation (STIC) in the Comprehensive Assessment of the Fetal Heart Using FetalHQ[®]. *J. Clin. Med.* **2022**, *11*, 1414. <https://doi.org/10.3390/jcm11051414>

Academic Editor: Vlasta Fesslova

Received: 13 January 2022

Accepted: 2 March 2022

Published: 4 March 2022

Publisher's Note: MDPI stays neutral with regard to jurisdictional claims in published maps and institutional affiliations.



Copyright: © 2022 by the authors. Licensee MDPI, Basel, Switzerland. This article is an open access article distributed under the terms and conditions of the Creative Commons Attribution (CC BY) license (<https://creativecommons.org/licenses/by/4.0/>).

Abstract: Fetal Heart Quantification (FetalHQ[®]) is a novel speckle tracking software that permits the study of global and regional ventricular shape and function from a 2D four-chamber-view loop. The 4D-Spatio Temporal Image Correlation (STIC) modality enables the offline analysis of optimized and perfectly aligned cardiac planes. We aimed to evaluate the feasibility and reproducibility of 4D-STIC speckle tracking echocardiography (STE) using FetalHQ[®] and to compare it to 2D STE. We conducted a prospective study including 31 low-risk singleton pregnancies between 20 and 40 weeks of gestation. Four-chamber view volumes and 2D clips were acquired with an apex pointing at 45° and with a frame rate higher than 60 Hz. Morphometric and functional echocardiography was performed by FetalHQ[®]. Intra- and interobserver reproducibility were evaluated by the intraclass correlation coefficient (ICC). Our results showed excellent reproducibility (ICC > 0.900) for morphometric evaluation (biventricular area, longitudinal and transverse diameters). Reproducibility was also good (ICC > 0.800) for functional evaluation (biventricular strain, Fractional Area Change, left ventricle volumes, ejection fraction and cardiac output). On the contrary, the study of the sphericity index and shortening fraction of the different ventricular segments showed lower reproducibility (ICC < 0.800). To conclude, 4D-STIC is feasible, reproducible and comparable to 2D echocardiography for the assessment of cardiac morphometry and function.

Keywords: fetal echocardiography; speckle tracking echocardiography; STIC; strain; fetal cardiac function; prenatal ultrasound

1. Introduction

Fetal echocardiography has dramatically improved in recent decades. The 2D modality has been mainly used for congenital heart disease (CHD) diagnosis [1–3]. However, advances in fetal imaging and technology, with the incorporation of new modalities such as M-mode [4], tissue Doppler [5], 4D-Spatio-Temporal Image Correlation (4D-STIC) [6,7] and, more recently, speckle tracking echocardiography (STE) [8–10] have led to an improvement in fetal cardiac evaluation, not only in CHD detection, but also to carry out a comprehensive evaluation of cardiac morphometry and function [11]. By tracking the endocardial border, STE allows one to evaluate myocardial deformation and global and segmental biventricular morphometry and function. Although STE has been widely used in pediatric and adult cardiology [12–14], its application in fetal life is scarce [15–22], probably due to the difficulty in adapting adult-designed software to prenatal cardiac evaluation [23]. On

the one hand, fetal echocardiography has its own constraints including limited access and small size of the fetal heart, fetal movements, high heart rate and technical aspects in image acquisition. On the other hand, STE has specific and inherent limitations such as variability of reference values when using different equipment, nonsystematic image settings and processing (spatial resolution, frame rate), and the use of different software's [24,25].

In this context, fetal specific STE software Fetal Heart Quantification (FetalHQ®) was recently developed as a promising offline tool that permits the study of global and regional (24-segment) ventricular shape and function [26–33]. Some groups have reported the application of this novel technology to the study of CHD [34,35], and fetal cardiac adaptation to different fetal conditions (fetal growth restriction [36], diabetes mellitus [37], twin-to-twin transfusion syndrome [38]). Despite its potential for further studying the fetal heart, its applicability is limited given the requirement of a high resolution four-chamber view in a specific angle of insonation. The use of 4D-fetal echocardiography (4D-STIC) permits the acquisition of cardiac volumes for offline analysis, also with high frame rate and good resolution and the possibility of postprocessing modification of parameters such as the angle of insonation, the cardiac plane, and the frame for evaluation [7,23,39]. However, no previous studies have specifically compared 2D- and 4D-STIC STE using FetalHQ® for morphometric and functional assessment of the fetal heart.

The aim of this study was to evaluate the feasibility and reproducibility of 4D-STIC STE by FetalHQ® for morphometric and functional parameters in healthy fetuses and to compare it to 2D STE.

2. Materials and Methods

2.1. Study Design and Participants

Prospective study including 31 singleton pregnancies from 20 + 0 to 40 + 0 weeks of gestation attended at the Maternal-Fetal Medicine Department of BCNatal (Hospital Clínic and Hospital Sant Joan de Déu) between September 2020 and January 2021. Low-risk pregnant women were eligible and invited to participate in the study. Exclusion criteria were age <18 years old, ultrasound or chromosomal anomalies and maternal and fetal conditions with known cardiovascular impairment such as diabetes or hypertension, antiretroviral treatment and fetal growth restriction (fetal growth <10th centile according to local standards [40]). Baseline and perinatal data were obtained from the medical records. Gestational age (GA) was calculated according to crown-rump length in first-trimester ultrasound. All participants underwent a single fetal standard ultrasound and echocardiography, performed by two expert sonographers (L.N. and O.G.), to exclude cardiac or extracardiac anomalies following recommended guidelines [41,42]. Estimated fetal weight was calculated according to Hadlock et al. [43], in cases in which it was not available in the two weeks prior to the fetal echocardiography. Fetal weight centile was calculated according to local references adjusted by GA and fetal gender. Doppler pulsatility indices of umbilical, middle cerebral artery and ductus venosus, as well as maximum systolic peak velocity of the middle cerebral artery, were also evaluated.

Study protocol was approved by the Ethical Committee of the institution (Reg. HCB/2019/0540), and written consent was obtained from all participants.

2.2. Fetal Echocardiography

Fetal cardiac 2D clips and 4D-STIC volumes were acquired using a Voluson E10 (GE Healthcare Ultrasound, Milwaukee, WI, USA) with a C2-9D convex probe (3–9 MHz) and RM6C convex matrix-array volume probe (2–6 MHz), respectively. All cardiac images were acquired using Speckle Reduction Imaging (SRI) 3 and Compound Resolution Imaging (CRI) 2 and stored in 4D View (GE Medical Systems, Milwaukee, WI, USA) for offline STE analysis.

Two-dimensional 4-chamber clips were obtained at an apical 4-chamber plane with an angle of insonation between the ultrasound beam and the interventricular septum of $45^\circ \pm 20^\circ$, including at least three complete heart cycles without maternal and fetal

movements. Acquisition was made with a frame rate higher than 60 Hz and adequate zoom so that the thorax filled most of the ultrasound screen [20].

Cardiac volumes were acquired preferably in the same projection as 2D clips. The acquisition of 4D-STIC volumes was standardized as follows: acquisition time of 7.5 s, angle range of 20–30° and no fetal or maternal movements. Prior to STE evaluation, 4D-STIC volume was adjusted to obtain a perfectly aligned 4-chamber view according to the following steps: 1. The reference dot was placed at the crux cordis in the A plane of a multiplanar view. 2. The Z-axis was rotated until the apex was placed at 0°. 3. The X and Y axes were rotated to systematically obtain an improved 4-chamber view (Figure 1).

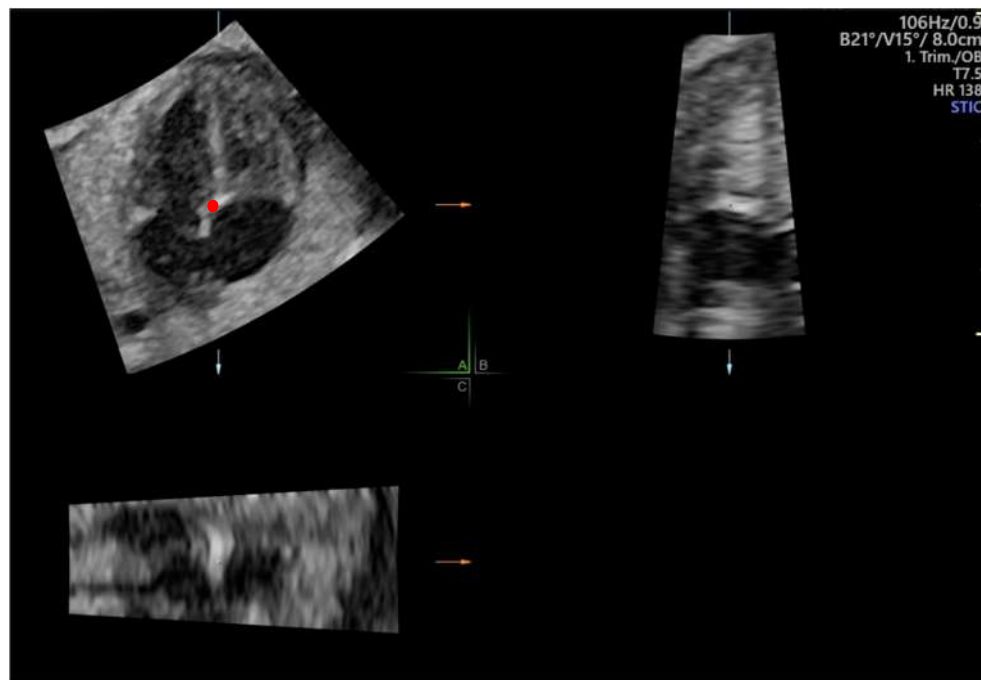


Figure 1. Multiplanar display of a 4D-Spatio Temporal Image Correlation (STIC) volume. In plane A, the reference dot (red dot) is placed at the crux cordis and Z axis rotated until apex is placed at 0°.

2.3. Speckle Tracking Analysis

Two dimensional 4-chamber clips and 4D-STIC cardiac volumes were loaded onto FetalHQ (BT20, GE, Medical Systems). M-mode trace obtained across lateral right ventricle wall at the level of tricuspid annulus was used to define a single cardiac cycle by identifying end-systole and end-diastole, as previously described [20]. The septal, the lateral atrioventricular (AV) valve annulus and the apex of each ventricle were manually identified in the previously defined end-systole frame. Endocardial border was tracked semi-automatically, obtaining a speckle-tracking algorithm, along the cardiac cycle (Figure 2). End-diastolic endocardial tracking was then adjusted if necessary, especially the RV, so that the endocardium, the muscular trabeculations and the moderator band were considered the RV cavity [44]. Both ventricles were divided into 24 segments automatically [27] to allow analysis of the base (segments 1–8), mid ventricle (segments 9–16) and apex (segments 17–24).

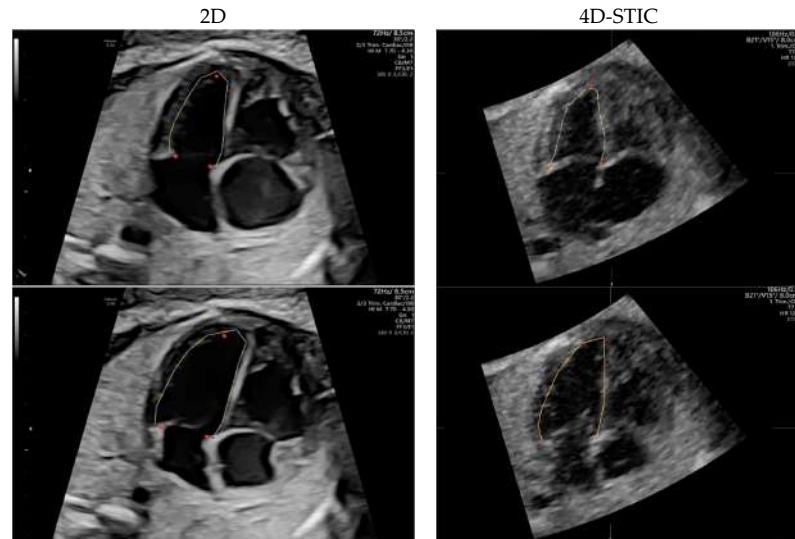


Figure 2. Speckle tracking analysis in a 2-Dimensional (2D) (left) and 4D-Spatio Temporal Image Correlation (4D-STIC) volume (right) using Fetal Heart Quantification (FetalHQ[®]). Four chamber view in the end systole with the three reference dots at the septal and lateral mitral valve annulus and at the apex, and tracking of the endocardial border (superior). Tracking of the left ventricle endocardial border at the end diastole (inferior).

Biventricular global longitudinal strain (GLS) and area derivative as a function of time derivative graphs after the analysis are displayed (Figure 3). The end-systolic frame was adjusted in the area derivative as a function of the time derivative graph at the time the function crossed 0 on the Y axis.

FetalHQ[®] analysis automatically calculated the global and segmental cardiac morphometric parameters, which included biventricular end-diastolic areas and lengths and LV volumes, as well as the transverse and longitudinal diameters and sphericity indices (SI), for 24 defined segments of both ventricles as described by DeVore et al. [27,32]. Global cardiac function was also assessed by calculating biventricular fractional area change (FAC) [30] and LV ejection fraction (EF), stroke volume (SV) and cardiac output (CO) [28,45]. Since the measurement of estimated fetal weight in the same scan is necessary to obtain the result for CO, CO was only assessed in 24 fetuses, unlike the other parameters, which were assessed in 31 fetuses. Additionally, biventricular GLS [31,46] and the fractional shortening of the 24 previously defined ventricular segments were also calculated to evaluate biventricular longitudinal and radial function [26], respectively. The results of the analysis were exported as a comma-separated values (CSV) file and converted to an Excel spreadsheet (Microsoft Corp., Redmond, WA, USA).

All measurements were performed offline by three expert Fetal Medicine operators (LN, MB and OG) for interobserver reproducibility and to compare 2D- and 4D-STIC modalities. A second analysis by a single observer (LN) was performed at least 1 month after the first measurement for the intraobserver reproducibility. All operators had a learning curve of more than 20 fetuses prior to the study.

Additionally, new FetalHQ[®] software (BT21, GE, Medical Systems) with the introduction of Quiver [47], a new tool specially designed to enhance the identification of the septal and lateral atrioventricular annulus was used to reanalyze 10 cases and to compare with no Quiver tool.

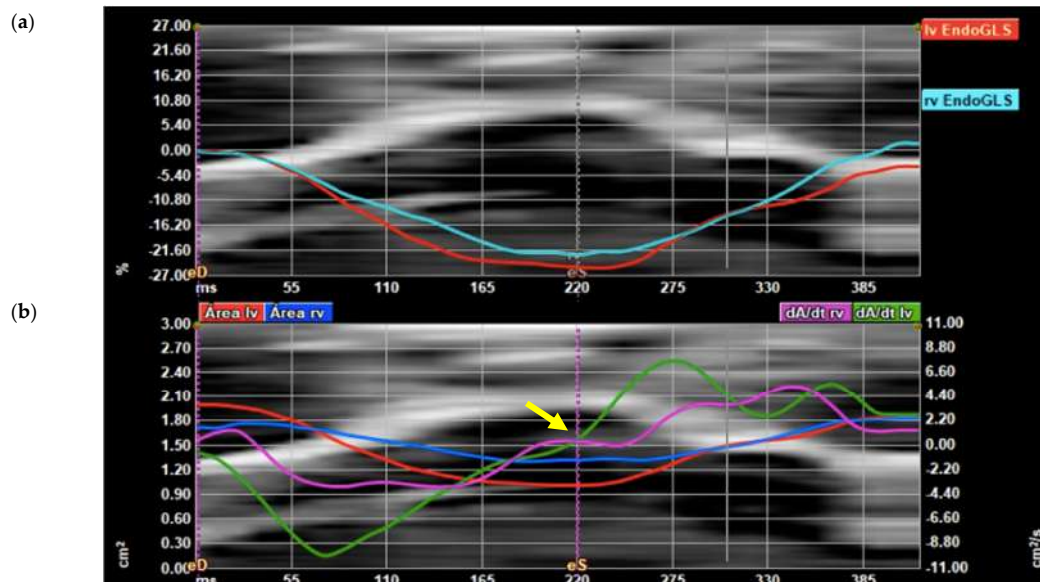


Figure 3. FetalHQ[®] graphic display. (a) Graphic display of left ventricle (LV) global longitudinal strain (GLS) (red line) and right ventricle (RV) GLS (light blue line) with superimposed anatomic M-mode representing tricuspid annulus; (b) graphic display of the derivative of the area (dA/dt) of the LV (green line) and the RV (pink line), LV and RV area (red and blue lines, respectively). Systolic frame (eS) is adjusted in the area derivate as a function of the time derivate graph at the time the function crosses 0 (yellow arrow).

2.4. Sample Size Calculation

The sample size required for reproducibility analysis (30 fetuses) was calculated following Bonnet's et al. formula [48].

2.5. Statistical Analysis

Statistical analysis was performed using IBM SPSS Statistics for Windows statistical package (version 25, IBM Corp., Armonk, NY, USA).

Inter- and intraobserver reproducibility of STE using 4D-STIC was assessed using Intraclass Correlation Coefficients (ICC) and their 95% confidence intervals using a two-way random model. In addition, ICC was used to assess reproducibility of STE using 2D vs. 4D-STIC. Inter- and intraobserver reproducibility of the 4D-STIC STE using Quiver tool was calculated using ICC. Agreement between operators was studied with the Student t test. Limits of agreement, standard error and 95% limit of agreement were calculated and Bland–Altman plots were obtained.

3. Results

3.1. Characteristics of the Study Population

Maternal and perinatal characteristics of the study population are described in Table 1. Median GA at ultrasound was 28.3 weeks (20.3–39.3 weeks) (20 patients between 20–30 weeks and 11 between 30–40). Fetal ultrasound showed a mean estimated fetal weight of 1428 ± 663 g with a mean centile of 51 ± 31.3 . Normal umbilical and fetal Doppler parameters were confirmed in all cases.

Table 1. Maternal and perinatal characteristics of the study population.

| Variable | Result |
|---|-------------|
| MATERNAL BASELINE CHARACTERISTICS | |
| Maternal age, years | 33.3 ± 6.16 |
| Body mass index, kg/m ² | 22.1 ± 2.5 |
| Chronic diseases (hypothyroidism, ulcerative colitis) | 2 (6.4%) |
| Race | |
| White | 28 (80%) |
| Latin American | 2 (5.7%) |
| Asian | 1 (2.9%) |
| Smoking habit | 1 (3.2%) |
| Nulliparity | 18 (58.1%) |
| Use of artificial reproductive technologies | 2 (6.5 %) |
| PERINATAL RESULTS | |
| Gestational age at birth, weeks | 39.5 ± 1.1 |
| Cesarean section | 3 (9.7%) |
| Birthweight, g | 3513 ± 417 |
| Birthweight centile | 53.7 ± 28 |
| Five minutes APGAR score below 7 | 0 (0%) |
| Data expressed as mean ± standard deviation, median (range) or <i>n</i> (%) | |

3.2. Feasibility

Adequate speckle tracking analysis was achieved in all 4D-STIC volumes and in all except one 2D clip due to the poor delimitation of the right ventricular cavity. A frame rate above 60 Hz was achieved in all cases with a mean frame rate of 80 Hz in 2D clips and 107 Hz in 4D-STIC.

3.3. Reproducibility

The 4D-STIC intraobserver and interobserver reproducibility ICC for the most relevant FetalHQ[®] parameters is detailed in Table 2, Figure S1 and Table 3, Figure 4, respectively. Our results show excellent reproducibility (ICC > 0.900) for global morphometric parameters, including biventricular areas, longitudinal, midventricular and apical diameters. Reproducibility was also good (ICC > 0.800) for biventricular basal diameters. On the contrary, the study of the SI of the different ventricular segments showed poor reproducibility. The repeatability of global functional parameters was also good. LV GLS and LV volumes showed excellent intraobserver reproducibility, while RV GLS, biventricular FAC and LV EF and cardiac output demonstrated good intra, and interobserver reliability. Nevertheless, biventricular FS showed a lower reproducibility, especially FS of the basal segments of both ventricles. No statistically significant differences between operators were observed neither systematic bias for the studied parameters.

Table 2. Intraobserver reproducibility of the fetal heart speckle tracking analysis results using 4D-STIC.

| Variable | ICC | 95% Confidence Interval | p-Value | ICC | 95% Confidence Interval | p-Value |
|---|-------|-------------------------|---------|-------|-------------------------|---------|
| FETAL CARDIAC MORPHOMETRY | | | | | | |
| | | Left Ventricle | | | Right Ventricle | |
| Ventricular Area | 0.976 | 0.950 to 0.988 | <0.001 | 0.970 | 0.936 to 0.986 | <0.001 |
| Longitudinal diameter | 0.933 | 0.862 to 0.968 | <0.001 | 0.970 | 0.938 to 0.9585 | <0.001 |
| Basal diameter (segment 1) | 0.853 | 0.696 to 0.929 | <0.001 | 0.855 | 0.702 to 0.930 | <0.001 |
| Mid-ventricular diameter (segment 9) | 0.924 | 0.841 to 0.964 | <0.001 | 0.936 | 0.867 to 0.969 | <0.001 |
| Apical diameter (segment 17) | 0.912 | 0.818 to 0.958 | <0.001 | 0.943 | 0.881 to 0.972 | <0.001 |
| Basal sphericity index (segment 1) | 0.440 | −0.201 to 0.736 | 0.067 | 0.526 | −0.042 to 0.872 | 0.061 |
| Mid-ventricular sphericity index (segment 9) | 0.702 | 0.392 to 0.855 | <0.001 | 0.665 | 0.298 to 0.840 | 0.002 |
| Apical sphericity index (segment 17) | 0.787 | 0.561 to 0.897 | <0.001 | 0.609 | 0.129 to 0.812 | 0.006 |
| FETAL CARDIAC FUNCTION | | | | | | |
| | | Left Ventricle | | | Right Ventricle | |
| Global longitudinal strain | 0.906 | 0.807 to 0.955 | <0.001 | 0.732 | 0.437 to 0.873 | <0.001 |
| Fractional area change | 0.845 | 0.665 to 0.926 | <0.001 | 0.746 | 0.482 to 0.877 | <0.001 |
| Basal shortening fraction (segment 1) | 0.302 | −0.561 to 0.684 | 0.188 | 0.775 | 0.526 to 0.895 | <0.001 |
| Mid-ventricular shortening fraction (Segment 9) | 0.748 | 0.472 to 0.879 | <0.001 | 0.801 | 0.579 to 0.906 | <0.001 |
| Apical shortening fraction (segment 17) | 0.805 | 0.599 to 0.906 | <0.001 | 0.619 | 0.188 to 0.820 | 0.007 |
| End-diastolic volume | 0.968 | 0.933 to 0.985 | <0.001 | | | |
| End-systolic volume | 0.936 | 0.866 to 0.969 | <0.001 | | | |
| Ejection fraction | 0.760 | 0.501 to 0.885 | <0.001 | | | |
| Cardiac Output | 0.782 | 0.500 to 0.904 | <0.001 | | | |

ICC: Intraclass Correlation Coefficient.

Table 3. Interobserver reproducibility of the fetal heart speckle tracking analysis results using 4D-STIC.

| Variable | ICC | 95% Confidence Interval | p-Value | ICC | 95% Confidence Interval | p-Value |
|--|-------|-------------------------|---------|-------|-------------------------|---------|
| FETAL CARDIAC MORPHOMETRY | | | | | | |
| | | Left Ventricle | | | Right Ventricle | |
| Ventricular area | 0.931 | 0.857 to 0.967 | <0.001 | 0.966 | 0.930 to 0.984 | <0.001 |
| Longitudinal diameter | 0.756 | 0.483 to 0.885 | <0.001 | 0.909 | 0.797 to 0.958 | <0.001 |
| Basal diameter (segment 1) | 0.746 | 0.464 to 0.881 | <0.001 | 0.891 | 0.751 to 0.950 | <0.001 |
| Mid-ventricular diameter (segment 9) | 0.841 | 0.666 to 0.924 | <0.001 | 0.921 | 0.835 to 0.962 | <0.001 |
| Apical diameter (segment 17) | 0.884 | 0.675 to 0.925 | <0.001 | 0.882 | 0.745 to 0.994 | <0.001 |
| Basal sphericity index (segment 1) | 0.390 | −0.161 to 0.694 | 0.064 | 0.333 | −0.227 to 0.659 | 0.095 |
| Mid-ventricular sphericity index (segment 9) | 0.495 | −0.11 to 0.754 | 0.027 | 0.683 | 0.329 to 0.850 | 0.001 |
| Apical sphericity index (segment 17) | 0.445 | −0.101 to 0.728 | 0.047 | 0.628 | 0.212 to 0.823 | 0.005 |

Table 3. Cont.

| Variable | ICC | 95% Confidence Interval | p-Value | ICC | 95% Confidence Interval | p-Value |
|---|-------|-------------------------|---------|-------|-------------------------|---------|
| FETAL CARDIAC FUNCTION | | | | | | |
| | | Left Ventricle | | | Right Ventricle | |
| Global longitudinal strain | 0.825 | 0.634 to 0.916 | <0.001 | 0.767 | 0.508 to 0.889 | <0.001 |
| Fractional area change | 0.831 | 0.646 to 0.920 | <0.001 | 0.843 | 0.671 to 0.925 | <0.001 |
| Basal shortening fraction (segment 1) | 0.116 | −0.951 to 0.595 | 0.378 | 0.506 | −0.055 to 0.772 | 0.036 |
| Mid-ventricular shortening fraction (Segment 9) | 0.742 | 0.466 to 0.875 | <0.001 | 0.666 | 0.303 to 0.839 | 0.002 |
| Apical shortening fraction (segment 17) | 0.782 | 0.554 to 0.894 | <0.001 | 0.745 | 0.476 to 0.876 | <0.001 |
| End-diastolic volume | 0.872 | 0.718 to 0.942 | <0.001 | | | |
| End-systolic volume | 0.773 | 0.497 to 0.898 | <0.001 | | | |
| Ejection fraction | 0.769 | 0.516 to 0.890 | <0.001 | | | |
| Cardiac Output | 0.602 | 0.082 to 0.828 | 0.016 | | | |

ICC: Intraclass Correlation Coefficient.

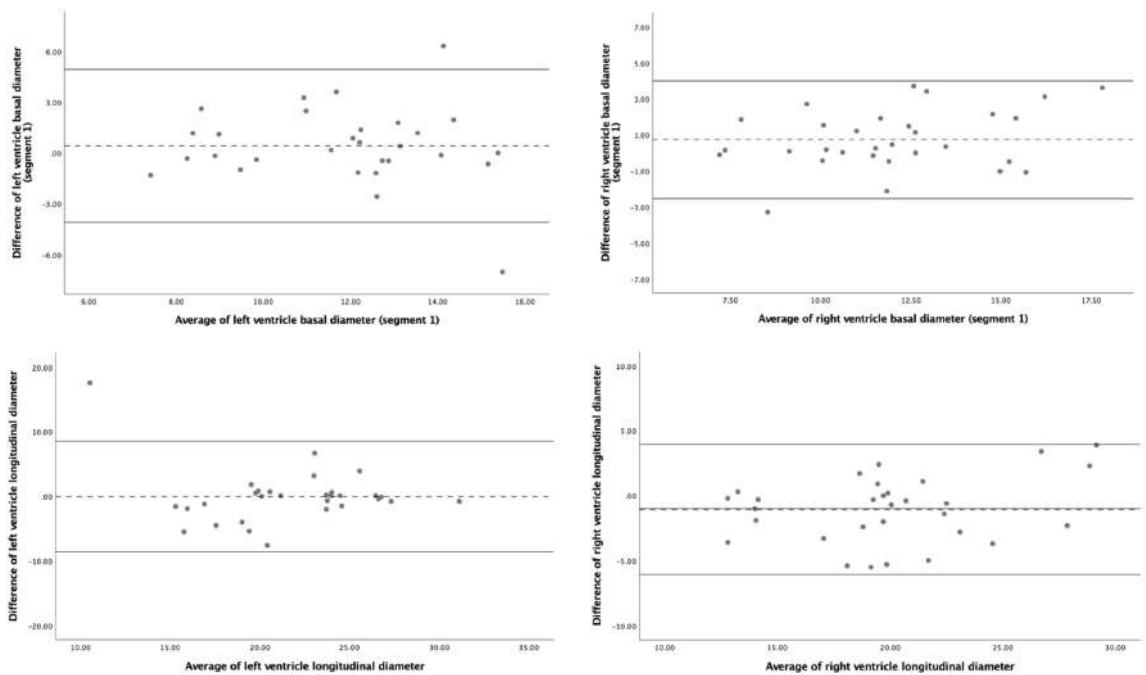


Figure 4. Cont.

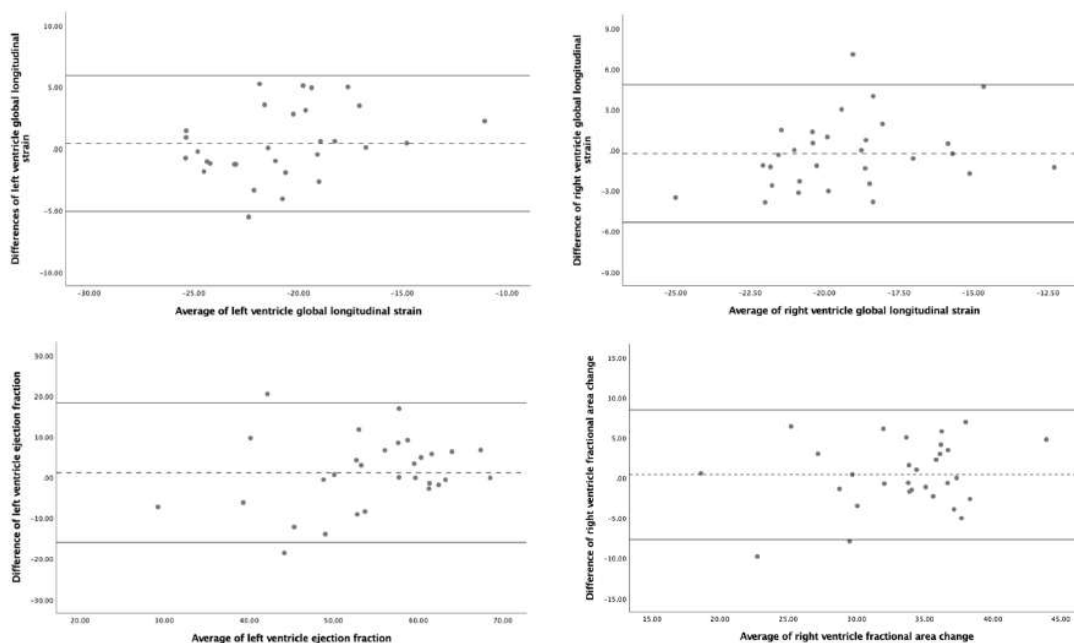


Figure 4. Bland–Altman plots for interobserver reproducibility of fetal heart speckle tracking analysis of morphometric and functional parameters using 4D-Spatio Temporal Image Correlation (4D-STIC). **Upper figures:** left ventricle basal diameter (segment 1) (left) and right ventricle basal diameter (segment 1) (right). **Middle upper figures:** left ventricle longitudinal diameter (left) and right ventricle longitudinal diameter (right). **Middle bottom figures:** left ventricle global longitudinal strain (left) and right ventricle global longitudinal strain (right). **Bottom figures:** left ventricle ejection fraction (left) and right ventricle fractional area change (right).

Comparison between 2D- and 4D-STIC echocardiographic modalities showed similar data (Table 4, Figure 5). The repeatability was good for global biventricular morphometric and functional parameters and poor for the SI and SF of the different ventricular segments, especially for the segments corresponding to the base of both ventricles. The best concordance was found for biventricular areas and LV volume. Again, no statistically significant differences between operators were observed neither systematic bias for the studied parameters.

Table 4. Comparison of Interobserver reproducibility of the fetal heart speckle tracking analysis results using 2D- vs. 4D-STIC.

| Variable | ICC | 95% Confidence Interval | p-Value | ICC | 95% Confidence Interval | p-Value |
|--------------------------------------|-------|-------------------------|---------|-------|-------------------------|---------|
| CARDIAC MORPHOMETRY | | | | | | |
| | | Left Ventricle | | | Right Ventricle | |
| Ventricular area | 0.930 | 0.817 to 0.970 | <0.001 | 0.949 | 0.895 to 0.975 | <0.001 |
| Longitudinal diameter | 0.745 | 0.480 to 0.876 | <0.001 | 0.907 | 0.806 to 0.955 | <0.001 |
| Basal diameter (segment 1) | 0.833 | 0.529 to 0.930 | <0.001 | 0.912 | 0.803 to 0.959 | <0.001 |
| Mid-ventricular diameter (segment 9) | 0.858 | 0.461 to 0.947 | <0.001 | 0.825 | 0.638 to 0.915 | <0.001 |

Table 4. Cont.

| Variable | ICC | 95% Confidence Interval | p-Value | ICC | 95% Confidence Interval | p-Value |
|---|-------|-------------------------|---------|-------|-------------------------|---------|
| Apical diameter (segment 17) | 0.871 | 0.661 to 0.944 | <0.001 | 0.871 | 0.753 to 0.938 | <0.001 |
| Basal sphericity index (segment 1) | 0.222 | −0.401 to 0.601 | 0.211 | 0.637 | 0.226 to 0.823 | 0.003 |
| Mid-ventricular sphericity index (segment 9) | 0.463 | −0.062 to 0.737 | 0.018 | 0.738 | 0.457 to 0.873 | <0.001 |
| Apical sphericity index (segment 17) | 0.589 | 0.172 to 0.799 | 0.005 | 0.698 | 0.370 to 0.855 | 0.001 |
| CARDIAC FUNCTION | | | | | | |
| | | Left Ventricle | | | Right Ventricle | |
| Global longitudinal strain | 0.898 | 0.779 to 0.952 | <0.001 | 0.878 | 0.746 to 0.941 | <0.001 |
| Fractional area change | 0.682 | 0.350 to 0.846 | 0.001 | 0.667 | 0.307 to 0.842 | 0.002 |
| Basal shortening fraction (segment 1) | 0.643 | 0.227 to 0.838 | 0.003 | 0.339 | −0.521 to 0.710 | 0.163 |
| Mid-ventricular shortening fraction (Segment 9) | 0.387 | −0.196 to 0.695 | 0.078 | −0.05 | −1.1 to 0.493 | 0.553 |
| Apical shortening fraction (segment 17) | 0.501 | −0.021 to 0.758 | 0.030 | 0.480 | −0.091 to 0.752 | 0.043 |
| End-diastolic volume | 0.936 | 0.669 to 0.978 | <0.001 | | | |
| End-systolic volume | 0.896 | 0.774 to 0.952 | <0.001 | | | |
| Ejection fraction | 0.628 | 0.243 to 0.819 | 0.004 | | | |
| Cardiac Output | 0.562 | −0.149 to 0.826 | 0.001 | | | |

ICC: Intraclass Correlation Coefficient.

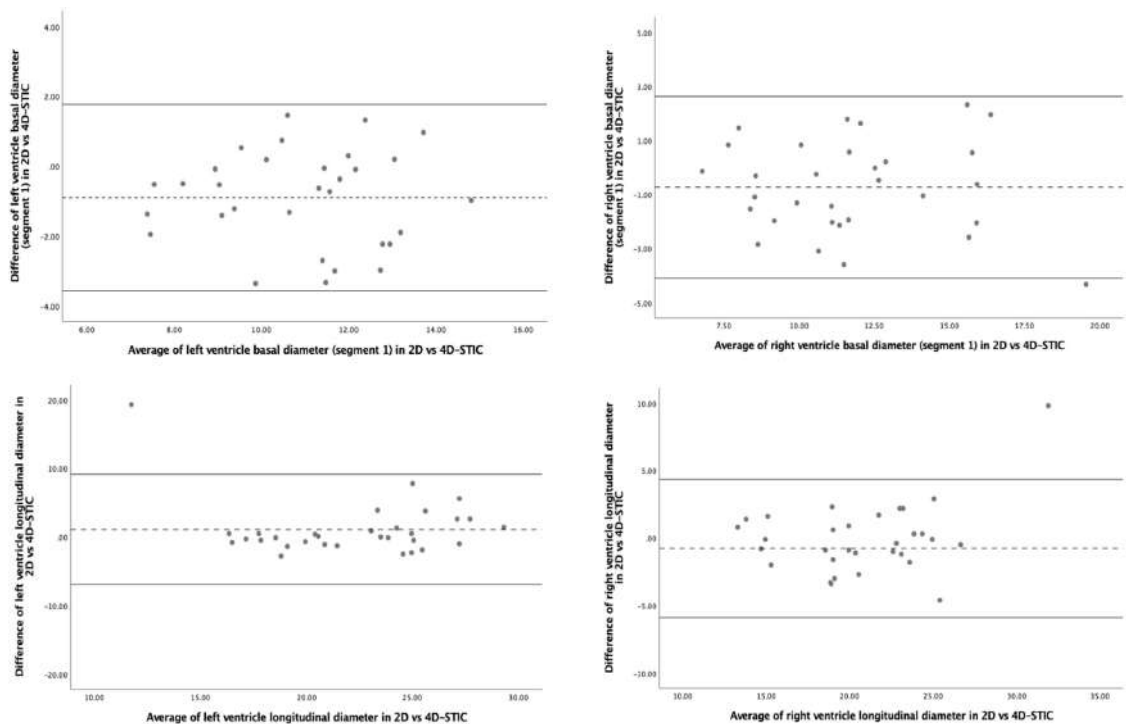


Figure 5. Cont.

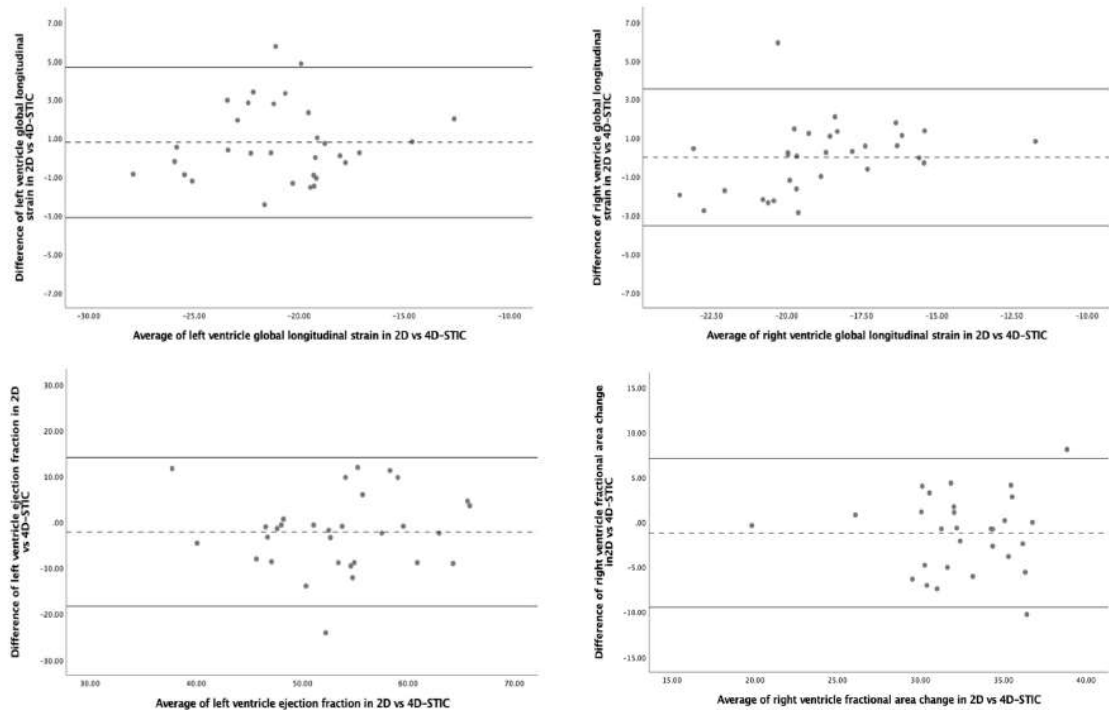


Figure 5. Bland–Altman plots for interobserver reproducibility of fetal heart speckle tracking analysis of morphometric parameters with 2D- versus 4D-Spatio Temporal Image Correlation (4D-STIC). **Upper figures:** left ventricle basal diameter (segment 1) (left) and right ventricle basal diameter (segment 1) (right). **Middle upper figures:** left ventricle longitudinal diameter (left) and right ventricle longitudinal diameter (right). **Middle bottom figures:** left ventricle global longitudinal strain (left) and right ventricle global longitudinal strain (right). **Bottom figures:** left ventricle ejection fraction (left) and right ventricle fractional area change (right).

3.4. Subanalysis Using Quiver Tool

The subanalysis performed in 10 cases using the Quiver tool demonstrated a slightly better reproducibility for most global morphometric and functional parameters but again low reproducibility for the SI and SF of the different biventricular segments, both using 2D- and 4D-STIC. Additionally, ICC and 95% confidence intervals of the Quiver tool analysis as well as the comprehensive study of the 24 biventricular segments are provided in the Supplemental Material.

4. Discussion

This study first demonstrates that 4D-STIC STE is feasible, reproducible and comparable to 2D STE when assessing global cardiac morphometry and function using FetalHQ®. Our results show excellent reproducibility for most of the global cardiac morphometry and function variables evaluated, but worse results for segmental analysis of SI and SF.

4.1. Speckle Tracking Echocardiography Using 2D- and 4D-STIC

Since the first use of 2D STE in fetal cardiology in 2008, only a few publications have focused on the analysis of biventricular GLS on healthy fetuses, reporting a good reproducibility [49,50]. However, there are still limited data on GLS normality ranges throughout the pregnancy [16,22,31,51–54] and its application in different clinical scenarios. In fact, more recent studies, which have incorporated the latest technological advances, point to

the need to better evaluate STE reproducibility and its correlation with other morphometric and functional echocardiographic parameters before introducing STE into clinical practice. In recent years, FetalHQ[®] has shown excellent reproducibility for the analysis of morphometric and functional cardiac parameters [26,27,30,32,55–58]. FetalHQ[®] automatically defines 24 segments of the ventricles and provides information of the shape (SI) and radial systolic function (SF) by the calculation of the longitudinal and transverse diameter of each segment. Although the reproducibility of this segmental analysis was initially reported to be very good [26,27], more recent studies have reported worse data [55,57]. Additionally, none of the previous studies have reported results on the reproducibility conducting a comprehensive study of global and regional cardiac morphometric and functional data.

Focusing on 4D-STIC, the only group that had applied 4D-STIC for STE study in fetal life was Dodaro et al. The authors analyzed the feasibility and reproducibility of LV function evaluation in a cohort of fetuses between 20 and 40 weeks of gestation, reporting moderate interobserver (0.562) and good intraobserver (0.857) agreement for LV GLS and moderate interobserver (0.544) and intraobserver (0.647) repeatability for LV EF [59]. Our data showed better results on LV GLS and EF reproducibility using 4D-STIC STE (Tables 2 and 3) which could be explained for different reasons. First, we defined a standardized protocol both for the acquisition of cardiac volumes and for the subsequent processing in order to always carry out the offline cardiac evaluation in the same way. Second, this strict protocol allowed us to obtain all cardiac volumes with a very high FR (mean of 107 Hz), which was even higher than that achieved with 2D STE (80 Hz). Third, our study was conducted by experienced fetal medicine specialists with previous expertise in 4D-STIC, while e-STIC evaluations were performed by less experienced sonographers with only three weeks training on FetalHQ[®]. Finally, we evaluated a greater cardiac morphometric and functional parameters comparing 4D-STIC and 2D STE, being able to demonstrate that both techniques are reproducible, with the best performance for global cardiac morphometric and functional parameters and the worst for segmental cardiac shape analysis (SI) and radial function (FS).

4.2. Fetal Cardiac Morphometric and Functional Assessment Using 4D-STIC STE

To our knowledge, this is the first study to assess 4D-STIC STE feasibility for a comprehensive morphometric and functional cardiac evaluation and to compare its reproducibility to 2D STE. Our 4D-STIC results showing a good reproducibility for global cardiac morphometric evaluation are in accordance to most previously 2D STE published data, which supports the use of FetalHQ[®] with both modalities. On the contrary, the available studies on 2D STE reproducibility for segmental cardiac morphometric evaluation show discrepant data. While some recent studies [55] have reported a good reproducibility for biventricular SI (ICC > 0.758), other studies such as ours have shown poorer results, especially for assessing the shape of the basal segments of both ventricles [57]. We hypothesize that manual adjustment applied for improving the delineation of both ventricles, especially the RV, led to differences in the endocardial delineation, in particular variations of transverse diameters that compute for the SI and FS segmental analysis. In our study, we performed a manual adjustment of the semi-automatic tracking of both ventricles in most of our cases, especially for the RV, considering the endocardium and moderator band as part of the ventricular cavity [44]. Furthermore, SI and FS are calculated by a mathematical formula (SI: end-diastolic longitudinal diameter/end-diastolic transverse diameter, for each segment; FS: (end-diastolic transverse diameter-end-systolic transverse diameter)/end-diastolic transverse diameter, for each of the 24 segments), which may increase the error of both measures and explain the poorer reproducibility compared to other parameters that do not apply formulas. Finally, different orientation of the four-chamber view acquisition (apical vs. transverse) between studies could also explain discrepant results. It is important to note that due to lateral resolution echographic properties, some of the echoes of the lateral walls and the upper part of the septum can be missed when analyzing an apical compared to a transverse four-chamber view. Further studies are necessary to better define these

methodological issues and their impact on STE reproducibility of biventricular segmental morphometric evaluation [23].

With respect to functional heart assessment, our study is the first one that has so far included the most extensive analysis of the reproducibility of a large number of cardiac functional parameters using both 4D-STIC and 2D STE. We demonstrate a good 4D-STIC STE reliability for biventricular systolic function assessment, with better performance for LV systolic evaluation, including both GLS and FAC, in comparison with the RV. This can be explained by the more complex 3D structure of the RV. Regarding LV systolic parameters (LV volumes, EF and CO), we also report good reproducibility. CO ICC was the lowest regarding LV systolic function, but we only included 24 cases to assess the reproducibility of this parameter, since evaluation of the estimated fetal weight in the same exploration is necessary to calculate CO. On the other hand, biventricular SF showed a poor reproducibility, a finding that has also been reported by other groups [55,56] and that correlates with the poorer reproducibility that we also found for the SI of the different segments of both ventricles. Again, differences in four-chamber-view orientation, methodology and manual tracking could explain our poorer reproducibility results.

4.3. Subanalysis Using Quiver Tool

To better understand our poor results on the segmental ventricular evaluation using fetal HQ, we evaluated 10 cases using Quiver technology, which is supposed to facilitate the identification of the septal and lateral AV valve annulus by displaying two frames before and after end-systole and end-diastole frame [47]. However, our study failed to demonstrate a better performance with Quiver. We are aware that the analysis was carried out in a relatively small number of fetuses, and this technique may need a learning curve to obtain better results; furthermore, more studies are needed to validate previous studies on this technology.

4.4. Strengths and Limitations

We report a rigorously defined acquisition protocol both in 2D- and 4D-STIC modalities defining clear anatomic landmarks postprocessing analysis and recommendable frame rate, which allowed us to obtain a good reproducibility for most of the echocardiographic parameters studied. We also included fetuses ranging from 20 to 40 weeks of gestation to validate the results in both second and third trimesters. Moreover, the comprehensive evaluations of the fetal heart we perform in our study allow us to compare the reproducibility between global and segmental cardiac parameters and to identify our worse results for the segmental analysis. On the other hand, this study also has some limitations. Firstly, we are aware that the sample size of our study could be a weakness, especially for the assessment of CO, as we only included 24 fetuses. Secondly, although 2D STE has been previously validated with normal and abnormal hearts, we have only included in the study healthy fetuses. Thus, more studies would be necessary in order to confirm our results in fetuses with cardiac or extracardiac anomalies. Finally, we are aware that all of our 2D clips and 4D-STIC volumes are in an apical oblique four-chamber view that can be difficult to achieve in the third trimester, or in other fetal conditions such as oligohydramnios. DeVore et al. described that apex-down four-chamber views are eligible indistinctly from apical views for 2D-STE [20], but more studies using basal four-chamber view 4D-STIC volumes should be carried out in order to validate their results.

5. Conclusions

To conclude, we confirm that 4D-STIC STE is feasible, reproducible and comparable to 2D echocardiography for the assessment of global cardiac morphometry and systolic function, including GLS. Although it requires a learning curve, the results of this study are encouraging in using FetalHQ® in future studies to assess fetal cardiac remodeling in different maternal and fetal conditions. If our results are confirmed, 4D-STIC would allow not only structural evaluation of fetal cardiac anatomy but a comprehensive structural and

functional evaluation by a unique cardiac volume acquired in the four-chamber view. This would enable the use of FetalHQ[®] for telemedicine. Future technical improvements in the semi-automatic tracking of the endocardium—to avoid manual correction—are warranted to improve reproducibility of segmental fetal cardiac evaluation.

Supplementary Materials: The following supporting information can be downloaded at: <https://www.mdpi.com/article/10.3390/jcm11051414/s1>, Table S1: Intraobserver reproducibility of the fetal heart 4D-Spatio Temporal Image Correlation (4D-STIC) speckle tracking analysis results using the Quiver technique. Table S2: Interobserver reproducibility of the fetal heart 4D-STIC speckle tracking analysis results using the Quiver technique. Table S3: Comparison of 2D- vs. 4D-STIC Interobserver reproducibility of the fetal heart speckle tracking analysis results using the Quiver technique. Table S4: Intraobserver reproducibility of the fetal heart speckle tracking segmental analysis results using 4D-STIC. Table S5: Interobserver reproducibility of the fetal heart speckle tracking segmental analysis results using 4D-STIC. Table S6: Comparison of interobserver reproducibility of the fetal heart speckle tracking segmental analysis results using 2D- vs. 4D-STIC. Figure S1. Bland–Altman plots for intraobserver reproducibility of fetal heart speckle tracking analysis of morphometric and functional parameters using 4D-Spatio Temporal Image Correlation (4D-STIC). Upper figures: left ventricle basal diameter (segment 1) (left) and right ventricle basal diameter (segment 1) (right). Middle upper figures: left ventricle longitudinal diameter (left) and right ventricle longitudinal diameter (right), Middle bottom: left ventricle global longitudinal strain (left) and right ventricle global longitudinal strain (right). Bottom figures: left ventricle ejection fraction (left) and right ventricle fractional area change (right).

Author Contributions: Conceptualization, L.N., M.B., O.G. and F.C.; methodology, M.B., O.G. and F.C.; software, G.D.; investigation, L.N.; data curation, N.I. and C.M.; writing—original draft preparation, L.N.; writing—review and editing, M.B., O.G., F.C., N.M., J.M.M. and E.G.; supervision, M.B., O.G., F.C. All authors have read and agreed to the published version of the manuscript.

Funding: This research was supported by grants from Hospital Clínic de Barcelona (Premi Fi de Residència “Emili Letang” 2019) (Spain), Instituto Carlos III (INT21/00027, PI17/00675, PI18/00073 and PI20/00246) integrados en el Plan Nacional de I + D + I y cofinanciados por el ISCIII-Subdirección General de Evaluación y el Fondo Europeo de Desarrollo Regional (FEDER) “Una manera de hacer Europa” (Spain), Centro de Investigación Biomédica en Red de Enfermedades Raras (ERPR04G719/2016) (Spain), Cerebra Foundation for the Brain Injured Child (Carmarthen, Wales, UK) and AGAUR 2017 SGR grant No. 1531 (Spain) and Fundació La Marató de TV3–Ref 202016-30-31.

Institutional Review Board Statement: The study was conducted according to the guidelines of the Declaration of Helsinki, and approved by the Ethics Committee of Hospital Clínic de Barcelona (protocol code HCB/2019/0540).

Informed Consent Statement: Informed consent was obtained from all subjects involved in the study.

Data Availability Statement: Study data can be made available upon documented request.

Conflicts of Interest: The authors declare no conflict of interest.

References

1. Shapiro, I.; Degani, S.; Leibovitz, Z.; Ohel, G.; Tal, Y.; Abinader, E.G. Fetal Cardiac Measurements Derived by Transvaginal and Transabdominal Cross-Sectional Echocardiography from 14 Weeks of Gestation to Term. *Ultrasound Obs. Gynecol* **1998**, *12*, 404–418. [[CrossRef](#)]
2. Firpo, C.; Silverman, N.H. Evaluation of Fetal Heart Dimensions from 12 Weeks to Term. *Am. J. Cardiol.* **2001**, *87*, 594–600. [[CrossRef](#)]
3. Kleinman, S.; Lynch, C.; Hobbins, C.; Talner, S. Echocardiographic Studies of the Human Fetus: Prenatal Diagnosis of Congenital Heart Disease and Cardiac Dysrhythmias. *Pediatrics* **2021**, *65*, 1059–1067. [[CrossRef](#)]
4. Allan, L.D.; Joseph, M.C.; Boyd, E.G.C.A.; Campbell, S.; Tynan, M. M-Mode Echocardiography in the Developing Human Fetus. *Br Hear. J* **1982**, *47*, 573–583. [[CrossRef](#)] [[PubMed](#)]
5. Comas, M.; Crispi, F. Assessment of Fetal Cardiac Function Using Tissue Doppler Techniques. *Fetal Diagn. Ther.* **2012**, *32*, 30–38. [[CrossRef](#)]

6. Bennasar, M.; Mart, J.M.I.; Figueras, F.; Olivella, A.; Puerto, B. Intra- and Interobserver Repeatability of Fetal Cardiac Examination Using Four-Dimensional Spatiotemporal Image Correlation in Each Trimester of Pregnancy. *Ultrasound Obstet. Gynecol.* **2010**, *35*, 318–323. [[CrossRef](#)]
7. DeVore, G.R.; Satou, G.; Sklansky, M. 4D Fetal Echocardiography—An Update. *Echocardiography* **2017**, *34*, 1788–1798. [[CrossRef](#)]
8. Langeland, S.; Jan, D.; Wouters, P.F.; Leather, H.A.; Claus, P.; Bijmens, B.; Sutherland, G.R. Experimental Validation of a New Ultrasound Method for the Simultaneous Assessment of Radial and Longitudinal Myocardial Deformation Independent of Insonation Angle. *Circulation* **2005**, *112*, 2157–2162. [[CrossRef](#)]
9. Kocabay, G.; Muraru, D.; Peluso, D.; Cucchini, U.; Mihaila, S.; Padayattil-jose, S.; Gentian, D.; Iliceto, S.; Vinereanu, D.; Badano, L.P. Normal Left Ventricular Mechanics by Two-Dimensional Speckle-Tracking Echocardiography. Reference Values in Healthy Adults. *Rev. Esp. Cardiol.* **2014**, *67*, 651–658. [[CrossRef](#)]
10. Pirat, B.; Khoury, D.S.; Hartley, C.J.; Tiller, L.; Schulz, D.G.; Nagueh, S.F.; Zoghbi, W.A. A Novel Feature-Tracking Echocardiographic Method for the Quantitation of Regional Myocardial Function: Validation in an animal model of ischemia-reperfusion. *J. Am. Coll. Cardiol.* **2008**, *51*, 651–659. [[CrossRef](#)]
11. Crispi, F.; Valenzuela-Alcaraz, B.; Gratacós, E. Ultrasound Assessment of Fetal Cardiac Function. *AJUM* **2013**, *16*, 158–167. [[CrossRef](#)] [[PubMed](#)]
12. Forsey, J.; Friedberg, M.K.; Mertens, L. Speckle Tracking Echocardiography in Pediatric and Congenital Heart Disease. *Echocardiography* **2013**, *30*, 447–459. [[CrossRef](#)] [[PubMed](#)]
13. Geyer, H.; Caracciolo, G.; Abe, H.; Wilansky, S.; Carerj, S. Assessment of Myocardial Mechanics Using Speckle Tracking Echocardiography: Fundamentals and Clinical Applications. *J. Am. Soc. Echocardiogr.* **2010**, *23*, 351–369. [[CrossRef](#)] [[PubMed](#)]
14. Levy, P.T.; Machevsky, A.; Sanchez, A.A.; Patel, M.D.; Rogal, S.; Singh, G.K. Reference Ranges of Left Ventricular Strain Measures by Two-Dimensional Speckle Tracking Echocardiography in Children: A Systematic Review and Meta-Analysis. *J. Am. Soc. Echocardiogr.* **2017**, *29*, 209–225. [[CrossRef](#)]
15. Di Salvo, G.; Russo, M.G.; Paladini, D.; Felicetti, M.; Castaldi, B.; Tartaglione, A.; Pietto, L.; Ricci, C.; Morelli, C.; Pacileo, G. Two-Dimensional Strain to Assess Regional Left and Right Ventricular Longitudinal Function in 100 Normal Fetuses. *Eur. J. Echocardiogr.* **2008**, *9*, 754–756. [[CrossRef](#)]
16. Ta-shma, A.; Perles, Z.; Gavri, S.; Golender, J. Analysis of Segmental and Global Function of the Fetal Heart Using Novel Automatic Functional Imaging. *Congenit. Heart Dis.* **2008**, *21*, 146–150. [[CrossRef](#)]
17. Willruth, A.M.; Geipel, A.K.; Fimmers, R.; Gembruch, U.G. Assessment of Right Ventricular Global and Regional Longitudinal Peak Systolic Strain, Strain Rate and Velocity in Healthy Fetuses and Impact of Gestational Age Using a Novel Speckle / Feature-Tracking Based Algorithm. *Ultrasound Obs. Gynecol* **2011**, *37*, 143–149. [[CrossRef](#)]
18. Ishii, T.; McElhinney, D.B.; Harrild, D.M.; Marcus, E.N.; Sahn, D.J.; Truong, U.; Tworetzky, W.T. Circumferential and Longitudinal Ventricular Strain in the Normal Human Fetus. *J. Am. Soc. Echocardiogr.* **2012**, *25*, 105–111. [[CrossRef](#)]
19. Germanakis, I. Assessment of Fetal Myocardial Deformation Using Speckle Tracking Techniques. *Fetal Diagn. Ther.* **2012**, *32*, 39–46. [[CrossRef](#)]
20. Devore, G.R.; Polanco, B.; Satou, G.; Sklansky, M. Two-Dimensional Speckle Tracking of the Fetal Heart. *J. Ultrasound Med.* **2016**, *35*, 1765–1781. [[CrossRef](#)]
21. Day, T.G.; Charakida, M.; Simpson, J.M. Using Speckle-Tracking Echocardiography to Assess Fetal Myocardial Deformation: Are We There Yet? *Ultrasound Obstet. Gynecol.* **2019**, *54*, 575–581. [[CrossRef](#)] [[PubMed](#)]
22. van Oostrum, N.H.; de Vet, C.M.; van der Woude, D.A.; Kempes, H.M.; Oei, S.G.; van Laar, J.O. Fetal Strain and Strain Rate during Pregnancy Measured with Speckle Tracking Echocardiography: A Systematic Review. *Eur. J. Obstet. Gynecol.* **2020**, *250*, 178–187. [[CrossRef](#)]
23. Semmler, J.; Day, T.; Georgiopoulos, G.; Garcia-Gonzalez, C.; Aguilera, J.; Vigneswaran, T.; Zidere, V.; Miller, O.I.; Sharland, G.; Charakida, M.; et al. Fetal Speckle-Tracking: Impact of Angle of Insonation and Frame Rate on Global Longitudinal Strain. *J. Am. Soc. Echocardiogr.* **2020**, *33*, 1141–1146.e2. [[CrossRef](#)] [[PubMed](#)]
24. Voigt, J.-U.; Pedrizzetti, G.; Lysyansky, P.; Marwick, T.H.; Houle, H.; Baumann, R.; Pedri, S.; Ito, Y.; Abe, Y.; Metz, S.; et al. Definitions for a common standard for 2D speckle tracking echocardiography: Consensus document of the EACVI/ASE/Industry Task Force to standardize deformation imaging. *Eur. Heart J.-Cardiovasc. Imaging* **2014**, *16*, 1–11. [[CrossRef](#)] [[PubMed](#)]
25. Moen, C.A.; Salminen, P.-R.; Dahle, G.O.; Hjertaas, J.J.; Grong, K.; Matre, K. Is strain by Speckle Tracking Echocardiography dependent on user controlled spatial and temporal smoothing? An experimental porcine study. *Cardiovasc. Ultrasound* **2013**, *11*, 32. [[CrossRef](#)] [[PubMed](#)]
26. Devore, G.R.; Klas, B.; Satou, G.; Sklansky, M. Twenty-Four Segment Transverse Ventricular Fractional Shortening: A new technique to evaluate fetal cardiac function. *J. Ultrasound Med.* **2018**, *37*, 1129–1141. [[CrossRef](#)] [[PubMed](#)]
27. Devore, G.R.; Klas, B.; Satou, G.; Sklansky, M. 24-Segment Sphericity Index: A New Technique to Evaluate Fetal Cardiac Diastolic Shape. *Ultrasound Obstet. Gynecol.* **2018**, *51*, 650–658. [[CrossRef](#)]
28. Devore, G.R.; Klas, B.; Satou, G.; Sklansky, M. Evaluation of Fetal Left Ventricular Size and Function Using Speckle-Tracking and the Simpson Rule. *J. Ultrasound Med.* **2018**, *38*, 1209–1221. [[CrossRef](#)]
29. Devore, G.R.; Klas, B.; Satou, G.; Sklansky, M. Speckle Tracking of the Basal Lateral and Septal Wall Annular Plane Systolic Excursion of the Right and Left Ventricles of the Fetal Heart. *J. Ultrasound Med.* **2019**, *38*, 1309–1318. [[CrossRef](#)]

30. Devore, G.R.; Klas, B.; Satou, G.; Sklansky, M. Quantitative Evaluation of Fetal Right and Left Ventricular Fractional Area Change Using Speckle-Tracking Technology. *Ultrasound Obs. Gynecol.* **2019**, *53*, 219–228. [[CrossRef](#)]
31. Devore, G.R.; Klas, B.; Satou, G.; Sklansky, M. Longitudinal Annular Systolic Displacement Compared to Global Strain in Normal Fetal Hearts and Those With Cardiac Abnormalities. *J. Ultrasound Med.* **2018**, *37*, 1156–1171. [[CrossRef](#)] [[PubMed](#)]
32. Devore, G.R.; Cuneo, B.; Klas, B.; Satou, G.; Sklansky, M. Comprehensive Evaluation of Fetal Cardiac Ventricular Widths and Ratios Technique. *J. Ultrasound Med.* **2019**, *38*, 1039–1047. [[CrossRef](#)] [[PubMed](#)]
33. Devore, G.R.; Klas, B.; Satou, G.; Sklansky, M. Evaluation of the Right and Left Ventricles: An Integrated Approach Measuring the Area, Length and Width of the Chambers in Normal Fetuses. *Prenat. Diagn.* **2019**, *37*, 1203–1212. [[CrossRef](#)] [[PubMed](#)]
34. Devore, G.R.; Haxel, C.; Satou, G.; Sklansky, M. Improved Detection of Coarctation of the Aorta Using Speckle Tracking Analysis of the Fetal Heart Using the Last Examination Prior to Delivery. *Ultrasound Obs. Gynecol.* **2021**, *57*, 282–291. [[CrossRef](#)]
35. Devore, G.R.; Satou, G.M.; Afshar, Y.; Harake, D.; Sklansky, M. Evaluation of Fetal Cardiac Size and Shape: A New Screening Tool to Identify Fetuses at Risk for Tetralogy of Fallot. *J. Ultrasound Med.* **2021**, *40*, 2537–2548. [[CrossRef](#)]
36. Devore, G.R.; Gumina, D.L.; Hobbins, J.C. Assessment of ventricular contractility in fetuses with an estimated fetal weight less than the tenth centile. *Am. J. Obstet. Gynecol.* **2019**, *221*, 498.e1–498.e22. [[CrossRef](#)]
37. Georgiopoulos, G.; Nicolaidis, K.H.; Charakida, M.; Sciences, I. Impact of Gestational Diabetes Mellitus on Fetal Cardiac Morphology and Function: Cohort Comparison of Second- and Third-Trimester Fetuses. *Ultrasound Obstet. Gynecol.* **2021**, *57*, 607–613. [[CrossRef](#)]
38. Harbison, A.L.; Chmait, R.H.; Pruetz, J.D.; Ma, S.; Sklansky, M.S.; Devore, G.R. Evaluation of Cardiac Function in the Recipient Twin in Successfully Treated Twin-to-Twin Transfusion Syndrome Using a Novel Fetal Speckle-Tracking Analysis. *Prenat. Diagn.* **2021**, *41*, 136–144. [[CrossRef](#)]
39. Bennasar, M.; Martínez, J.M.; Gómez, O.; Bartrons, J.; Olivella, A.; Puerto, B.; Gratacós, E. Accuracy of Four-Dimensional Spatiotemporal Image Correlation Echocardiography in the Prenatal Diagnosis of Congenital Heart Defects. *Ultrasound Obstet. Gynecol.* **2010**, *36*, 458–464. [[CrossRef](#)]
40. Figueras, F.; Meler, E.; Iraola, A.; Eixarch, E.; Coll, O.; Figueras, J. Customized Birthweight Standards for a Spanish Population. *Eur. J. Obs. Gynecol. Reprod. Biol.* **2008**, *136*, 20–24. [[CrossRef](#)]
41. Carvalho, J.S.; Allan, L.D.; Chaoui, R.; Copel, J.A.; DeVore, G.R.; Hecher, K.; Lee, W.; Munoz, H.; Paladini, D.; Tutschek, B.; et al. ISUOG Practice Guidelines (Updated): Sonographic Screening Examination of the Fetal Heart. *Ultrasound Obstet. Gynecol.* **2013**, *41*, 348–359. [[CrossRef](#)] [[PubMed](#)]
42. Salomon, L.J.; Alfirevic, Z.; Berghella, V.; Bilardo, C.; Hernandez-Andrade, E.; Johnsen, S.L.; Kalache, K.; Leung, K.-Y.; Malinger, G.; Munoz, H.; et al. Practice Guidelines for Performance of the Routine Mid-Trimester Fetal Ultrasound Scan. *Ultrasound Obstet. Gynecol.* **2011**, *37*, 116–126. [[CrossRef](#)] [[PubMed](#)]
43. Hadlock, F.P.; Harrist, R.B.; Shah, Y.P.; King, D.E.; Park, S.K.; Sharman, R.S. Estimating Fetal Age Using Multiple Parameters: A Prospective Evaluation in a Racially Mixed Population. *Am. J. Obstet. Gynecol.* **1987**, *156*, 955–957. [[CrossRef](#)]
44. Guirado, L.; Crispi, F.; Soveral, I.; Valenzuela-alcaraz, B.; Rodriguez-López, M.; García-Otero, L.; Torres, X.; Sepúlveda-Martínez, Á.; Escobar-Díaz, M.C.; Martínez, J.M.; et al. Nomograms of Fetal Right Ventricular Fractional Area Change by 2D Echocardiography. *Fetal Diagn. Ther.* **2020**, *47*, 399–410. [[CrossRef](#)]
45. Lang, R.M.; Badano, L.P.; Mor-avi, V.; Afilalo, J.; Armstrong, A.; Ernande, L.; Flachskampf, F.A.; Foster, E.; Goldstein, S.A.; Kuznetsova, T.; et al. Recommendations for Cardiac Chamber Quantification by Echocardiography in Adults: An Update from the American Society of Echocardiography and the European Association of Cardiovascular Imaging. *Eur. Heart J.-Cardiovasc. Imaging* **2015**, *16*, 233–271. [[CrossRef](#)]
46. Devore, G.R.; Satou, G.; Sklansky, M. Using Speckle-Tracking Echocardiography to Assess Fetal Myocardial Deformation: Are We There yet? Yes We Are! *Ultrasound Obs. Gynecol.* **2019**, *54*, 703–704. [[CrossRef](#)]
47. Devore, G.R.; Satou, G.; Sklansky, M. Comparing the Non-Quiver and Quiver Techniques for Identification of the Endocardial Borders Used for Speckle-Tracking Analysis of the Ventricles of the Fetal Heart. *J. Ultrasound Med.* **2020**, *40*, 1955–1961. [[CrossRef](#)]
48. Watson, P.F.; Petrie, A. Method Agreement Analysis: A Review of Correct Methodology. *Theriogenology* **2010**, *73*, 1167–1179. [[CrossRef](#)]
49. Crispi, F.; Sepulveda-swatson, E.; Cruz-lemini, M. Original Paper: Techniques Feasibility and Reproducibility of a Standard Protocol for 2D Speckle Tracking and Tissue Doppler-Based Strain and Strain Rate Analysis of the Fetal Heart. *Fetal Diagn. Ther.* **2012**, *32*, 96–108. [[CrossRef](#)]
50. Enzensberger, C.; Achterberg, F.; Degenhardt, J.; Wolter, A.; Graupner, O.; Herrmann, J.; Axt-fliedner, R. Feasibility and Reproducibility of Two-Dimensional Wall Motion Tracking (WMT) in Fetal Echocardiography Study Population. *Ultrasound Int. Open* **2017**, *3*, 26–33.
51. Younoszai, A.K.; Saudek, D.E.; Emery, S.P.; Thomas, J.D. Evaluation of Myocardial Mechanics in the Fetus by Velocity Vector Imaging. *J. Am. Soc. Echocardiogr.* **2008**, *21*, 470–474. [[CrossRef](#)] [[PubMed](#)]
52. Belghiti, H.; Brette, S.; Lafitte, S.; Reant, P.; Picard, F.; Serri, K.; Lafitte, M.; Courregelongue, M.; Dos Santos, P.; Douard, H.; et al. Automated Function Imaging: A New Operator-Independent Strain Method for Assessing Left Ventricular Function Imagerie Paramétrique Fonctionnelle Automatique. *Arch. Cardiovasc. Dis.* **2008**, *101*, 163–169. [[CrossRef](#)]

53. Barker, P.C.A.; Houle, H.; Li, J.S.; Miller, S.; Herlong, J.R.; Camitta, M.G.W. Global Longitudinal Cardiac Strain and Strain Rate for Assessment of Fetal Cardiac Function: Novel Experience with Velocity Vector Imaging. *Echocardiography* **2009**, *26*, 28–36. [[CrossRef](#)] [[PubMed](#)]
54. Maskatia, S.A.; Pignatelli, R.H.; Ayres, N.A.; Altman, C.A.; Sangi-haghpeykar, H.; Lee, W. Longitudinal Changes and Interobserver Variability of Systolic Myocardial Deformation Values in a Prospective Cohort of Healthy Fetuses across Gestation and after Delivery. *J. Am. Soc. Echocardiogr.* **2016**, *29*, 341–349. [[CrossRef](#)]
55. Huntley, E.S.; Hernandez-Andrade, E.; Soto, E.; Devore, G.; Sibai, B.M. Novel Speckle Tracking Analysis Showed Excellent Reproducibility for Size and Shape of the Fetal Heart and Good Reproducibility for Strain and Fractional Shortening. *Fetal Diagn. Ther.* **2021**, *48*, 541–550. [[CrossRef](#)]
56. Hata, T.; Koyanagi, A.; Yamanishi, T.; Bouno, S.; Takayoshi, R. A 24-Segment Fractional Shortening of the Fetal Heart Using Fetal HQ. *J. Perinat. Med.* **2021**, *49*, 371–376. [[CrossRef](#)]
57. Hata, T.; Koyanagi, A.; Yamanishi, T.; Bouno, S.; Ahmed, M.; Aboellail, M.; Miyake, T. Evaluation of 24-Segment Sphericity Index of Fetal Heart Using Fetal HQ. *J. Matern. Neonatal Med.* **2020**, 1–7. [[CrossRef](#)]
58. Luo, Y.; Xiao, F.; Long, C.; Kuang, H.; Jiang, M. Evaluation of the Sphericity Index of the Fetal Heart during Middle and Late Pregnancy Using FetalHQ. *J. Matern. Neonatal Med.* **2021**, 1–6. [[CrossRef](#)]
59. Dodaro, M.G.; Montaguti, E.; Balducci, A.; Perolo, A.; Angeli, E.; Lenzi, J.; Lombardo, L.; Donti, A.; Pilu, G.; Gaia, M.; et al. Fetal Speckle-Tracking Echocardiography: A Comparison between Two-Dimensional and Electronic Spatio-Temporal Image Correlation (e-STIC) Technique Two-Dimensional and Electronic Spatio-Temporal Image Correlation. *J. Matern. Neonatal Med.* **2021**, 1–7. [[CrossRef](#)]

Table S1. Intraobserver reproducibility of the fetal heart 4D-Spatio Temporal Image Correlation (4D-STIC) speckle tracking analysis results using Quiver technique.

| Variable | ICC | 95% confidence interval | <i>p</i> -value | ICC | 95% confidence interval | <i>p</i> -value |
|---|----------------|-------------------------|-----------------|-----------------|-------------------------|-----------------|
| FETAL CARDIAC MORPHOMETRY | | | | | | |
| | Left Ventricle | | | Right Ventricle | | |
| Ventricular Area | 0.854 | 0.406 to 0.964 | 0.005 | 0.878 | 0.533 to 0.969 | 0.002 |
| Longitudinal diameter | 0.906 | 0.634 to 0.977 | 0.001 | 0.926 | 0.718 to 0.981 | <0.001 |
| Basal diameter (segment 1) | 0.798 | 0.190 to 0.950 | 0.005 | 0.910 | 0.447 to 0.980 | <0.001 |
| Mid-ventricular diameter (segment 9) | 0.681 | -0.436 to 0.923 | 0.063 | 0.887 | 0.571 to 0.972 | 0.001 |
| Apical diameter (segment 17) | 0.549 | -1.136 to 0.902 | 0.157 | 0.851 | 0.375 to 0.963 | 0.006 |
| Basal sphericity index (segment 1) | 0.244 | -0.524 to 0.750 | 0.258 | 0.661 | -0.128 to 0.911 | 0.034 |
| Mid-ventricular sphericity index (segment 9) | 0.616 | -0.725 to 0.907 | 0.098 | 0.738 | 0.072 to 0.933 | 0.018 |
| Apical sphericity index (segment 17) | 0.432 | -1.778 to 0.865 | 0.224 | 0.691 | -0.387 to 0.925 | 0.058 |
| FETAL CARDIAC FUNCTION | | | | | | |
| | Left Ventricle | | | Right Ventricle | | |
| Global longitudinal strain | 0.983 | 0.936 to 0.996 | <0.001 | 0.928 | 0.730 to 0.982 | <0.001 |
| Fractional area change | 0.940 | 0.683 to 0.986 | <0.001 | 0.883 | 0.562 to 0.970 | 0.002 |
| Basal shortening fraction (Segment 1) | 0.564 | -0.239 to 0.886 | 0.018 | 0.726 | -0.118 to 0.933 | 0.008 |
| Mid-ventricular shortening fraction (Segment 9) | 0.830 | 0.297 to 0.958 | 0.009 | 0.877 | 0.537 to 0.969 | 0.002 |
| Apical shortening fraction (Segment 17) | 0.687 | -0.071 to 0.919 | 0.035 | 0.731 | -0.191 to 0.935 | 0.040 |
| End-diastolic volume | 0.795 | 0.140 to 0.950 | 0.017 | | | |
| End-systolic volume | 0.545 | -1.159 to 0.891 | 0.145 | | | |
| Ejection fraction | 0.920 | 0.569 to 0.980 | <0.001 | | | |

| | | | |
|--|-------|----------------|-------|
| Cardiac Output | 0.898 | 0.585 to 0.977 | 0.002 |
| ICC: Intraclass Correlation Coefficient. | | | |

Table S2. Interobserver reproducibility of the fetal heart 4D-STIC speckle tracking analysis results using Quiver technique.

| Variable | ICC | 95% confidence interval | p-value | ICC | 95% confidence interval | p-value |
|---|-------|-------------------------|---------|-------|-------------------------|---------|
| FETAL CARDIAC MORPHOMETRY | | | | | | |
| | | Left Ventricle | | | Right Ventricle | |
| Ventricular Area | 0.989 | 0.790 to 0.998 | <0.001 | 0.946 | 0.789 to 0.987 | <0.001 |
| Longitudinal diameter | 0.952 | 0.806 to 0.988 | <0.001 | 0.938 | 0.636 to 0.986 | <0.001 |
| Basal diameter (segment 1) | 0.786 | 0.204 to 0.946 | 0.015 | 0.986 | 0.948 to 0.997 | <0.001 |
| Mid-ventricular diameter (segment 9) | 0.959 | 0.836 to 0.990 | <0.001 | 0.837 | 0.312 to 0.960 | 0.008 |
| Apical diameter (segment 17) | 0.825 | 0.267 to 0.957 | 0.010 | 0.886 | 0.566 to 0.971 | 0.001 |
| Basal sphericity index (segment 1) | 0.011 | -1.562 to 0.715 | 0.492 | 0.696 | -0.202 to 0.924 | 0.048 |
| Mid-ventricular sphericity index (segment 9) | 0.507 | -1.371 to 0.882 | 0.171 | 0.578 | -0.912 to 0.898 | 0.121 |
| Apical sphericity index (segment 17) | 0.260 | -2.088 to 0.818 | 0.334 | 0.598 | -0.806 to 0.903 | 0.110 |
| FETAL CARDIAC FUNCTION | | | | | | |
| | | Left Ventricle | | | Right Ventricle | |
| Global longitudinal strain | 0.907 | 0.621 to 0.977 | 0.001 | 0.713 | -0.239 to 0.935 | 0.051 |
| Fractional area change | 0.796 | 0.133 to 0.950 | 0.017 | 0.938 | 0.753 to 0.985 | <0.001 |
| Basal shortening fraction (Segment 1) | 0.119 | -0.275 to 0.608 | 0.309 | 0.491 | -1.451 to 0.878 | 0.182 |
| Mid-ventricular shortening fraction (Segment 9) | 0.308 | -2.401 to 0.836 | 0.309 | 0.629 | -0.690 to 0.910 | 0.091 |
| Apical shortening fraction (Segment 17) | 0.759 | 0.140 to 0.938 | 0.016 | 0.359 | -1.863 to 0.845 | 0.269 |
| End-diastolic volume | 0.986 | 0.930 to 0.997 | <0.001 | | | |

| | | | |
|--|-------|-----------------|--------|
| End-systolic volumen | 0.948 | 0.787 to 0.987 | <0.001 |
| Ejection fraction | 0.668 | -0.501 to 0.920 | 0.070 |
| Cardiac Output | 0.925 | 0.679 to 0.983 | <0.001 |
| ICC: Intraclass Correlation Coefficient. | | | |

Table S3. Comparison of 2D vs 4D-STIC Interobserver reproducibility of the fetal heart speckle tracking analysis results using Quiver technique.

| Variable | ICC | 95% confidence interval | p-value | ICC | 95% confidence interval | p-value |
|--|-------|-------------------------|---------|-------|-------------------------|---------|
| FETAL CARDIAC MORPHOMETRY | | | | | | |
| | | Left Ventricle | | | Right Ventricle | |
| Ventricular Area | 0.930 | 0.728 to 0.982 | <0.001 | 0.964 | 0.864 to 0.991 | <0.001 |
| Longitudinal diameter | 0.946 | 0.779 to 0.987 | <0.001 | 0.965 | 0.806 to 0.955 | <0.001 |
| Basal diameter (segment 1) | 0.802 | 0.264 to 0.950 | 0.011 | 0.949 | 0.805 to 0.987 | <0.001 |
| Mid-ventricular diameter (segment 9) | 0.888 | 0.554 to 0.972 | 0.002 | 0.930 | 0.735 to 0.982 | <0.001 |
| Apical diameter (segment 17) | 0.966 | 0.863 to 0.992 | <0.001 | 0.935 | 0.745 to 0.984 | <0.001 |
| Basal sphericity index (segment 1) | 0.347 | -1.872 to 0.841 | 0.276 | 0.607 | -0.553 to 0.902 | 0.093 |
| Mid-ventricular sphericity index (segment 9) | 0.662 | -0.283 to 0.915 | 0.061 | 0.487 | -1.117 to 0.874 | 0.176 |
| Apical sphericity index (segment 17) | 0.434 | -1.730 to 0.865 | 0.221 | 0.236 | -3.642 to 0.838 | 0.368 |
| FETAL CARDIAC FUNCTION | | | | | | |
| | | Left Ventricle | | | Right Ventricle | |
| LV Global longitudinal strain | 0.763 | 0.149 to 0.939 | 0.017 | 0.959 | 0.837 to 0.990 | <0.001 |
| LV Fractional area change | 0.791 | 0.241 to 0.947 | 0.010 | 0.889 | 0.540 to 0.972 | 0.002 |
| FS Segment 1 (base) | 0.096 | -2.755 to 0.793 | 0.444 | 0.806 | 0.227 to 0.951 | 0.011 |
| FS Segment 9 (mid-ventricular) | 0.662 | -0.511 to 0.918 | 0.072 | 0.445 | -1.662 to 0.867 | 0.213 |
| FS Segment 17 (apex) | 0.564 | -0.415 to 0.885 | 0.093 | 0.551 | -0.581 to 0.885 | 0.115 |

| | | | |
|--|-------|----------------|-------|
| LV End diastolic volume | 0.919 | 0.686 to 0.980 | 0.001 |
| LV End systolic volume | 0.880 | 0.527 to 0.970 | 0.002 |
| Ejection fraction | 0.844 | 0.408 to 0.961 | 0.005 |
| Cardiac Output | 0.869 | 0.419 to 0.970 | 0.006 |
| ICC: Intraclass Correlation Coefficient. | | | |

Table S4. Intraobserver reproducibility of the fetal heart speckle tracking segmental analysis results using 4D-STIC

| Variable | ICC | 95% confidence interval | ICC | 95% confidence interval |
|----------------------------------|----------------|-------------------------|-----------------|-------------------------|
| FETAL CARDIAC MORPHOMETRY | | | | |
| End-diastolic diameter | | | | |
| | Left ventricle | | Right ventricle | |
| Segment 1 | 0.853 | 0.696 to 0.929 | 0.855 | 0.702 to 0.930 |
| Segment 2 | 0.888 | 0.770 to 0.946 | 0.884 | 0.760 to 0.944 |
| Segment 3 | 0.916 | 0.825 to 0.959 | 0.906 | 0.804 to 0.955 |
| Segment 4 | 0.923 | 0.839 to 0.963 | 0.920 | 0.833 to 0.961 |
| Segment 5 | 0.920 | 0.833 to 0.961 | 0.930 | 0.854 to 0.966 |
| Segment 6 | 0.917 | 0.828 to 0.960 | 0.938 | 0.871 to 0.970 |
| Segment 7 | 0.916 | 0.827 to 0.960 | 0.945 | 0.885 to 0.973 |
| Segment 8 | 0.917 | 0.828 to 0.96 | 0.949 | 0.894 to 0.975 |
| Segment 9 | 0.924 | 0.841 to 0.964 | 0.936 | 0.867 to 0.969 |
| Segment 10 | 0.920 | 0.835 to 0.961 | 0.954 | 0.904 to 0.978 |
| Segment 11 | 0.922 | 0.839 to 0.962 | 0.955 | 0.907 to 0.979 |
| Segment 12 | 0.922 | 0.838 to 0.962 | 0.955 | 0.907 to 0.978 |
| Segment 13 | 0.919 | 0.832 to 0.961 | 0.954 | 0.905 to 0.978 |
| Segment 14 | 0.915 | 0.824 to 0.959 | 0.953 | 0.903 to 0.977 |
| Segment 15 | 0.911 | 0.816 to 0.957 | 0.952 | 0.900 to 0.977 |
| Segment 16 | 0.909 | 0.812 to 0.956 | 0.948 | 0.892 to 0.975 |
| Segment 17 | 0.912 | 0.818 to 0.958 | 0.943 | 0.881 to 0.972 |
| Segment 18 | 0.923 | 0.839 to 0.963 | 0.938 | 0.871 to 0.970 |
| Segment 19 | 0.933 | 0.861 to 0.968 | 0.934 | 0.862 to 0.968 |
| Segment 20 | 0.938 | 0.872 to 0.970 | 0.929 | 0.852 to 0.966 |
| Segment 21 | 0.937 | 0.870 to 0.970 | 0.924 | 0.841 to 0.963 |
| Segment 22 | 0.933 | 0.862 to 0.968 | 0.919 | 0.832 to 0.961 |
| Segment 23 | 0.930 | 0.856 to 0.966 | 0.915 | 0.824 to 0.959 |
| Segment 24 | 0.929 | 0.853 to 0.966 | 0.912 | 0.818 to 0.958 |
| Sphericity index | | | | |
| | Left ventricle | | Right ventricle | |

| | | | | |
|------------|-------|-----------------|-------|-----------------|
| Segment 1 | 0.440 | -0.201 to 0.736 | 0.526 | -0.042 to 0.872 |
| Segment 2 | 0.494 | -0.015 to 0.752 | 0.344 | -0.368 to 0.685 |
| Segment 3 | 0.565 | 0.114 to 0.789 | 0.457 | -0.122 to 0.738 |
| Segment 4 | 0.582 | 0.134 to 0.798 | 0.558 | 0.093 to 0.786 |
| Segment 5 | 0.575 | 0.110 to 0.796 | 0.624 | 0.231 to 0.817 |
| Segment 6 | 0.571 | 0.099 to 0.795 | 0.666 | 0.318 to 0.838 |
| Segment 7 | 0.591 | 0.141 to 0.804 | 0.694 | 0.375 to 0.851 |
| Segment 8 | 0.610 | 0.181 to 0.813 | 0.701 | 0.389 to 0.855 |
| Segment 9 | 0.702 | 0.392 to 0.855 | 0.665 | 0.298 to 0.840 |
| Segment 10 | 0.664 | 0.296 to 0.839 | 0.705 | 0.396 to 0.857 |
| Segment 11 | 0.694 | 0.359 to 0.853 | 0.702 | 0.388 to 0.855 |
| Segment 12 | 0.710 | 0.392 to 0.861 | 0.693 | 0.370 to 0.851 |
| Segment 13 | 0.729 | 0.435 to 0.870 | 0.684 | 0.350 to 0.847 |
| Segment 14 | 0.750 | 0.480 to 0.880 | 0.676 | 0.333 to 0.843 |
| Segment 15 | 0.77 | 0.522 to 0.889 | 0.659 | 0.298 to 0.835 |
| Segment 16 | 0.779 | 0.541 to 0.893 | 0.641 | 0.24 to 0.827 |
| Segment 17 | 0.787 | 0.561 to 0.897 | 0.609 | 0.192 to 0.812 |
| Segment 18 | 0.798 | 0.584 to 0.902 | 0.575 | 0.118 to 0.795 |
| Segment 19 | 0.903 | 0.597 to 0.905 | 0.537 | 0.036 to 0.777 |
| Segment 20 | 0.799 | 0.589 to 0.903 | 0.499 | -0.048 to 0.760 |
| Segment 21 | 0.793 | 0.576 to 0.900 | 0.466 | -0.122 to 0.744 |
| Segment 22 | 0.789 | 0.566 to 0.897 | 0.448 | -0.163 to 0.736 |
| Segment 23 | 0.784 | 0.558 to 0.895 | 0.437 | -0.187 to 0.731 |
| Segment 24 | 0.782 | 0.552 to 0.894 | 0.432 | -0.199 to 0.894 |

FETAL CARDIAC FUNCTION

| Shortening fraction | | | | |
|---------------------|----------------|-----------------|-----------------|----------------|
| | Left ventricle | | Right ventricle | |
| Segment 1 | 0.302 | -0.561 to 0.684 | 0.775 | 0.526 to 0.894 |
| Segment 2 | 0.502 | -0.049 to 0.764 | 0.681 | 0.351 to 0.844 |
| Segment 3 | 0.569 | 0.084 to 0.796 | 0.684 | 0.358 to 0.846 |
| Segment 4 | 0.633 | 0.218 to 0.826 | 0.667 | 0.322 to 0.838 |
| Segment 5 | 0.655 | 0.279 to 0.834 | 0.638 | 0.260 to 0.824 |
| Segment 6 | 0.700 | 0.375 to 0.856 | 0.621 | 0.221 to 0.816 |
| Segment 7 | 0.729 | 0.436 to 0.870 | 0.635 | 0.247 to 0.823 |
| Segment 8 | 0.741 | 0.460 to 0.876 | 0.669 | 0.317 to 0.84 |
| Segment 9 | 0.748 | 0.472 to 0.879 | 0.801 | 0.579 to 0.906 |
| Segment 10 | 0.760 | 0.499 to 0.885 | 0.817 | 0.613 to 0.913 |
| Segment 11 | 0.777 | 0.535 to 0.892 | 0.809 | 0.598 to 0.909 |
| Segment 12 | 0.790 | 0.566 to 0.899 | 0.776 | 0.530 to 0.893 |
| Segment 13 | 0.801 | 0.589 to 0.904 | 0.729 | 0.432 to 0.871 |

| | | | | |
|------------|-------|----------------|-------|----------------|
| Segment 14 | 0,809 | 0,607 to 0,908 | 0,683 | 0,334 to 0,849 |
| Segment 15 | 0,814 | 0,618 to 0,910 | 0,647 | 0,254 to 0,833 |
| Segment 16 | 0,813 | 0,616 to 0,909 | 0,624 | 0,201 to 0,822 |
| Segment 17 | 0,805 | 0,599 to 0,906 | 0,619 | 0,188 to 0,820 |
| Segment 18 | 0,794 | 0,575 to 0,900 | 0,634 | 0,221 to 0,827 |
| Segment 19 | 0,782 | 0,551 to 0,895 | 0,654 | 0,264 to 0,837 |
| Segment 20 | 0,772 | 0,530 to 0,890 | 0,666 | 0,288 to 0,842 |
| Segment 21 | 0,765 | 0,515 to 0,887 | 0,665 | 0,288 to 0,842 |
| Segment 22 | 0,760 | 0,504 to 0,884 | 0,612 | 0,161 to 0,819 |
| Segment 23 | 0,756 | 0,496 to 0,882 | 0,607 | 0,152 to 0,817 |
| Segment 24 | 0,754 | 0,492 to 0,881 | 0,604 | 0,146 to 0,815 |

ICC: Intraclass Correlation Coefficient.

Table S5. Interobserver reproducibility of the fetal heart speckle tracking segmental analysis results using 4D-STIC.

| Variable | ICC | 95% confidence interval | ICC | 95% confidence interval |
|----------------------------------|----------------|-------------------------|-----------------|-------------------------|
| FETAL CARDIAC MORPHOMETRY | | | | |
| End-diastolic diameter | | | | |
| | Left ventricle | | Right ventricle | |
| Segment 1 | 0.746 | 0.464 to 0.881 | 0.891 | 0.751 to 0.950 |
| Segment 2 | 0.836 | 0.659 to 0.921 | 0.914 | 0.802 to 0.961 |
| Segment 3 | 0.856 | 0.698 to 0.931 | 0.926 | 0.828 to 0.966 |
| Segment 4 | 0.860 | 0.707 to 0.932 | 0.933 | 0.847 to 0.969 |
| Segment 5 | 0.854 | 0.698 to 0.929 | 0.937 | 0.860 to 0.970 |
| Segment 6 | 0.847 | 0.686 to 0.926 | 0.937 | 0.865 to 0.970 |
| Segment 7 | 0.842 | 0.676 to 0.923 | 0.933 | 0.860 to 0.968 |
| Segment 8 | 0.841 | 0.671 to 0.923 | 0.927 | 0.848 to 0.965 |
| Segment 9 | 0.841 | 0.666 to 0.924 | 0.921 | 0.835 to 0.962 |
| Segment 10 | 0.852 | 0.693 to 0.928 | 0.920 | 0.836 to 0.961 |
| Segment 11 | 0.861 | 0.713 to 0.933 | 0.923 | 0.842 to 0.963 |
| Segment 12 | 0.869 | 0.729 to 0.937 | 0.926 | 0.846 to 0.964 |
| Segment 13 | 0.870 | 0.733 to 0.937 | 0.925 | 0.844 to 0.964 |
| Segment 14 | 0.866 | 0.723 to 0.935 | 0.922 | 0.837 to 0.962 |
| Segment 15 | 0.858 | 0.707 to 0.931 | 0.914 | 0.822 to 0.959 |
| Segment 16 | 0.850 | 0.691 to 0.927 | 0.902 | 0.796 to 0.953 |
| Segment 17 | 0.884 | 0.675 to 0.925 | 0.882 | 0.745 to 0.994 |
| Segment 18 | 0.841 | 0.674 to 0.923 | 0.866 | 0.725 to 0.935 |

| | | | | |
|------------|-------|----------------|-------|----------------|
| Segment 19 | 0,829 | 0,648 to 0,917 | 0,845 | 0,681 to 0,925 |
| Segment 20 | 0,804 | 0,598 to 0,905 | 0,822 | 0,634 to 0,914 |
| Segment 21 | 0,776 | 0,538 to 0,892 | 0,799 | 0,588 to 0,902 |
| Segment 22 | 0,754 | 0,492 to 0,881 | 0,781 | 0,551 to 0,894 |
| Segment 23 | 0,739 | 0,461 to 0,874 | 0,769 | 0,527 to 0,888 |
| Segment 24 | 0,730 | 0,443 to 0,87 | 0,762 | 0,513 to 0,884 |

Sphericity index

| | Left ventricle | | Right ventricle | |
|------------|----------------|-----------------|-----------------|-----------------|
| Segment 1 | 0.390 | -0.161 to 0.694 | 0.333 | -0.227 to 0.659 |
| Segment 2 | 0,548 | 0,097 to 0,778 | 0,560 | 0,103 to 0,786 |
| Segment 3 | 0,605 | 0,178 to 0,81 | 0,624 | 0,207 to 0,821 |
| Segment 4 | 0,630 | 0,217 to 0,823 | 0,675 | 0,295 to 0,847 |
| Segment 5 | 0,625 | 0,218 to 0,82 | 0,706 | 0,355 to 0,862 |
| Segment 6 | 0,609 | 0,201 to 0,81 | 0,717 | 0,385 to 0,867 |
| Segment 7 | 0,586 | 0,169 to 0,797 | 0,709 | 0,379 to 0,862 |
| Segment 8 | 0,575 | 0,150 to 0,791 | 0,691 | 0,353 to 0,851 |
| Segment 9 | 0,495 | -0,110 to 0,754 | 0,683 | 0,329 to 0,850 |
| Segment 10 | 0,604 | 0,204 to 0,806 | 0,648 | 0,286 to 0,829 |
| Segment 11 | 0,628 | 0,249 to 0,818 | 0,635 | 0,263 to 0,822 |
| Segment 12 | 0,652 | 0,295 to 0,830 | 0,617 | 0,229 to 0,813 |
| Segment 13 | 0,666 | 0,322 to 0,837 | 0,604 | 0,201 to 0,806 |
| Segment 14 | 0,668 | 0,326 to 0,838 | 0,602 | 0,194 to 0,806 |
| Segment 15 | 0,656 | 0,303 to 0,832 | 0,602 | 0,189 to 0,807 |
| Segment 16 | 0,630 | 0,254 to 0,819 | 0,596 | 0,169 to 0,805 |
| Segment 17 | 0,445 | -0,101 to 0,728 | 0,628 | 0,212 to 0,823 |
| Segment 18 | 0,495 | -0,006 to 0,751 | 0,552 | 0,059 to 0,785 |
| Segment 19 | 0,345 | -0,296 to 0,677 | 0,533 | 0,016 to 0,777 |
| Segment 20 | 0,134 | -0,719 to 0,573 | 0,514 | -0,024 to 0,768 |
| Segment 21 | 0,28 | -0,507 to 0,657 | 0,502 | -0,044 to 0,761 |
| Segment 22 | 0,148 | -0,800 to 0,596 | 0,494 | -0,056 to 0,757 |
| Segment 23 | 0,280 | -1,548 to 0,374 | 0,491 | -0,060 to 0,755 |
| Segment 24 | 0,008 | -1,118 to 0,531 | 0,488 | -0,063 to 0,753 |

FETAL CARDIAC FUNCTION

Shortening fraction

| | Left ventricle | | Right ventricle | |
|-----------|----------------|-----------------|-----------------|-----------------|
| Segment 1 | 0,116 | -0,951 to 0,595 | 0,506 | -0,055 to 0,772 |
| Segment 2 | 0,261 | -0,595 to 0,646 | 0,661 | 0,287 to 0,841 |
| Segment 3 | 0,299 | -0,502 to 0,669 | 0,666 | 0,268 to 0,843 |
| Segment 4 | 0,388 | -0,312 to 0,712 | 0,761 | 0,421 to 0,893 |
| Segment 5 | 0,486 | -0,100 to 0,757 | 0,796 | 0,526 to 0,907 |

| | | | | |
|------------|-------|----------------|-------|-----------------|
| Segment 6 | 0,648 | 0,265 to 0,831 | 0,782 | 0,541 to 0,895 |
| Segment 7 | 0,692 | 0,359 to 0,852 | 0,740 | 0,469 to 0,874 |
| Segment 8 | 0,720 | 0,420 to 0,865 | 0,694 | 0,369 to 0,852 |
| Segment 9 | 0,742 | 0,466 to 0,875 | 0,666 | 0,303 to 0,839 |
| Segment 10 | 0,768 | 0,520 to 0,888 | 0,669 | 0,305 to 0,841 |
| Segment 11 | 0,794 | 0,573 to 0,901 | 0,695 | 0,36 to 0,853 |
| Segment 12 | 0,813 | 0,611 to 0,910 | 0,725 | 0,429 to 0,868 |
| Segment 13 | 0,823 | 0,632 to 0,914 | 0,746 | 0,476 to 0,877 |
| Segment 14 | 0,825 | 0,637 to 0,915 | 0,755 | 0,496 to 0,882 |
| Segment 15 | 0,820 | 0,629 to 0,913 | 0,757 | 0,501 to 0,882 |
| Segment 16 | 0,806 | 0,602 to 0,906 | 0,754 | 0,494 to 0,881 |
| Segment 17 | 0,782 | 0,544 to 0,894 | 0,745 | 0,476 to 0,876 |
| Segment 18 | 0,748 | 0,485 to 0,878 | 0,732 | 0,453 to 0,870 |
| Segment 19 | 0,703 | 0,394 to 0,855 | 0,605 | 0,151 to 0,816 |
| Segment 20 | 0,648 | 0,288 to 0,828 | 0,557 | 0,058 to 0,793 |
| Segment 21 | 0,594 | 0,184 to 0,801 | 0,693 | 0,331 to 0,859 |
| Segment 22 | 0,552 | 0,104 to 0,766 | 0,670 | 0,286 to 0,849 |
| Segment 23 | 0,524 | 0,050 to 0,766 | 0,479 | -0,082 to 0,754 |
| Segment 24 | 0,508 | 0,020 to 0,758 | 0,649 | 0,244 to 0,839 |

ICC: Intraclass Correlation Coefficient.

Table S6. Comparison of Interobserver reproducibility of the fetal heart speckle tracking segmental analysis results using 2D vs 4D-STIC.

| Variable | ICC | 95% confidence interval | ICC | 95% confidence interval |
|----------------------------------|----------------|-------------------------|-----------------|-------------------------|
| FETAL CARDIAC MORPHOMETRY | | | | |
| End-diastolic diameter | | | | |
| | Left ventricle | | Right ventricle | |
| Segment 1 | 0,833 | 0,529 to 0,930 | 0,912 | 0,803 to 0,959 |
| Segment 2 | 0,849 | 0,540 to 0,939 | 0,917 | 0,793 to 0,963 |
| Segment 3 | 0,857 | 0,510 to 0,944 | 0,919 | 0,785 to 0,965 |
| Segment 4 | 0,856 | 0,498 to 0,945 | 0,915 | 0,775 to 0,963 |
| Segment 5 | 0,855 | 0,494 to 0,944 | 0,909 | 0,768 to 0,960 |
| Segment 6 | 0,855 | 0,492 to 0,944 | 0,905 | 0,767 to 0,957 |
| Segment 7 | 0,856 | 0,485 to 0,945 | 0,902 | 0,771 to 0,955 |
| Segment 8 | 0,858 | 0,479 to 0,946 | 0,899 | 0,775 to 0,953 |
| Segment 9 | 0,858 | 0,461 to 0,947 | 0,825 | 0,638 to 0,915 |
| Segment 10 | 0,860 | 0,425 to 0,949 | 0,888 | 0,768 to 0,946 |

| | | | | |
|------------|-------|----------------|-------|----------------|
| Segment 11 | 0,863 | 0,381 to 0,952 | 0,881 | 0,755 to 0,942 |
| Segment 12 | 0,864 | 0,356 to 0,953 | 0,873 | 0,739 to 0,939 |
| Segment 13 | 0,861 | 0,370 to 0,951 | 0,868 | 0,729 to 0,936 |
| Segment 14 | 0,858 | 0,423 to 0,948 | 0,868 | 0,729 to 0,936 |
| Segment 15 | 0,857 | 0,495 to 0,945 | 0,871 | 0,734 to 0,937 |
| Segment 16 | 0,861 | 0,578 to 0,944 | 0,872 | 0,737 to 0,938 |
| Segment 17 | 0,871 | 0,661 to 0,944 | 0,871 | 0,753 to 0,938 |
| Segment 18 | 0,885 | 0,736 to 0,947 | 0,866 | 0,725 to 0,935 |
| Segment 19 | 0,893 | 0,776 to 0,948 | 0,855 | 0,701 to 0,930 |
| Segment 20 | 0,889 | 0,772 to 0,946 | 0,838 | 0,662 to 0,922 |
| Segment 21 | 0,879 | 0,748 to 0,942 | 0,818 | 0,621 to 0,913 |
| Segment 22 | 0,867 | 0,723 to 0,936 | 0,803 | 0,589 to 0,905 |
| Segment 23 | 0,859 | 0,706 to 0,932 | 0,793 | 0,568 to 0,901 |
| Segment 24 | 0,853 | 0,695 to 0,930 | 0,787 | 0,556 to 0,898 |

Sphericity index

| | Left ventricle | | Right ventricle | |
|------------|----------------|-----------------|-----------------|-----------------|
| Segment 1 | 0,222 | -0,401 to 0,601 | 0,637 | 0,226 to 0,823 |
| Segment 2 | 0,222 | -0,376 to 0,591 | 0,689 | 0,368 to 0,849 |
| Segment 3 | 0,264 | -0,301 to 0,612 | 0,723 | 0,432 to 0,866 |
| Segment 4 | 0,305 | -0,240 to 0,636 | 0,736 | 0,459 to 0,872 |
| Segment 5 | 0,340 | -0,192 to 0,658 | 0,748 | 0,483 to 0,878 |
| Segment 6 | 0,375 | -0,151 to 0,680 | 0,752 | 0,493 to 0,880 |
| Segment 7 | 0,401 | -0,124 to 0,696 | 0,756 | 0,500 to 0,881 |
| Segment 8 | 0,416 | -0,109 to 0,706 | 0,752 | 0,492 to 0,879 |
| Segment 9 | 0,463 | -0,062 to 0,737 | 0,738 | 0,457 to 0,873 |
| Segment 10 | 0,441 | -0,090 to 0,723 | 0,715 | 0,408 to 0,862 |
| Segment 11 | 0,458 | -0,081 to 0,735 | 0,689 | 0,352 to 0,851 |
| Segment 12 | 0,474 | -0,071 to 0,746 | 0,674 | 0,317 to 0,843 |
| Segment 13 | 0,490 | -0,049 to 0,755 | 0,676 | 0,320 to 0,844 |
| Segment 14 | 0,520 | 0,000 to 0,771 | 0,691 | 0,352 to 0,852 |
| Segment 15 | 0,546 | 0,056 to 0,782 | 0,706 | 0,386 to 0,859 |
| Segment 16 | 0,566 | 0,115 to 0,789 | 0,713 | 0,402 to 0,862 |
| Segment 17 | 0,589 | 0,172 to 0,799 | 0,698 | 0,370 to 0,855 |
| Segment 18 | 0,598 | 0,192 to 0,803 | 0,666 | 0,300 to 0,840 |
| Segment 19 | 0,596 | 0,175 to 0,804 | 0,620 | 0,201 to 0,818 |
| Segment 20 | 0,577 | 0,121 to 0,796 | 0,561 | 0,075 to 0,790 |
| Segment 21 | 0,545 | 0,044 to 0,782 | 0,508 | -0,036 to 0,765 |
| Segment 22 | 0,519 | -0,015 to 0,770 | 0,477 | -0,101 to 0,750 |
| Segment 23 | 0,501 | -0,053 to 0,762 | 0,459 | -0,140 to 0,741 |
| Segment 24 | 0,491 | -0,076 to 0,757 | 0,452 | -0,155 to 0,738 |

| FETAL CARDIAC FUNCTION | | | | |
|------------------------|----------------|-----------------|-----------------|-----------------|
| Shortening fraction | | | | |
| | Left ventricle | | Right ventricle | |
| Segment 1 | 0,643 | 0,227 to 0,838 | 0,339 | -0,521 to 0,710 |
| Segment 2 | 0,378 | -0,170 to 0,689 | 0,237 | -0,697 to 0,658 |
| Segment 3 | 0,246 | -0,366 to 0,614 | 0,309 | -0,509 to 0,684 |
| Segment 4 | 0,137 | -0,602 to 0,565 | 0,225 | -0,657 to 0,640 |
| Segment 5 | 0,390 | -0,167 to 0,693 | 0,188 | -0,705 to 0,617 |
| Segment 6 | 0,356 | -0,239 to 0,677 | 0,298 | -0,474 to 0,673 |
| Segment 7 | 0,342 | -0,271 to 0,671 | 0,246 | -0,536 to 0,641 |
| Segment 8 | 0,356 | -0,250 to 0,679 | 0,068 | -1,447 to 0,531 |
| Segment 9 | 0,387 | -0,196 to 0,695 | 0,160 | -0,769 to 0,607 |
| Segment 10 | 0,410 | -0,160 to 0,708 | 0,171 | -0,794 to 0,616 |
| Segment 11 | 0,407 | -0,178 to 0,708 | 0,142 | -0,855 to 0,597 |
| Segment 12 | 0,384 | -0,246 to 0,699 | 0,269 | -0,580 to 0,656 |
| Segment 13 | 0,367 | -0,309 to 0,694 | 0,371 | -0,347 to 0,703 |
| Segment 14 | 0,382 | -0,301 to 0,704 | 0,436 | -0,190 to 0,732 |
| Segment 15 | 0,422 | -0,224 to 0,724 | 0,470 | -0,108 to 0,747 |
| Segment 16 | 0,466 | -0,117 to 0,744 | 0,480 | -0,085 to 0,752 |
| Segment 17 | 0,501 | -0,021 to 0,758 | 0,480 | -0,091 to 0,752 |
| Segment 18 | 0,519 | 0,035 to 0,764 | 0,479 | -0,105 to 0,753 |
| Segment 19 | 0,629 | 0,242 to 0,821 | 0,464 | -0,146 to 0,747 |
| Segment 20 | 0,524 | 0,233 to 0,818 | 0,429 | -0,226 to 0,731 |
| Segment 21 | 0,615 | 0,217 to 0,814 | 0,385 | -0,320 to 0,710 |
| Segment 22 | 0,608 | 0,204 to 0,811 | 0,351 | -0,391 to 0,694 |
| Segment 23 | 0,596 | 0,159 to 0,809 | 0,330 | -0,437 to 0,684 |
| Segment 24 | 0,595 | 0,156 to 0,808 | 0,327 | -0,462 to 0,678 |

ICC: Intraclass Correlation Coefficient.

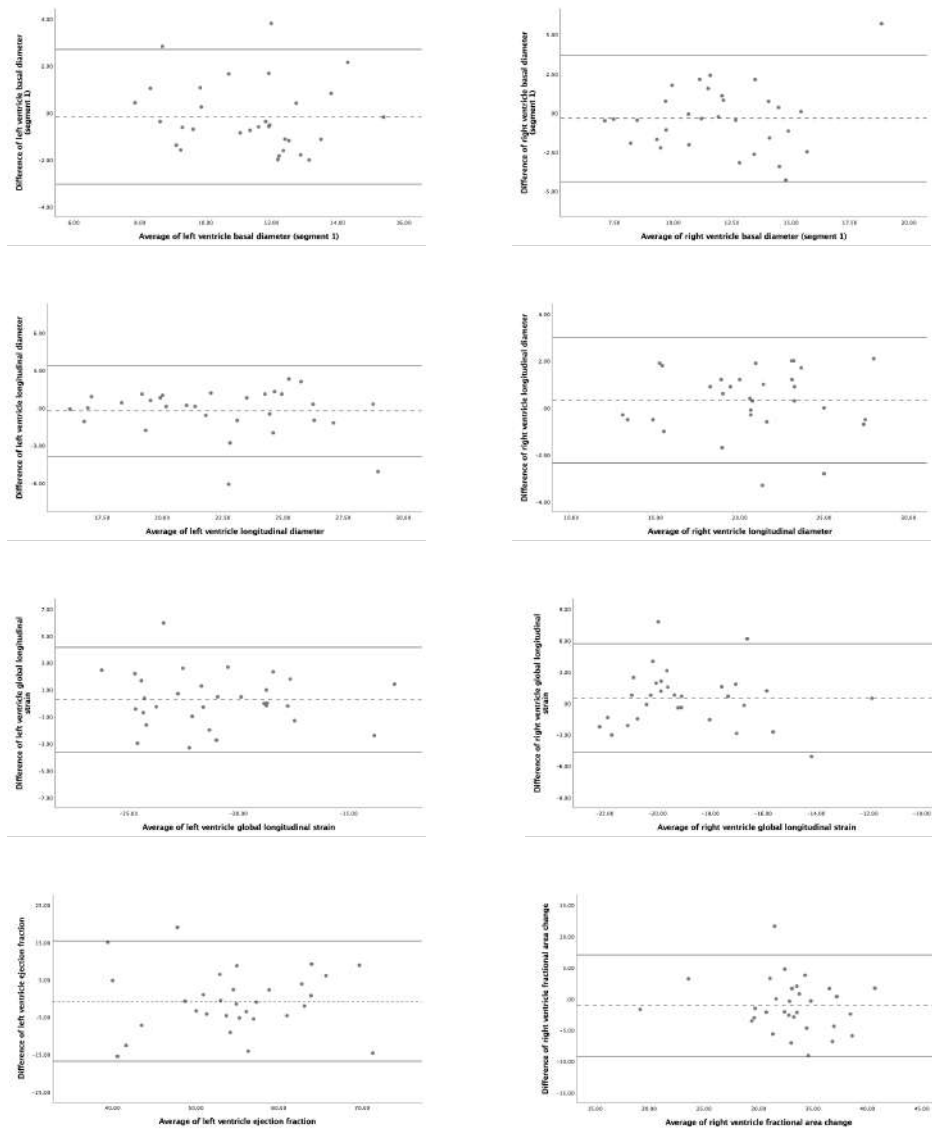


Figure S1. Bland-Altman plots for intraobserver reproducibility of fetal heart speckle tracking analysis of morphometric and functional parameters using 4D-Spatio Temporal Image Correlation (4D-STIC). Upper figures: left ventricle basal diameter (segment 1) (left) and right ventricle basal diameter (segment 1) (right); Middle upper figures: left ventricle longitudinal diameter (left) and right ventricle longitudinal diameter (right); Middle bottom: left ventricle global longitudinal strain (left) and right ventricle global longitudinal strain (right); bottom figures: left ventricle ejection fraction (left) and right ventricle fractional area change.

Study 2

Nogué L, Bennasar M, Guirado L, Dall'Asta A, Ghi T, Masoller N, Escobar-Diaz MC, Bijmens B, Martínez JM, Crispi F, Gómez O. Incremental value of 2D strain fetal echocardiography in the prediction of neonatal valvuloplasty in isolated mild to critical pulmonary valve stenosis.

Status: under 3rd review in Ultrasound in Obstetrics and Gynecology



INCREMENTAL VALUE OF 2D STRAIN FETAL ECHOCARDIOGRAPHY IN THE PREDICTION OF NEONATAL VALVULOPLASTY IN ISOLATED MILD TO CRITICAL PULMONARY VALVE STENOSIS

| | |
|-------------------------------|---|
| Journal: | <i>Ultrasound in Obstetrics and Gynecology</i> |
| Manuscript ID | UOG-2023-0359.R2 |
| Wiley - Manuscript type: | Original Article |
| Date Submitted by the Author: | n/a |
| Complete List of Authors: | Nogué, Laura; BCNatal Fetal Medicine Research Center (Hospital Clínic and Hospital Sant Joan de Déu); Institut d'Investigacions Biomèdiques August Pi i Sunyer (IDIBAPS) Bennasar, Mar; BCNatal Fetal Medicine Research Center (Hospital Clínic and Hospital Sant Joan de Déu); Institut d'Investigacions Biomèdiques August Pi i Sunyer (IDIBAPS) Guirado, Laura; BCNatal Fetal Medicine Research Center (Hospital Clínic and Hospital Sant Joan de Déu) Dall'Asta, Andrea; University of Parma Department of Medicine and Surgery, Obstetrics and Gynecology Unit Ghi, Tullio; University of Parma Department of Medicine and Surgery, Obstetrics and Gynecology Unit Masoller Casas, Narcís; BCNatal Fetal Medicine Research Center (Hospital Clínic and Hospital Sant Joan de Déu); Institut d'Investigacions Biomèdiques August Pi i Sunyer (IDIBAPS) Escobar, Maria Clara; Pediatric Cardiology Department, Sant Joan de Déu Hospital; Cardiovascular Research Group, Sant Joan de Deu Research Institute Bijnens, Bart; ICREA, Universitat Pompeu Fabra; Universitat Pompeu Fabra Martínez, Josep M; BCNatal Fetal Medicine Research Center (Hospital Clínic and Hospital Sant Joan de Déu); Institut d'Investigacions Biomèdiques August Pi i Sunyer (IDIBAPS); Center for Biomedical Research on Rare Diseases (CIBER-ER) Crispi, Fàtima; BCNatal Fetal Medicine Research Center (Hospital Clínic and Hospital Sant Joan de Déu); Institut d'Investigacions Biomèdiques August Pi i Sunyer (IDIBAPS); Center for Biomedical Research on Rare Diseases (CIBER-ER) Gómez, Olga; BCNatal Fetal Medicine Research Center (Hospital Clínic and Hospital Sant Joan de Déu); Institut d'Investigacions Biomèdiques August Pi i Sunyer (IDIBAPS); Center for Biomedical Research on Rare Diseases (CIBER-ER) |
| Manuscript Categories: | Obstetrics |
| Keywords: | congenital heart disease, pulmonary stenosis, fetal echocardiography, speckle tracking echocardiography, strain, neonatal valvuloplasty, |

| | |
|--|-------------------------|
| | mechanical dyssynchrony |
| | |

SCHOLARONE™
Manuscripts

**INCREMENTAL VALUE OF 2D STRAIN FETAL ECHOCARDIOGRAPHY IN THE
PREDICTION OF NEONATAL VALVULOPLASTY IN ISOLATED MILD TO
CRITICAL PULMONARY VALVE STENOSIS**

**Nogué L^{1,2}, Bennasar M^{1,2} (*), Guirado L¹, Dall'Asta A³, Ghi T³, Masoller N^{1,2}, Escobar-Diaz MC^{4,5},
Bijnens B^{6,7}, Martínez JM^{1,2,8}, Crispí F^{1,2,8} (†) and Gómez O^{1,2,8}(†); for the BCNatal and Parma
University investigators**

¹ BCNatal Fetal Medicine Research Center (Hospital Clínic and Hospital Sant Joan de Déu),
University of Barcelona, Barcelona, Spain

² Institut d'Investigacions Biomèdiques August Pi i Sunyer (IDIBAPS), Barcelona, Spain

³ Department of Medicine and Surgery, Unit of Surgical Sciences, Obstetrics and Gynecology,
University of Parma, Parma, Italy

⁴ Pediatric Cardiology Department, Sant Joan de Déu Hospital, Esplugues de Llobregat,
Barcelona, Spain

⁵ Cardiovascular Research Group, Sant Joan de Deu Research Institute, Esplugues de Llobregat,
Barcelona, Spain

⁶ ICREA, Barcelona, Spain

⁷ Universitat Pompeu Fabra, Barcelona, Spain.

⁸ Centre for Biomedical Research on Rare Diseases (CIBER-ER), Madrid, Spain

(†) F.C. and O.G. share last authorship

*** Correspondence:** Mar Bennasar Sans

BCNatal, Fetal Medicine Research Center (Hospital Clínic and Hospital Sant Joan de Déu), Sabino de Arana street 1, 08028 Barcelona, Spain. Telephone: +34 932279904. E-mail: bennasar@clinic.cat

Short title: Strain for valvuloplasty prediction in prenatal pulmonar stenosis

Keywords: congenital heart disease, pulmonary stenosis, fetal echocardiography, speckle tracking echocardiography, strain, neonatal valvuloplasty, mechanical dyssynchrony

For Peer Review

1 **INCREMENTAL VALUE OF 2D STRAIN FETAL ECHOCARDIOGRAPHY IN THE**
2 **PREDICTION OF NEONATAL VALVULOPLASTY IN ISOLATED MILD TO**
3 **CRITICAL PULMONARY VALVE STENOSIS**

4
5 **Nogué L^{1,2}, Bennasar M^{1,2} (*), Guirado L¹, Dall'Asta A³, Ghi T³, Masoller N^{1,2}, Escobar-Diaz MC^{4,5},**
6 **Bijnens B^{6,7}, Martínez JM^{1,2,8}, Crispí F^{1,2,8} (†) and Gómez O^{1,2,8}(†); for the BCNatal and Parma**
7 **University investigators**

8
9 ¹ BCNatal Fetal Medicine Research Center (Hospital Clínic and Hospital Sant Joan de Déu),
10 University of Barcelona, Barcelona, Spain

11 ² Institut d'Investigacions Biomèdiques August Pi i Sunyer (IDIBAPS), Barcelona, Spain

12 ³ Department of Medicine and Surgery, Unit of Surgical Sciences, Obstetrics and Gynecology,
13 University of Parma, Parma, Italy

14 ⁴ Pediatric Cardiology Department, Sant Joan de Déu Hospital, Esplugues de Llobregat,
15 Barcelona, Spain

16 ⁵ Cardiovascular Research Group, Sant Joan de Deu Research Institute, Esplugues de Llobregat,
17 Barcelona, Spain

18 ⁶ ICREA, Barcelona, Spain

19 ⁷ Universitat Pompeu Fabra, Barcelona, Spain.

20 ⁸ Centre for Biomedical Research on Rare Diseases (CIBER-ER), Madrid, Spain

21

22 (†) F.C. and O.G. share last authorship

23

24 *** Correspondence:** Mar Bennasar Sans

25 BCNatal, Fetal Medicine Research Center (Hospital Clínic and Hospital Sant Joan de Déu), Sabino
26 de Arana street 1, 08028 Barcelona, Spain. Telephone: +34 932279904. E-mail:
27 bennasar@clinic.cat

28

29 **Short title:** Strain for valvuloplasty prediction in prenatal pulmonar stenosis

30 **Keywords:** congenital heart disease, pulmonary stenosis, fetal echocardiography, speckle
31 tracking echocardiography, strain, neonatal valvuloplasty, mechanical dyssynchrony

32

33 **Contribution:**

34 **What are the novel findings of this work?**

35 Pulmonary stenosis presents decreased right ventricle (RV) deformation that correlates with
36 mechanical dyssynchrony. A scoring system is provided for neonatal valvuloplasty prediction,
37 combining ductus venosus pulsatility index centile, RV global longitudinal strain, reversed flow
38 at the ductus arteriosus and significant tricuspid regurgitation.

39 **What are the clinical implications of this work?**

40 Our results provide a combination of prenatal parameters to predict, with high accuracy, the
41 need of neonatal valvuloplasty. This information is clinically relevant since it enables early
42 assessments by specialists in neonatal cardiology for high-risk fetuses.

43

44 **Referee nominations:**

- 45 1. Mark Friedberg
- 46 2. Giuseppe Rizzo
- 47 3. Ulrike Herberg

48 ABSTRACT**49 Objectives**

50 To evaluate a prediction model of neonatal valvuloplasty by fetal echocardiography including
51 speckle tracking echocardiography (STE) in a series of isolated pulmonary stenosis (PS).

52 Methods

53 A prospective cohort study was conducted, which included 24 cases of isolated PS, comprising
54 7 critical and 17 mild-moderate cases. Cases were matched with 48 healthy controls adjusted
55 for gestational age at echocardiography. The study was conducted at BCNatal, a referral center
56 for congenital heart defects in Spain. Fetal ultrasound, comprehensive echocardiography and
57 off-line STE were performed at the time of PS diagnosis. Semiautomated tracking of both right
58 (RV) and left ventricles (LV) was carried-out for STE to obtain RV and LV global longitudinal strain
59 (GLS), tricuspid and mitral annular plane systolic excursion (TAPSE, MAPSE), RV fractional area
60 change (FAC) and LV ejection fraction. STE segmental analysis was performed to explore the
61 evaluation of mechanical dyssynchrony. Maternal and perinatal characteristics were obtained
62 from medical records. Echocardiographic parameters were analyzed according to the need for
63 neonatal valvuloplasty to identify possible predictors of early intervention.

64

65 Results

66 Maternal and perinatal characteristics were similar in both groups. Mean gestational age at
67 echocardiography was 31.4 weeks (Median 32.5 weeks (27.4-35.1)) with 12.5% of the cases
68 evaluated <24 weeks. Half of the PS fetuses required valvuloplasty within the first month of life.
69 Critical PS fetuses showed global RV functional impairment with significantly reduced GLS, FAC
70 (which correlated with mechanical dyssynchrony), TAPSE, a more pulsatile DV, and no changes
71 in LV parameters. Worse RV function was observed in the valvuloplasty group. A combination of
72 DV PI centile (cut-off value $\geq 79\%$), RV GLS (cut-off value of $\geq -15.85\%$), reversed flow in the DA,

73 and significant tricuspid regurgitation were predictors of neonatal valvuloplasty, and when
74 combined in a scoring system the area under the curve was 0.931, $p=0.001$. Giving a score of 1
75 for each present variable, values ≥ 2 predicted the need of neonatal valvuloplasty with a
76 sensitivity of 91.7% and specificity of 100%. The prediction model based only on conventional
77 echocardiographic parameters also had excellent performance with slightly lower sensitivity.

78

79 **Conclusions**

80 Decreased RV deformation is observed in critical PS fetuses, and correlates with mechanical
81 dyssynchrony. A scoring system combining the DV PI centile and RV GLS with the presence of
82 reversed ductus arteriosus flow and significant tricuspid regurgitation, is provided to identify
83 those fetuses in need of neonatal valvuloplasty, who will thus benefit from an early neonatal
84 assessment by pediatric cardiologists. Further studies are needed to evaluate the performance
85 of the suggested scoring system, which seems promising.

86

87 1. INTRODUCTION

88 Pulmonary stenosis (PS) is one of the most frequent congenital heart defects (CHD) diagnosed
89 postnatally with an incidence of 10% of CHD newborns¹. Its severity varies from mild forms,
90 which will not require intervention, to very severe forms requiring postnatal univentricular
91 repair²⁻⁵. Given the wide spectrum of postnatal outcome, fetal echocardiography has been
92 proposed to assess cardiovascular remodeling and dysfunction. This could potentially
93 differentiate those fetuses that will progress to the more severe forms requiring neonatal
94 valvuloplasty and would benefit from early assessment by neonatal echocardiography.
95 Recently, new data has been published to better define biventricular remodeling in fetal PS⁶ and
96 classify severe PS forms beyond the presence of significant tricuspid regurgitation (TR) and
97 reversed ductus arteriosus (DA) flow. However, to date, no single echocardiographic parameter
98 has shown to be useful in predicting the need for neonatal valvuloplasty^{7,8}. Therefore, the wide
99 variability of echocardiographic indexes points to the need a combination of classic parameters
100 or to define new ones to better determine postnatal evolution.
101 Novel diagnostic parameters have been described for the study of systolic and diastolic function,
102 with standard echocardiography and with novel myocardial imaging techniques, such as global
103 longitudinal strain (GLS), a measurement of myocardial deformation widely used in adult and
104 pediatric cardiology⁹⁻¹¹ to detect preclinical myocardial dysfunction in risk patients^{12,13}.
105 Decreased right ventricle (RV) GLS in PS newborns has been reported, with an improvement
106 after valvuloplasty¹⁴. GLS has been described for prenatal cardiac evaluation in different CHD¹⁵.
107 However, its clinical application has not yet been proven.
108 Additionally, the use of novel techniques such as speckle tracking (STE)¹⁶⁻¹⁸ enables the off-line
109 study of mechanical dyssynchrony, which consists of the difference in timing of mechanical
110 shortening or lengthening between different ventricular segments. This has shown good
111 correlation with ventricular function parameters and response to treatment in a pediatric
112 population with CHD¹⁹, and may be useful for better outcome prediction.

113 The aim of our study is to evaluate morphometric and functional parameters using STE in a large
114 cohort of mild and critical PS. Additionally, we aim to develop a prediction model for neonatal
115 valvuloplasty based on echocardiographic indexes, including STE.

For Peer Review

116 **2. METHODS**

117 *Study design and participants*

118 A cohort study including 35 fetuses with diagnosis of isolated PS recruited between 20+0 and
119 39+0 weeks of gestation, and healthy controls matched by gestational age and estimated fetal
120 weight (EFW) at scan (2:1 control: case ratio) was designed. Cases were prospectively recruited
121 from January 2019 to September 2021, from a consecutive series of 819 fetuses with CHD
122 evaluated in the **Fetal Cardiology Unit of BCNatal (Hospital Clínic of Barcelona and Hospital Sant**
123 **Joan de Deu)**, which operates as a referral center for pregnancies at risk for CHD. Thirteen PS
124 cases were included from a historical cohort (2014-2019). The study population consisted of
125 fetuses with isolated valvular PS with anterograde flow through the pulmonary valve at
126 diagnosis regardless of the flow in the DA (anterograde or reversed). PS was defined by the
127 presence of pulmonary valve dysplasia signs (such as hyperechogenicity, thickening and/or
128 hypomobility of the valve) combined with systolic flow acceleration (peak systolic velocity above
129 120 cm/s in the second trimester or >140cm/s in the third trimester). Fetuses affected by
130 pulmonary atresia at the moment of the first echocardiography in our unit, as well as cases with
131 additional cardiac defects were not included in the study. Monochorionic twin pregnancies with
132 PS of the recipient twin were also excluded from the study (**Figure 1**). Controls were recruited
133 from consecutive low-risk pregnancies that were invited to participate in the study and were
134 matched with PS cases by gestational age at scan +/- 1 week. Maternal age, smoking status,
135 parity, and the presence of maternal diseases such as hypertension and diabetes were retrieved
136 from patients' medical records. Perinatal outcome including gestational age, mode of delivery,
137 birthweight and Apgar score were also obtained. PS diagnosis and severity were confirmed
138 postnatally²⁰, and all newborns were followed-up at least for 10 months. The need for intensive
139 care unit admission, prostaglandin infusion and valvuloplasty were obtained in all cases.
140 Prenatal diagnosis of PS usually accounts for the more severe spectrum of the disease and a
141 fraction of the total neonatal PS population. Therefore, we reviewed the registry of neonatal

142 pulmonary valvuloplasty at our center to determine the prenatal detection rate of PS requiring
143 neonatal valvuloplasty. Study protocol was approved by the Ethical Committee of the institution
144 (Reg. HCB/2019/0540) and written consent was obtained from all pregnant women from both
145 prospective and retrospective cohorts.

146

147 *Feto-placental ultrasound and standard echocardiography*

148 All participants underwent a feto-placental standard ultrasound and echocardiography to rule
149 out other cardiac or extracardiac anomalies according to the existing Guidelines^{21,22}. In addition,
150 an amniocentesis for microarray analysis, to rule out chromosomal abnormalities, was offered
151 and performed in all PS cases. Gestational age was calculated according to crown-rump length
152 at first trimester ultrasound²³ and EFW was obtained according to Hadlock et al²⁴. Weight centile
153 was determined according to local references, adjusted by GA and fetal gender²⁵. Doppler
154 pulsatility index (PI) of umbilical, middle cerebral artery, ductus venosus (DV), as well as
155 cerebral-placental ratio²⁶ (middle cerebral artery PI/umbilical artery PI) were also evaluated. PS
156 cases were subclassified into: *critical* in presence of reverse flow in the DA at first
157 echocardiography, or *mild-moderate* in the remaining cases (including cases with the existence
158 of RV hypertrophy with significant TR, defined as holosystolic regurgitation and peak velocity
159 higher than 200cm/s, with anterograde flow in the DA).

160 A comprehensive echocardiography was performed, at first evaluation at our center, using a
161 Voluson E10 (GE Healthcare Ultrasound, Milwaukee, WI, USA) with a C2-9D convex probe (3-
162 9MHz) using 2D and Doppler⁶. Methodology of morphometric and functional parameters
163 assessed by 2D echocardiography are detailed in **Supplementary Table 1**. Additionally, cardiac
164 timing parameters were evaluated in all cases, as described by Soveral et. al²⁷, to evaluate their
165 predictive value. **Regarding the historical cohort, all cases were recruited prospectively for a
166 previous study by our group on PS⁶. Therefore, they followed the same strict echocardiographic**

167 protocol on 4-chamber clip acquisition as in the prospective cohort⁶. STE analysis and timing
168 parameters were measured retrospectively from the ultrasound performed at diagnosis.

169

170 *Fetal speckle tracking echocardiography*

171 Apical or basal 4-chamber view clips including both RV and LV apex, containing at least three
172 heart cycles with a frame rate higher than 60Hz, were obtained for STE¹⁶ at first
173 echocardiography at our center. All cardiac images were acquired using Speckle Reduction
174 Imaging (SRI) 3 and Compound Resolution Imaging (CRI) 2, stored in DICOM (Digital Imaging and
175 Communication in Medicine) and imported to cardiac software program 2D STRAIN (Fetal)
176 developed by TomTec imaging systems, GmbH (Munich, Germany). All STE analysis were
177 performed by the same experienced operator (L.N.).

178 End-systolic and end-diastolic frames of a single cardiac cycle were identified from an M-mode
179 display of the tricuspid annulus. To allow semiautomated tracking of the endocardial border
180 throughout the entire cardiac cycle, septal and lateral atrioventricular valve annulus and apex
181 of the RV and LV were indicated in the end-systolic frame¹⁶. Semiautomated tracking was
182 manually adjusted when necessary, including endocardium, muscular trabeculations and
183 moderator band as RV cavity^{28,29}. Biventricular strain curves were generated at basal, mid-
184 ventricular and apical segments of the free LV and RV walls and interventricular septum (6
185 segments). Biventricular morphometric parameters (area, longitudinal and transverse
186 diameters) were automatically obtained as described by DeVore et al³⁰. Longitudinal cardiac
187 deformation was evaluated with RV and LV global longitudinal strain (GLS) (changes in strain are
188 reported in absolute value)^{31,32} and RV and LV lateral wall annular plane systolic excursion
189 (TAPSE, MAPSE)³³. Both TAPSE and MAPSE are calculated automatically by STE software as the
190 movement of the endocardium closest to the tricuspid and mitral annulus towards the
191 ventricular apex. Global RV function was assessed by calculation of fractional area change
192 (FAC)³⁴ and LV function with ejection fraction (EF)³⁵. Segmental analysis of sphericity index and

193 shortening fraction was not included in the analysis due to previously reported modest
194 reproducibility of these parameters²⁹. The results of the analysis were exported to an Excel
195 spreadsheet (Microsoft Corp., Redmond, WA, USA) for further analysis.

196

197 *STE segmental analysis and mechanical dyssynchrony*

198 Segmental STE analysis was performed to explore mechanical dyssynchrony. Both ventricles
199 were automatically divided into 6 ventricular segments (free-wall basal, mid-ventricular and
200 apical and septum apical, mid-ventricular and basal). Peak systolic strain in each of the 6 RV and
201 LV segments, and their timing, were measured to evaluate mechanical dyssynchrony. Time-to-
202 peak shortening (ms) was defined as the time interval from the onset of myocardial shortening
203 to peak systolic strain. Difference of time to peak strain between basal and apical segments of
204 both RV and LV free wall was calculated (RV and LV free wall peak strain delay). Standard
205 deviation of the time-to-peak shortening of the 6 ventricular segments was assessed (intra-RV
206 and intra-LV dyssynchrony index) as an indicator of mechanical dyssynchrony(**Figure 2**)³⁶.

207

208 *Statistical analysis*

209 Statistical analysis was performed using IBM SPSS Statistics for Mac (version 25, IBM Corp.,
210 Armonk, NY, USA). A Kolmogorov-Smirnov test of normality was performed on all continuous
211 variables. Differences between PS and controls were assessed by Student's t-test and Mann-
212 Whitney U test for non-normally distributed continuous variables, and **Fisher's exact** for
213 categorical variables. Comparisons between critical PS, mild-moderate PS and control group
214 were studied applying One-way ANOVA followed by post hoc Bonferroni test for pairwise
215 comparison or Kruskal-Wallis one-way ANOVA for non-normally distributed variables, and
216 **Fisher's exact** for categorical variables. **P-values were adjusted for potentially confounding**
217 **factors that were significantly different between groups, such as estimated fetal weight and**
218 **ventricular length**. Additionally, the PS group was analyzed according to the need of neonatal

219 balloon valvuloplasty by Student's t-test. Linear regression analysis was performed in order to
220 find any association between dyssynchrony and functional parameters. Receiver-operating
221 characteristics (ROC) curves and area under the curve were calculated to measure the sensitivity
222 and specificity of RV functional parameters for the prediction of neonatal valvuloplasty. Cut-off
223 points were extracted from ROC analysis. A subanalysis of the performance of the scoring system
224 was done in early (before 24 weeks) and late pregnancy (after 24 weeks). Statistical significance
225 for all analysis was considered when p value was <0.05 .

For Peer Review

226 3. RESULTS

227 *Characteristics of the study population*

228 Characteristics of the PS fetuses included in the study are shown in **Figure 1**. From the initial
229 cohort of 35 PS fetuses, 11 were excluded due to different reasons such as termination of
230 pregnancy (n=1), monochorionic twin pregnancies (n=3), lost to follow up (n=2), non-isolated PS
231 (n=1) and poor quality of 4-chamber view clips (n=4). The 24 remaining PS cases were included
232 in the study. Mean gestational age at echocardiography was 31.4 weeks (Median 32.5 weeks
233 (27.4-35.1)), (range 20.0 to 39.1). PS fetuses were subclassified in 7 critical PS due to retrograde
234 flow at the DA at first echocardiography, and 17 mild-moderate PS. Twenty-two fetus (91.6%)
235 were referred to our fetal cardiac unit for CHD suspicion during the screening ultrasound, mainly
236 because of RV hypertrophy or aliasing at the pulmonary flow, one fetus was referred because of
237 a sibling with a PS and another case for reversed ductus venosus flow at first trimester
238 ultrasound. Thirty neonatal pulmonary valvuloplasties were performed since 2014. The prenatal
239 detection rate was 50%, increasing to 64% during the last period of the study (2019-2021). It
240 should be noted that our center is a national referral center for interventional catheterization,
241 so many children were referred from other centers. The implementation of color Doppler in
242 cardiac evaluation in second and third trimester ultrasound screening, as well as the
243 technological improvement of ultrasound equipment, would explain the increase in prenatal
244 detection of PS over the study period.

245 Maternal, fetal and perinatal characteristics of the study population are detailed in **Table 1** and
246 **Supplementary Table 2**. There were no statistical differences in maternal baseline
247 characteristics such as ethnicity, smoking or presence of chronic diseases. Gestational diabetes
248 was more frequent (n=2, 8.3%) in PS cases without reaching statistical significance ($p=0.108$).
249 Preterm delivery was significantly increased in PS (n=4, 16.67%), mainly spontaneously,
250 although, in one case of critical PS, delivery was induced because of cardiac function
251 deterioration at 35 weeks. Fetuses with critical PS had lower birthweight and birthweight centile

252 at similar gestational age at birth. Median postnatal follow up was 5.2 years (interquartile range:
253 2.4-9.3), and confirmed all cases of PS. Prostaglandin infusion was required in 9 newborns
254 (37.5%) of which 2 had an antegrade DA. Although this is a series of mostly mild-moderate
255 cases, half of them required neonatal valvuloplasty at a median age of 3.5 days (interquartile
256 range: 3-12.8).

257

258 *Fetal ultrasound and standard 2D echocardiographic results*

259 Mean gestational age and EFW at ultrasound were similar between groups, while Doppler
260 evaluation in critical PS fetuses revealed a more pulsatile DV (**Table 2 and Supplementary Table**
261 **3**). Comprehensive echocardiography results confirmed previous data of biventricular impact of
262 fetal PS⁶ (**Supplementary Table 4 and 5**). In addition, right filling time fraction was significantly
263 shorter in critical PS, with 57.1% of the cases below minus 2 z-scores. On the contrary, right
264 ejection time fraction showed a non-significant trend to lengthen in critical PS fetuses.

265

266 *Fetal speckle tracking echocardiography results*

267 STE morphometric evaluation of the RV showed a non-significant trend to a smaller area and
268 longitudinal diameter in critical PS group and a higher mid-ventricular diameter in mild-
269 moderate PS fetuses as compared to controls (**Table 3 and Supplementary Table 6**). Regarding
270 RV function, critical PS fetuses presented a global impairment compared to controls and mild-
271 moderate PS, with significant decrease in longitudinal (reduced GLS and TAPSE) and global
272 function (FAC) (**Supplementary Table 6**). No statistically significant changes were observed in LV
273 morphometry or function between the three groups. Reproducibility of STE analysis was
274 analyzed previously by our group²⁹.

275

276 *Mechanical dyssynchrony in relation to echocardiographic parameters*

277 PS fetuses, in particular critical PS, showed signs of RV mechanical dyssynchrony as compared
278 to the mild-moderate PS and control groups, with a higher intra RV dyssynchrony index and
279 higher free wall time to peak strain delay (**Table 3** and **Supplementary Table 6**), indicating the
280 presence of mechanical dispersion. Moreover, the association between mechanical
281 dyssynchrony and echocardiographic parameters was studied and a strong negative association
282 between RV dyssynchrony index and RV FAC ($r=-0.727$, $p<0.001$) and moderate negative
283 correlation with RV GLS ($r=-0.685$, $p<0.001$) were found (**Figure 3**). No correlation was found
284 between mechanical dyssynchrony and timing parameters.

285

286 *Association of prenatal echocardiography and need for neonatal valvuloplasty*

287 Results were evaluated regarding the need for neonatal valvuloplasty (**Tables 1, 2, 3** and
288 **Supplementary Table 4**). Fetuses that needed valvuloplasty in the first month of life had smaller
289 birthweight, higher DV PI centile, higher incidence of significant TR and reversed flow at the DA
290 than those who did not require a neonatal intervention (**Tables 1 and 2**). Furthermore, smaller
291 RV area and transverse diameters and more impaired RV function (**decreased GLS and FAC**) were
292 observed in the valvuloplasty group, with no changes in terms of LV morphometry and function
293 (**Table 3**). Although not significant, fetuses that needed a neonatal valvuloplasty presented with
294 an increased intra RV dyssynchrony index when compared to those not needing valvuloplasty
295 (**Table 3**). Prenatal and postnatal cardiac characteristics of 12 fetuses that underwent neonatal
296 valvuloplasty are detailed in **Table 4**.

297 All echocardiographic and dyssynchrony parameters were assessed in a univariate predictive
298 diagnostic test for neonatal valvuloplasty. Logistic regression analysis identified TR as the best
299 performing echocardiographic parameter (Odds ratio 2.44, 95% confidence interval (1.15-
300 114.02); $p=0.038$). Analysis of ROC curves identified DV PI centile, RV GLS, presence of reversed
301 flow in the DA and significant TR as the only associated variables for prediction of neonatal

302 valvuloplasty. DV PI centile area under the curve (AUC) was 0.782 with a cut-off value of 79 to
303 obtain the maximal sensitivity and specificity, RV GLS AUC was 0.833, cut-off value of -15.85%,
304 reversed flow in the DA AUC was 0.750 and significant TR AUC 0.806 (**Table 5, Figure 4**).

305 Using the previously described thresholds as well as the presence of TR and reversed flow at the
306 DA, a scoring system for the prediction of neonatal valvuloplasty was created. Patients were
307 assigned a score of 1 for each present variable (1 for DV IP centile > 79, 1 for RV GLS > -15.85, 1
308 when reversed DA flow at diagnosis was present and 1 for significant TR). The maximum score
309 was 4 and the minimum was 0. This scoring system showed a significant association with the
310 need of neonatal valvuloplasty (AUC: 0.931, $p=0.001$). A score higher than or equal to 2
311 predicted neonatal valvuloplasty with a sensitivity of 91.7% and specificity of 100%. Scores of
312 fetuses that required neonatal valvuloplasty are shown in **Table 4**. The performance of the
313 prediction model based only on conventional echocardiographic parameters was also excellent,
314 although it showed a lower sensitivity (83%) and 100% specificity (**Figure 5**). A subanalysis of the
315 performance of the model in mid pregnancy (<24 weeks) and late pregnancy (>24 weeks) was
316 conducted showing a sensitivity and specificity of 100% before 24 weeks and 87.5% sensitivity
317 and 100% specificity after 24 weeks. These numbers must be taken with caution as only 3 patients
318 were diagnosed in mid pregnancy.

319

320 4. DISCUSSION

321 This is the first study that evaluates GLS by STE in a series of PS fetuses. We demonstrate a
322 decreased RV GLS in critical PS and its correlation with mechanical dyssynchrony evaluated
323 through the RV dyssynchrony index. Moreover, we propose a new score system that combines
324 GLS with conventional echocardiographic parameters, achieving >90% sensitivity in the
325 prediction of neonatal valvuloplasty, even in early gestational ages.

326

327 *PS is associated with reduced RV GLS and mechanical dyssynchrony*

328 RV GLS measurement is a reliable parameter for decision-making in RV dysfunction in adult
329 cardiology, mainly secondary to pulmonary hypertension³⁷, and also in CHD follow-up¹³. Gozar
330 et al. reported that RV GLS is reduced in PS in the neonatal period and that it improves after
331 valvuloplasty¹⁴. Previous reports of strain in fetal life are scarce, and studies have shown a wide
332 distribution of GLS that overlap with normal values^{18,38}

333 Our results, showing a decreased RV GLS in PS which correlates with severity and the need for
334 neonatal valvuloplasty, are consistent with those published pre and postnatally, although
335 previous studies did not include the moderator band as part of the RV cavity, so differences in
336 methodology need to be considered^{30,34}.

337 Previous studies have shown that increased interventricular dyssynchrony is associated with
338 lower TAPSE and RV GLS in children^{37,38}. It has been previously described, in a cohort of mainly
339 mild-moderate PS fetuses, that RV function is preserved⁶. However, we report RV hypertrophy
340 and myocardial dysfunction in critical PS, that is also associated with mechanical dyssynchrony,
341 and can explain RV systolic dysfunction in more severe PS. The cause of this dyssynchrony is not
342 known, but Hui et al. hypothesized it may be due to a right bundle branch block (RBBB) induced
343 by subendocardial wall stress in RV pressure overload. The RBBB causes early apical septal
344 contraction (septal flash)³⁶, which is linked to decreased RV GLS¹⁹. Our study found similar results

345 and a septal flash can be identified in some severe PS cases, but more research is needed to
346 confirm this hypothesis.

347 Previous studies have shown that adverse RV-LV interaction and LV volume overload can cause
348 LV diastolic dysfunction in PS fetuses⁶, consistent with a study in young adults with neonatal
349 valvuloplasty that reported a worsening in LV circumferential strain associated with greater RV
350 volume load⁴⁰. However, the present study did not find differences in LV deformation, although
351 further studies are needed to clarify the different results.

352

353 *Predictors of neonatal pulmonary valvuloplasty*

354 While reversed DA flow is often used as a predictor for neonatal valvuloplasty, a significant
355 number of newborns requiring intervention have antegrade flow in the DA, 50% in our series.
356 Other studies have also found that reversed DA flow is not always present in fetuses requiring
357 intervention for pulmonary stenosis or prostaglandin E1 treatment^{6,41}, indicating a need for
358 additional reliable parameters.

359 The current parameters for predicting the need for neonatal pulmonary valvuloplasty are not
360 optimal. Thus, a new scoring system is proposed that includes well-established parameters and
361 a more sensitive parameter (RV GLS) to detect cases with antegrade flow in the DA that may
362 require neonatal valvuloplasty, with excellent sensitivity and specificity. This is especially
363 relevant to detect those cases with antegrade flow in the DA, that will need prostaglandin E1
364 or neonatal intervention. In our series, the scoring system would have increased the prediction
365 of neonatal valvuloplasty in 50% of cases that did not have reversed DA flow or significant TR at
366 diagnosis. The scoring system was evaluated without RV GLS and still performed excellent,
367 although with slightly lower sensitivity. Referring PS cases before delivery to referral centers can
368 help select those who will benefit from an early echocardiographic assessment.

369 To date, only Wang et al.⁴¹ studied postnatal management in critical PS and pulmonary atresia
370 with intact interventricular septum with biventricular management at birth. They found

371 pulmonary valve regurgitation in the second trimester and RV/LV length ratio >0.86 in the third
372 trimester as predictors of ductal dependency, but the current study did not confirm the utility
373 of those parameters, which might be explained by the different outcomes studied. Our group
374 also identified decreased TAPSE, mitral E' peak velocity and increased LV cardiac output as
375 possible predictors; however, in this study we could not determine their role in predicting the
376 outcome due to limited sample size⁶.

377

378 *Strengths and limitations*

379 This study reports fetal adaptation to RV pressure overload in PS evaluated by STE. For the first
380 time a scoring system to predict the need for neonatal valvuloplasty in PS fetuses is described
381 that can be applied either in the second or third trimester. This score consists of parameters
382 easily assessed in the echocardiographic follow up.

383 The study has limitations, including a small sample size and a potential selection bias, as only a
384 small portion of neonatal PS cases were detected prenatally (more frequently moderate and
385 severe cases), retrospective analysis of 13 cases, and lack of external validation of the scoring
386 system. STE results reproducibility, especially evaluation of mechanical dyssynchrony, is also a
387 concern due to differences between vendors¹⁸ and the need for further validation of
388 dyssynchrony index, of which we evaluated its potential use; however, further studies are
389 needed to validate its effectiveness since EKG is not available in fetal life. The low sample size of
390 PS could affect the performance of the scoring system, which can be used as early as 21 weeks,
391 although few fetuses are diagnosed at early gestational ages and multicentric studies with a
392 larger number of cases are needed to validate the applicability of our results.

393

394 *Conclusions*

395 We describe the clinical utility of GLS in functional evaluation of PS fetuses and its role in
396 neonatal management prediction. Decreased RV deformation is observed in critical PS stenosis

397 fetuses, and it correlates with mechanical dyssynchrony. In addition, neonatal valvuloplasty may
398 be accurately predicted by combining DV PI centile, RV GLS, reversed flow at the DA and
399 significant TR in a scoring system. This information is relevant since it helps to refer fetuses with
400 higher scores for early assessment by neonatal cardiology experts.
401

For Peer Review

402 Acknowledgments and funding

403 We thank the study participants for their personal time and commitment to this project.

404 The research leading to these results has received funding from Hospital Clinic de Barcelona

405 (Ajut Josep Font 2015 and Premi Emili Letang 2019, Barcelona, Spain), Instituto de Salud Carlos

406 III (ISCIII) (PI15/00263, PI17/00675, PI20/00246, INT21/00027) co-funded by the European

407 Union, Cerebra Foundation for the Brain Injured Child (Carmarthen, Wales, UK), Fundació La

408 Marató de TV3 (Ref 202016-30-31), and the Maternal and Child Health and Development

409 Network (SAMID), RD16/0022/0015. Additionally, we would like to thank the Fundació Jesús

410 Serra of the Grup Catalana Occident for the Fundació Jesús Serra Research Prize in the Clinical

411 category awarded to the Researcher Fatima Crispi in its 4th edition for the project titled

412 "Cardiovascular prevention from fetal life: benefits of Mediterranean diet during gestation".

413 This publication reflects the views of the authors only, and the Commission cannot be held

414 responsible for any usage, which may be made of the information contained therein. No industry

415 funding was used in the development of this work.

416

417 **Collaborators**

418 BCNatal and Parma University Group information:

419 **Gaeta G:** BCNatal Fetal Medicine Research Center (Hospital Clínic and Hospital Sant Joan de
420 Déu), University of Barcelona, Barcelona, Spain421 **Di Tonto A:** Department of Medicine and Surgery, Unit of Surgical Sciences, Obstetrics and
422 Gynecology, University of Parma, Parma, Italy423 **Izquierdo N:** BCNatal Fetal Medicine Research Center (Hospital Clínic and Hospital Sant Joan de
424 Déu), University of Barcelona, Barcelona, Spain425 **Caballero M:** BCNatal Fetal Medicine Research Center (Hospital Clínic and Hospital Sant Joan de
426 Déu), University of Barcelona, Barcelona, Spain427 **Pérez-Cruz M:** BCNatal Fetal Medicine Research Center (Hospital Clínic and Hospital Sant Joan
428 de Déu), University of Barcelona, Barcelona, Spain

429

430 **Author contributions**

431 Conceptualization, L.N., O.G., M.B. and F.C.; methodology, L.N., O.G. and F.C.; software, L.N.;
432 validation, L.G. formal analysis, L.N., L.G., O.G. and F.C.; investigation, O.G., L.N., L.G., N.I., M.C,
433 N.M., M.C.E.-D., B.B, A.D.T, A.D.A, M.B., and F.C.; resources O.G., M.B., F.C., J.M.M., A.D.A., T.G.,
434 data curation, L.N., G.G, N.I., M.C.; writing—original draft preparation, L.N, M.B., O.G; writing—
435 review and editing, O.G., L.N., L.G., N.I., M.C, N.M., M.C.E.-D., B.B., A.D.A, T.G., J.M.M., M.B., and
436 F.C.; visualization, L.N.; supervision, O.G., M.B. and F.C.; project administration, O.G., M.B. and
437 F.C.; funding acquisition, L.N., O.G., J.M.M., M.B. and F.C. All authors have read and agreed to
438 the published version of the manuscript.
439

For Peer Review

440 **5. REFERENCES**

- 441 1. van der Linde D, Konings EE, Slager MA, Witsenburg M, Helbing WA, Takkenberg JJ, Roos-
442 Hesselink JW. Birth prevalence of congenital heart disease worldwide: a systematic review
443 and meta-analysis. *J Am Coll Cardiol.* 2011 Nov 15;58(21):2241–7.
- 444 2. Yamamoto Y, Hornberger LK. Progression of outflow tract obstruction in the fetus. *Early*
445 *Hum Dev.* 2012 May;88(5):279–85.
- 446 3. Gottschalk I, Strizek B, Menzel T, Herberg U, Breuer J, Brockmeier K, Geipel A, Gembruch
447 U, Berg C. Severe pulmonary stenosis or atresia with intact ventricular septum in the fetus:
448 the natural history. *Fetal Diagn Ther.* 2020;47(5):420–428.
- 449 4. Todros T, Paladini D, Chiappa E, Russo MG, Gaglioti P, Pacileo G, Cau MA, Martinelli P.
450 Pulmonary stenosis and atresia with intact ventricular septum during prenatal life.
451 *Ultrasound Obstet Gynecol.* 2003 Mar;21(3):228–33.
- 452 5. Villalain C, Moon-Grady AJ, Herberg U, Strainic J, Cohen JL, Shah A, Levi DS, Gómez-Montes
453 E, Herraiz I, Galindo A. Prediction of postnatal circulation in pulmonary atresia/critical
454 stenosis with intact ventricular septum: systematic review and external validation of
455 models. *Ultrasound Obstet Gynecol.* 2023 Jul;62(1)14–22.
- 456 6. Guirado L, Crispi F, Masoller N, Bennasar M, Marimon E, Carretero J, Gratacós E, Martínez
457 JM, Friedberg MK, Gómez O. Biventricular impact of mild to moderate fetal pulmonary
458 valve stenosis. *Ultrasound Obstet Gynecol.* 2018 Mar;51(3):349–356.
- 459 7. Roman KS, Fouron JC, Nii M, Smallhorn JF, Chaturvedi R, Jaeggi ET. Determinants of
460 outcome in fetal pulmonary valve stenosis or atresia with intact ventricular septum. *Am J*
461 *Cardiol.* 2007 Mar 1;99:699–703.
- 462 8. Gómez-Montes E, Herraiz I, Mendoza A, Albert L, Hernández-García JM, Galindo A.
463 Pulmonary atresia/critical stenosis with intact ventricular septum: prediction of outcome
464 in the second trimester of pregnancy. *Prenat Diagn.* 2011 Apr;31(4):372–9.
- 465 9. Forsey J, Ch B, Friedberg MK, Mertens L. Speckle Tracking echocardiography in pediatric
466 and congenital heart disease. *Echocardiography.* 2013 Apr;30(4):447–59.
- 467 10. Geyer H, Caracciolo G, Abe H, Wilansky S, Carerj S, Gentile F, Nesser HJ, Khandheria B,
468 Narula J, Sengupta PP. Assessment of myocardial mechanics using speckle tracking
469 echocardiography: fundamentals and clinical applications. *J Am Soc Echocardiogr.* 2010
470 Apr;23(4):351–69.
- 471 11. Levy PT, Machevsky A, Sanchez AA, Patel MD, Rogal S, Fowler S, Yaeger L, Hardi A, Holland
472 MR, Hamvas A, Singh GK. Reference ranges of left ventricular strain measures by two-
473 dimensional speckle tracking echocardiography in children: a systematic review and meta-
474 analysis. *J Am Soc Echocardiogr.* 2016 Mar;29(3):209–225.
- 475 12. Colquitt JL, Pignatelli RH. Strain imaging: the emergence of speckle tracking
476 echocardiography into clinical pediatric cardiology. *Congenit Heart Dis.* 2016 Mar-
477 Apr;11(2):199–207.
- 478 13. Huntgeburth M, Germund I, Geerdink LM, Sreeram N, Udink Ten Cate FEA. Emerging

- 479 clinical applications of strain imaging and three-dimensional echocardiography for the
480 assessment of ventricular function in adult congenital heart disease. *Cardiovasc Diagn*
481 *Ther.* 2019 Oct;9(Suppl 2):S326–345.
- 482 14. Gozar L, Iancu M, Gozar H, Sglimbea A, Cerghit Paler A, Gabor-Miklosi D, Toganel R,
483 Fagarasan A, Iurian DR, Toma D. Assessment of biventricular myocardial function with 2-
484 dimensional strain and conventional echocardiographic parameters: a comparative
485 analysis in healthy infants and patients with severe and critical pulmonary stenosis. *J Pers*
486 *Med.* 2022 Jan 6;12(1):57.
- 487 15. Germanakis I, Matsui H, Gardiner HM. Myocardial strain abnormalities in fetal congenital
488 heart disease assessed by speckle tracking echocardiography. *Fetal Diagn Ther.* 2012;32(1–
489 2):123–30.
- 490 16. Devore GR, Polanco B, Satou G, Sklansky M. Two-Dimensional speckle tracking of the fetal
491 heart: a practical step-by-step approach for the fetal sonologist. *J Ultrasound Med.* 2016
492 Aug;35(8):1765–81.
- 493 17. Day TG, Charakida M, Simpson JM. Using speckle-tracking echocardiography to assess fetal
494 myocardial deformation: are we there yet? *Ultrasound Obstet Gynecol.* 2019
495 Nov;54(5):575–581.
- 496 18. Germanakis I, Gardiner H. Assessment of fetal myocardial deformation using speckle
497 tracking techniques. *Fetal Diagn Ther.* 2012;32(1-2):39–46.
- 498 19. Yim D, Hui W, Larios G, Dragulescu A, Grosse-Wortmann L, Bijnens B, Mertens L, Friedberg
499 MK. Quantification of right ventricular electromechanical dyssynchrony in relation to right
500 ventricular function and clinical outcomes in children with repaired tetralogy of fallot. *J*
501 *Am Soc Echocardiogr.* 2018 Jul;31(7):822–30.
- 502 20. Cuyper JA, Witsenburg M, van der Linde D, Roos-Hesselink JW. Pulmonary stenosis:
503 update on diagnosis and therapeutic options. *Heart.* 2013 Mar;99(5):339–47.
- 504 21. Salomon LJ, Alfirevic Z, Berghella V, Bilardo CM, Chalouhi GE, Da Silva Costa F, Hernandez-
505 Andrade E, Malinger G, Munoz H, Paladini D, Perfumo F, Sotiriadis A, Toi A, Lee W. ISUOG
506 Practice guidelines (updated): performance of the routine mid-trimester fetal ultrasound
507 scan. *Ultrasound Obstet Gynecol.* 2022 Jun;59(6):840–856.
- 508 22. Carvalho JS, Allan LD, Chaoui R, Copel JA, DeVore GR, Hecher K, Lee W, Munoz H, Paladini
509 D, Tutschek B, Yagel S. ISUOG Practice Guidelines (updated): sonographic screening
510 examination of the fetal heart. *Ultrasound Obstet Gynecol.* 2013 Mar;41(3):348–59.
- 511 23. Robinson HP, Sweet EM, Adam AH. The accuracy of radiological estimates of gestational
512 age using early fetal crown-rump length measurements by ultrasound as a basis for
513 comparison. *Br J Obstet Gynaecol.* 1979 Jul;86(7):525–8.
- 514 24. Hadlock FP, Harrist RB, Shah YP, King DE, Park SK, Sharman RS. Estimating fetal age using
515 multiple parameters: a prospective evaluation in a racially mixed population. *Am J Obstet*
516 *Gynecol.* 1987 Apr;156(4):955–7.
- 517 25. Figueras F, Meler E, Iraola A, Eixarch E, Coll O, Figueras J, Francis A, Gratacos E, Gardosi J.
518 Customized birthweight standards for a Spanish population. *Eur J Obstet Gynecol Reprod*
519 *Biol.* 2008 Jan;136(1):20–4.

- 520 26. Baschat AA, Gembruch U. The cerebroplacental Doppler ratio revisited. *Ultrasound Obstet*
521 *Gynecol.* 2003 Feb;21(2):124–7.
- 522 27. Soveral I, Crispi F, Guirado L, García-Otero L, Torres X, Bennasar M, Sepúlveda-Martínez Á,
523 Nogué L, Gratacós E, Martínez JM, Bijns B, Friedberg M, Gómez O. Fetal cardiac filling
524 and ejection time fractions by pulsed-wave Doppler: reference ranges and potential
525 clinical application. *Ultrasound Obstet Gynecol.* 2021 Jul;58(1):83–91.
- 526 28. Guirado L, Crispi F, Soveral I, Valenzuela-Alcaraz B, Rodríguez-López M, García-Otero L,
527 Torres X, Sepúlveda-Martínez Á, Escobar-Díaz MC, Martínez JM, Friedberg MK, Gratacós E,
528 Gómez O. Nomograms of Fetal Right Ventricular Fractional Area Change by 2D
529 Echocardiography. *Fetal Diagn Ther.* 2020;47:399–410.
- 530 29. Nogué L, Gómez O, Izquierdo N, Mula C, Masoller N, Martínez JM, Gratacós E, Devore G,
531 Crispi F, Bennasar M. Feasibility of 4D-Spatio Temporal Image Correlation (STIC) in the
532 Comprehensive Assessment of the Fetal Heart Using FetalHQ®. *J Clin Med.* 2022 Mar
533 4;11(5):1414.
- 534 30. DeVore GR, Klas B, Satou G, Sklansky M. Evaluation of the right and left ventricles: An
535 integrated approach measuring the area, length, and width of the chambers in normal
536 fetuses. *Prenat Diagn.* 2017 Dec;37(12):1203–1212.
- 537 31. Devore GR, Klas B, Satou G, Sklansky M, M- U. Longitudinal annular systolic displacement
538 compared to global strain in normal fetal hearts and those with cardiac abnormalities. *J*
539 *Ultrasound Med.* 2018;37(5):1156–1171.
- 540 32. Devore GR, Satou G, Sklansky M. Using speckle-tracking echocardiography to assess fetal
541 myocardial deformation: are we there yet? Yes we are! *Ultrasound Obstet Gynecol.* 2019
542 Nov;54(5):703–704.
- 543 33. Devore GR, Klas B, Satou G, Sklansky M. Speckle tracking of the basal lateral and septal
544 wall annular plane systolic excursion of the right and left ventricles of the fetal heart. *J*
545 *Ultrasound Med.* 2019 May;38(5):1309–1318.
- 546 34. Devore GR, Klas B, Satou G, Sklansky M. Quantitative evaluation of fetal right and left
547 ventricular fractional area change using speckle-tracking technology. *Ultrasound Obstet*
548 *Gynecol.* 2019 Feb;53(2):219–228.
- 549 35. Devore GR, Klas B, Satou G, Sklansky M. Evaluation of fetal left ventricular tracking and the
550 simpson rule. *J Ultrasound Med.* 2019 May;38(5):1209–1221.
- 551 36. Hui W, Slorach C, Dragulescu A, Mertens L, Bijns B, Friedberg MK. Mechanisms of right
552 ventricular electromechanical dyssynchrony and mechanical inefficiency in children after
553 repair of tetralogy of fallot. *Circ Cardiovasc Imaging.* 2014 Jul;7(4):610–8.
- 554 37. Haji K, Marwick TH. Clinical utility of echocardiographic strain and strain rate
555 measurements. *Curr Cardiol Rep.* 2021 Feb 16;23(3):18.
- 556 38. Barker PC, Houle H, Li JS, Miller S, Herlong JR, Camitta MG. Global longitudinal cardiac
557 strain and strain rate for assessment of fetal cardiac function: novel experience with
558 velocity vector imaging. *Echocardiography.* 2009 Jan;26(1):28–36.
- 559 39. Mahfouz RA, Moustafa TM, Gouda M, Gad M. Longitudinal function and ventricular

- 560 dyssynchrony are restored in children with pulmonary stenosis after percutaneous balloon
561 pulmonary valvuloplasty. *Int J Cardiovasc Imaging*. 2017 Apr;33(4):533–538.
- 562 40. Li SJ, Yu HK, Wong SJ, Cheung YF. Right and left ventricular mechanics and interaction late
563 after balloon valvoplasty for pulmonary stenosis. *Eur Heart J Cardiovasc Imaging*. 2014
564 Sep;15(9):1020–8.
- 565 41. Wang Q, Wu YR, Jiao XT, Wu PF, Zhao LQ, Chen S, Sun K. Fetal pulmonary valve stenosis or
566 atresia with intact ventricular septum: Predictors of need for neonatal intervention. *Prenat*
567 *Diagn*. 2018 Mar;38(4):273–279.
- 568

For Peer Review

570 **Figure legends**

571 **Figure 1.** Flow chart of fetuses with pulmonary stenosis included in the study. PS: pulmonary
572 stenosis.

573 **Figure 2.** Right ventricle segmental strain curves display in a fetus with mild pulmonary stenosis.
574 Segment 1 (free-wall basal) corresponds to light blue curve, segment 2 (free-wall mid-ventricle)
575 dark blue curve, segment 3 (free-wall apical) red line, segment 4 (septum basal) orange curve,
576 segment 5 (septum mid-ventricular) yellow curve, segment 6 (septum apical) green curve. White
577 curve represents global strain. (a) Time-to-peak shortening (ms) of global strain and segments
578 1, 2, 3. (b) Peak systolic strain (%) (global strain and segment 1, 2, 3). eD is end diastolic frame
579 and eS end systolic frame.

580 **Figure 3.** Linear association between mechanical dispersion and right ventricle (RV) fractional
581 area change (FAC) (left graphic), and RV global longitudinal strain (GLS) absolute value (right
582 graphic).

583 **Figure 4.** Values of right ventricle global longitudinal strain (RV GLS) (left) and ductus venosus
584 pulsatility index centile (DV centile) (right) of pulmonary stenosis fetuses classified according to
585 the need of neonatal valvuloplasty. Reference line is set at -15.85% RV GLS and DV centile 79%,
586 identified at receiver operating characteristic curves.

587 **Figure 5.** Receiver-operating characteristic (ROC) curves of Scoring System (red thick line) area
588 under the curve (AUC) 0.931, scoring System without right ventricle global longitudinal strain
589 (RV GLS) (dashed line) AUC 0.917, ductus venosus pulsatility index centile (DV PI) (blue line) AUC:
590 0.782, RV GLS (Orange line) AUC 0.833 , reversed flow at the ductus arteriosus (DA) (yellow line)
591 AUC 0.750 and significant tricuspid regurgitation (TR) (green line) AUC 0.806; as predictors for
592 neonatal valvuloplasty.

593 **Table 1.** Maternal and perinatal characteristics in pulmonary stenosis (PS) versus healthy control
 594 fetuses, as well as PS subdivided according to the need of neonatal valvuloplasty

| Variable | Pulmonary Stenosis (n=24) | Control group (n=48) | p value* | Neonatal valvuloplasty (n=12) | No neonatal valvuloplasty (n=12) | p value† |
|--|---------------------------|---------------------------|--------------|----------------------------------|----------------------------------|--------------|
| MATERNAL CHARACTERISTICS | | | | | | |
| Maternal age (years) | 35.12 ± 5.53 | 33.30 ± 4.50 | 0.141 | 37.51 (36.00-39.75) | 33.54 (28.25-36.00) | 0.018 |
| Body mass index (kg/m ²) | 23.63 ± 3.97 | 22.78 ± 3.90 | 0.282 | 23.93 ± 3.32 | 23.82 ± 4.38 | 0.948 |
| Nulliparity | 11 (45.83%) | 21 (43.75%) | 1.000 | 5 (41.67%) | 5 (41.67%) | 1.000 |
| Artificial Reproductive Technologies | 4 (16.67%) | 6 (12.50%) | 0.722 | 3 (25.00%) | 1 (8.33%) | 0.590 |
| PERINATAL CHARACTERISTICS | | | | | | |
| Gestational age at birth (weeks.days) | 39.0 ± 2.7 | 39.6 ± 1.3 | 0.562 | 39.3 ± 1.4 | 38.6 ± 3.4 | 0.562 |
| Cesarean section | 5 (20.83%) | 11 (22.92%) | 1.000 | 1 (8.33%) | 4 (33.33%) | 0.317 |
| Birthweight (g) | 2992.00 (2910.00-3645.00) | 3400.00 (3195.50-3754.75) | 0.090 | 2930.00 (2800.00-2977.50) | 3645.00 (3118.50-3850.00) | 0.020 |
| Five-minute APGAR <7 | 2 (8.33%) | 0 (0.00%) | 0.108 | 0 (0.00%) | 2 (16.67%) | 0.478 |
| Umbilical artery pH | 7.24 ± 0.07 | 7.24 ± 0.08 | 0.995 | 7.21 ± 0.08 | 7.26 ± 0.05 | 0.101 |
| <p>Data expressed as mean ± standard deviation, median (interquartile range) or n (percentage). *P-value comparing pulmonary stenosis (PS) versus controls calculated by t-test for continuous variables and Fisher's exact for categorical variables. †P-value comparing PS that required neonatal valvuloplasty versus those that did not, calculated by t-test for continuous variables and Fisher's exact for categorical variables.</p> | | | | | | |

595

596

597 **Table 2.** Feto-placental ultrasonographic results in pulmonary stenosis (PS) fetuses and healthy
 598 controls, and also PS cases subdivided according to the need of neonatal valvuloplasty
 599

| Variable | Pulmonary Stenosis (n=24) | Controls (n=48) | p value* | Neonatal valvuloplasty (n=12) | No neonatal valvuloplasty (n=12) | p value† |
|--|-------------------------------|--------------------------|------------------|-------------------------------|----------------------------------|--------------|
| Gestational age ultrasound (weeks.days) | 33.4 (27.1-35.5) | 32.3 (29.1-36.5) | 0.496 | 29.4 (24.0-34.5) | 34.4 (31.3-37.5) | 0.077 |
| Estimated fetal weight (g) | 2443.00 (1669.50-2962.00) | 2141.50 (1341.00-2838.5) | 0.383 | 1917.50 (1081.75-2652.75) | 2958.00 (1981.50-3062.00) | 0.068 |
| Estimated fetal weight centile | 43.00 (28.50-76.50) | 49.00 (31.50-85.00) | 0.740 | 45.50 (28.75-72.50) | 36.00 (28.00-68.00) | 0.821 |
| FETAL DOPPLER | | | | | | |
| Umbilical artery PI | 0.95 ± 0.26 | 1.01 ± 0.16 | 0.288 | 0.98 ± 0.24 | 0.91 ± 0.27 | 0.536 |
| Middle cerebral artery PI | 2.11 ± 0.54 | 1.84 ± 0.34 | 0.046 | 2.15 ± 0.65 | 2.04 ± 0.45 | 0.653 |
| Cerebroplacental ratio | 2.20 (1.84-2.57) | 1.86 (1.50-2.17) | 0.102 | 2.21 (1.78-2.49) | 2.07 (1.55-2.81) | 0.539 |
| Ductus venosus PI centile | 89.00 (30.11-99.43) | 19.06 (4.25-53.00) | <0.001 | 99.44 (86.75-100.00) | 38.18 (16.51-80.54) | 0.028 |
| Tricuspid regurgitation | 13 (54.17%) | 0 (0.00%) | <0.001 | 9 (75.00%) | 4 (33.33%) | 0.100 |
| Ductus arteriosus reversed flow | 7 (29.17%) | 0 (0.00%) | <0.001 | 7 (58.33%) | 0 (0.00%) | 0.005 |
| PULMONARY VALVE | | | | | | |
| Pulmonary valve peak systolic velocity (cm/s) | 172.11 (141.00-319.50) | 79.00 (72.00-86.25) | <0.001 | 320.00 (304.00-373.00) | 146.40 (127.50-168.50) | 0.001 |
| <i>PI: Pulsatility Index.</i> <i>Data expressed as mean ± standard deviation, median (interquartile range) or n (percentage).</i> <i>*P-value comparing pulmonary stenosis (PS) versus controls calculated by t-test or Mann-Whitney U test according to its distribution (normal or non-normal) for continuous variables and Fisher's exact for categorical variables.</i> <i>†P-value comparing PS that required neonatal valvuloplasty versus those that did not calculated by t-test or Mann-Whitney U test according to its distribution (normal or non-normal) for continuous variables and Fisher's exact for categorical variables.</i> | | | | | | |

600

601

602 **Table 3.** Speckle tracking echocardiographic results in fetuses with pulmonary stenosis (PS) and
 603 healthy controls, as well as PS cases subdivided according to the need of neonatal valvuloplasty

| Parameter | Pulmonary Stenosis (n=24) | Control group (n=48) | p value* | Neonatal valvuloplasty (n=12) | No neonatal valvuloplasty (n=12) | p value† |
|---|----------------------------|----------------------|--------------|-------------------------------|----------------------------------|--------------|
| RIGHT VENTRICLE MORPHOMETRY | | | | | | |
| Ventricular Area (cm ²) | 3.03 ± 1.28 | 3.28 ± 1.24 | 0.488 | 2.61 ± 0.88 | 3.51 ± 1.24 | 0.045 |
| Longitudinal diameter (mm) | 23.91 ± 5.14 | 26.06 ± 4.48 | 0.113 | 22.32 ± 3.70 | 25.86 ± 4.85 | 0.101 |
| Basal diameter (mm) | 14.10 ± 3.73 | 13.88 ± 3.61 | 0.807 | 12.66 ± 2.48 | 15.57 ± 3.83 | 0.044 |
| Mid-ventricular diameter (mm) | 13.97 ± 4.12 | 14.04 ± 3.20 | 0.923 | 12.72 ± 2.19 | 15.64 ± 4.46 | 0.039 |
| RIGHT VENTRICLE FUNCTION | | | | | | |
| Global longitudinal strain (%) | -16.33 ± 5.88 | -18.87 ± 3.07 | 0.047 | -13.51 ± 6.23 | -20.13 ± 4.66 | 0.005 |
| Fractional area change (%) | 27.04 ± 13.31 | 30.72 ± 5.15 | 0.307 | 21.77 ± 14.25 | 33.09 ± 8.32 | 0.026 |
| Tricuspid annular plane systolic excursion (mm) ‡ | 4.25 ± 2.04 | 6.00 ± 1.66 | 0.002 | 3.49 ± 1.30 | 5.11 ± 2.03 | 0.135 |
| RIGHT VENTRICLE DYSSYNCHRONY | | | | | | |
| RV free wall peak systolic strain delay (ms) | 42.00 (28.50-80.00) | 13.00 (0.00-35.00) | 0.30 | 45.00 (28.50-123.50) | 39.50 (30.25-65.00) | 0.684 |
| IntraRV dyssynchrony index | 41.31 (31.47-74.93) | 33.59 (21.23-37.88) | 0.042 | 82.34 (45.00-115.51) | 40.89 (28.49-45.81) | 0.198 |
| LEFT VENTRICLE MORPHOMETRY | | | | | | |
| Ventricular Area (cm ²) | 3.03 ± 0.88 | 3.09 ± 0.82 | 0.586 | 2.89 ± 0.85 | 3.15 ± 0.72 | 0.246 |
| Longitudinal diameter (mm) | 25.31 ± 3.60 | 27.18 ± 4.55 | 0.080 | 25.03 ± 4.19 | 26.21 ± 2.20 | 0.319 |
| Basal diameter (mm) | 11.98 (9.31-14.24) | 11.81 (10.50-14.11) | 0.830 | 12.04 (8.33-14.36) | 12.72 (9.61-14.18) | 0.079 |
| Mid-ventricular diameter (mm) | 13.53 ± 2.76 | 13.22 ± 2.29 | 0.671 | 13.07 ± 3.02 | 14.17 ± 2.41 | 0.771 |
| LEFT VENTRICLE FUNCTION | | | | | | |
| Global longitudinal strain (%) | -21.09 ± 4.00 | -20.21 ± 3.33 | 0.629 | -21.10 ± 3.97 | -20.19 ± 3.31 | 0.629 |
| Ejection fraction (%) | 50.45 ± 12.81 | 48.66 ± 9.69 | 0.495 | 50.48 ± 12.81 | 48.68 ± 9.71 | 0.495 |
| Mitral annular plane systolic excursion (mm) ‡ | 4.89 ± 1.37 | 5.71 ± 1.52 | 0.101 | 4.94 ± 1.36 | 5.84 ± 1.52 | 0.869 |
| LEFT VENTRICLE DYSSYNCHRONY | | | | | | |
| LV free wall peak systolic strain delay (ms) | 39.00 (20.00-48.00) | 21.50 (3.00-36.75) | 0.234 | 27.00 (10.00-47.50) | 40.00 (21.50-47.50) | 0.414 |
| IntraLV dyssynchrony index | 27.75 (20.62-41.44) | 33.59 (21.23-37.88) | 0.989 | 24.84 (12.24-40.62) | 32.33 (22.03-43.64) | 0.414 |

Data expressed as mean \pm standard deviation or median (interquartile range).
Intra LV dyssynchrony index: Standard deviation of the time-to-peak systolic shortening of the 6 ventricular segments
*P-value comparing pulmonary stenosis (PS) versus controls calculated by t-test or Mann-Whitney U test according to its distribution (normal or non-normal).
†P-value comparing PS that required neonatal valvuloplasty versus those that did not by t-test or Mann-Whitney U test according to its distribution (normal or non-normal), adjusted by estimated fetal weight.
‡ Tricuspid/Mitral annular plane systolic excursion p-values are adjusted by RV/LV longitudinal diameter.

604

For Peer Review

605 **Table 4.** Prenatal and postnatal cardiac characteristics of 12 cases who required neonatal pulmonary valvuloplasty

| Case | GA at diagnosis (weeks, days) | Referral indication | GA at US (weeks, days) | Pulmonary valve PVS (cm/s) | Prenatal severity | TR (cm/s) | DA flow | DV/PI | RV GLS (%) | Scoring system | Postnatal pulmonary valve gradient (mmHg) | PG administration | Age at valvuloplasty (days) | Postnatal severity |
|------|-------------------------------|--------------------------|------------------------|----------------------------|-------------------|-----------|-----------|-------|------------|----------------|---|-------------------|-----------------------------|--------------------|
| 1 | 29.5 | CHD suspicion | 34.5 | 320 | Critical | 300 | Reversed | 0.72 | -7.53 | 4 | - | Yes | 7 | Critical |
| 2 | 37.4 | CHD suspicion | 37.4 | 440 | Critical | 450 | Reversed | 0.80 | -8.43 | 4 | - | Yes | 2 | Critical |
| 3 | 35.0 | CHD suspicion | 35.0 | 323 | Critical | 250 | Reversed | 0.68 | -18.41 | 3 | 40 | Yes | 3 | critical |
| 4 | 25.1 | CHD suspicion | 31.6 | 344 | Critical | 500 | Reversed | 0.86 | -12.53 | 4 | 100 | Yes | 1 | Critical |
| 5 | 22.0 | First trimester RVD flow | 26.0 | 62 | Critical | 410 | Reversed | 1.23 | -5.35 | 4 | 75 | Yes | 3 | Critical |
| 6 | 21.4 | CHD suspicion | 21.4 | 350 | Critical | 210 | Reversed | 1.21 | -4.00 | 4 | 95 | Yes | 3 | Critical |
| 7 | 33.1 | CHD suspicion | 35.6 | 378 | Moderate | 510 | Antegrade | 0.30 | -15.35 | 2 | 30 | Yes | 3 | Severe |
| 8 | 21.2 | CHD suspicion | 26.0 | 304 | Moderate | No | Antegrade | 1.08 | -14.77 | 2 | 90 | Yes | 3 | Severe |
| 9 | 20.5 | CHD suspicion | 28.6 | 373 | Critical | No | Reversed | 0.96 | -14.68 | 3 | 81 | Yes | 4 | Severe |
| 10 | 21.5 | CHD suspicion | 21.5 | 319 | Moderate | 219 | Antegrade | 0.98 | -1.70 | 3 | 70 | No | 6 | Moderate |
| 11 | 21.1 | Family history | 30.3 | 315 | Moderate | 200 | Antegrade | 1.29 | -10.12 | 3 | 60 | No | 10 | Moderate |
| 12 | 34.0 | CHD suspicion | 34.6 | 287 | Moderate | No | Antegrade | 0.31 | -21.75 | 0 | 65 | No | 29 | Moderate |

GA: gestational age; US: ultrasound; PVS: peak systolic velocity; TR: tricuspid regurgitation; DA: ductus arteriosus; DV/PI: Ductus venosus pulsatility index; RV GLS: right ventricle global longitudinal strain; PG: prostaglandin E₁; CHD: congenital heart defect; RVD: reversed ductus venosus.

606

607
608
609
610
611
612
613

Table 5. Receiver operating curves for the Scoring system, scoring system without right ventricle global longitudinal strain (RV GLS), Ductus venosus pulsatility index centile, right ventricle global longitudinal strain, ductus arteriosus reversed flow and significant tricuspid regurgitation for neonatal valvuloplasty prediction

| Parameter | AUC | Cut-off | 95% Confidence interval | p value | Sensitivity | Specificity |
|-------------------------------|-------|----------|-------------------------|---------|-------------|-------------|
| Scoring system* | 0.935 | ≥2 | 0.809-1 | 0.001 | 92% | 100% |
| Scoring system without RV GLS | 0.917 | ≥2 | 0.786-1 | 0.001 | 83% | 100% |
| DV PI centile | 0.782 | >79.00% | 0.567-0.998 | 0.030 | 82% | 91% |
| RV GLS | 0.833 | >-15.85 | 0.649-1 | 0.011 | 75% | 83% |
| DA flow | 0.750 | Reversed | 0.539-0.961 | 0.045 | 50% | 92% |
| Significant TR | 0.806 | Present | 0.602-1 | 0.019 | 83% | 75% |

AUC: area under the curve; RV GLS: right ventricle global longitudinal strain; DV PI: Ductus venosus pulsatility index; DA: ductus arteriosus; TR: tricuspid regurgitation
 * Scoring system includes DV PI centile, RV GLS, DA reversed flow and significant TR.
 A score of 1 was assigned for each present variable (DV IP centile > 79.00%, RV GLS > -15.85, reversed DA flow and significant TR). Cut-off ≥2 was considered when more than 2 variables were present.

614

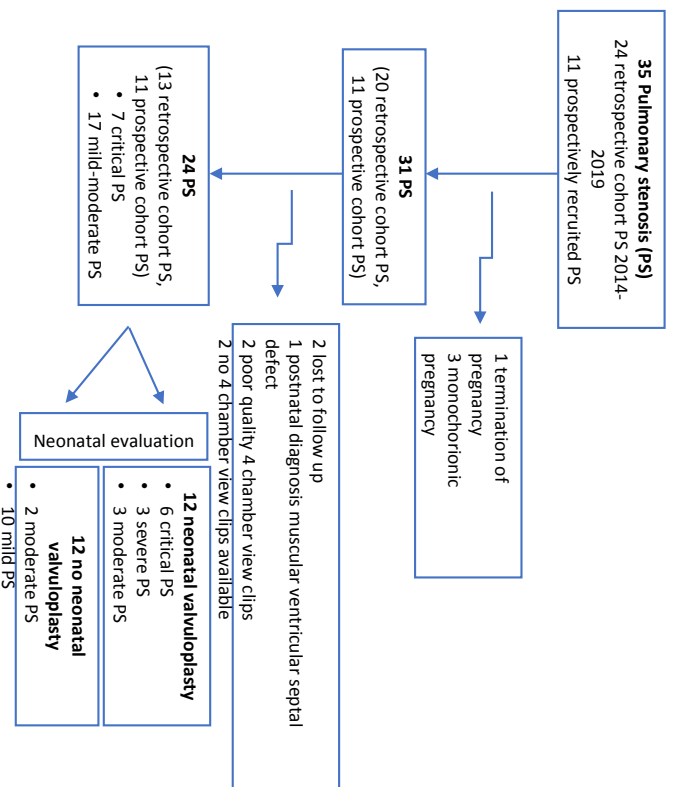
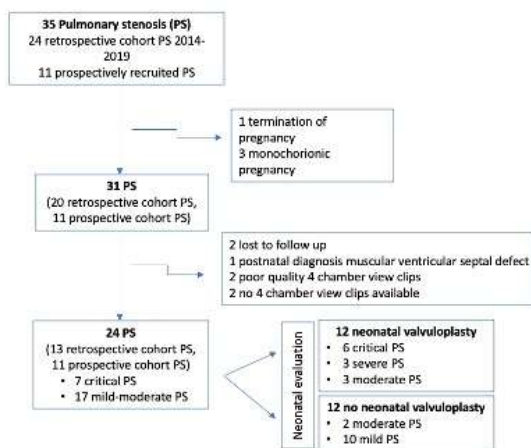


Figure 1. Flow chart of fetuses with pulmonary stenosis included in the study. PS: pulmonary stenosis.



Flow chart of fetuses with pulmonary stenosis included in the study. PS: pulmonary stenosis.

146x120mm (72 x 72 DPI)

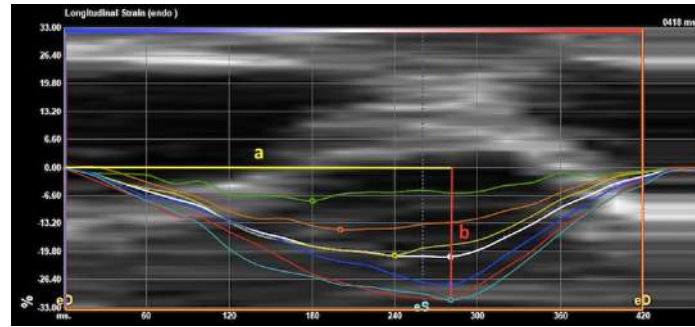
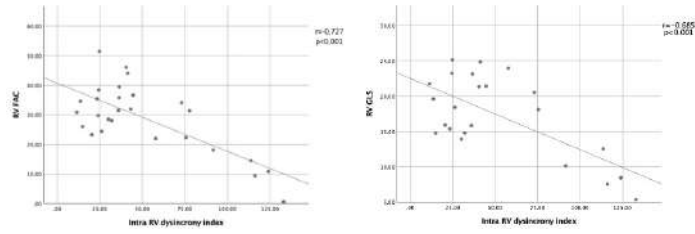


Figure 2. Right ventricle segmental strain curves display in a fetus with mild pulmonary stenosis. Segment 1 (free-wall basal) corresponds to light blue curve, segment 2 (free-wall mid-ventricle) dark blue curve, segment 3 (free-wall apical) red line, segment 4 (septum basal) orange curve, segment 5 (septum mid-ventricular) yellow curve, segment 6 (septum apical) green curve. White curve represents global strain. (a) Time-to-peak shortening (ms) of global strain and segments 1, 2, 3. (b) Peak systolic strain (%) (global strain and segment 1, 2, 3). eD is end diastolic frame and eS end systolic frame

287x133mm (72 x 72 DPI)



Linear association between mechanical dispersion and right ventricle (RV) fractional area change (FAC) (left graphic), and RV global longitudinal strain (GLS) absolute value (right graphic).

310x104mm (72 x 72 DPI)

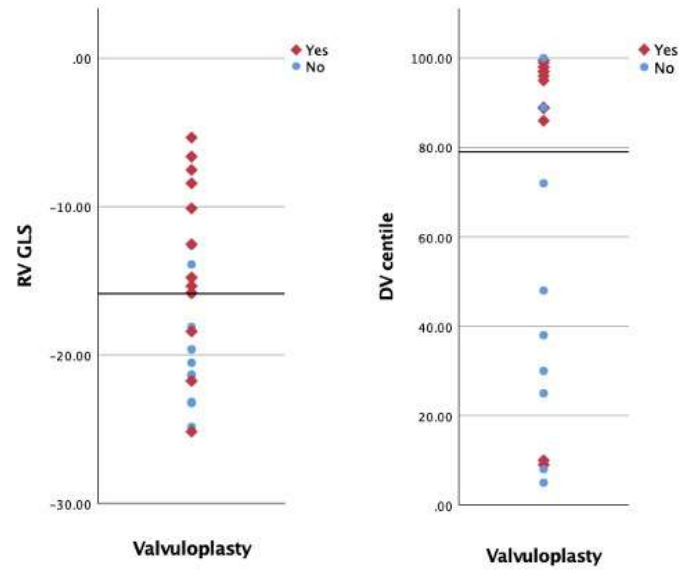


Figure 4. Values of right ventricle global longitudinal strain (RV GLS) (left) and ductus venosus pulsatility index centile (DV centile) (right) of pulmonary stenosis fetuses classified according to the need of neonatal valvuloplasty. Reference line is set at -15.85% RV GLS and DV centile 79%, identified at receiver operating characteristic curves.

177x154mm (72 x 72 DPI)

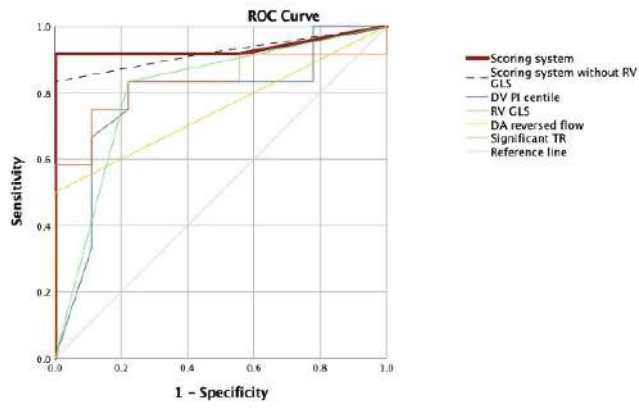


Figure 5. Receiver-operating characteristic (ROC) curves of Scoring System (red thick line) area under the curve (AUC) 0.931, scoring System without right ventricle global longitudinal strain (RV GLS) (dashed line) AUC 0.917, ductus venosus pulsatility index centile (DV PI) (blue line) AUC: 0.782, RV GLS (Orange line) AUC 0.833, reversed flow at the ductus arteriosus (DA) (yellow line) AUC 0.750 and significant tricuspid regurgitation (TR) (green line) AUC 0.806; as predictors for neonatal valvuloplasty.

230x138mm (72 x 72 DPI)

1 **Supplementary Table 1.** Methodology for conventional echocardiographic parameters
2

| | |
|---|--|
| Cardio thoracic ratio | Apical or transverse 4-chamber view in end-diastole. Cardiac area/Thoracic area*100 |
| Global sphericity index | Longitudinal cardiac diameter/transverse cardiac diameter |
| Free-wall and septal thickness | In end-diastole using M-mode from a transverse 4-chamber view ¹ |
| Ventricular transverse diameters | In end-diastole using M-mode from a transverse 4-chamber view(1) |
| Right and left ventricle relative wall thickness (RWT) | $RWT = (\text{septal wall thickness} + \text{free wall thickness})/\text{ventricular transverse diameter}^1$ |
| Septal to right or left free wall thickness ratio (SRWT, SLWT) | Is a measurement of wall thickness asymmetry $SRWT, SLWT = \text{septal wall thickness}/\text{free wall thickness}^1$ |
| Filling time fraction (FTF) | Measured from tricuspid and mitral diastolic spectral Doppler $FTF = \text{Filling time}/\text{Cardiac cycle} * 100^2$ |
| Ejection time fraction (ETF) | Measured from systolic pulmonary and aortic pulsed Doppler $ETF: \text{ejection time}/\text{cardiac cycle} * 100^2$ |
| Pulmonary and aortic valves diameter | Measured during systole with the valve opened ³ |
| Pulmonary and aortic systolic flows | Obtained in a right and left ventricle (RV, LV) outflow tract view with an angle to ultrasound beam close to 0°, from whose spectral Doppler peak systolic velocity, heart rate (HR) and velocity-time integral (VTI) (area under the curve of aortic and pulmonary flow traced manually) were assessed. |
| Right and left ventricle cardiac outputs (CO) | $CO = VTI \times \text{valve diameter} \times HR$ |
| Cardiac Index (CI) | Cardiac index accounts for combined right and left cardiac outputs. $CI = (RV-CO + LV-CO)/EFW \text{ (ml/min/Kg)}^4$ |

3

4 **Supplementary Table 2.** Maternal and perinatal characteristics in critical pulmonary stenosis
 5 (PS), mild-to-moderate PS and healthy control fetuses

| Variable | Critical Pulmonary Stenosis (n=7) | Mild Pulmonary Stenosis (n=17) | Control group (n=48) | p value |
|---|-----------------------------------|--------------------------------|---------------------------|--------------|
| MATERNAL CHARACTERISTICS | | | | |
| Maternal age (years) | 38.00 ± 2.24 | 33.94 ± 6.10 | 33.30 ± 4.50 | 0.061 |
| Body mass index (kg/m ²) | 21.98 ± 2.94 | 24.35 ± 4.23 | 22.78 ± 3.90 | 0.273 |
| Nulliparity | 3 (42.86%) | 8 (47.06%) | 21 (43.75%) | 1.000 |
| Artificial Reproductive Technologies | 0 (0.00%) | 4 (23.53%) | 6 (12.50%) | 0.422 |
| PERINATAL CHARACTERISTICS | | | | |
| Gestational age at birth (weeks.days) | 38.0 ± 1.6 | 39.2 ± 2.6 | 39.6 ± 1.3 | 0.060 |
| Cesarean section | 1 (14.28%) | 4 (23.53%) | 11 (22.92%) | 1.000 |
| Birthweight (g) | 2800.00 (2789.00-2950.00)*† | 3370.00 (2962.50-3767.50) | 3400.00 (3195.50-3754.75) | 0.013 |
| Five-minute APGAR <7 | 2 (28.57%) | 0 (0.00%) | 0 (0.00%) | 0.108 |
| Umbilical artery pH | 7.28 ± 0.06 | 7.23 ± 0.07 | 7.24 ± 0.08 | 0.654 |
| Data expressed as mean ± standard deviation or n (percentage). P-value comparing critical pulmonary stenosis (PS) vs mild-moderate PS vs controls calculated by ANOVA for continuous variables and Fisher's exact for categorical variables. *Denotes P<0.05 between critical PS as compared to controls (post-hoc comparisons using Dunn-Bonferroni for continuous variables). | | | | |

6

7

8 **Supplementary Table 3.** Feto-placental ultrasonographic results in critical pulmonary stenosis
 9 (PS), mild-to-moderate PS and healthy control fetuses

10

| Variable | Critical Pulmonary Stenosis (n=7) | Mild-moderate Pulmonary Stenosis (n=17) | Controls (n=48) | p value |
|--|-----------------------------------|---|---------------------------|------------------|
| Gestational age ultrasound (weeks.days) | 29.4 (24.0-33.5) | 33.4 (28.3-35.5) | 32.3 (29.1-36.5) | 0.305 |
| Estimated fetal weight (g) | 1619.00 (1039.50-2553.00) | 2474.00 (1895.00-2984.50) | 2141.50 (1341.00-2838.50) | 0.356 |
| Estimated fetal weight centile | 48.00 (35.50-89.00) | 37.00 (28.75.00-55.25) | 49.00 (31.50-85.00) | 0.650 |
| FETAL DOPPLER | | | | |
| Umbilical artery PI | 0.94 ± 0.23 | 0.96 ± 0.27 | 1.01 ± 0.16 | 0.554 |
| Middle cerebral artery PI | 2.08 ± 0.56 | 2.12 ± 0.54 | 1.84 ± 0.34 | 0.055 |
| Cerebroplacental ratio | 2.25 (1.85-2.46) | 2.12 (1.55-2.73) | 1.86 (1.50-2.17) | 0.181 |
| Ductus venosus PI centile | 99.11 (89.43-100.00)*† | 43.57 (9.75-99.25)‡ | 19.06 (4.25-53.00) | <0.001 |
| Tricuspid regurgitation | 7 (100.00%)*† | 6 (35.29%)‡ | 0 (0.00%) | <0.001 |
| Ductus arteriosus reversed flow | 7 (100.00%)*† | 0 (0.00%) | 0 (0.00%) | <0.001 |
| PULMONARY VALVE | | | | |
| Pulmonary valve peak systolic velocity (cm/s) | 333.00 (320.00-365.00) | 167.00 (140.00-287.00) | 79.00 (72.00-86.25) | <0.001 |
| <i>PI: Pulsatility Index.</i> <i>Data expressed as mean ± standard deviation, median (interquartile range) or n (percentage).</i> <i>P-value comparing critical pulmonary stenosis (PS) vs mild-moderate PS vs controls calculated by ANOVA or Kruskal-Wallis one-way ANOVA according to its distribution (normal or non-normal) for continuous variables, and Fisher's exact for categorical variables.</i> <i>*Denotes P<0.05 between critical PS as compared to controls (post-hoc comparisons using Dunn-Bonferroni for continuous and Chi-squared for categorical variables)</i> <i>† Denotes P<0.05 between critical PS as compared to mild PS (post-hoc comparisons using Dunn-Bonferroni for continuous and Chi-squared for categorical variables).</i> <i>‡ Denotes P<0.05 between mild PS as compared to controls (post-hoc comparisons using Dunn-Bonferroni for continuous and Chi-squared for categorical variables).</i> | | | | |

11

12

13 **Supplementary Table 4.** Standard echocardiographic results in pulmonary stenosis (PS) and
 14 healthy control fetuses, as well as PS cases subdivided according to the need of neonatal
 15 valvuloplasty

| Variable | Pulmonary Stenosis (n=24) | Controls (n=48) | p value* | Neonatal valvuloplasty (n=12) | No neonatal valvuloplasty (n=12) | p value† |
|---|---------------------------|-----------------|----------------|-------------------------------|----------------------------------|----------------|
| GLOBAL CARDIAC PARAMETERS | | | | | | |
| Cardio thoracic ratio | 0.36 ± 0.09 | 0.30 ± 0.04 | < 0.001 | 0.36 ± 0.06 | 0.38 ± 0.11 | 0.734 |
| Global sphericity index | 1.17 ± 0.19 | 1.24 ± 0.09 | 0.001 | 1.25 ± 0.24 | 1.08 ± 0.09 | 0.063 |
| Cardiac index (ml/min/kg) | 617.52 ± 212.60 | 353.69 ± 77.48 | < 0.001 | 579.61 ± 162.55 | 649.26 ± 249.52 | 0.824 |
| RIGHT VENTRICLE MORPHOMETRY | | | | | | |
| Pulmonary valve (mm) | 5.40 ± 1.80 | 6.70 ± 1.42 | < 0.001 | 3.93 ± 1.10 | 6.64 ± 1.27 | < 0.001 |
| Right ventricle wall thickness (mm) | 4.44 ± 1.09 | 3.38 ± 0.64 | 0.001 | 4.63 ± 1.20 | 4.47 ± 0.84 | 0.350 |
| Septal to right ventricle free wall thickness ratio | 0.92 ± 0.39 | 0.99 ± 0.11 | 0.078 | 1.09 ± 0.37 | 0.68 ± 0.28 | 0.074 |
| Right ventricle relative wall thickness | 1.85 ± 1.26 | 0.49 ± 0.09 | < 0.001 | 1.65 ± 0.70 | 1.98 ± 1.74 | 0.602 |
| RIGHT VENTRICLE FUNCTION | | | | | | |
| Right ventricle output (ml/min) | 918.55 ± 639.58 | 431.85 ± 220.52 | < 0.001 | 752.73 ± 412.08 | 1069.30 ± 782.81 | 0.148 |
| Tricuspid filling time fraction (%) | 36.27 ± 5.70 | 39.54 ± 2.25 | 0.021 | 36.27 ± 5.70 | 39.54 ± 2.25 | 0.246 |
| Pulmonary ejection time fraction (%) | 43.04 ± 5.12 | 41.93 ± 1.87 | 0.356 | 33.63 ± 5.22 | 38.37 ± 5.07 | 0.062 |
| LEFT VENTRICLE MORPHOMETRY | | | | | | |
| Aortic valve (mm) | 5.93 ± 1.24 | 5.78 ± 1.36 | 0.638 | 5.33 ± 0.80 | 6.52 ± 1.26 | 0.016 |
| Septal wall thickness (mm) | 4.41 ± 1.67 | 3.32 ± 0.63 | 0.001 | 5.13 ± 2.12 | 3.80 ± 2.12 | 0.062 |
| Left ventricle wall thickness (mm) | 3.90 ± 0.87 | 3.22 ± 0.64 | 0.001 | 3.86 ± 0.93 | 4.08 ± 0.77 | 0.816 |
| Septal to left ventricular free wall thickness ratio | 1.15 ± 0.41 | 1.04 ± 0.13 | 0.936 | 1.35 ± 0.49 | 0.92 ± 0.12 | 0.087 |
| Left ventricle relative wall thickness | 0.89 ± 0.43 | 0.59 ± 0.66 | < 0.001 | 0.98 ± 0.54 | 0.81 ± 0.29 | 0.663 |
| LEFT VENTRICLE FUNCTION | | | | | | |
| Aortic valve peak systolic velocity (cm/s) | 101.18 ± 19.66 | 81.08 ± 10.71 | < 0.001 | 106.67 ± 17.60 | 95.19 ± 20.60 | 0.156 |
| Left ventricle output (ml/min) | 517.55 ± 258.28 | 326.33 ± 195.35 | 0.001 | 416.51 ± 216.38 | 593.32 ± 269.49 | 0.123 |
| Mitral Filling time fraction (%) | 42.52 ± 5.56 | 43.07 ± 2.92 | 0.688 | 41.07 ± 2.64 | 43.39 ± 7.47 | 0.393 |
| Aortic ejection time fraction (%) | 41.72 ± 5.82 | 40.96 ± 1.74 | 0.321 | 42.62 ± 7.41 | 41.19 ± 4.71 | 0.608 |
| <i>Data expressed as mean ± standard deviation</i> | | | | | | |
| <i>*P-value comparing pulmonary stenosis (PS) versus controls calculated by t-test.</i> | | | | | | |
| <i>†P-value comparing PS that required neonatal valvuloplasty versus those that did not calculated by t-test.</i> | | | | | | |
| <i>The p-value for morphometric parameters has been adjusted for estimated fetal weight.</i> | | | | | | |

16 **Supplementary Table 5.** Standard echocardiographic results in critical pulmonary stenosis (PS),
 17 mild-to-moderate PS and healthy control fetuses

18

| Variable | Critical Pulmonary Stenosis (n=7) | Mild-moderate Pulmonary Stenosis (n=17) | Controls (n=48) | p value |
|---|-----------------------------------|---|-----------------|------------------|
| GLOBAL CARDIAC PARAMETERS | | | | |
| Cardio thoracic ratio | 0.34 ± 0.04 | 0.37 ± 0.10‡ | 0.30 ± 0.04 | 0.001 |
| Global sphericity index | 1.21 ± 0.10 | 1.15 ± 0.22‡ | 1.24 ± 0.09 | 0.001 |
| Cardiac index (ml/min/kg) | 563.01 ± 201.99* | 640.81 ± 220.05‡ | 353.69 ± 77.48 | <0.001 |
| RIGHT VENTRICLE MORPHOMETRY | | | | |
| Pulmonary valve (mm) | 3.99 ± 1.06*† | 5.98 ± 1.72 | 6.70 ± 1.46 | <0.001 |
| Right ventricle wall thickness (mm) | 4.42 ± 1.54* | 4.45 ± 0.89‡ | 3.38 ± 0.64 | <0.001 |
| Septal to right ventricle free wall thickness ratio | 1.21 ± 0.41 | 0.77 ± 0.29†† | 0.99 ± 0.11 | 0.026 |
| Right ventricle relative wall thickness | 1.97 ± 0.69* | 1.79 ± 1.48‡ | 0.49 ± 0.09 | <0.001 |
| RIGHT VENTRICLE FUNCTION | | | | |
| Right ventricle output (ml/min) | 707.30 ± 471.74 | 1003.05 ± 691.46‡ | 431.85 ± 220.52 | <0.001 |
| Tricuspid filling time fraction (%) | 33.94 ± 5.62* | 37.27 ± 5.64 | 39.54 ± 2.25 | 0.018 |
| Pulmonary ejection time fraction (%) | 45.28 ± 4.27 | 42.29 ± 5.29 | 41.93 ± 1.87 | 0.126 |
| LEFT VENTRICLE MORPHOMETRY | | | | |
| Aortic valve (mm) | 5.53 ± 0.82 | 6.10 ± 1.36 | 5.58 ± 1.36 | 0.799 |
| Septal wall thickness (mm) | 5.50 ± 2.44* | 3.82 ± 0.64‡ | 3.32 ± 0.63 | 0.022 |
| Left ventricle wall thickness (mm) | 3.55 ± 0.90 | 4.09 ± 0.82‡ | 3.22 ± 0.64 | <0.001 |
| Septal to left ventricular free wall thickness ratio | 1.51 ± 0.44*† | 0.96 ± 0.22 | 1.04 ± 0.13 | 0.001 |
| Left ventricle relative wall thickness | 0.76 ± 0.19 | 0.96 ± 0.51 | 0.59 ± 0.66 | 0.054 |
| LEFT VENTRICLE FUNCTION | | | | |
| Aortic valve peak systolic velocity (cm/s) | 104.29 ± 17.50* | 99.90 ± 20.85‡ | 81.08 ± 10.71 | <0.001 |
| Left ventricle output (ml/min) | 549.32 ± 259.09* | 504.84 ± 265.93‡ | 326.33 ± 195.35 | 0.004 |
| Mitral Filling time fraction (%) | 41.73 ± 3.89 | 42.81 ± 6.15 | 43.07 ± 2.92 | 0.756 |
| Aortic ejection time fraction (%) | 39.61 ± 2.11 | 42.37 ± 6.49 | 40.96 ± 1.74 | 0.336 |
| <p>Data expressed as mean ± standard deviation P-value comparing critical pulmonary stenosis (PS) vs mild-moderate PS vs controls calculated by ANOVA. *Denotes P<0.05 between critical PS as compared to controls (post-hoc comparisons using Dunn-Bonferroni). † Denotes P<0.05 between critical PS as compared to mild PS (post-hoc comparisons using Dunn-Bonferroni). ‡ Denotes P<0.05 between mild PS as compared to controls (post-hoc comparisons using Dunn-Bonferroni). The p-value for morphometric parameters has been adjusted for estimated fetal weight.</p> | | | | |

19

20

21 **Supplementary Table 6.** Speckle tracking echocardiographic results in fetuses with
 22 critical pulmonary stenosis (PS), mild-to-moderate PS and healthy controls
 23

| Parameter | Critical Pulmonary Stenosis (n=7) | Mild-moderate Pulmonary Stenosis (n=17) | Control group (n=48) | p value |
|--|-----------------------------------|---|----------------------|------------------|
| RIGHT VENTRICLE MORPHOMETRY | | | | |
| Ventricular Area (cm ²) | 2.11 ± 0.92 | 3.46 ± 1.24 | 3.28 ± 1.24 | 0.442 |
| Longitudinal diameter (mm) | 20.55 ± 4.61 | 25.37 ± 4.83 | 26.06 ± 4.48 | 0.057 |
| Basal diameter (mm) | 11.68 ± 2.72 | 15.04 ± 11.30 | 13.88 ± 3.61 | 0.436 |
| Mid-ventricular diameter (mm) | 11.24 ± 2.69 | 15.22 ± 4.16 | 14.04 ± 3.20 | 0.307 |
| RIGHT VENTRICLE FUNCTION | | | | |
| Global longitudinal strain (%) | -12.07 ± 7.31*† | -18.72 ± 4.29 | -18.87 ± 3.07 | <0.001 |
| Fractional area change (%) | 16.94 ± 16.83*† | 31.14 ± 9.25 | 30.72 ± 5.15 | 0.019 |
| Tricuspid annular plane systolic excursion (mm) § | 2.97 ± 1.75* | 4.76 ± 1.91 | 6.00 ± 1.66 | 0.004 |
| RIGHT VENTRICLE DYSSYNCHRONY | | | | |
| RV free wall peak strain delay (ms) | 123.50 (60.00-220.00)*† | 37.00 (28.00-60.00) | 13.00 (0.00-35.00) | 0.037 |
| IntraRV dyssynchrony index | 93.38 (60.02-115.51)*† | 38.73 (28.49-51.71) | 33.59 (21.23-37.88) | 0.013 |
| LEFT VENTRICLE MORPHOMETRY | | | | |
| Ventricular Area (cm ²) | 3.06 ± 1.33 | 3.03 ± 0.74 | 3.09 ± 0.82 | 0.108 |
| Longitudinal diameter (mm) | 23.92 ± 5.34* | 25.78 ± 2.62 | 27.18 ± 4.55 | 0.004 |
| Basal diameter (mm) | 13.64 (9.47-15.52) | 11.48 (8.91-14.07) | 11.81 (10.50-14.11) | 0.100 |
| Mid-ventricular diameter (mm) | 13.41 ± 4.16 | 13.52 ± 2.25 | 13.22 ± 2.29 | 0.836 |
| LEFT VENTRICLE FUNCTION | | | | |
| Global longitudinal strain (%) | -24.33 ± 5.58 | -19.72 ± 2.19 | -20.21 ± 3.33 | 0.075 |
| Ejection fraction (%) | 53.95 ± 16.09 | 49.11 ± 11.34 | 48.66 ± 9.69 | 0.491 |
| Mitral annular plane systolic excursion (mm) § | 5.12 ± 1.45 | 4.75 ± 1.47 | 5.71 ± 1.52 | 0.052 |
| LEFT VENTRICLE DYSSYNCHRONY | | | | |
| LV free wall peak strain delay (ms) | 39.50 (24.75-51.25) | 36.00 (20.00-41.00) | 21.50 (3.00-36.75) | 0.327 |
| IntraLV dyssynchrony index | 26.29 (21.65-36.94) | 31.70 (20.66-42.74) | 33.59 (21.23-37.88) | 0.685 |
| Data expressed as mean ± standard deviation or median (interquartile range). P-value calculated by ANOVA or Kruskal-Wallis one-way ANOVA according to its distribution (normal or non-normal). *Denotes P<0.05 between critical pulmonary stenosis (PS) as compared to controls (post-hoc comparisons using Dunn-Bonferroni). † Denotes P<0.05 between critical PS as compared to mild PS (post-hoc comparisons using Dunn-Bonferroni). ‡ Denotes P<0.05 between mild PS as compared to controls (post-hoc comparisons using Dunn-Bonferroni). The p-value for morphometric parameters has been adjusted for estimated fetal weight. § Tricuspid/Mitral annular plane systolic excursion p-values are adjusted by RV/LV longitudinal diameter. | | | | |

24
 25

26 REFERENCES

- 27 1. García-Otero L , Soveral I , Sepúlveda-Martínez Á, Rodríguez-López M, Torres X, Guirado L,
28 Nogué L, Valenzuela-Alcaraz B, Martínez JM, Gratacós E, Gómez O, Crispí F. Reference ranges
29 for fetal cardiac, ventricular and atrial relative size, sphericity, ventricular dominance, wall
30 asymmetry and relative wall thickness from 18 to 41 weeks of gestation. *Ultrasound Obstet
31 Gynecol.* 2021 Sep;58(3):388-397.
- 32 2. Soveral I, Crispí F, Guirado L, García-Otero L, Torres X, Bennasar M, Sepúlveda-Martínez Á,
33 Nogué L, Gratacós E, Martínez JM, Bijns B, Friedberg M, Gómez O. Cardiac filling and ejection
34 time fractions by pulsed Doppler: fetal nomograms and potential clinical application. *Ultrasound
35 Obstet Gynecol.* 2021 Jul;58(1):83-91.
- 36 3. Schneider C, McCrindle BW, Carvalho JS, Hornberger LK, McCarthy KP, Daubeney PE.
37 Development of Z -scores for fetal cardiac dimensions from echocardiography. *Ultrasound
38 Obstet Gynecol.* 2005 Nov;(26(6):599-605.
- 39 4. Kiserud T, Ebbing C, Kessler J, Rasmussen S. Fetal cardiac output , distribution to the placenta
40 and impact of placental compromise. *Ultrasound Obstet Gynecol.* 2006;(July):126–36.

41

Study 3

Gómez O, **Nogué L**, Soveral I, Guirado L, Izquierdo N, Pérez-Cruz M, Masoller N, Escobar MC, Sánchez de Toledo J, Martínez JM, Bennasar M*, Crispi F*. Cord blood cardiovascular biomarkers in Tetralogy of Fallot and D-transposition of the great arteries. *Frontiers in pediatrics*. 2023, Apr 28;11:1151814

*These authors have contributed equally to this article.

Impact factor: 3.569. **1r quartile**



OPEN ACCESS

EDITED BY
Biagio Castaldi,
University of Padua, Italy

REVIEWED BY
John Simpson,
Guy's and St Thomas' NHS Foundation Trust,
United Kingdom
Monique Haak,
Leiden University Medical Center (LUMC),
Netherlands

*CORRESPONDENCE
Olga Gómez
✉ ogomez@clinic.cat

†These authors share last authorship

RECEIVED 26 January 2023
ACCEPTED 10 April 2023
PUBLISHED 28 April 2023

CITATION

Gómez O, Nogué L, Soveral I, Guirado L,
Izquierdo N, Pérez-Cruz M, Masoller N,
Escobar MC, Sanchez-de-Toledo J,
Martínez-Crespo JM, Bennasar M and Crispí F
(2023) Cord blood cardiovascular biomarkers in
tetralogy of fallot and D-transposition of great
arteries.
Front. Pediatr. 11:1151814.
doi: 10.3389/fped.2023.1151814

COPYRIGHT

© 2023 Gómez, Nogué, Soveral, Guirado,
Izquierdo, Pérez-Cruz, Masoller, Escobar,
Sanchez-de-Toledo, Martínez-Crespo,
Bennasar and Crispí. This is an open-access
article distributed under the terms of the
Creative Commons Attribution License (CC BY).
The use, distribution or reproduction in other
forums is permitted, provided the original
author(s) and the copyright owner(s) are
credited and that the original publication in this
journal is cited, in accordance with accepted
academic practice. No use, distribution or
reproduction is permitted which does not
comply with these terms.

Cord blood cardiovascular biomarkers in tetralogy of fallot and D-transposition of great arteries

Olga Gómez^{1,2,3*}, Laura Nogué^{1,2}, Iris Soveral^{1,4}, Laura Guirado¹,
Nora Izquierdo¹, Miriam Pérez-Cruz^{1,5,6}, Narcís Masoller^{1,2},
María Clara Escobar^{5,7}, Joan Sanchez-de-Toledo^{5,7}, Josep
Maria Martínez-Crespo^{1,2,3}, Mar Bennasar^{1,2†} and Fàtima Crispí^{1,2,3†}

¹BCNatal Fetal Medicine Research Center, Sant Joan de Déu Hospital, Barcelona, Spain, ²August Pi i Sunyer Biomedical Research Institute (IDIBAPS), Barcelona, Spain, ³Fetal Medicine Department, Centro de Investigación Biomédica en Red de Enfermedades Raras (CIBERER), Madrid, Spain, ⁴Department of Obstetrics, Hospital General de Hospitalet, Barcelona, Spain, ⁵Sant Joan de Déu Research Institute (IRSJD), Barcelona, Spain, ⁶Primary Care Interventions to Prevent Maternal and Child Chronic Diseases of Perinatal and Developmental Origin Network, Carlos III Health Institute, Madrid, Spain, ⁷Pediatric Cardiology Department, Sant Joan de Déu Hospital, Esplugues de Llobregat, Barcelona, Spain

Previous reports suggest that cord blood biomarkers could serve as a prognostic tool for conotruncal congenital heart defects (CHD). We aimed to describe the cord blood profile of different cardiovascular biomarkers in a prospective series of fetuses with tetralogy of Fallot (ToF) and D-transposition of great arteries (D-TGA) and to explore their correlation with fetal echocardiography and perinatal outcome.

Methods: A prospective cohort study (2014–2019), including fetuses with isolated ToF and D-TGA and healthy controls, was conducted at two tertiary referral centers for CHD in Barcelona. Obstetric ultrasound and fetal echocardiography were performed in the third trimester and cord blood was obtained at delivery. Cord blood concentrations of N-terminal precursor of B-type natriuretic peptide, Troponin I, transforming growth factor β (TGF β), placental growth factor, and soluble fms-like tyrosine kinase-1 were determined.

Results: Thirty-four fetuses with conotruncal-CHD (22 ToF and 12 D-TGA) and 36 controls were included. ToF-fetuses showed markedly increased cord blood TGF β (24.9 ng/ml (15.6–45.3) vs. normal heart 15.7 ng/ml (7.2–24.3) vs. D-TGA 12.6 ng/ml (8.7–37.9); $P = 0.012$). These results remained statistically significant even after adjusting for maternal body mass index, birth weight and mode of delivery. TGF β levels showed a negative correlation with the pulmonary valve diameter z-score at fetal echocardiography ($r = -0.576$, $P = 0.039$). No other differences were found in the rest of cord blood biomarkers among the study populations. Likewise, no other significant correlations were identified between cardiovascular biomarkers, fetal echocardiography and perinatal outcome.

Conclusions: This study newly describes increased cord blood TGF β concentrations in ToF compared to D-TGA and normal fetuses. We also demonstrate that TGF β levels correlate with the severity of right ventricle outflow obstruction. These novel findings open a window of research opportunities on new prognostic and potential preventive strategies.

KEYWORDS

transforming growth factor beta, Troponin I, angiogenic factors, congenital heart disease, fetal echocardiography, NT-pro-brain natriuretic peptide, tetralogy of fallot, transposition of the great arteries

1. Introduction

Conotruncal anomalies are a common group of congenital heart defects (CHD) involving the outflow tracts and great vessels. The inclusion of the outflow tracts views into fetal heart screening ultrasound (1) has greatly improved the prenatal detection of conotruncal anomalies, particularly tetralogy of Fallot (ToF) and D-transposition of great arteries (D-TGA), the two most commonly prenatally diagnosed cyanotic CHD (2). Multidisciplinary care from fetal life has also contributed to greatly increase neonatal survival (3). Therefore, fetal cardiology is now focused on improving medium- and long-term prognostic evaluation.

Several blood cardiovascular biomarkers have been proposed as potential prognostic factors. Previous reports suggest altered circulating concentrations of angiogenic factors in fetuses with CHD. Placental growth factor (PlGF) is a glycoprotein mainly produced in placental trophoblast to promote endothelial growth but also expressed by cardiomyocytes in response to stress (4). The soluble form of fms-like tyrosine kinase-1 (sFlt-1) is a potent antagonist of PlGF that prevents its interaction with cell receptors (5). However, only a few studies have evaluated the pattern of these biomarkers in fetuses with CHD showing controversial results. An antiangiogenic imbalance, with significantly increased cord blood sFlt-1 levels, was firstly described in a mixed group of CHD (6). Recently, a proangiogenic profile with drastically reduced cord blood sFlt1 concentrations, has been reported in a group of left univentricular CHD including hypoplastic left heart syndrome, severe aortic stenosis and Shone syndrome (7). Nonetheless, the role of PlGF and sFlt1 in different types of CHD and their correlation with cardiac dysfunction and perinatal outcome has been insufficiently studied to date.

Additional biomarkers with a potential role in CHD are B-type natriuretic peptide (BNP) and its N-terminal precursor (NT-proBNP). They are released from ventricular myocytes in response to pressure/volume overload or hypoxia, and are clinically useful for CHD screening in neonatal stage (8). Moreover, increased cord blood levels of NT-proBNP and Troponin I, a specific marker of myocardial damage (9), have been described in fetuses with single ventricle (7, 10). Nonetheless, elevated cord blood levels of NT-proBNP and Troponin I have also been reported in neonates with acidosis (11) and intrauterine growth restriction (12).

Lastly, transforming growth factor β 1 (TGF β) is a cytokine produced by different cells with an essential role in the development of heart remodeling and fibrosis (13). Several studies describe elevated plasmatic concentrations of TGF β in adolescents and young adults with repaired ToF, indicating altered TGF β signaling in ToF correlating with aortic root dilation (14, 15). To our knowledge, only one study has evaluated this biomarker in fetal life, demonstrating a significant elevation in aortic coarctation, aortic stenosis and Shone syndrome with biventricular outcome (7).

Thus, the study of these biomarkers in a series specifically composed of common conotruncal anomalies could be of interest to preliminarily define its cardiac biomarker profile from fetal life, evaluating its potential clinical applicability in subsequent studies. We aimed to first describe the cord blood levels of PlGF, sFlt1, BNP, Troponin I and TGF β in a prospective series of fetuses

with ToF and D-TGA and to explore their correlation with fetal echocardiography and perinatal outcome.

2. Materials and methods

2.1. Study population

A prospective cohort study was conducted between January 2014 and December 2019, including fetuses diagnosed with ToF and D-TGA at the Fetal Cardiology Unit of BCNatal, which groups two tertiary referral centers for CHD in Barcelona (Clinic and Sant Joan de Déu hospitals). Fetuses with structurally normal hearts were also recruited from low-risk pregnancies attended at BCNatal and included as a control group. Pregnancies of women older than 18 years with accurate gestational age (GA) calculated by first-trimester crown-rump length (16) were considered eligible. Fetal ultrasound and echocardiography were performed in the third trimester, cord blood was obtained at delivery and perinatal results and cardiovascular outcome data were collected postnatally. The study was approved by the institutional Ethics Committee (Reg. HCB/2019/0540). Written consent was obtained from all pregnant women.

ToF was defined by the combination of a subaortic ventricular septal defect with an overriding aorta and infundibular pulmonary obstruction. ToF-cases were sub-classified as ToF with pulmonary stenosis or atresia, based on the presence or absence of anterograde flow through the pulmonary valve, respectively. To obtain a homogeneous group, infrequent cases of TOF with absent pulmonary valve or with major aortopulmonary collaterals were not considered eligible for the study. D-TGA was defined based on the presence a discordant ventricular arterial connection and it was later subdivided into two categories: simple-D-TGA and complex-D-TGA (in the presence of a ventricular septal defect, pulmonary stenosis and/or coarctation of the aorta). All fetuses underwent prenatal genetic testing with microarray analysis and complete extracardiac anatomical ultrasound at diagnosis and during follow-up. Fetuses with pre or postnatal diagnosis of additional major cardiac defects, major extracardiac malformations and/or chromosomal abnormalities were excluded from the study.

Control fetuses were recruited from singleton, spontaneously conceived and low-risk pregnancies attended at the maternal-fetal Medicine Department at BCNatal. Control fetuses were matched for GA (± 2 weeks) at delivery with conotruncal-CHD fetuses. Exclusion criteria for controls were pre or postnatal diagnosis of CHD, major extracardiac malformations, chromosomal abnormalities and/or those conditions potentially affecting cord blood biomarkers such as intrauterine growth restriction (12, 17–19), macrosomia (20), pregestational diabetes (20, 21), pregestational hypertension or exposure to toxics (22).

2.2. Baseline, perinatal characteristics and cardiovascular outcome

Maternal age, body mass index, ethnicity, smoking status, pre-gestational medical conditions and parity were collected from

medical records. Pregnancy outcome, including the presence of intrauterine growth restriction, preeclampsia, pregnancy induced hypertension, gestational diabetes and prematurity below 37 weeks and perinatal characteristics as GA at delivery, mode of delivery, birthweight, neonatal height and head circumference, umbilical artery pH and Apgar score were also recorded. Intrauterine growth restriction was defined as EFW and birthweight below the 3rd centile or below the 10th centile with abnormal uterine, umbilical or middle cerebral artery Doppler values (23). In all cases, CHD subtype was confirmed by postnatal echocardiography and clinical outcome was obtained from medical records at least one year after birth and reevaluated yearly if necessary.

2.3. Fetal ultrasound and echocardiography

Fetal ultrasound and echocardiography were performed using a Siemens Sonoline Antares (Siemens Medical Systems, Malvern, PA, USA) or Voluson E10 (General Electric, Zipf, Austria) using a curved-array 2–6 MHz transducer. Structural fetal ultrasound encompassed a detailed extra-cardiac and cardiac examination, following recommended guidelines (24, 25).

Third trimester standard obstetric ultrasound comprised estimation of fetal weight, measurement of mean uterine arteries pulsatility index (PI), umbilical artery PI, middle cerebral artery PI, aortic isthmus PI (26) and ductus venosus PI (27). Estimated fetal weight (EFW) was calculated according to the method of Hadlock et al. (28). EFW centile was calculated using institutional reference curves (29). The cerebroplacental ratio was calculated by dividing the middle cerebral artery PI by the umbilical artery PI (30).

Following the echocardiographic protocol of our center in CHD, in fetuses with ToF and D-TGA, a detailed study of cardiac morphometry and functionalism was performed including measurement of cardiac area, cardiothoracic ratio, ventricular widths, lengths, right-to-left and sphericity indices (SI) and septal thickness from an apical or transverse four-chamber view at end-diastole (31, 32). Aortic and pulmonary valve diameters at mid-systole and aortic-to-pulmonary valve ratio were also obtained. Aortic and pulmonary valve size were normalized for gestational age and the z-scores were calculated (33). Cardiac function evaluation included aortic and pulmonary peak systolic velocities, mitral (MAPSE) and tricuspid annular-plane systolic excursion (TAPSE) (34).

2.4. Cord blood biomarkers

Cord blood samples were obtained from the umbilical vein after cord clamping at birth. Plasma was separated from ethylenediaminetetraacetic acid-treated blood using centrifugation at $1,400\times g$ for 10 min at 4°C. Serum was separated using centrifugation at $2,000\times g$ for 10 min at room temperature. Sample aliquots were immediately stored at -80°C until assayed.

Cord blood biomarkers were measured as previously described (7). Briefly, concentrations of PlGF and sFlt1 were determined in

serum by the fully automated Elecsys assays on an electrochemiluminescence immunoassay platform Cobas analyzer (Roche Diagnostics, Mannheim, Germany). NT-proBNP and Troponin I concentrations were measured in plasma by electrochemiluminescence immunoassay using Siemens Atellica IM NT-proBNP and High Sensitivity Troponin I (sensitivity of the technique: 0.0025 pg/ml), respectively (Siemens Healthcare, Erlangen, Germany). TGF β was measured in serum by conventional ELISA assay Quantikine Human TGF-beta1 (R&D Systems, Minneapolis, MN, USA). Concentrations of cord concentrations of PlGF, sFlt1, NT-proBNP and TGF β are presented as continuous variables. Given the different behavior of troponin I (acute increase in response to ischemia or hypoxia), Troponin I was treated as dichotomous variable: concentrations above 0.0093 pg/ml (which corresponds to the 75th centile of the troponin level among the control group), were considered to be high.

2.5. Statistical analysis

IBM SPSS Statistics version 25 statistical package (IBM Corp., Armonk, NY, USA) was used for statistical analysis. Kolmogorov-Smirnov test of normality was performed in all continuous variables. Measurements were expressed as mean \pm standard deviation or as median (range) for continuous variables as appropriate, and frequencies with percentages for categorical variables. Differences between study groups were examined using parametric analysis of variance (one-way ANOVA) followed by *post hoc* Bonferroni tests for pairwise comparison for normally distributed variables, Kruskal-Wallis one-way ANOVA followed by *post-hoc* pairwise comparisons using the Dunn-Bonferroni approach for non-normally distributed variables and χ^2 test for categorical variables.

Baseline variables were analyzed to identify possible confounders including maternal age, maternal body mass index (BMI), nulliparity, smoking, pregestational diabetes, gestational diabetes, preeclampsia, GA at delivery, birth weight, gender and mode of delivery. Potentially confounders factors such as maternal BMI, birth weight and mode of delivery were significantly different between groups, therefore were adjusted in the model. Spearman correlation coefficient to compare associations between biomarkers and the previously described standard obstetric ultrasound and echocardiographic parameters was used in the ToF and D-TGA groups. For all analyses, *P*-values <0.05 were considered statistically significant.

3. Results

3.1. Study population and obstetric standard ultrasound

From the original cohort of 84 ToF and D-TGA fetuses, 18 pregnant women elected for termination of pregnancy. We excluded from the analysis 6 cases with ToF: 1 case with absent pulmonary valve, 1 case with major aorto-pulmonary collateral arteries (MAPCAs), 1 case with intrauterine fetal demise, 1 monochorionic twin pregnancy, 1 case with a chromosomal

abnormality and a last case with an associated multicystic kidney disease. We didn't obtain cord blood at delivery in 23 cases, 1 patient was lost to follow-up and 2 refused to participate. The final study population consisted of 34 fetuses with conotruncal CHD (22 ToF and 12 D-TGA cases) and 36 controls.

As shown in **Figure 1**, the ToF group included 19 fetuses with pulmonary stenosis and 3 cases with pulmonary atresia. Only one case of ToF with pulmonary stenosis presented retrograde flow at the ductus arteriosus, with the remaining cases presenting forward flow until birth. Blalock-Taussig shunt was required prior to the ToF corrective surgery only in the 3 cases with pulmonary atresia.

The D-TGA-group included 6 fetuses with a simple-D-TGA, 5 cases with a subpulmonary ventricular septal defect and one fetus with an associated pulmonary stenosis (complex-D-TGA group). Rashkind atrioseptostomy was performed prior to arterial switch procedure in 58.3% of the D-TGA fetuses (7/12). The cardiovascular outcome was favorable in all conotruncal CHD cases, with no significant postnatal complications and with a median follow-up of 46 months (interquartile range 28.0–50.5).

Maternal baseline characteristics and perinatal results are shown in **Table 1**. Most baseline characteristics were similar in the three study populations; however, BMI was significantly higher in pregnant women with ToF-fetuses compared to the other two groups. Additionally, the prevalence of small for GA

fetuses was higher in the ToF group [31.8% (7/22)] and cesarean section was more frequently performed in the ToF and D-TGA groups compared to controls. Additional perinatal outcomes such as GA at delivery was similar across groups and there were no differences in the five-minute Apgar score and umbilical artery pH. No cases of fetal acidosis were found. Regarding biometrics at birth, ToF-fetuses had a significantly lower birth weight compared to D-TGA and control groups, with only 2 ToF cases with pulmonary stenosis presenting a birth weight below the 3th percentile. The head circumference at birth was also significantly reduced in both conotruncal CHD groups as compared to controls. As shown in **Table 1**, birth length did not significantly differ between the three groups.

Table 2 details the results of fetal ultrasound in the study populations. Interestingly, there were no significant differences in estimated fetal weight or head circumference at the time of ultrasound. There were also no differences in uterine or umbilical-fetal and ductus venosus Doppler between the three groups.

3.2. Cord blood biomarkers

Results of cord blood biomarkers in ToF, D-TGA and control-groups are presented in **Table 3** and **Figure 2**. Concentrations of

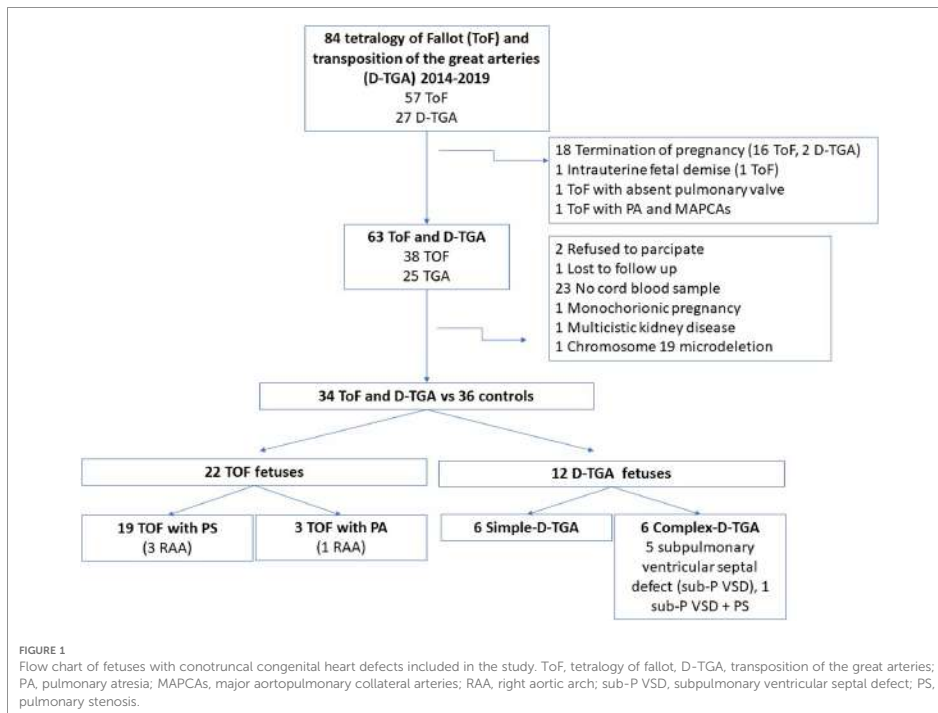


TABLE 1 Maternal characteristics and perinatal outcome in the study populations.

| Variable | Tetralogy of fallot (n = 22) | Transposition of the great arteries (n = 12) | Controls (n = 36) | P-value |
|--|------------------------------|--|---------------------|----------------|
| MATERNAL CHARACTERISTICS | | | | |
| Maternal age (years) | 35.27 ± 6.35 | 33.58 ± 5.14 | 33.88 ± 4.67 | 0.560 |
| Body mass index (kg/m ²) | 28.4 (24.29–29.31)* | 26.51 (24.24–30.85) | 22.92 (21.36–24.39) | <0.001 |
| Chronic diseases | 6 (27.27%) | 2 (16.67%) | 11 (30.6%) | 0.576 |
| Ethnicity | | | | 0.596 |
| Caucasian | 15 (68.2%) | 11 (91.7%) | 26 (72.2%) | |
| Latin American | 2 (9.1%) | 1 (8.3%) | 2 (5.6%) | |
| Maghreb | 4 (18.2%) | 0 (0%) | 3 (8.3%) | |
| Asian | 1 (4.5%) | 0 (0%) | 4 (11.1%) | |
| African | 0 (0%) | 0 (0%) | 1 (2.8%) | |
| Smoking habit | 0 (0%) | 1 (8.3%) | 1 (2.8%) | 0.378 |
| Nulliparity | 11 (50%) | 8 (66.7%) | 17 (47.2%) | 0.499 |
| PERINATAL CHARACTERISTICS | | | | |
| Gestational age at birth (weeks) | 39.4 (38.2–40.0) | 40 (39.5–41.1) | 39.5 (39.0–40.2) | 0.326 |
| Pregnancy complications: | | | | |
| Small for gestational age | 7 (31.8%)* | 2 (16.7%)* | 0 (0%) | 0.002 |
| Intrauterine growth restriction | 2 (9.1%) | 1 (8.3%) | 0 (0%) | 0.189 |
| Preeclampsia or pregnancy induced hypertension | 0 (0%) | 0 (0%) | 0 (0%) | 1 |
| Gestational diabetes | 1 (4.5%) | 0 (0%) | 3 (8.3%) | 0.538 |
| Prematurity (Birth <37 weeks) | 0 (0.0%) | 0 (0.0%) | 1 (2.8%) | 0.619 |
| Cesarean section | 12 (54.5%)* | 4 (33.3%)* | 8 (22.2%) | 0.042 |
| Birth weight (g) | 2,935 (2,729–3,305)* | 3,235 (3,077–3,465) | 3,390 (3,132–3,637) | 0.004 |
| Birth weight centile | 32 (9–59)* | 35 (20–64) | 43 (38–70) | 0.007 |
| Birth weight <3rd centile | 2 (9.1%) | 0 (0%) | 0 (0%) | 0.106 |
| Birth weight >4,000 g | 0 (0%) | 0 (0%) | 0 (0%) | 1 |
| Five-minute Apgar <7 | 2 (9.1%) | 1 (8.3%) | 2 (5.6%) | 0.866 |
| Umbilical artery pH | 7.25 (7.20–7.28) | 7.24 (7.2–7.29) | 7.21 (7.16–7.28) | 0.164 |
| Female fetal gender | 4 (18.2%) | 6 (50%) | 16 (44.4%) | 0.080 |
| Head circumference at birth (cm) | 33.6 (32.3–38.8)* | 33.7 (32.1–34.4)* | 35.4 (34.5–36.0) | < 0.001 |
| Head circumference centile | 34 (13.5–80.7) | 21 (4.25–39.75)* | 72 (52.75–84.25) | < 0.001 |
| Height (cm) | 50 (47–51.25) | 50.5 (49–52.5) | 51 (50–52) | 0.125 |
| Height centile | 34 (13.5–80.75) | 59.5 (31.75–89.25) | 70.5 (40.5–89.8) | 0.066 |
| CARDIOVASCULAR OUTCOME | | | | |
| Follow-up (months) | 47 (33.5–51.5) | 35.5 (6.5–50.7) | NA | |

Data expressed as mean ± standard deviation, median (interquartile range) or n (percentage). ToF, tetralogy of fallot; PS, pulmonary stenosis; D-TGA, transposition of the great arteries; NA, non-applicable.

P-value calculated by ANOVA.

*Bold numbers means statistically significant.

*Denotes P < 0.05 as compared to controls (Post-hoc comparisons using Dunn–Bonferroni for continuous and χ^2 for categorical variables).

TABLE 2 Feto-placental ultrasound in the study populations.

| Variable | Tetralogy of Fallot (n = 22) | Transposition of the great arteries (n = 12) | Controls (n = 36) | P-value |
|---------------------------------------|------------------------------|--|-------------------|---------|
| Gestational age at ultrasound (weeks) | 33.3 (31.5–33.2) | 34.1 (31.1–34.6) | 33.1 (29–35.1) | 0.193 |
| Estimated fetal weight (g) | 2,033.48 ± 405.06 | 2,144.08 ± 579.13 | 1,908.72 ± 694.40 | 0.464 |
| Estimated fetal weight centile | 28 (13–61) | 51 (30–83) | 43 (17–62) | 0.221 |
| Head circumference (mm) | 304 (292–319) | 294 (272–313) | 295 (255–312) | 0.271 |
| Mean uterine artery PI centile | 56.85 ± 28.67 | 49.17 ± 17.48 | 35.81 ± 31.98 | 0.098 |
| Mean uterine artery PI > p95 | 2 (15.4%) | 0 (0%) | 2 (6.3%) | 0.415 |
| Umbilical artery PI centile | 51.76 ± 24.10 | 39.0 ± 21.70 | 44.34 ± 23.31 | 0.302 |
| Umbilical artery PI < p95 | 0 (0%) | 0 (0%) | 0 (0%) | 1 |
| Middle cerebral artery PI centile | 52 (32.5–74) | 39 (18–95) | 51 (21–71) | 0.785 |
| Middle cerebral artery PI < P5 | 0 (0%) | 0 (0%) | 1 (2.9%) | 0.629 |
| Cerebroplacental ratio | 2.05 ± 0.67 | 2.43 ± 1.03 | 2.04 ± 0.52 | 0.216 |
| Cerebroplacental ratio centile | 40.10 ± 26.87 | 51.55 ± 37.86 | 47.49 ± 30.63 | 0.561 |
| Cerebroplacental ratio < P5 | 0 (0%) | 0 (0%) | 2 (5.7%) | 0.401 |
| Ductus venosus PI centile | 52.18 ± 29.65 | 46.70 ± 30.78 | 36.18 ± 31.46 | 0.207 |
| Aortic isthmus PI centile | 58.36 ± 12.70 | 65.86 ± 20.09 | 71.41 ± 14.41 | 0.056 |

Data expressed as mean ± standard deviation, median (interquartile range) or n (percentage). PI, pulsatility index.

P-value calculated by ANOVA.

TABLE 3 Concentrations of biomarkers in cord blood the study populations.

| Variable | Tetralogy of fallot (n = 22) | Transposition of the great arteries (n = 12) | Controls (n = 36) | Adjusted P-value |
|--|------------------------------|--|----------------------------|------------------|
| Placental growth factor (PIGF) (pg/ml) | 12.7 (10.9–20.2) | 14.6 (11.15–29.55) | 17.5 (13.7–23.55) | 0.222 |
| Soluble fms-like tyrosin kinase 1 (sFlt-1) (pg/ml) | 1,116.6 (856.9–1,966.2) | 1,121.2 (912.75–1,946.9) | 1,962.3 (1,379.9–2,726.25) | 0.711 |
| sFlt-1/PIGF ratio | 80.36 (57.76–115.73) | 91.46 (63.89–125.03) | 106.25 (78.48–155.22) | 0.401 |
| High troponin I [†] positive | 5 (19%) | 6 (50%) | 8 (25%) | |
| Pro-Brain natriuretic peptide (pg/ml) | 1,005 (466.5–1,588) | 607 (471.75–1,157.75) | 508 (288.5–740.75) | 0.154 |
| Transforming growth factor β (ng/ml) | 24.85 (15.75–45.28)* | 12.6 (8.7–37.9) | 15.7 (7.25–24.3) | 0.012 |

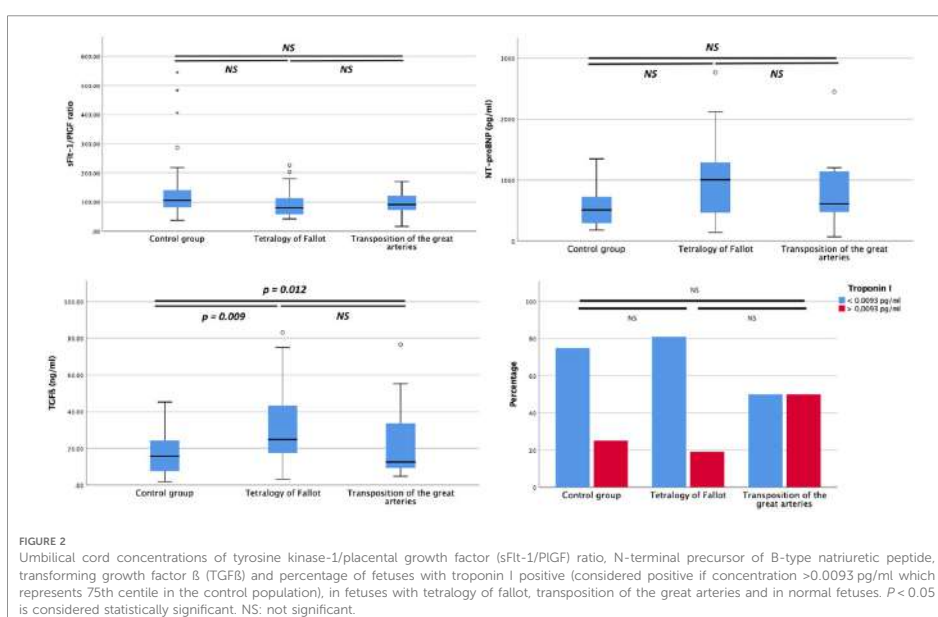
Data expressed as mean ± standard deviation, median (interquartile range) or n (percentage).

[†]Troponin considered positive if concentration >0.0093 pg/ml which represents 75th centile in the control population.

P-value calculated by logistic regression adjusted by body mass index, cesarean section and birthweight.

Bold numbers means statistically significant.

*Denotes P<0.05 between Tetralogy of Fallot and Controls (post-hoc comparisons using Dunn-Bonferroni for continuous variables).



cord blood angiogenic factors including PIGF, sFlt1 and sFlt1/PIGF ratio, did not show significant differences among the study populations. Compared with the controls, ToF fetuses presented a marked increase in cord blood concentrations of TGFβ. Troponin showed a non-significant tendency to higher concentrations in the D-TGA group (Figure 2).

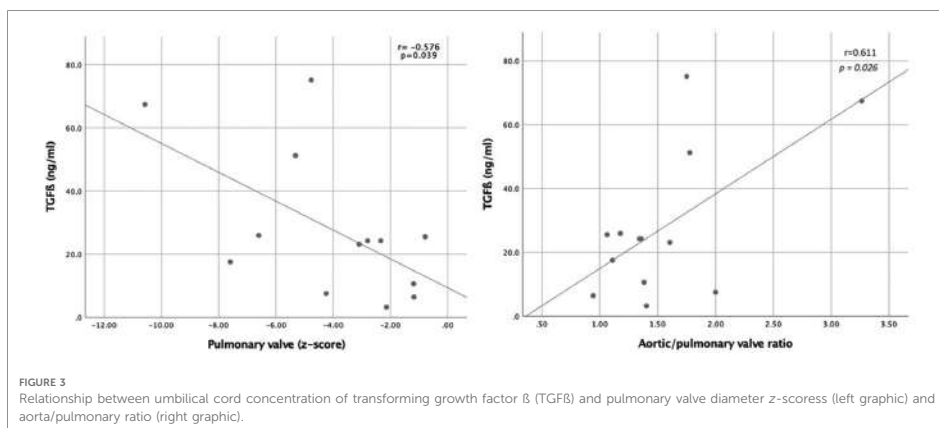
Cord blood biomarkers were not correlated with any obstetric ultrasound parameter, such as umbilical artery, middle cerebral artery and aortic isthmus PI, nor with any perinatal outcome including mode of delivery, estimated fetal weight, head circumference, umbilical artery pH and 5 min Apgar score.

Finally, and as shown in Figure 3, cord blood levels of TGFβ showed a negative correlation with the pulmonary valve diameter z-score ($r = -0.576$, $P = 0.039$) and positive correlation with

aortic/pulmonary valve ratio ($r = 0.611$, $P = 0.026$) in ToF fetuses. No additional correlations were found between cord blood biomarkers and the rest of morphometric and functional echocardiographic parameters evaluated in ToF and D-TGA fetuses, including aortic peak systolic velocity.

4. Discussion

This study first describes the pattern of different cord blood biomarkers in a cohort of fetuses diagnosed with isolated ToF and D-TGA. Our main findings are: (1) TGFβ is significantly increased in ToF from fetal stage and (2) cord blood TGFβ levels correlate with the severity of the prenatal right ventricular



outflow tract obstruction. Only a few prior studies have evaluated cord blood cardiovascular biomarkers in fetuses with CHD with conflicting results. Differences in the CHD groups included among the studies, together with their small sample size, precludes direct comparison of results. A series of 39 fetuses with a mixed group of CHD, which included some cases with conotruncal anomalies reported an anti-angiogenic pattern with increased cord blood sFlt-1 levels (6). On the contrary, a prior study by our group, evaluating 45 fetuses with left-CHD, found only modestly decreased PlGF in the left-CHD group compared to normal fetuses, and markedly decreased sFlt1 only in fetuses with univentricular left-CHD conferring a proangiogenic profile of PlGF and sFlt1 in the poor prognostic group (7). In our study, no differences were found in cord blood levels of PlGF and sFlt1 among the study groups. Given that sFlt1 is downregulated by hypoxia (35), our results in conotruncal CHD suggest that there is little ventricular hypoxic damage *in utero* in these cyanotic CHD. Further studies are needed to better define which groups of CHD are related to abnormal angiogenesis at the cardiac level and its possible relationship with a concomitant deficient placental angiogenesis (36).

Several studies have reported cord blood NT-proBNP to be elevated in CHD, including 10 cases with mixed CHD (12), 15 fetuses with functional single ventricle associated to neonatal death (10), 16 fetuses with univentricular left-CHD (7) and 6 cases with non-immune hydrops of cardiac origin (10). Although these studies group a limited number of cases, the results are consistent with prior data reporting elevated NT-proBNP in pediatric patients (37) with heart failure, indicating that NT-proBNP is a useful predictor in the setting of severe cardiac anomalies. In our study, NT-proBNP was slightly elevated in the ToF group and preserved in D-TGA cases, which is in accordance with the favorable biventricular outcome and lack of major postnatal complications of our series.

Finally, there is very limited data on Troponin I behavior in fetuses with CHD. We previously reported positive cord blood Troponin I to be more frequent in the group of fetuses with left-

CHD with favorable cardiac outcome (7). In the present study, a higher proportion of fetuses with D-TGA presented positive values above the 75th centile (Figure 2), but this difference was not significant possibly due to the limited number of cases. Troponin I is a very sensitive biomarker for endocardial hypoxia and myocardial damage. It has also been found to be elevated in newborns requiring NICU admission (38), in neonates with acidemia (39) and in fetuses with intrauterine growth restriction (40). Thus, larger populations studies are needed to better describe the profile of all these biomarkers not only in different groups of CHD but also in clinical conditions associated with cardiac dysfunction.

4.1. Increased cord blood TGFB in ToF compared with D-TGA

This is the first prenatal report of increased cord blood TGFB concentrations in ToF. This increase may be explained by different mechanisms. First, TGFB has been identified as a primary factor responsible for cardiovascular fibrosis (41) and upregulation of TGFB signaling has been shown to be associated with pro-fibrotic molecular signaling in cardiac pressure overload (42). In this regard, limited data is available on blood flow mechanics and its effect on biventricular remodeling in fetal ToF (43). Nonetheless, a recent computational model evaluating fluid dynamics in fetuses with ToF has shown that although biventricular pressure is equalized by the presence of the ventricular septal defect, biventricular pressure is globally elevated in ToF compared to normal hearts leading to mild right ventricle hypertrophy in fetal life (44). These findings could plausibly explain the higher levels of TGFB in the ToF group. Furthermore, the ventricular walls around the ventricular septal defect consistently experienced high stress due to a shear flow effect, a mechanism which has also been described to induce cardiovascular tissue growth and remodeling (45).

Secondly, in normal fetal circulation there is a preferential shunting across the foramen ovale that comprises 30% of the cardiac output (46). However, tricuspid flow has been described to be increased in ToF (44), as a lower resistance alternative to the foramen ovale. As such, some of the right atrial flow is derived through the right ventricle and the ventricular septal defect instead of flowing through the foramen ovale, further contributing to the increased endothelial shear stress at the ventricular septal defect.

Finally, TGF β has also a central role in vascular morphogenesis and extracellular matrix homeostasis, thus there is a growing interest to better understand its contribution to vascular remodeling. Altered TGF β signaling has been reported in bicuspid aortopathy as a key component in the pathogenesis of thoracic aneurysms (47) as well as in Marfan syndrome, in which circulating levels of TGF β are correlated with aortic root dilation (48). Moreover, overexpression of TGF β in the ascending aorta has been described in patients with ToF, tricuspid atresia and double-outlet right ventricle in association with abnormal elastic fibers. Interestingly, increased TGF β levels have been recently found in a study evaluating adolescents and young adults with ToF after surgery in comparison with controls (14). TGF β was also slightly elevated after atrial switch operation in corrected TGA and Fontan procedures but was preserved after arterial switch surgery in D-TGA. These data suggest that different mechanisms may be involved in the neo-aortic root dilation that progressively occurs in repaired D-TGA compared to other CHD. Our data, showing similar results in fetuses with ToF and D-TGA, reinforce the hypothesis that an underlying lesion of the aorta may already be present in ToF from very early stages of development. In fact, a decreased aortic compliance, evaluated by fetal echocardiography, has already been reported in fetuses with Marfan syndrome and ToF compared to normal fetuses (49). Therefore, future studies evaluating fetal aortic characteristics in different CHD are warranted.

4.2. TGF β correlates with the severity of the right ventricle obstruction in ToF

Prior studies have demonstrated a positive correlation between circulating levels of TGF β and aortic sinus dimension in patients with repaired-ToF (14). Moreover, TGF β levels have also been correlated with the aortic stiffness evaluated by echocardiography in patients with ToF before the surgical repair (15). Our data are consistent with these findings. As shown in **Figure 3**, TGF β concentration showed a negative correlation with the pulmonary valve diameter and a positive correlation with aortic/pulmonary valve ratio in ToF fetuses. Thus, we could hypothesize that increasing right ventricular obstruction severity results in progressive aortic volume overload, which may be associated with a more pronounced deleterious hemodynamic effect and higher TGF β levels. However, we could not demonstrate any correlation between TGF β levels and fetal right ventricular morphometry and functionalism, assessed by the sphericity index and tricuspid annular-plane systolic excursion, respectively; nor

with peak pulmonary/aortic systolic velocity, findings that require to be conformation with a larger number of cases.

In agreement with previous reports, ToF-newborns had a significantly lower birth weight compared to D-TGA and control groups (50). Additionally, head circumference perimeter at birth was also significantly reduced in both conotruncal CHD groups (51). However, cord blood biomarkers were neither correlated with any ultrasound parameter and perinatal outcome. Likewise, no cord blood biomarker was correlated with any echocardiographic parameter in the D-TGA and control groups. However, these results may be limited by the small sample size of our study.

4.3. Strengths and limitations

To our knowledge, this is the first study to perform a comprehensive assessment of cord blood cardiac biomarkers profile in a specific series of fetuses diagnosed with conotruncal anomalies. It is also the first study to identify increased cord blood TGF β concentrations in ToF and its correlation with the severity of right ventricular outflow tract obstruction.

However, this is an exploratory study and, therefore, future studies are necessary to confirm our findings and subsequently evaluate the potential clinical applicability of TGF β in the prognostic evaluation of ToF. The main limitation of our study is the limited number of cases, especially in the D-TGA group. However, the group of ToF is quite homogeneous since most of the cases correspond to ToF with pulmonary stenosis. Although cord blood biomarkers concentrations were analyzed after adjustment for identified confounders we recognize that additional confounders might exist. Finally, we are aware that we have neither the weight of the placenta at birth nor a placental biopsy, which could also provide relevant information.

5. Conclusions

This study newly describes increased cord blood TGF β concentrations in ToF compared to D-TGA and normal fetuses. Moreover, we demonstrate that TGF β levels correlate with the severity of right ventricle outflow obstruction. These novel findings open a window of research opportunities into new prognostic and potential preventive strategies. For this, larger multicenter studies, including enough cases in each category of conotruncal anomalies and other groups of CHD, both in fetal and postnatal stages, are warranted. Additionally, the study of these cardiovascular biomarkers in maternal blood and as well as in the amniotic fluid would allow to expand their potential clinical applicability to earlier stages of gestation.

Data availability statement

The raw data supporting the conclusions of this article will be made available by the authors, without undue reservation.

Ethics statement

The studies involving human participants were reviewed and approved by Ethics Committee Hospital Clínic de Barcelona (Reg. HCB/2019/0540). The patients/participants provided their written informed consent to participate in this study.

Author contributions

Conceptualization, IS, OG, MB and FC; methodology, IS, LN, OG and FC; software, LN; validation, IS and LG; formal analysis, LN, IS, OG and FC; investigation, OG, LN, IS, LG, NI, MP, NM, MCE, JST, JMM, MB and FC; resources OG, LN, IS, LG, NI, MP, NM, MCE, JST, JMM, MB and FC; data curation, LN, IS; writing—original draft preparation, OG; writing—review and editing, OG, LN, IS, LG, NI, MP, NM, MCE, JST, JMM, MB and FC; visualization, LN; supervision, OG, MB and FC; project administration, OG, MB and FC; funding acquisition, LN, OG, JMM, MB and FC. All authors contributed to the article and approved the submitted version.

Funding

The research leading to these results has received funding from Hospital Clínic de Barcelona (Ajut Josep Font 2015 and Premi Emili Letang 2019, Barcelona, Spain), Instituto de Salud Carlos III (ISCIII) (PI15/00263, PI17/00675, PI20/00246, INT21/00027) co-funded by the European Union, Cerebra Foundation for the Brain Injured Child (Carmarthen, Wales, UK), Fundació La Marató de TV3 (Ref 202016-30-31), and the Maternal and Child

Health and Development Network (SAMID), RD16/0022/0015. Additionally, we would like to thank the Fundació Jesús Serra of the Grup Catalana Occident for the Fundació Jesús Serra Research Prize in the Clinical category awarded to the Researcher Fatima Crispí in its 4th edition for the project titled “Cardiovascular prevention from fetal life: benefits of Mediterranean diet during gestation”.

Acknowledgments

We would like to thank Biobanks of Clínic-IDIBAPS and Fundació Sant Joan de Déu for the valuable management of samples.

Conflict of interest

The authors declare that the research was conducted in the absence of any commercial or financial relationships that could be construed as a potential conflict of interest.

Publisher's note

All claims expressed in this article are solely those of the authors and do not necessarily represent those of their affiliated organizations, or those of the publisher, the editors and the reviewers. Any product that may be evaluated in this article, or claim that may be made by its manufacturer, is not guaranteed or endorsed by the publisher.

References

- International Society of Ultrasound in Obstetrics and Gynecology null, Carvalho JS, Allan LD, Chaoui R, Copel JA, DeVore GR, Hecher K, et al. ISUOG practice guidelines (updated): sonographic screening examination of the fetal heart. *Ultrasound Obstet Gynecol.* (2013) 41(3):348–59. doi: 10.1002/uog.12403
- Shinebourne EA, Babu-Narayan SV, Carvalho JS. Tetralogy of fallot: from fetus to adult. *Heart.* (2006) 92(9):1353–9. doi: 10.1136/hrt.2005.061143
- Donofrio MT, Moon-Grady AJ, Hornberger LK, Copel JA, Sklansky MS, Abuhamad A, et al. Diagnosis and treatment of fetal cardiac disease: a scientific statement from the American heart association. *Circulation.* (2014) 129(21):2183–242. doi: 10.1161/01.cir.0000437597.44550.5d
- Iwama H, Uemura S, Naya N, Imagawa KI, Takemoto Y, Asai O, et al. Cardiac expression of placental growth factor predicts the improvement of chronic phase left ventricular function in patients with acute myocardial infarction. *J Am Coll Cardiol.* (2006) 47(8):1559–67. doi: 10.1016/j.jacc.2005.11.064
- Maglione D, Guerriero V, Vignietto G, Delli-Bovi P, Persico MG. Isolation of a human placenta cDNA coding for a protein related to the vascular permeability factor. *Proc Natl Acad Sci U S A.* (1991) 88(20):9267–71. doi: 10.1073/pnas.88.20.9267
- Llurba E, Sánchez O, Ferrer Q, Nicolaidis KH, Ruiz A, Dominguez C, et al. Maternal and foetal angiogenic imbalance in congenital heart defects. *Eur Heart J.* (2014) 35(11):701–7. doi: 10.1093/eurheartj/ehz389
- Severall I, Guirado L, Escobar-Diaz MC, Alcaide MJ, Martínez JM, Rodríguez-Sureda V, et al. Cord blood cardiovascular biomarkers in left-sided congenital heart disease. *J Clin Med.* (2022) 11(23):7119. doi: 10.3390/jcm11237119
- Mitchell ME, Sander TL, Klinkner DB, Tomita-Mitchell A. The molecular basis of congenital heart disease. *Semin Thorac Cardiovasc Surg.* (2007) 19(3):228–37. doi: 10.1053/j.semtcv.2007.07.013
- Agewall S, Giannitsis E, Jernberg T, Katus H. Troponin elevation in coronary vs. non-coronary disease. *Eur Heart J.* (2011) 32(4):404–11. doi: 10.1093/eurheartj/ehq456
- Lee SM, Kwon JE, Song SH, Kim GB, Park JY, Kim BJ, et al. Prenatal prediction of neonatal death in single ventricle congenital heart disease. *Prenat Diagn.* (2016) 36(4):346–52. doi: 10.1002/pd.4787
- Irmak K, Tüten N, Karaoglu G, Madazli R, Tüten A, Malik E, et al. Evaluation of cord blood creatine kinase (CK), cardiac troponin T (cTnT), N-terminal-pro-B-type natriuretic peptide (NT-proBNP), and s100B levels in nonreassuring foetal heart rate. *J Matern Fetal Neonatal Med.* (2021) 34(8):1249–54. doi: 10.1080/14767058.2019.1632285
- Kocylowski RD, Dubiel M, Gudmundsson S, Sieg I, Fritzer E, Alkasi O, et al. Biochemical tissue-specific injury markers of the heart and brain in postpartum cord blood. *Am J Obstet Gynecol.* (2009) 200(3):273.e1–25. doi: 10.1016/j.ajog.2008.10.009
- Ren LL, Li XJ, Duan TT, Li ZH, Yang JZ, Zhang YM, et al. Transforming growth factor- β signaling: from tissue fibrosis to therapeutic opportunities. *Chem Biol Interact.* (2023) 369:110289. doi: 10.1016/j.cbi.2022.110289
- Cheung YF, Chow PC, So EKF, Chan KW. Circulating transforming growth factor- β and aortic dilation in patients with repaired congenital heart disease. *Sci Rep.* (2019) 9(1):162. doi: 10.1038/s41598-018-36458-1
- Seki M, Kurishima C, Saiki H, Masutani S, Arakawa H, Tamura M, et al. Progressive aortic dilation and aortic stiffness in children with repaired tetralogy of fallot. *Heart Vessels.* (2014) 29(1):83–7. doi: 10.1007/s00380-013-0326-1
- Robinson HP, Sweet EM, Adam AH. The accuracy of radiological estimates of gestational age using early fetal crown-rump length measurements by ultrasound as

- a basis for comparison. *Br J Obstet Gynaecol.* (1979) 86(7):525–8. doi: 10.1111/j.1471-0528.1979.tb10804.x
17. Rodríguez-López M, Cruz-Lemini M, Valenzuela-Alcaraz B, García-Otero L, Sitges M, Bijmens B, et al. Descriptive analysis of different phenotypes of cardiac remodeling in fetal growth restriction. *Ultrasound Obstet Gynecol.* (2017) 50(2):207–14. doi: 10.1002/uog.17365
 18. Crispi F, Bijmens B, Figueras F, Bartrons J, Eixarch E, Le Noble F, et al. Fetal growth restriction results in remodeled and less efficient hearts in children. *Circulation.* (2010) 121(22):2427–36. doi: 10.1161/CIRCULATIONAHA.110.937995
 19. Barker DJP. Adult consequences of fetal growth restriction. *Clin Obstet Gynecol.* (2006) 49(2):270–83. doi: 10.1097/00003081-200606000-00009
 20. Mert MK, Satar M, Özbarlas N, Yaman A, Özgüven FT, Asker HS, et al. Troponin T and NT ProBNP levels in gestational, type 1 and type 2 diabetic mothers and macrosomic infants. *Pediatr Cardiol.* (2016) 37(1):76–83. doi: 10.1007/s00246-015-1242-1
 21. Patey O, Carvalho JS, Thilaganathan B. Perinatal changes in fetal cardiac geometry and function in diabetic pregnancy at term. *Ultrasound Obstet Gynecol.* (2019) 54(5):634–42. doi: 10.1002/uog.20187
 22. García-Otero L, López M, Gómez O, Goncá A, Bannasar M, Martínez JM, et al. Zidovudine treatment in HIV-infected pregnant women is associated with fetal cardiac remodeling. *AIDS.* (2016) 30(9):1393–401. doi: 10.1097/QAD.0000000000001066
 23. Figueras F, Gratacós E. Update on the diagnosis and classification of fetal growth restriction and proposal of a stage-based management protocol. *Fetal Diagn Ther.* (2014) 36(2):86–98. doi: 10.1159/000357592
 24. Yagel S, Cohen SM, Achiron R. Examination of the fetal heart by five short-axis views: a proposed screening method for comprehensive cardiac evaluation. *Ultrasound Obstet Gynecol.* (2001) 17(5):367–9. doi: 10.1046/j.1469-0705.2001.00414.x
 25. Lee W, Carvalho JS, Chauvi R, Copel J, Hecher K, Paladini D. Cardiac screening examination of the fetus: guidelines for performing the “basic” and “extended basic” cardiac scan. *Ultrasound Obstet Gynecol.* (2006) 27(1):107–13. doi: 10.1002/uog.2677
 26. Bhidé A, Acharya G, Bilardo CM, Brezinka C, Cafici D, Hernandez-Andrade E, et al. ISUOG Practice guidelines: use of Doppler ultrasonography in obstetrics. *Ultrasound Obstet Gynecol.* (2013) 41(2):233–9. doi: 10.1002/uog.12396
 27. Hecher K, Campbell S, Snijders R, Nicolaides K. Reference ranges for fetal venous and atrioventricular blood flow parameters. *Ultrasound Obstet Gynecol.* (1994) 4(5):381–90. doi: 10.1046/j.1469-0705.1994.04050381.x
 28. Hadlock FP, Harrist RB, Shah YP, King DE, Park SK, Sharman RS. Estimating fetal age using multiple parameters: a prospective evaluation in a racially mixed population. *Am J Obstet Gynecol.* (1987) 156(4):955–7. doi: 10.1016/0002-9378(87)90365-6
 29. Figueras F, Meler E, Iraola A, Eixarch E, Coll O, Figueras J, et al. Customized birthweight standards for a Spanish population. *Eur J Obstet Gynecol Reprod Biol.* (2008) 136(1):20–4. doi: 10.1016/j.ejogrb.2006.12.015
 30. Baschat AA, Gembruch U. The cerebroplacental Doppler ratio revisited. *Ultrasound Obstet Gynecol.* (2003) 21(2):124–7. doi: 10.1002/uog.20
 31. García-Otero L, Soveral I, Sepúlveda-Martínez Á, Rodríguez-López M, Torres X, Guirado L, et al. Reference ranges for fetal cardiac, ventricular and atrial relative size, sphericity, ventricular dominance, wall asymmetry and relative wall thickness from 18 to 41 gestational weeks. *Ultrasound Obstet Gynecol.* (2021) 58(3):388–97. doi: 10.1002/uog.23127
 32. García-Otero L, Gómez O, Rodríguez-López M, Torres X, Soveral I, Sepúlveda-Martínez Á, et al. Nomograms of fetal cardiac dimensions at 18–41 weeks of gestation. *Fetal Diagn Ther.* (2020) 47(5):387–98. doi: 10.1159/000494838
 33. Schneider C, McCrindle BW, Carvalho JS, Hornberger LK, McCarthy KP, Daubeney PEF. Development of z-scores for fetal cardiac dimensions from echocardiography. *Ultrasound Obstet Gynecol.* (2005) 26(6):599–605. doi: 10.1002/uog.2597
 34. Cruz-Lemini M, Crispi F, Valenzuela-Alcaraz B, Figueras F, Sitges M, Gómez O, et al. Value of annular M-mode displacement vs tissue Doppler velocities to assess cardiac function in intrauterine growth restriction. *Ultrasound Obstet Gynecol.* (2013) 42(2):175–81. doi: 10.1002/uog.12374
 35. Ikeda T, Sun L, Tsuruoka N, Ishigaki Y, Yoshitomi Y, Yoshitake Y, et al. Hypoxia down-regulates sFlt-1 (sVEGFR-1) expression in human microvascular endothelial cells by a mechanism involving mRNA alternative processing. *Biochem J.* (2011) 436(2):399–407. doi: 10.1042/BJ20101490
 36. Snoep MC, Aliasi M, van der Meer LE, Jongbloed MRM, DeRuiter MC, Haak MC. Placenta morphology and biomarkers in pregnancies with congenital heart disease - A systematic review. *Placenta.* (2021) 112:189–96. doi: 10.1016/j.placenta.2021.07.297
 37. Di Angelantonio E, Chowdhury R, Sarwar N, Ray KK, Gobin R, Saleheen D, et al. B-type natriuretic peptides and cardiovascular risk: systematic review and meta-analysis of 40 prospective studies. *Circulation.* (2009) 120(22):2177–87. doi: 10.1161/CIRCULATIONAHA.109.884866
 38. Mondal T, Ryan PM, Gupta K, Radovanovic G, Pugh E, Chan AKC, et al. Cord-blood high-sensitivity troponin-I reference interval and association with early neonatal outcomes. *Am J Perinatol.* (2022) 29(14):1548–54. doi: 10.1055/s-0041-1722944
 39. Alexandre SM, D’Almeida V, Guinsburg R, Nakamura MU, Tufik S, Moron A. Cord blood cardiac troponin I, fetal Doppler velocimetry, and acid base status at birth. *Int J Gynaecol Obstet.* (2008) 100(2):136–40. doi: 10.1016/j.ijgo.2007.08.007
 40. Perez-Cruz M, Crispi F, Fernández MT, Parra JA, Valls A, Gomez Roig MD, et al. Cord blood biomarkers of cardiac dysfunction and damage in term growth-restricted fetuses classified by severity criteria. *Fetal Diagn Ther.* (2018) 44(4):271–6. doi: 10.1159/000484315
 41. Goumans MJ, Liu Z, ten Dijke P. TGF-beta signaling in vascular biology and dysfunction. *Cell Res.* (2009) 19(1):116–27. doi: 10.1038/cr.2008.326
 42. Dobaczewski M, Chen W, Frangogiannis NG. Transforming growth factor (TGF)- β signaling in cardiac remodeling. *J Mol Cell Cardiol.* (2011) 51(4):600–6. doi: 10.1016/j.yjmcc.2010.10.033
 43. Jatavan P, Tongprasert F, Srisupundit K, Luewan S, Traisrisilp K, Tongsong T. Quantitative cardiac assessment in fetal tetralogy of fallot. *J Ultrasound Med.* (2016) 35(7):1481–8. doi: 10.7863/ultra.15.08017
 44. Wiputra H, Chen CK, Talbi E, Lim GL, Soomarr SM, Biswas A, et al. Human fetal hearts with tetralogy of fallot have altered fluid dynamics and forces. *Am J Physiol Heart Circ Physiol.* (2018) 315(6):H1649–59. doi: 10.1152/ajpheart.00235.2018
 45. Groenendijk BCW, Hierck BP, Gittenberger-De Groot AC, Poelmann RE. Development-related changes in the expression of shear stress responsive genes KLF-2, ET-1, and NOS-3 in the developing cardiovascular system of chicken embryos. *Dev Dyn.* (2004) 230(1):57–68. doi: 10.1002/dvdy.20029
 46. Sun L, van Amerom JFP, Marini D, Portnoy S, Lee FT, Saini BS, et al. MRI Characterization of hemodynamic patterns of human fetuses with cyanotic congenital heart disease. *Ultrasound Obstet Gynecol.* (2021) 58(6):824–36. doi: 10.1002/uog.23707
 47. El-Hamamsy I, Yacoub MH. Cellular and molecular mechanisms of thoracic aortic aneurysms. *Nat Rev Cardiol.* (2009) 6(12):771–86. doi: 10.1038/nrcardio.2009.191
 48. Franken R, den Hartog AW, de Waard V, Engle L, Radonic T, Lutter R, et al. Circulating transforming growth factor- β as a prognostic biomarker in Marfan syndrome. *Int J Cardiol.* (2013) 168(3):2441–6. doi: 10.1016/j.ijcard.2013.03.033
 49. Taketazu M, Sugimoto M, Saiki H, Ishido H, Masutani S, Senzaki H. Developmental changes in aortic mechanical properties in normal fetuses and fetuses with cardiovascular disease. *Pediatr Neonatol.* (2017) 58(3):245–50. doi: 10.1016/j.pedneo.2016.05.004
 50. Ghanchi A, Rahshenas M, Bonnet D, Derridj N, LeLong N, Salomon LJ, et al. Prevalence of growth restriction at birth for newborns with congenital heart defects: a population-based prospective cohort study EPICARD. *Front Pediatr.* (2021) 9:676994. doi: 10.3389/fped.2021.676994
 51. Escobar-Diaz MC, Pérez-Cruz M, Arráez M, Cascant-Vilaplana MM, Albiach-Delgado A, Kuligowski J, et al. Brain oxygen perfusion and oxidative stress biomarkers in fetuses with congenital heart disease: A retrospective, case-control pilot study. *Antioxidants.* (2022) 11(2):299. doi: 10.3390/antiox11020299

Study 4

Biventricular remodeling and dysfunction in fetuses with Tetralogy of Fallot. A speckle tracking echocardiography study.

Status: in preparation

METHODS

Study design and participants

A multicenter prospective cohort study was designed including singleton fetuses with isolated Tetralogy of Fallot (ToF) from 20 to 40 weeks of gestation and healthy control fetuses matched by gestational age at scan, with a 1:1 control - case ratio. Forty-two ToF fetuses were prospectively recruited from September 2011 to January 2023 among 2724 fetuses with congenital heart defects (CHD) evaluated in the Fetal Cardiology Unit at BCNatal (Hospital Clínic de Barcelona and Hospital Sant Joan de Deu), a national referral center for CHD. Twenty-nine ToF fetuses were prospectively recruited from June 2019 to January 2023 in the division of perinatal medicine and fetal therapy of Universitätsklinikum Gießen and Marburg, reference center for CHD in Germany. ToF was diagnosed as a combination of outlet ventricular septal defect (VSD) with overriding of the aorta and pulmonary stenosis (PS), with anterograde flow through the ductus arteriosus (DA), or pulmonary atresia (PA) with retrograde DA flow. Controls were recruited from low-risk pregnancies followed at BCNatal with no maternal conditions that could potentially induce fetal cardiovascular remodeling, who were invited to participate in the study. Exclusion criteria included other types of ToF such as ToF-absent pulmonary valve, as well as fetuses with additional major cardiac or extracardiac malformations, including genetic anomalies and poor image quality for speckle tracking echocardiography (STE). Maternal characteristics (age, body mass index, smoking status), comorbidities (such as hypertension and diabetes) and gestational complications were retrieved from patients' medical records. Perinatal outcome including gestational age and mode of delivery, birthweight and Apgar score and umbilical artery pH were also obtained. ToF was confirmed postnatally in all cases, and newborns were followed-up for at least for 9 months. Information on admission to the intensive care unit, the need for prostaglandins, oxygen saturation, type, and age at surgery was obtained for all cases. The study protocol was approved by the Ethical Committee of the institution and written consent was obtained from all pregnant women.

Feto-placental ultrasound standard echocardiography

All participants underwent a feto-placental ultrasound and echocardiography to rule out other cardiac or extracardiac anomalies according to the existing Guidelines^{1,2}. Doppler and echocardiographic evaluations were performed using either Voluson E8, E10 (GE Healthcare Ultrasound, Milwaukee, WI, USA) with a M6C-D and C2-9D convex probe (3-9MHz), or Toshiba Artida an Aplio 500 or an Aplio i900 system (Toshiba Medical Systems Corporation, Otawara, Tochigi, Japan) with a 1-5-MHz curved array probe (PVT 375 BT). Gestational age was calculated based on the crown-rump length at first trimester ultrasound³ and the estimated fetal weight (EFW) was obtained according to Hadlock et al⁴. Weight centile was determined according to local references, adjusted by gestational age and fetal gender⁵. Doppler evaluation included the measurement of umbilical artery pulsatility index (PI), middle cerebral artery PI, ductus venosus PI, and cerebro-placental ratio (middle cerebral artery PI/umbilical artery PI) ⁶.

A comprehensive echocardiography was conducted to evaluate fetal cardiac morphometric and functional parameters, preferably at third trimester of gestation. The methodology used to evaluate morphometric and functional parameters through 2D echocardiography has been previously published and is detailed in **Supplementary Table 1**. In all measurements right ventricle (RV) trabeculations and moderator band were considered as RV cavity^{7,8}.

Fetal speckle tracking echocardiography

Four-chamber view clips containing at least three heart cycles with a high frame rate were used for STE. Clips were stored in DICOM (Digital Imaging and Communication in Medicine) format and were analyzed using the 2D STRAIN (Fetal) software developed by TomTec imaging systems, GmbH (Munich, Germany). All STE analysis were performed by the same experienced operator (L.N.). STE reproducibility was previously tested by our group⁸.

As fetal EKG is not available, the end-systolic and end-diastolic frames of a cardiac cycle were identified using an M-mode display of the tricuspid annulus. To semi-automatically track the endocardial border, the septal and lateral atrioventricular valve annulus and apex of the RV and left ventricle (LV) were indicated in the end-systolic frame⁹. Semi-

automated tracking was manually adjusted as needed. STE software generated automatically strain curves for six segments of the LV and RV walls and interventricular septum (basal, mid-ventricular and apical). Morphometric parameters included in the analysis were biventricular area, longitudinal and transverse diameters¹⁰. Biventricular global longitudinal strain (GLS) was analyzed and reported as an absolute value^{11,12}. RV and LV lateral wall annular plane systolic excursion (TAPSE, MAPSE) were calculated automatically by STE software as the movement of the endocardium closest to the tricuspid and mitral annulus towards the ventricular apex¹³. Both were evaluated to assess longitudinal function.

The global RV function was evaluated using fractional area change (FAC)¹⁴ and LV function was assessed using ejection fraction¹⁵. Segmental analysis of SI and SF were not considered due to their limited reproducibility⁸.

STE segmental analysis and mechanical dyssynchrony

Segmental STE analysis was performed to explore mechanical dyssynchrony. Both ventricles were automatically divided into 6 ventricular segments (free-wall basal, mid-ventricular and apical and septum apical, mid-ventricular and basal). Mean free wall and septal wall peak strain was calculated for each ventricle. Peak systolic strain in each of the 6 RV and LV segments, and their timing, were measured to evaluate mechanical dyssynchrony. Time-to-peak shortening (ms) was defined as the time interval from the onset of myocardial shortening to peak systolic strain. Difference of time to peak strain between basal and apical segments of both RV and LV free wall was calculated (RV and LV free wall peak strain delay). Standard deviation of the time-to-peak shortening of the 6 ventricular segments was assessed (intra-RV and intra-LV dyssynchrony index) as an indicator of mechanical dyssynchrony¹⁶.

Statistical analysis

Statistical analysis was performed using IBM SPSS Statistics for Mac (version 25, IBM Corp., Armonk, NY, USA). A Kolmogorov-Smirnov test of normality was performed in all continuous variables. Data are presented as mean (standard deviation), mean (interquartile range) for non-parametric variables or number (percentage) for

categorical variables. Comparisons between groups were assessed by Student's t test for continuous variables, Mann-Whitney U test for non-normally distributed variables and Chi-square test for categorical variables. Cardiac morphometric parameters were adjusted by EFW. P- values below 0.05 were considered statistically significant. Spearman correlation coefficient was used to assess potential associations between echocardiographic parameters and mechanical dyssynchrony and postnatal outcome.

Intraobserver and interobserver reproducibility

The intra- and interobserver reproducibility were previously assessed by our group⁸. We reported good reproducibility for biventricular global morphometric and functional parameters as well as segmental morphometric diameters. On the other side, lower intraclass correlation coefficient for segmental sphericity index and shortening fraction was observed, reason by we don't assess such indices in the present study.

RESULTS

Characteristics of the study population

Figure 1 represents a flowchart of the included ToF cases. A total of 68 ToF fetuses were recruited, 41 from BCNatal and 27 from Universitätsklinikum Gießen and Marburg. Three cases lost to follow-up were excluded from the original cohort. Additionally, two cases were excluded due to insufficient quality of 4-chamber view clips for STE. The final analysis included a cohort of 63 ToF fetuses and 66 healthy controls. Among them, five had a prenatal diagnosis of ToF-PA and 58 ToF-PS. Associated mirror cardiac anomalies were found in 19 ToF fetuses (39.7%); 19 right aortic arch (30.2%) and 6 persistent left superior vena cava (9.5%). Amniocentesis for microarray analysis was offered and performed in 54 ToF fetuses (85.7%) to exclude genetic anomalies. Genetic syndromes were ruled out postnatally in the remaining cases. Three patients (4.76%) opted for a termination of pregnancy in the second trimester and there was one fetal demise of unknown cause.

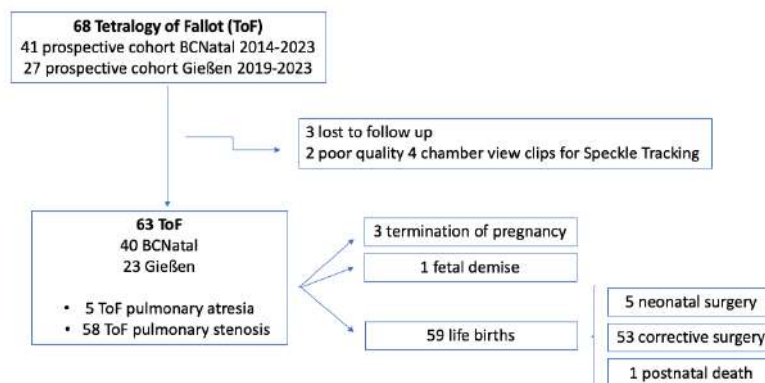


Figure 1. Flowchart of fetuses with Tetralogy of Fallot included in the study. ToF: Tetralogy of Fallot.

The maternal and perinatal characteristics of the study population are detailed in **Table 1**. There were no significant differences between both groups in terms of maternal

baseline characteristics except for maternal body mass index, which was higher in the ToF group (24.90 ± 5.32 ToF group vs. 22.96 ± 3.99 control group). Gestational diabetes (n=6, 9.5%) and placental diseases such as preeclampsia (n=4, 6.35%) and fetal growth restriction (n=12, 19.1%) were more frequently observed in the ToF group. A higher cesarean section rate was observed in the ToF group, with no differences in arterial pH at delivery or in 5-minute APGAR score. Moreover, ToF neonates showed lower birthweight and birthweight centile at a similar gestational age at birth. Postnatal echocardiography confirmed ToF in all fetuses. The median postnatal follow-up was 7.08 years (range: 3.54-8.65). Eight ToF fetuses (12.7%) required prostaglandin infusion and underwent an early procedure within the first month of age (5 Blalock-Taussig shunt and 3 ductus arteriosus stent) and one died before corrective surgery due to septic shock after Blalock-Taussig shunt procedure. Up to 75% of the newborns required β -blocker treatment until corrective surgery.

Table 1. Maternal characteristics and perinatal outcome in Tetralogy of Fallot (ToF) fetuses and healthy controls

| Variable | Tetralogy of Fallot (n=63) | Controls (n=66) | p value* |
|--------------------------------------|----------------------------|---------------------|------------------|
| MATERNAL CHARACTERISTICS | | | |
| Maternal age (years) | 33.30 (30.00-37.49) | 33.00 (30.00-36.80) | 0.593 |
| Body mass index (kg/m ²) | 24.90 \pm 5.32 | 22.96 \pm 3.99 | 0.028 |
| Ethnicity | | | |
| Caucasian | 47 (74.60%) | 59 (89.40%) | 0.097 |
| Latin American | 5 (7.93%) | 6 (9.10%) | |
| Maghreb | 2 (3.17%) | 1 (1.50%) | |
| Asian | 6 (9.52%) | 0 (0.00%) | |
| African | 2 (3.17%) | 0 (0.00%) | |
| Smoking habit | 3 (4.76%) | 5 (7.60%) | 0.508 |
| Nulliparity | 37 (58.73%) | 31 (47.00%) | 0.181 |
| PERINATAL CHARACTERISTICS | | | |
| Gestational age at birth, (weeks) | 39.0 (38.0-39.6) | 40.0 (39.0-40.4) | 0.154 |
| Gestational complications | | | |
| Fetal growth restriction | 12 (19.05%) | 0 (0.00%) | <0.001 |
| Preeclampsia | 4 (6.35%) | 0 (0.00%) | 0.038 |
| Gestational diabetes | 6 (9.50%) | 0 (0.00%) | 0.012 |
| Prematurity (Birth <37 weeks) | 1 (1.60%) | 1 (1.52%) | 0.982 |
| Cesarean section | 25 (39.68%) | 12 (18.18%) | 0.007 |

| | | | |
|--|---------------------------|---------------------------|--------------|
| Birthweight (g) | 3075.00 (2600.50-3377.50) | 3430.00 (3210.00-3737.50) | 0.001 |
| Birthweight centile | 27.50 (7.78-70.81) | 60.00 (36.50-78.00) | 0.015 |
| Five-minute APGAR <7 | 0 (0.00%) | 0 (0.00%) | 1.000 |
| Umbilical artery pH | 7.24 ± 0.05 | 7.23 ± 0.08 | 0.225 |
| Female fetal gender | 33 (52.38%) | 30 (45.50%) | 0.431 |
| CARDIOVASCULAR OUTCOME | | | |
| Neonatal intensive care unit stay (days) | 5.00 (3.00-9.25) | NA | |
| O2 saturation (%) | 95.54 ± 2.26 | NA | |
| Prostaglandin infusion | 8 (12.70%) | NA | |
| β-blocker treatment | 44 (74.58%) | NA | |
| Age at corrective surgery (months) | 5.62 (3.38-6.78) | NA | |
| Follow-up (years) | 7.08 (3.54-8.65) | NA | |
| <small>Data expressed as mean ± standard deviation, median (interquartile range) or n (percentage). NA: not applicable *P-value comparing Tetralogy of Fallot (ToF) versus controls calculated by t-test or Mann-Whitney U test for continuous variables according to its distribution (normal or non-normal) and chi-squared for categorical variables.</small> | | | |

Fetal ultrasound and comprehensive 2D echocardiographic results

Characteristics of the ToF fetuses and obstetric ultrasound are presented in **Tables 2 and 3**. Minor cardiac abnormalities, such as right aortic arch or persistent left superior vena cava, were found in 25 (39.7%) fetuses. Although the median gestational age at ultrasound was similar between groups (31.6 (30.3-34.0 vs 31.5 (29.5-34.0), $p=0.893$), ToF fetuses showed a lower EFW centile and a more pulsatile ductus venosus. Additionally, five fetuses (7.94%) showed reversed flow at the ductus arteriosus.

As expected, the pulmonary valve diameter in the ToF group was decreased with a higher transvalvular peak velocity compared to the controls. Additionally, the left ventricle outflow tract peak velocity and aortic valve diameter were increased when compared to controls (**Table 3**). Median VSD size was 4.96mm (4.23-6.16mm).

Table 2. Fetal characteristics and obstetric ultrasound parameters in Tetralogy of Fallot (ToF) fetuses and healthy controls

| Variable | Tetralogy of Fallot (n=63) | Controls (n=66) | p value* |
|---|----------------------------|---------------------|------------------|
| FETAL ULTRASOUND | | | |
| Gestational age ultrasound (weeks.days) | 31.6 (30.0-34.0) | 31.5 (29.4-34.0) | 0.893 |
| Estimated fetal weight (g) | 1724.38 ± 642.81 | 1869.92 ± 687.37 | 0.234 |
| Estimated fetal weight centile | 28.00 (5.50-61.50) | 48.00 (27.00-76.00) | 0.028 |
| Umbilical artery PI | 1.03 ± 0.20 | 1.00 ± 0.20 | 0.298 |
| Middle cerebral artery PI | 1.86 (1.63-2.17) | 2.00 (1.70-2.20) | 0.200 |
| Cerebroplacental ratio | 1.74 (1.55-2.18) | 1.93 (1.64-2.42) | 0.276 |
| Ductus venosus PI | 0.54 ± 0.21 | 0.39 ± 0.15 | <0.001 |
| Ductus venosus PI centile | 49.50 (13.00-82.75) | 16.00 (5.00-36.00) | 0.001 |
| Ductus arteriosus reversed flow | 5 (7.94%) | 0 (0.00%) | 0.008 |
| <i>PI: Pulsatility Index. NA: not applicable</i> <i>Data expressed as mean ± standard deviation, median (interquartile range) or n (percentage).</i> <i>*P-value comparing Tetralogy of Fallot (ToF) versus controls calculated by t-test or Mann-Whitney U test for continuous variables according to its distribution (normal or non-normal).</i> | | | |

The comprehensive 2D-echocardiography results are displayed in **Table 3**. ToF fetuses show signs of cardiac remodeling with a lower sphericity index, thicker septal, right and left ventricular walls, and increased right and left relative wall thickness, indicating biventricular concentric hypertrophy. Moreover, ToF fetuses have a higher aortic output (that comprises combined LV output and RV output), higher cardiac index, together with a higher fetal heart rate. Furthermore, prolonged tricuspid and mitral filling time fraction were observed in ToF fetuses, reflecting possibly in part subclinical diastolic dysfunction, due to the biventricular hypertrophy, as a moderate correlation between tricuspid filling time fraction and right ventricle wall thickness was demonstrated ($R=0.448$, $p<0.001$), **Figure 2**.

Table 3. Comprehensive 2D echocardiographic parameters in Tetralogy of Fallot (TOF) fetuses and healthy controls

| Variable | Tetralogy of Fallot (n=63) | Controls (n=66) | p value* |
|--|----------------------------|------------------------|------------------|
| GLOBAL CARDIAC PARAMETERS | | | |
| Cardio thoracic ratio | 0.30 (0.27-0.33) | 0.29 (0.37-0.31) | 0.431 |
| Global sphericity index | 1.16 ± 0.09 | 1.23 ± 0.10 | 0.002 |
| Fetal heart rate (bpm) | 143.38 ± 11.34 | 138.58 ± 10.97 | 0.016 |
| Cardiac index (ml/min/kg) | 514.83 (415.71-650.00) | 349.71 (306.33-409.65) | <0.001 |
| RIGHT VENTRICLE OUTFLOW PARAMETERS | | | |
| Pulmonary valve (mm) † | 4.70 ± 1.38 | 6.41 ± 1.04 | <0.001 |
| Pulmonary artery z-score | -2.84 ± 2.26 | -0.10 ± 0.48 | <0.001 |
| Right pulmonary artery (mm) | 2.90 (2.50-3.45) | NA | |
| Right pulmonary artery z-score | -1.17 (-1.75 - -0.18) | NA | |
| Left pulmonary artery (mm) | 3.00 (2.60-3.60) | NA | |
| Left pulmonary artery z-score | -0.18 (-0.91 - 0.24) | NA | |
| Pulmonary valve/aortic valve ratio | 0.70 ± 0.33 | 1.16 ± 0.14 | <0.001 |
| Pulmonary valve peak systolic velocity (cm/s) | 120.00 (92.00-141.50) | 79.00 (72.00-88.00) | 0.001 |
| RIGHT VENTRICLE MORPHOMETRY | | | |
| Right ventricle free wall thickness (mm) † | 4.00 (3.58-4.40) | 3.27 (2.94-3.34) | <0.001 |
| Septal to right ventricle free wall thickness ratio | 0.93 (0.76-1.10) | 1.03 (0.94-1.11) | 0.150 |
| Right ventricle relative wall thickness | 0.66 (0.54-0.87) | 0.50 (0.46-0.57) | 0.001 |
| RIGHT VENTRICLE FUNCTION | | | |
| Pulmonary output (ml/min) | 468.64 ± 318.73 | 487.83 ± 230.10 | 0.763 |
| Tricuspid filling time fraction (%) | 42.30 ± 4.85 | 38.78 ± 2.75 | 0.001 |
| Pulmonary ejection time fraction (%) | 40.97 ± 4.13 | 42.25 ± 2.36 | 0.147 |
| LEFT VENTRICLE OUTFLOW PARAMETERS | | | |
| Aortic valve (mm) † | 7.01 ± 1.57 | 5.56 ± 0.92 | <0.001 |
| Aortic valve z-score | 2.06 ± 1.61 | 0.45 ± 0.71 | <0.001 |
| Ascending aorta (mm) | 6.90 (6.33-7.50) | NA | |
| Ascending aorta z-score | 1.29 (0.59-1.81) | NA | |
| Aortic valve peak systolic velocity (cm/s) | 89.50 (76.00-101.25) | 79.00 (73.25-87.75) | 0.046 |
| LEFT VENTRICLE MORPHOMETRY | | | |
| Septal wall thickness (mm) † | 3.75 ± 0.98 | 3.40 ± 0.56 | 0.008 |
| Left ventricle wall thickness (mm) † | 3.85 (2.90-4.53) | 3.01 (2.80-3.34) | <0.001 |
| Septal to left ventricular free wall thickness ratio | 1.00 (0.88-1.06) | 1.08 (1.00-1.21) | 0.004 |
| Left ventricle relative wall thickness | 0.68 (0.52-0.92) | 0.51 (0.44-0.82) | 0.015 |
| LEFT VENTRICLE FUNCTION | | | |

| | | | |
|--|------------------------|------------------------|--------------|
| Aortic output (ml/min) | 574.00 (468.48-773.95) | 336.15 (211.13-571.21) | 0.001 |
| Mitral Filling time fraction (%) | 45.76 ± 5.34 | 43.06 ± 3.52 | 0.023 |
| Aortic ejection time fraction (%) | 40.63 (38.71-42.91) | 41.40 (40.25-42.59) | 0.499 |
| <i>Data expressed as mean ± standard deviation or median (interquartile range).</i> <i>*P-value comparing Tetralogy of Fallot (ToF) versus controls calculated by t-test or Mann-Whitney U test according to its distribution (normal or non-normal).</i> <i>† Morphometric parameters are adjusted by estimated fetal weight.</i> | | | |

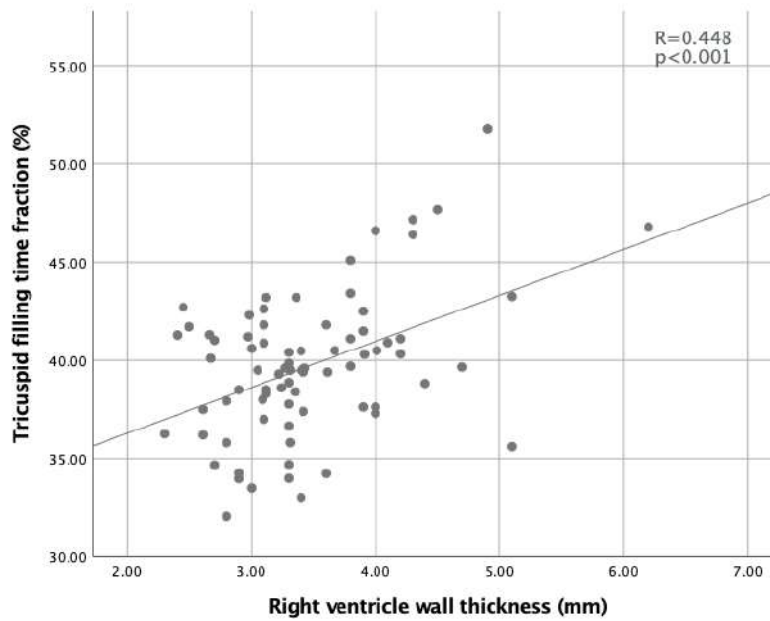


Figure 2. Scatter plot showing the relationship between tricuspid filling time fraction and right ventricle wall thickness.

Fetal speckle tracking echocardiographic results

Table 4 presents the STE morphometric and functional results. Fetuses with ToF exhibit signs of biventricular remodeling, with a reduced longitudinal diameter of both the RV and LV, as well as a smaller LV area and mid-ventricular diameter. In terms of RV function, a significant decrease in RV GLS and TAPSE is observed, while FAC remains

within normal ranges. Additionally, there is evidence of impaired LV function, as indicated by significantly lower LV GLS, LV EF, and MAPSE.

To evaluate differences in free wall and septal wall peak strain, segmental STE analysis was performed. The results showed a decrease in peak strain for both the RV free and septal wall ToF fetuses. However, the LV free wall peak strain was maintained, while LV septal wall was also decreased.

Table 4. Fetal speckle tracking echocardiographic results in fetuses with Tetralogy of Fallot (TOF) and healthy controls

| Parameter | Tetralogy of Fallot (n=63) | Controls (n=66) | p value* |
|--|----------------------------|-----------------|--------------|
| RIGHT VENTRICLE MORPHOMETRY | | | |
| Ventricular Area (cm ²) | 2.58 ± 0.81 | 2.81 ± 0.76 | 0.085 |
| Longitudinal diameter (mm) | 22.5 ± 3.38 | 24.57 ± 3.94 | <0.001 |
| Basal diameter (mm) | 13.06 ± 2.73 | 13.31 ± 2.73 | 0.781 |
| Mid-ventricular diameter (mm) | 12.63 ± 2.79 | 12.83 ± 3.40 | 0.989 |
| RIGHT VENTRICLE FUNCTION | | | |
| Global longitudinal strain(%) | -17.25 ± 3.76 | -19.33 ± 3.09 | 0.001 |
| Right ventricle free wall peak strain (%) | -21.47 ± 4.92 | -23.50 ± 3.76 | 0.021 |
| Right ventricle septal wall peak GLS (%) | -15.80 ± 5.07 | -17.62 ± 4.35 | 0.040 |
| Fractional area change (%) | 29.99 ± 7.05 | 29.87 ± 7.01 | 0.366 |
| Tricuspid annular plane systolic excursion (mm) | 4.77 ± 1.68 | 5.90 ± 1.71 | 0.032 |
| RIGHT VENTRICLE DYSSYNCHRONY | | | |
| Free right ventricle wall time to peak strain delay (ms) | 76.50 (50.75 – 109.25) | 55 (33.75 – 82) | 0.016 |
| Intra-right ventricle dyssynchrony index | 43.57 ± 20.76 | 32.92 ± 20.91 | 0.007 |
| LEFT VENTRICLE MORPHOMETRY | | | |
| Ventricular Area (cm ²) | 2.37 ± 0.85 | 2.81 ± 0.73 | <0.001 |
| Longitudinal diameter (mm) | 22.60 ± 4.14 | 25.34 ± 3.96 | <0.001 |
| Basal diameter (mm) | 11.10 ± 2.54 | 11.81 ± 2.01 | 0.073 |
| Mid-ventricular diameter (mm) | 11.51 ± 2.85 | 12.62 ± 2.16 | 0.004 |
| LEFT VENTRICLE FUNCTION | | | |
| Global longitudinal strain (%) | -17.96 ± 3.78 | -20.87 ± 3.45 | <0.001 |
| Left ventricle free wall peak strain (%) | -21.60 ± 5.06 | -23.30 ± 4.91 | 0.069 |
| Left ventricle septal wall peak strain (%) | -18.31 ± 4.88 | -20.16 ± 3.87 | 0.025 |

| | | | |
|---|---------------------|-------------------|------------------|
| Global circumferential strain (%) | -19.26 ± 8.68 | -21.80 ± 7.99 | 0.103 |
| Ejection fraction (%) | 43.01 ± 11.90 | 49.44 ± 10.30 | 0.001 |
| Mitral annular plane systolic excursion (mm) | 4.09 ± 1.47 | 5.45 ± 1.60 | <0.001 |
| LEFT VENTRICLE DYSSYNCHRONY | | | |
| Free left ventricle wall time to peak strain delay (ms) | 70.00 (42.00-91.00) | 35.5 (17.75 – 55) | <0.001 |
| Intra-left ventricle dyssynchrony index | 38.24 ± 18.33 | 19.95 ± 11.80 | <0.001 |
| <p><i>Data expressed as mean ± standard deviation or median (interquartile range).</i></p> <p><i>*P-value comparing Tetralogy of Fallot (ToF) versus controls calculated by t-test or Mann-Whitney U test according to its distribution (normal or non-normal).</i></p> <p><i>† Morphometric parameters are adjusted by estimated fetal weight.</i></p> <p><i>‡ Tricuspid/Mitral annular plane systolic excursion p-values are adjusted by RV/LV longitudinal diameter.</i></p> | | | |

STE segmental evaluation and mechanical dyssynchrony

Segmental STE analysis showed a biventricular increase in intra-RV and intra-LV dyssynchrony index and free wall time to peak strain delay in the ToF group compared to controls (**Table 4**).

Association between mechanical dyssynchrony and conventional and STE echocardiographic parameters was studied and a moderate negative correlation was found between RV GLS absolute value and intra-RV dyssynchrony index ($R=-0.483$, $p<0.001$) and between LV GLS absolute value and MAPSE with intra-LV dyssynchrony index (LV GLS: $R=-0.406$, $p<0.001$; MAPSE: $R=-0.375$, $p<0.001$) (**Figure 3**). No correlation was found between mechanical dyssynchrony and timing parameters, neither with severity of RV outflow tract obstruction.

Association between ToF severity and biventricular function and clinical parameters

The presence of an association between RV and LV GLS and the severity of RV outflow tract obstruction was evaluated. However only a weak correlation was found between biventricular GLS and pulmonary – aortic ratio (RV GLS: $R=0.215$, $p=0.021$; LV GLS: $R=0.254$, $p=0.006$).

The association between echocardiographic parameters and time to corrective surgery was evaluated but no significant correlation was found. Furthermore, the length of stay in the neonatal intensive care unit showed a negative moderate association with

pulmonary valve diameter ($R=-0.455$, $p=0.009$), pulmonary valve z-scores ($R=-0.566$, $p=0.001$), pulmonary peak systolic velocity ($R=-0.485$, $p=0.009$) and pulmonary – aortic valve ratio ($R=-0.471$, $p=0.007$). On the other hand, no predictors of early surgery (before 3 months of age) were identified.

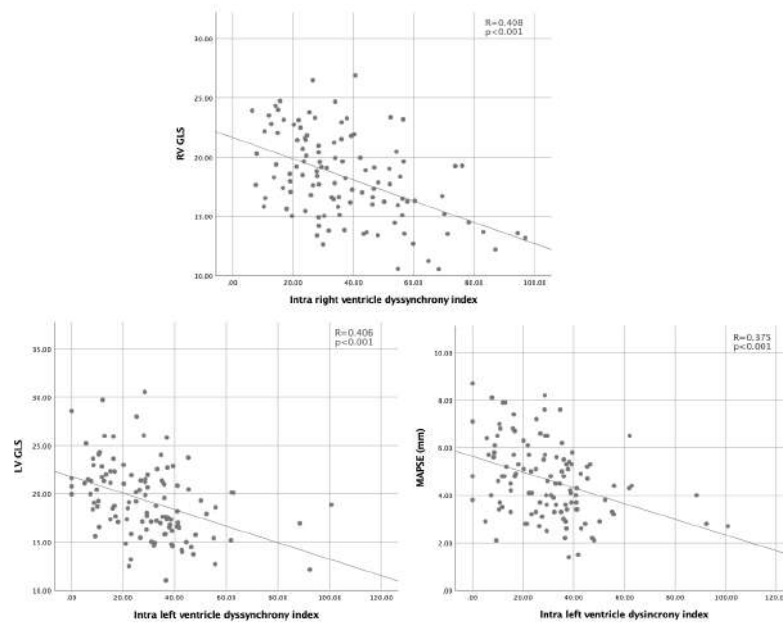


Figure 3. Scatterplots showing moderate negative relationship between mechanical dyssynchrony and right ventricle global longitudinal strain (RV GLS) (*upper graph*), left ventricle global longitudinal strain (LV GLS) (*lower left graph*) and mitral annular plane systolic excursion (MAPSE) (*lower right graph*).

REFERENCES

1. Salomon LJ, Alfievic Z, Berghella V, Bilardo C, Hernandez-Andrade E, Johnsen SL, et al. Practice guidelines for performance of the routine mid-trimester fetal ultrasound scan. *Ultrasound in Obstetrics & Gynecology*. 2011 Jan;37(1):116–26.
2. J S Carvalho, L D Allan, R Chaoui, J A Copel, G R DeVore, K Hecher, et al. ISUOG Practice Guidelines (updated): sonographic screening examination of the fetal heart. *Ultrasound in Obstetrics and Gynecology*. 2013;41(3):348–59.
3. Robinson H. P.; M. Sweet E.; Adam AH. The accuracy of radiological estimates of gestational age using early fetal crown-rump length measurements by ultrasound as a basis for comparison. *BJOG*. 1979;86(July):525–8.
4. Hadlock FP, Harrist RB, Shah YP, King DE, Park SK, Sharman RS. Estimating fetal age using multiple parameters: A prospective evaluation in a racially mixed population. *American Journal of Obstetrics and Gynecology*. 1987 Apr;156(4):955–7.
5. Figueras F, Meler E, Iraola A, Eixarch E, Coll O, Figueras J. Customized birthweight standards for a Spanish population. *Eur J Obstet Gynecol Reprod Biol*. 2008;136:20–4.
6. Baschat AA, Gembruch U. The cerebroplacental Doppler ratio revisited. *Ultrasound Obstet Gynecol*. 2003 Feb;21(2):124–7.
7. Guirado L, Crispi F, Soveral I, Valenzuela-alcaraz B, Rodriguez-López M, García-Otero L, et al. Nomograms of Fetal Right Ventricular Fractional Area Change by 2D Echocardiography. *Fetal Diagn Ther*. 2020;47:399–410.
8. Nogué L, Gómez O, Izquierdo N, Mula C, Masoller N, Martínez JM, et al. Feasibility of 4D-Spatio temporal image correlation (STIC) in the comprehensive assessment of the fetal heart using FetalHQ®. *J Clin Med*. 2022 Mar 4;11(5):1414.
9. Devore GR, Polanco B, Satou G, Sklansky M. Two-Dimensional Speckle Tracking of the Fetal Heart. *Journal Ultrasound Medicine*. 2016;35:1765–81.
10. DeVore GR, Klas B, Satou G, Sklansky M. Evaluation of the right and left ventricles: An integrated approach measuring the area, length, and width of the chambers in normal fetuses. *Prenat Diagn*. 2017 Dec;37(12):1203–12.
11. Devore GR, Klas B, Satou G, Sklansky M, M- U. Longitudinal annulae systolic displacement compared to global strain in normal fetal hearts and those with

- cardiac abnormalities. *J Ultrasound Med.* 2018;37(5):1156–71.
12. Devore GR, Satou G, Sklansky M. Using speckle-tracking echocardiography to assess fetal myocardial deformation: are we there yet? Yes we are! *Ultrasound Obstet Gynecol.* 2019;54:703–4.
 13. Devore GR, Klas B, Satou G, Sklansky M. Speckle tracking of the basal lateral and septal wall annular plane systolic excursion of the right and left ventricles of the fetal heart. *J Ultrasound Med.* 2019;38(5):1309–18.
 14. Devore GR, Klas B, Satou G, Sklansky M. Quantitative evaluation of fetal right and left ventricular fractional area change using speckle-tracking technology. *Ultrasound Obstet Gynecol.* 2019;53(2):219–28.
 15. Devore GR, Klas B, Satou G, Sklansky M. Evaluation of fetal left ventricular tracking and the simpson rule. *J Ultrasound Med.* 2019;38(5):1209–21.
 16. Hui W, Slorach C, Dragulescu A, Mertens L, Bijnens B, Friedberg MK. Mechanisms of right ventricular electromechanical dyssynchrony and mechanical inefficiency in children after repair of tetralogy of fallot. *Circ Cardiovasc Imaging.* 2014 Jul;7(4):610–8.

Supplementary Table 1. Methodology for conventional echocardiographic parameters

| MORPHOMETRY | |
|---|--|
| Cardio thoracic ratio | Apical or transverse 4-chamber view in end-diastole. Cardiac area/Thoracic area*100 |
| Global sphericity index | Longitudinal cardiac diameter/transverse cardiac diameter |
| Free-wall and septal thickness | In end-diastole using M-mode from a transverse 4-chamber view ¹ |
| Ventricular transverse diameters | In end-diastole using M-mode from a transverse 4-chamber view(1) |
| Right and left ventricle relative wall thickness (RWT) | RWT = (septal wall thickness + free wall thickness)/ventricular transverse diameter (1) |
| Septal to right or left free wall thickness ratio (SRWT, SLWT) | Is a measurement of wall thickness asymmetry SRWT, SLWT = septal wall thickness/free wall thickness(1) |
| Pulmonary and aortic valves diameter | Measured during systole with by the leading edge-to-edge method ² |
| Ascending aorta | Measured during systole ² |
| SYSTOLIC FUNCTION | |
| Pulmonary and aortic systolic flows | Obtained in a right and left ventricle (RV, LV) outflow tract view with an angle to ultrasound beam close to 0°, from whose spectral Doppler peak systolic velocity, heart rate (HR) and velocity-time integral (VTI) (area under the curve of aortic and pulmonary flow traced manually) were assessed. |
| Ejection time fraction (ETF) | Measured from systolic pulmonary and aortic pulsed Doppler ETF: ejection time/cardiac cycle*100) ³ |
| Right and left ventricle cardiac outputs (CO) | CO = VTI x valve diameter x HR |
| Cardiac Index (CI) | Cardiac index accounts for combined right and left cardiac outputs. CI = (RV-CO + LV-CO)/EFW (ml/min/Kg) ⁴ |
| DIASTOLIC FUNCTION | |
| Filling time fraction (FTF) | Measured from tricuspid and mitral diastolic spectral Doppler FTF = Filling time/Cardiac cycle*100 ³ |

REFERENCES

1. García-Otro L, Soveral I, Sepúlveda-Martínez Á, Rodríguez-López M, Torres X, Guirado L, et al. Reference ranges for fetal cardiac, ventricular and atrial relative size, sphericity, ventricular dominance, wall asymmetry and relative wall thickness from 18 to 41 weeks of gestation. *Ultrasound Obstet Gynecol.* 2021 Nov;58(5):788
2. Schneider C, McCrindle BW, Carvalho JS, Hornberger LK, McCarthy KP, Daubeney PE. Development of Z -scores for fetal cardiac dimensions from echocardiography. *Ultrasound Obstet Gynecol.* 2005 Nov;26(6):599–605.
3. Soveral I, Crispi F, Guirado L, García-Otero L, Torres X, Bennasar M. Cardiac filling and ejection time fractions by pulsed Doppler: fetal nomograms and potential clinical application. *Ultrasound Obstet Gynecol.* 2021 Jul;58(1):83-91
4. Kiserud T, Ebbing C, Kessler J, Rasmussen S. Fetal cardiac output, distribution to the placenta and impact of placental compromise. *Ultrasound Obstet Gynecol.* 2006;(July):126–36.

Discussion

This thesis has demonstrated the applicability and usefulness of new modalities to evaluate cardiovascular remodeling and function in healthy fetuses and in those with PS and ToF. The studies included in this thesis reflect the usefulness of STE and cord blood biomarkers to evaluate cardiovascular remodeling and postnatal outcome prediction. **Study 1** confirms the high feasibility and accuracy of STE using 4D-STIC volumes, that permits the obtention of perfectly aligned four chamber planes. In **Study 2** we demonstrate that STE echocardiography is also a useful tool to evaluate the RV response and mechanical dyssynchrony to pressure overload in fetuses with PS. A multiparametric scoring system including classical echocardiographic parameters and RV STE improves prenatal prediction of early neonatal valvuloplasty (**Study 2**). Moreover, we also demonstrate, for the first time, that cord blood TGF β concentration is increased in fetuses with ToF from fetal stages, a finding that correlates with the severity of right ventricular outflow tract obstruction (**Study 3**). Finally, we define the pattern of cardiovascular remodeling in ToF fetuses, showing a more spherical heart with biventricular hypertrophy. Additionally, morphometric changes are associated with both, biventricular diastolic dysfunction and decreased contractility, which correlates with the presence of mechanical dyssynchrony (**Study 4**).

1. [Study of cardiac morphometry and function using 4D-STIC speckle tracking echocardiography](#)

Study 1 demonstrates the feasibility of 2D and 4D-STIC STE using FetalHQ[®] through achieving correct endocardium tracking in 97% of 2D clips and 100% of 4D-STIC volumes included in the analysis. Additionally, the study confirms an excellent reproducibility for the most relevant morphometric and functional parameters evaluated, when comparing 4D-STIC and 2D echocardiographic modalities. However, segmental analysis of SI and SF showed poorer results. These findings validate the use of 4D-STIC STE and suggest its potential implementation in the clinical practice.

Speckle tracking echocardiography using 2D and 4D-STIC

2D STE for the evaluation of GLS has shown good reproducibility since its implementation in fetal cardiology(132,133). However, in recent years there has been a concern about the reproducibility between different software used for its analysis(134). Regarding prenatal implementation, there is limited data on GLS normality ranges throughout pregnancy(135–141) and the clinical application of GLS is still poor, thus, STE reproducibility and its correlation with other morphometric and functional echocardiographic parameters need to be further investigated. Recently, excellent interobserver and intraobserver reproducibility of FetalHQ® has been reported for the analysis of fetal global morphometric and functional cardiac parameters(142–145). However, there is some controversy regarding the reproducibility of certain parameters, such as segmental SI and SF(142–144,146), despite initial reports seemed to indicate that its reproducibility was also optimal (147,148).

Focusing on 4D-STIC STE, its use in prenatal life has been scarcely reported. A previous study reported moderate-good inter- and intraobserver reproducibility for LV GLS and LV ejection fraction evaluation(146). **Study 1** showed better reproducibility than previously reported, that could be explained by several reasons. First, a strictly standardized protocol was used for both the acquisition of cardiac volumes and the subsequent off-line processing, which allowed the obtention of higher frame rate clips (with a mean of 107Hz vs 80Hz in the previous study). Secondly, Fetal Medicine specialists participating in **Study 1** had a higher expertise when compared to less experienced sonographers with only three weeks training on FetalHQ® in the other study. To our knowledge, **Study 1** is the first to **demonstrate good reproducibility between 2D and 4D-STIC STE**.

Fetal cardiac morphometric and functional assessment using 4D-STIC STE

The results of **Study 1** showed **good to excellent intra- and interobserver reproducibility of 4D-STIC STE for global morphometric parameters**, which is similar to those reported by other groups with 2D STE(142). However, there are controversial results when assessing SI. On one hand, some groups reported moderate intra- and

interobserver reproducibility for cardiac transverse diameter and SI (>0.758). On the other hand, poor reproducibility has also been reported when assessing the shape of biventricular basal segments(144), which is in concordance with the results of **Study 1**. Several hypotheses may explain the poorer results. Manual adjustment of semi-automated tracking was needed in most cases to better delineate the endocardium, especially the transverse diameters used to calculate SI and FS segmental analysis. Moreover, delineation of the RV cavity may differ between groups due to its anatomy with more prominent trabeculations and the moderator band, which were considered part of the ventricular cavity in the present thesis(149). Furthermore, differences in methodology, such as acquisition angle of the 4-chamber view, could result in variations in ultrasound lateral resolution between the apical and transverse views, which may contribute to the results. Finally, a mathematical formula is used for calculation the SI (SI: end-diastolic longitudinal diameter/end-diastolic transverse diameter), which adds the error from each measurement in comparison with other parameters that do not apply formulas, and this may explain its lower reproducibility. Further studies focusing on methodological RV delineation and angle of acquisition are needed to define their impact on STE reproducibility(150).

Study 1 is the first to comprehensively assess the reproducibility of cardiac function using 2D and 4D-STIC STE. We demonstrated **good intra- and interobserver reliability for systolic function parameters commonly evaluated in fetuses** (GLS, FAC, LV ejection fraction, and cardiac output), with better performance of the LV than the RV, possibly due to RV's more complex 3D structure. However, similarly to SI, biventricular SF reproducibility was poor (<0.6), as previously reported by other groups(142,143). A recently developed technique, known as the Quiver technique, which displays two frames before and after the end-systolic and end-diastolic frames, could help in identifying the septal and lateral AV valve annulus. Its use might improve semi-automatic endocardial tracking and reproducibility(151). Quiver technique was evaluated in 10 fetuses, but it did not achieve better results. As the analysis was carried out on a small number of fetuses, we postulated that this technique may require further investigation. Therefore, more studies are needed to validate the superiority of Quiver technology.

From a clinical point of view, FetalHQ® has been proven to be a useful tool for assessing fetal cardiac morphometry and function with both 2D and 4D-STIC four chamber view acquisition, providing a comprehensive evaluation from a single endocardial trace. Although it requires a learning curve, the good results obtained in **Study 1** support the use of new fetal STE software in assessing fetal cardiac remodeling in different maternal and fetal conditions such as CHD (**Study 2 and 4**).

2. STE to evaluate cardiovascular remodeling and function in PS fetuses and neonatal valvuloplasty prediction

This thesis reports fetal adaptation to RV pressure overload in the largest cohort of mild to critical fetal PS and its correlation with mechanical dyssynchrony using STE. Additionally, a **scoring system to predict postnatal valvuloplasty is described** for the first time, with high accuracy. This score, valid from the second trimester, includes classical echocardiographic parameters typically evaluated in prenatal PS follow-up, such as DV PI centile, the presence of significant TR, and flow at the DA. Incorporating RV GLS into the score enhances the sensitivity of the scoring system.

PS is associated with reduced RV GLS and mechanical dyssynchrony

RV GLS measurement is no longer just a research tool in adult cardiology, but a reliable parameter that provides incremental value for decision-making in RV dysfunction, particularly in cases of pulmonary hypertension(43), as well as in CHD follow-up(33). Furthermore, studies show a reduced RV GLS in the neonatal period in PS, which improves after valvuloplasty(152). Although previous reports of strain in fetal life are limited and studies have shown a wide range of GLS values that overlap with normal values(45,153), we reported, in **Study 1**, that the use of STE in fetal life is reproducible and may be a useful tool for prenatal evaluation of CHD.

Fetal adaptation to pressure overload has been previously described by Crispi et al(12) and previous studies on fetal PS(20). In **Study 2**, an initial response to better tolerate wall stress is observed in mild PS, with an increased cardio-thoracic ratio and a more globular heart. Further biventricular concentric hypertrophy occurs in both mild and

critical PS to increase the contractile force. This hypertrophy leads to diastolic dysfunction (decreased tricuspid filling time fraction) in critical PS, while it remains preserved in mild forms of the disease. Furthermore, an increased cardiac index and biventricular cardiac output is observed in both PS groups, reflecting the volume overload in the RV due to tricuspid regurgitation and in the LV secondary to the higher blood flow through the foramen ovalis to the left atrium. Moreover, RV hypertrophy and myocardial dysfunction may lead to **mechanical dyssynchrony observed in critical PS, which correlates negatively with RV FAC and RV GLS**, and can explain the **RV systolic dysfunction in more severe PS**, which differs from a previous study describing preserved RV function in a cohort composed of mainly mild and moderate PS cases (20).

The assessment of mechanical dyssynchrony and its association with RV function has already been studied in the pediatric population using STE. In example, negative association between interventricular dyssynchrony and TAPSE was observed in a cohort of 48 fetuses with pulmonary stenosis before balloon valvuloplasty(154), showing decreased dyssynchrony and better contractility after successful pulmonary valvuloplasty. It is hypothesized that dyssynchrony is secondary to a mechanical delay due to a right bundle branch block induced by subendocardial wall stress in RV pressure overload, causing an early septal activation(155) (seen as a septal flash). Dyssynchrony was later correlated with decreased RV GLS(44). Our study yielded similar results in terms of RV dyssynchrony, and a septal flash was identified in some severe PS cases, suggesting that right bundle branch block may already exist from fetal life. Therefore, further studies are needed to verify our hypothesis.

Previous studies, with lower number of fetuses, have suggested that adverse RV-LV interaction and LV volume overload caused LV diastolic dysfunction in PS fetuses(20). This is consistent with a study in young adults with PS, reporting a worsening in LV circumferential strain associated with greater RV volume load after ballon pulmonary valvulopasty compared to controls(156). However, **Study 2** did not find any differences in LV function, even in more severe cases. Thus, further studies increasing the number of cases should be conducted to elucidate these different results.

Predictors of neonatal pulmonary valvuloplasty

With the increase in prenatal diagnosis of milder forms of PS, the attention has shifted towards identifying prenatal predictors of postnatal ductal dependency and early neonatal valvuloplasty in order to organize delivery in a tertiary care center. Historically, reversed DA flow was considered a reliable parameter, however 50% of the newborns in our series that required either intervention or prostaglandin infusion had DA antegrade flow in prenatal echocardiography. Other studies have also found that reversed DA flow is not always present in fetuses requiring intervention for PS or prostaglandin E1 treatment(20,118). Therefore, a multiparametric evaluation combining classical parameters with newer and more sensitive ones is needed (118). In example, several timing and morphometric echocardiographic parameters have been described to predict univentricular management in fetuses with the most severe forms of the disease (critical PS and pulmonary atresia). Furthermore, a metanalysis published in 2022(117) concludes that the combination of different echocardiographic parameters in scoring systems improves the prediction of postnatal surgical pathway.

In **Study 2** we identified several **echocardiographic parameters that, when combined in a 4-criteria scoring system, predict postnatal valvuloplasty with a sensitivity of 91.7% and specificity of 100%**. The scoring system was also evaluated without the inclusion of RV GLS variable, which is not universally available, and found a lower sensitivity (83%). As seen in **Figure 9**, the DA retrograde flow, which is currently the most used parameter to predict early neonatal valvuloplasty, shows an area under the curve of 0.750. Therefore, it performs worse than the proposed scoring system. Therefore, including RV GLS in the scoring system enables us to identify more cases with potential neonatal valvuloplasty requirement, who would benefit from delivery in a tertiary care center.

To date, only Wang et al.(118) have studied postnatal management in critical PS and pulmonary atresia with intact interventricular septum with biventricular management at birth. They found that pulmonary valve regurgitation in the second trimester and an RV/LV length ratio >0.86 in the third trimester were predictors of ductal dependency, but the current study did not confirm the utility of those parameters, which might be

explained by the different outcomes studied. Our group also identified decreased TAPSE, mitral E' peak velocity and increased LV cardiac output as possible predictors but in **Study 2** we could not determine their role in predicting the outcome due to the limited sample size(20).

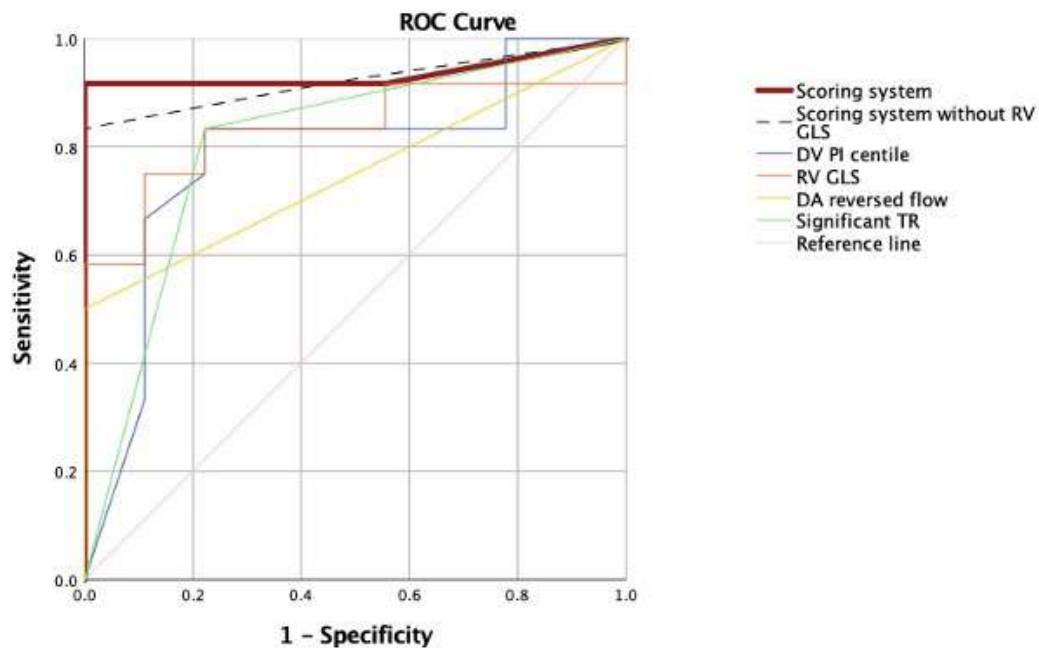


Figure 9. Receiver-operating characteristic (ROC) curves for neonatal valvuloplasty prediction. Red thick line: ROC curve of the scoring system: area under the curve (AUC) 0.931. Dashed line: ROC curve of the scoring system without right ventricle global longitudinal strain (RV GLS): AUC 0.917. Blue line: ROC curve of the ductus venosus pulsatility index centile (DV PI): AUC: 0.782. Orange line: ROC curve of RV GLS: AUC 0.833. Yellow line: ROC curve of the reversed flow at the ductus arteriosus (DA): AUC 0.750. Green line: ROC curve of the presence of significant tricuspid regurgitation (TR): AUC 0.806. (Original figure from study 2).

3. Cord blood cardiovascular biomarkers in conotruncal CHD

To the best of our knowledge, **Study 3** is the first to comprehensively assess the profile of cord blood cardiac biomarkers in fetuses diagnosed with conotruncal CHD. Additionally, is the first to identify **increased concentrations of TGF β in cord blood from fetal stages in ToF and its correlation with the severity of right ventricular outflow tract obstruction.** On the contrary, D-TGA fetuses show a tendency towards an

increased percentage of fetuses with Troponin I positive values, although not statistically significant. Further studies with large number of cases are needed to validate our hypothesis.

Previous studies on cord blood cardiac biomarkers in CHD

There is limited knowledge about cord blood angiogenic factors in fetuses with CHD, and the available studies report conflicting results. For instance, one study reported increased levels of sFlt-1, indicating an anti-angiogenic pattern, in a mixed group of fetal CHD(113). In contrast, a previous study from our group found a modest decrease in PlGF levels in fetuses with left-CHD and a pronounced sFlt1 decrease, but only in those with univentricular left-CHD, indicating a proangiogenic profile in the poor prognostic group(69). Differences between both studies may be attributed to the different CHD studied and the small sample sizes. Furthermore, **Study 3** shows no differences in cord blood levels of PlGF and sFlt1 among the conotruncal anomalies, indicating little ventricular hypoxic damage in utero in these cyanotic CHD. Further research is necessary to determine which types of congenital heart disease are associated with abnormal cardiovascular and placental angiogenesis(105).

NT-proBNP is a useful predictor for severe cardiac conditions, as evidenced by elevated plasmatic levels in pediatric patients with heart failure(157), and elevated cord blood levels in functional single ventricle associated with neonatal death(76), univentricular left-CHD(69), and non-immune hydrops of cardiac origin. In **Study 3**, NT-proBNP levels were slightly elevated in the ToF group but preserved in D-TGA cases, which is consistent with the favorable outcome and lack of complications in the study groups.

Troponin I is a sensitive biomarker for endocardial hypoxia and myocardial damage and has been found to be elevated in various clinical conditions associated with cardiac dysfunction (newborns requiring NICU admission(89), neonates with acidemia(91) and fetuses with intrauterine growth restriction(67)). **Study 3** found that a higher proportion of fetuses with D-TGA had Troponin I values above the 75th centile, but this difference was not statistically significant, probably due to the limited number of cases. The fact that less oxygenated blood reaches the coronary territory in fetal life could explain these

results. Additionally, our group had previously reported more positive values in a group of fetuses with left-CHD with favorable cardiac outcome(69). Larger population studies are needed to better understand the profile of these biomarkers in different groups of CHD and clinical conditions.

Increased TGF β in ToF compared with D-TGA

Increased cord blood TGF β concentrations in ToF is one of the main findings of this thesis. TGF β is upregulated by vascular shear stress and has a role in cardiovascular fibrosis(94) and pro-fibrotic molecular signaling in cardiac pressure overload(95). Hemodynamic factors and intrinsic histological changes may explain this TGF β increase in ToF fetuses.

Limited data is available on blood flow mechanics and its effect on biventricular remodeling in fetal ToF(122), but a recent computational model suggests that biventricular pressure is globally elevated in ToF, although is balanced by the presence of the VSD, and leads to mild RV hypertrophy in fetal life(158). The ventricular walls around the VSD consistently experienced high stress due to a shear flow effect, which has also been described to induce cardiovascular tissue growth and remodeling(159). Furthermore, in normal fetal circulation, there is a preferential shunting across the foramen ovale that accounts for 30% of the cardiac output(160). However, in ToF tricuspid flow through the VSD is increased, as an alternative to foramen ovale(158). This causes portion of the right atrial flow to pass through the VSD which increases aortic flow, leading to an increased endothelial shear stress at septal and aortic wall. All these hemodynamic mechanisms inducing high shear stress could explain the increase in TGF β .

There is a growing interest in understanding TGF β 's role in vascular morphogenesis and extracellular matrix homeostasis and its contribution to vascular remodeling. Altered TGF β signaling has been reported as a key component in the pathogenesis of thoracic aneurysms in bicuspid aortopathy(161), as well as in Marfan syndrome, where circulating levels of TGF β are correlated with aortic root dilation(162), two conditions with intrinsic aortopathy. Additionally, overexpression of TGF β in the ascending aorta

has been observed in patients with ToF, tricuspid atresia, and double-outlet RV, in association with abnormal elastic fibers. **Study 3** findings of an already increased TGF β from fetal life reinforce the hypothesis that an underlying lesion of the aorta may already be present from very early stages of development. In fact, a decreased aortic compliance, evaluated by fetal echocardiography, has already been reported in fetuses with Marfan syndrome and ToF compared to normal fetuses(124). However, we did not dispose of the values of ascending aorta diameter in our cohort. Therefore, future studies evaluating fetal aortic characteristics in different CHD are warranted.

TGF β correlates with the severity of the RV obstruction in ToF

Previous studies have shown a positive correlation between TGF β levels and aortic sinus dimension in patients with repaired-ToF(98), as well as a correlation with aortic stiffness in patients with ToF before surgical repair(99). **Study 3** supports these findings, showing a **negative correlation between TGF β concentration and pulmonary valve diameter z-score**, and a positive correlation with aortic/pulmonary valve ratio in ToF fetuses (**Figure 10**).

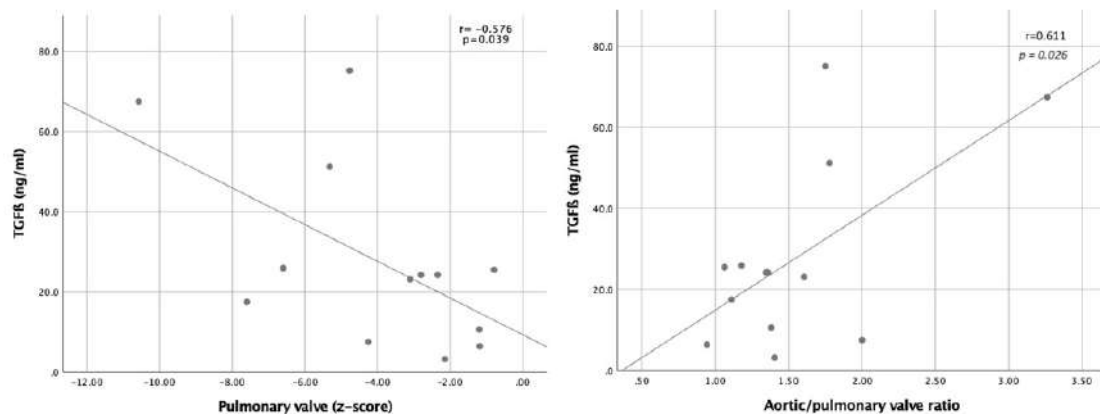


Figure 10. Correlation of transforming growth factor β (TGF β) and echocardiographic parameters. Left graphic: pulmonary valve diameter z score. Right graphic: aorta/pulmonary ratio. (Original figure from study 3).

A higher degree of RV outflow obstruction leads to increased aortic volume through the VSD, that would explain higher TGF β levels. However, no correlation was found between

TGF β levels and fetal RV morphometry (SI) and function (TAPSE, peak pulmonary peak systolic velocity), which requires further investigation with a larger number of cases.

In agreement with previous reports, newborns with ToF had a significantly lower birth weight compared to the D-TGA and control groups(163) that could also contribute to an increase in TGF β , as previous reports show increased concentrations in growth-restricted fetuses(101). Additionally, head circumference perimeter at birth was also significantly reduced in both conotruncal CHD groups(164). However, cord blood biomarkers were not correlated with any ultrasound parameter or perinatal outcome. Similarly, no cord blood biomarker was correlated with any echocardiographic parameter in the D-TGA and control groups. However, these results may be limited by the small sample size of our study.

4. STE to evaluate cardiovascular remodeling and function in ToF fetuses

In **Study 4**, we evaluate fetal cardiovascular remodeling and myocardial deformation using STE in the largest series of prenatal isolated ToF. Moreover, we explore the correlation with postnatal outcome. The results of the study show that **ToF has a biventricular impact from fetal life**. We describe a pattern of **cardiac remodeling** secondary to pressure overload (globular shape and concentric hypertrophy). Additionally, we demonstrate a **biventricular decrease in ventricular contractility which correlates with the presence of prenatal mechanical dyssynchrony**.

Biventricular remodeling in ToF fetuses

ToF is associated to an increased RV pressure as a result of RV outflow tract obstruction, which is balanced through the VSD towards the left ventricle. It has been demonstrated that both RV and LV pressures are higher than controls(158). Cardiac shape adaptation to better tolerate this mild pressure overload is observed in our ToF cohort, resulting in a more globular heart with concentric hypertrophy. Classically, it was believed that ToF fetuses did not present RV hypertrophy due to the characteristics of prenatal circulation. However, Jatavan et al were the first to demonstrate that RV hypertrophy is already

present from prenatal stage by analyzing a series of 20 fetuses at second trimester of pregnancy by means of STIC(122). This finding has been later confirmed by conventional echocardiography(53,60). **Our study confirms, in a largest series by STE, that mild hypertrophy is present in ToF fetuses, affecting RV as well as septal and LV walls,** demonstrating a global cardiac affection. Differences in gestational age at ultrasound, methodology and smaller series could explain the fact that previous studies did not find the LV response. More studies are needed to confirm our results as this novel finding is relevant. The presence of a more hypertrophic myocardium could potentially impact the biventricular response to hemodynamic and surgical changes, particularly in the RV.

Cardiac function in ToF fetuses

Timing parameters in fetal ToF are described for the first time in **Study 4**. We demonstrate prolonged **tricuspid and mitral time fractions, indicating mild impairment in right and left diastolic function**. This finding differs from fetal pulmonary stenosis, where the mitral filling time fraction is not affected(20). The decrease in biventricular diastolic function in ToF can be explained by a higher LV volume load proceeding from the RV through the VSD(158). This increase in LV load may affect left ventricular filling. On the contrary in fetal pulmonary stenosis the flow distributes through the foramen ovale to the left atrium, not directly to the ventricle. Moreover, the increased wall thickness may also difficult cardiac relaxation in both ventricles. In line with this, we found a moderate correlation between RV wall thickness and tricuspid filling time fraction.

Keelan reported a decrease in presurgical RV GLS in ductal dependent ToF compared to controls(165). Interestingly, decrease in ventricular deformation has also been demonstrated to be present *in utero*(53,60,166). Our results **decreased RV GLS in TOF fetuses**. Song et al. postulated that long-term pressure overload in the RV and increased wall shear stress may impact on ventricular contractility. An increased RV wall stress and biventricular increased pressure were described by Wiputra in a computational model of fluid dynamics(158). Increased wall stress, along with hypertrophy, may contribute to ischemia in the inner myocytes due to decreased coronary perfusion and explain decreased contractility. Finding an already impaired ventricular deformation from fetal

life would help monitoring postnatal adaptation to corrective surgery and long-term RV function.

Study 4 reports a lower LV deformation. The evaluation of LV dysfunction has been scarcely evaluated in prenatal and postnatal ToF. Devore et al found, in a series of 44 ToF fetuses, that up to 44% of cases had a MAPSE below the 5th centile, 48% decreased LV GLS and 64% a decreased LV ejection fraction(53). Song et al reported the same results, in accordance with our findings, showing that ToF fetuses present LV deformation in fetal life. They postulated that this may be due to an increased volume and pressure load in the LV, that may be explained by biventricular overload secondary to the presence of a VSD. This is in concordance with the finding of mainly preserved LV deformation in fetuses with pulmonary stenosis with intact septum, as they do not present increased LV pressure. In their study, Song et al. describe a normal LV ejection fraction, while our study and the one conducted by Devore et al suggest a decreased function. In addition, Song et al described a moderate negative association between RV outflow tract obstruction severity and RV and LV GLS absolute values(60). The results of our study didn't confirm this association. However, the study of Song et al was retrospective, cases were evaluated at lower gestational age and there were higher cases undergoing termination of pregnancy, which could explain the differences.

The biventricular dysfunction is also in accordance with pathologic abnormalities found in both ventricles. A study examining heart specimens affected with ToF showed a different fiber orientation in both ventricles compared to normal hearts. They found a more oblique orientation of the outer layer and the presence of a middle circumferential layer in the RV(167). The presence of more oblique fibers may contribute to a decrease in longitudinal function (GLS, MAPSE and TAPSE) while maintaining global and circumferential function (FAC and LV global circumferential strain).

The **results of the study also show a higher cardiac index** than controls. The increased cardiac index is at the expenses of an increase in fetal heart rate and increased aortic outflow, due to a dilated aortic valve, with a mean z-score of 2.06. The increased aortic output leads to higher wall shear stress, which is potentially responsible of TGF β

production together with biventricular hypertrophy. The **study 3** of this doctoral thesis identified increased cord blood concentrations of TGF β in ToF fetuses. TGF β at the endothelium plays a role in extracellular matrix formation and decreases endothelial elasticity, predisposing to dilation. In this line, a higher expression of TGF β has been found in young adults with ToF and aortic root dilation(98). More studies focusing on aortic root dilation and its implications in postnatal follow-up are needed. On the other hand, Devore et al reports a lower LV output in ToF than in controls(53). Methodological differences in the calculation of cardiac output may explain our different results. We calculated LV output by conventional echocardiography, combining heart rate, velocity time integral of aortic spectral Doppler and aortic valve diameter. In contrast, Devore et al used STE, which calculates LV output as the difference in LV volume between systole and diastole. This method does not reflect the fraction of RV output that contributes to the aortic flow. Similarly, a normal pulmonary output in ToF fetuses was observed in our study, as RV flow that crosses the VSD was neither accounted and there was only a mild increment in peak systolic velocity. This could also explain the difference with increased RV output reported in pulmonary stenosis fetuses, where all RV output is ejected through the pulmonary artery.

Mechanical dyssynchrony correlates with ventricular function

In **study 4** we report signs of mechanical dyssynchrony and its correlation with biventricular GLS and MAPSE. Song et al postulated that altered ventricular mechanics and interventricular interactions with a pressure loaded RV could explain lower LV deformation(60). Moreover, mechanical dyssynchrony is demonstrated in children with RV dysfunction after ToF repair, and correlates with lower TAPSE and RV GLS(44,155). They hypothesized that it could be caused by a right bundle branch block induced by subendocardial wall stress in RV pressure overload. Moreover, adverse RV-LV interactions lead to decreased LV contractility, affecting mostly the interventricular septum. Additionally, our results show a decrease in longitudinal peak strain in the septal wall compared to the RV and LV free wall. More research is needed in this field to confirm our results.

Fetal echocardiography and postnatal outcome

Although ToF is a CHD with an overall good prognosis, there is still debate regarding the timing and type of postnatal surgical procedure to be performed in cases with low oxygen saturation in the early neonatal period. Several authors have investigated potential predictors of early postnatal surgery in ToF newborns. They found echocardiographic parameters such as pulmonary valve diameter or z-score, size of pulmonary artery branches or reversed flow in the DA predicted early intervention with high sensitivity but lower specificity(128,129,168–172). Our study did not confirm these results, probably due to the lower percentage of children needing early surgery in our series (only 6 newborns required surgery before 90 days of age (9.5%)). However, we analyzed the need for an early systemic to pulmonary shunt, only in the subgroup of ToF fetuses with PS. We found that the pulmonary valve peak velocity had an area under the curve of 0.845 in receiving operative curve, although it was not statistically significant ($p=0.067$), probably due to the few number of cases (5.2%). Furthermore, we did find a moderate **correlation between valve size and peak velocity of the pulmonary valve and length of admission at the neonatal intensive care unit**. More severe RV outflow tract obstruction leads to lower oxygen saturation, needing more strict surveillance.

Previous studies reported that 9.7% of CHD fetuses, specially conotruncal CHD, have a birthweight lower than 3rd centile. Preeclampsia also is reported to be higher (5.7%) in CHD pregnancies compared to 1.2% in normal pregnancies(167). In our study we found a 19.05% of growth restricted fetuses and 6.35% mothers had preeclampsia. In addition, there was a 20% increase in cesarean section rate in our ToF cohort, suggesting, in part, a worse tolerance to the delivery. The cause of this increase in placental-related complications is not yet clearly understood. Llurba et al. described an antiangiogenic profile in a mixed CHD group(113) although the results of the **study 3** of this thesis did not find any differences in angiogenic factors in cord blood of ToF fetuses. However, a fraction of TGF β is also produced by the placenta, and increased TGF β is seen in ToF fetuses (**Study 3**).

We have shown that ToF is a CHD that affects prenatally right and left ventricle. Therefore, prenatal assessment of those fetuses should include a global comprehensive

evaluation of cardiac function. A longer admission, mainly due to lower oxygenation, was associated to smaller pulmonary valve, pulmonary valve z-score, pulmonary peak systolic velocity and pulmonary – aortic valve ratio. This information could be used when counseling parents and organizing delivery in referral centers. More studies including global assessment of the fetal heart are needed in order to better understand and detect predictors of early intervention and, therefore, the need for a tertiary care delivery.

5. Limitations

This thesis has several limitations that are worth commenting on. In all studies, the limited sample size is the main limitation, although **Study 2 and 4**, include the largest cohort of PS and ToF in fetal life, respectively. Additionally, in **Study 1**, we only included healthy fetuses, which may be considered a limitation, although 2D STE had been previously validated with normal and abnormal hearts.

Regarding technique limitations, in **Study 1**, all 2D clips and 4D-STIC volumes were obtained in an apical oblique 4-chamber view that can be difficult to achieve in the third trimester or in other fetal conditions such as oligohydramnios.

In **Study 2**, we included 13 cases from a retrospective cohort, which is a limitation, although the image acquisition protocol was the same and it was performed by the same operators as in **Study 2**. Currently, only a small portion of neonatal PS cases are detected prenatally, corresponding more frequently to moderate and severe cases, which could potentially introduce a selection bias. Additionally, we must consider the reproducibility of STE a limitation, especially for the evaluation of mechanical dyssynchrony, as it is a measurement that depends on segmental analysis. Furthermore, there is a need for further validation of the dyssynchrony index, as our results are not as accurate as postnatal results due to the unavailability of EKG in fetal life. Finally, the scoring system has not been externally validated, which is a limitation of **Study 2**.

In **Study 3**, the concentrations of cord blood biomarkers were analyzed after adjusting for identified confounders. However, we acknowledge that there may be additional confounders that were not accounted for. Furthermore, to better understand the role

of angiogenic factors in CHD, it would have been valuable to conduct an anatomopathological study of the placenta and assess its weight. Therefore, we consider this to be a limitation of the study. Moreover, we did not assess the diameter of the ascending aorta in ToF fetuses. Having this measure would have been interesting in order to correlate it with TGF β values. Finally, Troponin I behavior being positive or negative difficult the analysis.

Regarding **Study 4**, the main limitation is that the evaluation of mechanical dyssynchrony has not yet been validated in fetuses, although in **study 1** we published an overall good reproducibility for STE. To overcome this limitation all the analysis of our cases were performed by the same experienced operator (L.N.). The multicentric origin of the cases could also increase variability in some conventional cardiac measurements. The vast majority of our echocardiographies were performed at the third trimester of pregnancy, although in cases where families opted for termination of pregnancy, this ultrasound was performed earlier. Adjusting results for EFW or by z-scores partially reduce this limitation. Finally, the low rate of early surgery in our cohort did not provide the opportunity to evaluate possible predictors of neonatal outcome.

6. Future clinical perspectives

The use of 4D-STIC STE in the clinical setting could enable a comprehensive evaluation of both cardiac morphometry and function, facilitating the use of FetalHQ[®] for telemedicine.

The description of a new scoring system to predict neonatal valvuloplasty shows promise for prenatal follow-up of PS and identifying fetuses at high risk of needing a neonatal valvuloplasty. This could help to coordinate the delivery of those fetuses in a tertiary care center for early neonatal evaluation by pediatric cardiology specialists.

In addition, the study of cord biomarkers could subsequently evaluate the potential clinical applicability of TGF β in the prognostic evaluation of ToF. Further studies including higher number of cases and evaluation of aortic arch diameters present

research opportunities for new prognostic and preventive strategies. Additionally, studying these cardiovascular biomarkers in maternal blood and amniotic fluid could expand their potential clinical applicability to earlier stages of gestation.

We described the pattern of cardiovascular remodeling in ToF fetuses although finding predictors of early surgical correction is difficult for the low rate of early intervention. However, the application of machine learning techniques or computational models would help identify different clusters and clinical phenotypes in ToF population.

Conclusions

1. 4 dimension - Spatio Temporal Image Correlation speckle tracking echocardiography is feasible, reproducible and comparable to 2-dimensional echocardiography for the assessment of cardiac morphometry and function in healthy fetuses (**Study 1**).
2. Decreased right ventricle deformation is observed in critical pulmonary stenosis fetuses, and correlates with mechanical dyssynchrony. A scoring system combining the ductus venosus pulsatility index centile and right ventricle global longitudinal strain; with the presence of reversed ductus arteriosus flow and significant tricuspid regurgitation, enables to identify those fetuses in need of early neonatal valvuloplasty, who will thus benefit from an early neonatal assessment by pediatric cardiologists (**Study 2**).
3. Tetralogy of Fallot fetuses show increased cord blood transforming growth factor- β concentrations when compared to D-transposition of the great arteries and normal fetuses. Moreover, transforming growth factor- β levels correlate with the severity of right ventricle outflow obstruction (**Study 3**).
4. Fetuses with tetralogy of Fallot present signs of cardiovascular remodeling from prenatal life, characterized by a more spherical heart with biventricular concentric hypertrophy. Additionally, morphometric changes are associated with both, biventricular diastolic dysfunction and decreased contractility, which correlates with the presence of mechanical dyssynchrony (**Study 4**).

References

1. Allan LD, Sharland GK, Milburn A, Lockhart SM, Groves AM, Anderson RH, et al. Prospective diagnosis of 1,006 consecutive cases of congenital heart disease in the fetus. *J Am Coll Cardiol*. 1994 May;23(6):1452–8.
2. Donofrio MT, Moon-Grady AJ, Hornberger LK, Copel JA, Sklansky MS, Abuhamad A, et al. Diagnosis and treatment of fetal cardiac disease: A scientific statement from the American Heart Association. *Circulation*. 2014 May 27;129(21):2183–242.
3. Huhta J, Linask KK. Environmental origins of congenital heart disease: the heart-placenta connection. *Semin Fetal Neonatal Med*. 2013 Oct;18(5):245–50.
4. Boyd R, McMullen H, Beqaj H, Kalfa D. Environmental exposures and congenital heart disease. *Pediatrics*. 2022 Jan 1;149(1):e2021052151.
5. Lee CK. Prenatal counseling of fetal congenital heart disease. *Curr Treat Options Cardiovasc Med*. 2017 Jan;19(1):5.
6. Bakker MK, Bergman JEH, Krikov S, Amar E, Cocchi G, Cragan J, et al. Prenatal diagnosis and prevalence of critical congenital heart defects: an international retrospective cohort study. *BMJ Open*. 2019 Jul 2;9(7):e028139.
7. Lytzen R, Vejlstrop N, Bjerre J, Bjørn Petersen O, Leenskjold S, Keith Dodd J, et al. The accuracy of prenatal diagnosis of major congenital heart disease is increasing. *J Obstet Gynaecol*. 2020 Apr;40(3):308–15.
8. Holland BJ, Myers JA, Woods CR. Prenatal diagnosis of critical congenital heart disease reduces risk of death from cardiovascular compromise prior to planned neonatal cardiac surgery: a meta-analysis. *Ultrasound Obstet Gynecol*. 2015 Jun;45(6):631–8.
9. Masoller N, Martínez JM, Gómez O, Bennasar M, Crispi F, Sanz-Cortés M, et al. Evidence of second-trimester changes in head biometry and brain perfusion in fetuses with congenital heart disease. *Ultrasound Obstet Gynecol*. 2014 Aug;44(2):182–7.
10. Masoller N, Sanz-Cortés M, Crispi F, Gómez O, Bennasar M, Egaña-Ugrinovic G, et al. Mid-gestation brain Doppler and head biometry in fetuses with congenital heart disease predict abnormal brain development at birth. *Ultrasound in*

Obstetrics and Gynecology. 2016;47(1):65–73.

11. Thilaganathan B. Preeclampsia and fetal congenital heart defects: spurious association or maternal confounding? *Circulation*. 2017 Jul 4;136(1):49–51.
12. Crispi F, Sepúlveda-Martínez Á, Crovetto F, Gómez O, Bijmens B, Gratacós E. Main patterns of fetal cardiac remodeling. *Fetal Diagn Ther*. 2020;47(5):337–44.
13. Crispi F, Miranda J, Gratacós E. Long-term cardiovascular consequences of fetal growth restriction: biology, clinical implications, and opportunities for prevention of adult disease. *Am J Obstet Gynecol*. 2018 Feb;218(2S):S869–79.
14. García-Otero L, Gómez O, Rodríguez-López M, Torres X, Soveral I, Sepúlveda-Martínez Á, et al. Nomograms of fetal cardiac dimensions at 18–41 weeks of gestation. *Fetal Diagn Ther*. 2020;47(5):387–398.
15. Guirado L, Crispi F, Soveral I, Valenzuela-Alcaraz B, Rodríguez-López M, García-Otero L, et al. Nomograms of fetal right ventricular fractional area change by 2d echocardiography. *Fetal Diagn Ther*. 2020;47(5):399–410.
16. García-Otero L, Soveral I, Sepúlveda-Martínez Á, Rodríguez-López M, Torres X, Guirado L, et al. Reference ranges for fetal cardiac, ventricular and atrial relative size, sphericity, ventricular dominance, wall asymmetry and relative wall thickness from 18 to 41 gestational weeks. *Ultrasound Obstet Gynecol*. 2021 Sep;58(3):388–97.
17. Soveral I, Crispi F, Guirado L, García-Otero L, Torres X, Bennasar M, et al. Fetal cardiac filling and ejection time fractions by pulsed-wave Doppler: reference ranges and potential clinical application. *Ultrasound Obstet Gynecol*. 2021 Jul;58(1):83–91.
18. DeVore GR, Polanco B, Satou G, Sklansky M. Two-dimensional speckle tracking of the fetal heart: a practical step-by-step approach for the fetal sonologist. *J Ultrasound Med*. 2016 Aug;35(8):1765–81.
19. DeVore GR, Satou G, Sklansky M. 4D fetal echocardiography—An update. *Echocardiography*. 2017;34(12):1788–98.
20. Guirado L, Crispi F, Masoller N, Bennasar M, Marimon E, Carretero J, et al. Biventricular impact of mild to moderate fetal pulmonary valve stenosis. *Ultrasound Obstet Gynecol*. 2018;51(3):349–56.
21. Walter C, Soveral I, Bartrons J, Escobar MC, Carretero JM, Quirado L, et al.

- Comprehensive functional echocardiographic assessment of transposition of the great arteries: from fetus to newborn. *Pediatr Cardiol*. 2020 Apr 1;41(4):687–94.
22. Soveral I, Crispi F, Walter C, Guirado L, García-Cañadilla P, Cook A, et al. Early cardiac remodeling in aortic coarctation: insights from fetal and neonatal functional and structural assessment. *Ultrasound Obstet Gynecol*. 2020 Dec;56(6):837–49.
 23. Enzensberger C, Graupner O, Fischer S, Meister M, Reitz M, Götte M, et al. Evaluation of right ventricular myocardial deformation properties in fetal hypoplastic left heart by two-dimensional speckle tracking echocardiography. *Arch Gynecol Obstet*. 2023 Mar;307(3):699–708.
 24. Schneider C, McCrindle BW, Carvalho JS, Hornberger LK, McCarthy KP, Daubeney PEF. Development of Z-scores for fetal cardiac dimensions from echocardiography. *Ultrasound Obstet Gynecol*. 2005 Nov;26(6):599–605.
 25. Barker DJP. Adult consequences of fetal growth restriction. *Clin Obstet Gynecol*. 2006 Jun;49(2):270–83.
 26. Cruz-Lemini M, Crispi F, Valenzuela-Alcaraz B, Figueras F, Sitges M, Bijmens B, et al. Fetal cardiovascular remodeling persists at 6 months in infants with intrauterine growth restriction. *Ultrasound Obstet Gynecol*. 2016 Sep;48(3):349–56.
 27. Miranda JO, Cerqueira RJ, Ramalho C, Areias JC, Henriques-Coelho T. Fetal cardiac function in maternal diabetes: a conventional and speckle-tracking echocardiographic study. *J Am Soc Echocardiogr*. 2018 Mar;31(3):333–41.
 28. García-Otero L, López M, Gómez O, Goncé A, Bennasar M, Martínez JM, et al. Zidovudine treatment in HIV-infected pregnant women is associated with fetal cardiac remodelling. *AIDS*. 2016 Jun 1;30(9):1393–401.
 29. Valenzuela-Alcaraz B, Serafini A, Sepulveda-Martínez A, Casals G, Rodríguez-López M, Garcia-Otero L, et al. Postnatal persistence of fetal cardiovascular remodelling associated with assisted reproductive technologies: a cohort study. *BJOG*. 2019 Jan;126(2):291–298.
 30. Boutet ML, Casals G, Valenzuela-Alcaraz B, García-Otero L, Crovetto F, Cívico MS, et al. Cardiac remodeling in fetuses conceived by ARTs: fresh versus frozen embryo transfer. *Hum Reprod*. 2021 Sep 18;36(10):2697–708.
 31. Lang RM, Badano LP, Mor-Avi V, Afzalpoor J, Armstrong A, Ernande L, et al.

Recommendations for cardiac chamber quantification by echocardiography in adults: an update from the American Society of Echocardiography and the European Association of Cardiovascular Imaging. *J Am Soc Echocardiogr*. 2015 Jan;28(1):1-39.e14.

32. Trivedi SJ, Altman M, Stanton T, Thomas L. Echocardiographic strain in clinical practice. *Heart Lung Circ*. 2019 Sep;28(9):1320–30.
33. Huntgeburth M, Germund I, Geerdink LM, Sreeram N, Udink Ten Cate FEA. Emerging clinical applications of strain imaging and three-dimensional echocardiography for the assessment of ventricular function in adult congenital heart disease. *Cardiovasc Diagn Ther*. 2019 Oct;9(Suppl 2):S326–45.
34. van Oostrum NHM, de Vet CM, van der Woude DAA, Kemps HMC, Oei SG, van Laar JOEH. Fetal strain and strain rate during pregnancy measured with speckle tracking echocardiography: A systematic review. *Eur J Obstet Gynecol Reprod Biol*. 2020 Jul;250:178–87.
35. Semmler J, Day TG, Georgiopoulos G, Garcia-Gonzalez C, Aguilera J, Vigneswaran TV, et al. Fetal speckle-tracking: impact of angle of insonation and frame rate on global longitudinal strain. *J Am Soc Echocardiogr*. 2020 Sep;33(9):1141-1146.e2.
36. Smiseth OA, Torp H, Opdahl A, Haugaa KH, Urheim S. Myocardial strain imaging: how useful is it in clinical decision making? *Eur Heart J*. 2016 Apr 14;37(15):1196–207.
37. DeVore GR, Klas B, Satou G, Sklansky M. Evaluation of the right and left ventricles: An integrated approach measuring the area, length, and width of the chambers in normal fetuses. *Prenat Diagn*. 2017 Dec;37(12):1203–12.
38. DeVore GR, Cuneo B, Klas B, Satou G, Sklansky M. Comprehensive evaluation of fetal cardiac ventricular widths and ratios using a 24-segment speckle tracking technique. *J Ultrasound Med*. 2019 Apr;38(4):1039–47.
39. DeVore GR, Klas B, Satou G, Sklansky M. Quantitative evaluation of fetal right and left ventricular fractional area change using speckle-tracking technology. *Ultrasound Obstet Gynecol*. 2019 Feb;53(2):219–28.
40. DeVore GR, Klas B, Satou G, Sklansky M. Evaluation of fetal left ventricular size and function using speckle-tracking and the simpson rule. *J Ultrasound Med*. 2019 May;38(5):1209–21.

41. DeVore GR, Klas B, Satou G, Sklansky M. Longitudinal annular systolic displacement compared to global strain in normal fetal hearts and those with cardiac abnormalities. *J Ultrasound Med*. 2018 May;37(5):1159–71.
42. DeVore GR, Klas B, Satou G, Sklansky M. Speckle tracking of the basal lateral and septal wall annular plane systolic excursion of the right and left ventricles of the fetal heart. *J Ultrasound Med*. 2019 May;38(5):1309–18.
43. Haji K, Marwick TH. Clinical utility of echocardiographic strain and strain rate measurements. *Curr Cardiol Rep*. 2021 Feb 16;23(3):18.
44. Yim D, Hui W, Larios G, Dragulescu A, Grosse-Wortmann L, Bijmens B, et al. Quantification of right ventricular electromechanical dyssynchrony in relation to right ventricular function and clinical outcomes in children with repaired tetralogy of fallot. *J Am Soc Echocardiogr*. 2018 Jul;31(7):822–30.
45. Barker PCA, Houle H, Li JS, Miller S, Herlong JR, Camitta MGW. Global longitudinal cardiac strain and strain rate for assessment of fetal cardiac function: novel experience with velocity vector imaging. *Echocardiography*. 2009 Jan;26(1):28–36.
46. Chelliah A, Dham N, Frank LH, Donofrio M, Krishnan A. Myocardial strain can be measured from first trimester fetal echocardiography using velocity vector imaging. *Prenat Diagn*. 2016 May;36(5):483–8.
47. DeVore GR, Gumina DL, Hobbins JC. Assessment of ventricular contractility in fetuses with an estimated fetal weight less than the tenth centile. *Am J Obstet Gynecol*. 2019 Nov;221(5):498.e1-498.e22.
48. Yovera L, Zaharia M, Jachymski T, Velicu-Scraba O, Coronel C, de Paco Matallana C, et al. Impact of gestational diabetes mellitus on fetal cardiac morphology and function: cohort comparison of second- and third-trimester fetuses. *Ultrasound Obstet Gynecol*. 2021 Apr;57(4):607–13.
49. Harbison AL, Pruetz JD, Ma S, Sklansky MS, Chmait RH, DeVore GR. Evaluation of cardiac function in the recipient twin in successfully treated twin-to-twin transfusion syndrome using a novel fetal speckle-tracking analysis. *Prenat Diagn*. 2021 Jan;41(1):136–44.
50. Huluta I, Wright A, Cosma LM, Dimopoulou S, Nicolaidis KH, Charakida M. Fetal cardiac function at midgestation and conception by in-vitro fertilization. *Ultrasound Obstet Gynecol*. 2023 May;61(5):587-592.

51. DeVore GR, Haxel C, Satou G, Sklansky M, Pelka MJ, Jone PN, et al. Improved detection of coarctation of the aorta using speckle-tracking analysis of fetal heart on last examination prior to delivery. *Ultrasound Obstet Gynecol.* 2021 Feb;57(2):282–91.
52. Moras P, Pasquini L, Rizzo G, Campanale CM, Masci M, Di Chiara L, et al. Prenatal prediction of Shone’s complex. The role of the degree of ventricular disproportion and speckle-tracking analysis. *J Perinat Med.* 2022 Nov 24; 51(4):550-558.
53. DeVore GR, Afshar Y, Harake D, Satou G, Sklansky M. Speckle-tracking analysis in fetuses with tetralogy of fallot: evaluation of right and left ventricular contractility and left ventricular function. *J Ultrasound Med.* 2022 Dec;41(12):2955–64.
54. DeVore GR, Cuneo B, Sklansky M, Satou G. Abnormalities of the width of the four-chamber view and the area, length, and width of the ventricles to identify fetuses at high-risk for d-transposition of the great arteries and tetralogy of fallot. *J Ultrasound Med.* 2023 Feb;42(3):637–46.
55. Patey O, Carvalho JS, Thilaganathan B. Urgent neonatal balloon atrial septostomy in simple transposition of the great arteries: predictive value of fetal cardiac parameters. *Ultrasound Obstet Gynecol.* 2021 May;57(5):756–68.
56. DeVore GR, Satou G, Sklansky M, Cuneo B. Speckle tracking analysis in fetuses with d-transposition: predicting the need for urgent neonatal balloon atrial septostomy. *Pediatr Cardiol.* 2023 Aug;44(6):1382-1396.
57. Cohen J, Binka E, Woldu K, Levasseur S, Glickstein J, Freud LR, et al. Myocardial strain abnormalities in fetuses with pulmonary atresia and intact ventricular septum. *Ultrasound Obstet Gynecol.* 2019 Apr;53(4):512–9.
58. Li T, Han J, Han Y, Liu X, Gu X, Zhang Y, et al. Evaluation of changes of cardiac morphology and function in fetuses with ductus arteriosus constriction by Speckle-tracking echocardiography. *Front Pediatr.* 2023;11:1085352.
59. Ma J, Yuan Y, Zhang L, Chen S, Cao H, Hong L, et al. Evaluation of right ventricular function and myocardial microstructure in fetal hypoplastic left heart syndrome. *J Clin Med.* 2022 Jul 30;11(15):4456.
60. Song X, Cao H, Hong L, Zhang L, Li M, Shi J, et al. Ventricular myocardial deformation in fetuses with tetralogy of fallot: a necessary field of investigation. *Front Cardiovasc Med.* 2021;8:764676.

61. Drop MCV, Möllers M, Hammer K, Oelmeier de Murcia K, Falkenberg MK, Braun J, et al. Strain and dyssynchrony in fetuses with congenital heart disease compared to normal controls using speckle tracking echocardiography (STE). *J Perinat Med*. 2019 Aug 27;47(6):598–604.
62. DeVore GR, Polanco B, Satou G, Sklansky M. Two-dimensional speckle tracking of the fetal heart: a practical step-by-step approach for the fetal sonologist. *J Ultrasound Med*. 2016 Aug;35(8):1765–81.
63. Bennasar M, Martínez JM, Gómez O, Bartrons J, Olivella A, Puerto B, et al. Accuracy of four-dimensional spatiotemporal image correlation echocardiography in the prenatal diagnosis of congenital heart defects. *Ultrasound in Obstetrics and Gynecology*. 2010;36(4):458–64.
64. Messing B, Gilboa Y, Lipschuetz M, Valsky DV, Cohen SM, Yagel S. Fetal tricuspid annular plane systolic excursion (f-TAPSE): evaluation of fetal right heart systolic function with conventional M-mode ultrasound and spatiotemporal image correlation (STIC) M-mode. *Ultrasound Obstet Gynecol*. 2013 Aug;42(2):182–8.
65. Bravo-Valenzuela NJ, Peixoto AB, Carrilho MC, Siqueira Pontes AL, Chagas CC, Simioni C, et al. Fetal cardiac function by three-dimensional ultrasound using 4D-STIC and VOCAL - an update. *J Ultrason*. 2019 Dec;19(79):287–94.
66. Liem DA, Cadeiras M, Setty SP. Insights and perspectives into clinical biomarker discovery in pediatric heart failure and congenital heart disease-a narrative review. *Cardiovasc Diagn Ther*. 2023 Feb 28;13(1):83–99.
67. Perez-Cruz M, Crispi F, Fernández MT, Parra JA, Valls A, Gomez Roig MD, et al. Cord blood biomarkers of cardiac dysfunction and damage in term growth-restricted fetuses classified by severity criteria. *Fetal Diagn Ther*. 2018;44(4):271–276.
68. Crispi F, Hernandez-Andrade E, Pelsers MMAL, Plasencia W, Benavides-Serralde JA, Eixarch E, et al. Cardiac dysfunction and cell damage across clinical stages of severity in growth-restricted fetuses. *Am J Obstet Gynecol*. 2008 Sep;199(3):254.e1-8.
69. Soveral I, Guirado L, Escobar-Diaz MC, Alcaide MJ, Martínez JM, Rodríguez-Sureda V, et al. Cord blood cardiovascular biomarkers in left-sided congenital heart disease. *J Clin Med*. 2022 Nov 30;11(23):7119.
70. Hopkins WE, Chen Z, Fukagawa NK, Hall C, Knot HJ, LeWinter MM. Increased atrial

and brain natriuretic peptides in adults with cyanotic congenital heart disease: enhanced understanding of the relationship between hypoxia and natriuretic peptide secretion. *Circulation*. 2004 Jun 15;109(23):2872–7.

71. Schwachtgen L, Herrmann M, Georg T, Schwarz P, Marx N, Lindinger A. Reference values of NT-proBNP serum concentrations in the umbilical cord blood and in healthy neonates and children. *Z Kardiol*. 2005 Jun;94(6):399–404.
72. Bahlmann F, Krummenauer F, Spahn S, Gallinat R, Kampmann C. Natriuretic peptide levels in intrauterine growth-restricted fetuses with absent and reversed end-diastolic flow of the umbilical artery in relation to ductus venosus flow velocities. *J Perinat Med*. 2011 Sep;39(5):529–37.
73. Kim HN, Januzzi JL. Natriuretic peptide testing in heart failure. *Circulation*. 2011 May 10;123(18):2015–9.
74. Holmgren D, Westerlind A, Berggren H, Lundberg PA, Wåhländer H. Increased natriuretic peptide type B level after the second palliative step in children with univentricular hearts with right ventricular morphology but not left ventricular morphology. *Pediatr Cardiol*. 2008 Jul;29(4):786–92.
75. Eindhoven JA, van den Bosch AE, Jansen PR, Boersma E, Roos-Hesselink JW. The usefulness of brain natriuretic peptide in complex congenital heart disease: a systematic review. *J Am Coll Cardiol*. 2012 Nov 20;60(21):2140–9.
76. Lee SM, Kwon JE, Song SH, Kim GB, Park JY, Kim BJ, et al. Prenatal prediction of neonatal death in single ventricle congenital heart disease. *Prenat Diagn*. 2016 Apr;36(4):346–52.
77. Johns MC, Stephenson C. Amino-terminal pro-B-type natriuretic peptide testing in neonatal and pediatric patients. *Am J Cardiol*. 2008 Feb 4;101(3A):76–81.
78. Lee SM, Suh DH, Kim SY, Kim MK, Oh S, Song SH, et al. Antenatal prediction of neonatal survival in sacrococcygeal teratoma. *J Ultrasound Med*. 2018 Aug;37(8):2003–9.
79. Lee SM, Jun JK, Kim SA, Kang MJ, Song SH, Lee J, et al. N-terminal pro-B-type natriuretic peptide and cardiac troponin T in non-immune hydrops. *J Obstet Gynaecol Res*. 2016 Apr;42(4):380–4.
80. Rouatbi H, Zigabe S, Gkiougki E, Vranken L, Van Linthout C, Seghaye MC. Biomarkers of neonatal stress assessment: A prospective study. *Early Hum Dev*.

2019 Oct;137:104826.

81. Habli M, Cnota J, Michelfelder E, Salisbury S, Schnell B, Polzin W, et al. The relationship between amniotic fluid levels of brain-type natriuretic peptide and recipient cardiomyopathy in twin-twin transfusion syndrome. *Am J Obstet Gynecol.* 2010 Oct;203(4):404.e1-7.
82. Miyoshi T, Hosoda H, Umekawa T, Asada T, Fujiwara A, Kurosaki KI, et al. Amniotic fluid natriuretic peptide levels in fetuses with congenital heart defects or arrhythmias. *Circ J.* 2018 Sep 25;82(10):2619–26.
83. Friedman KG, Sleeper LA, Fichorova RN, Weinau T, Tworetzky W, Wilkins-Haug LE. Myocardial injury in fetal aortic stenosis: Insights from amniotic fluid analysis. *Prenat Diagn.* 2018 Feb;38(3):190–5.
84. Eerola A, Jokinen EO, Savukoski TI, Pettersson KSI, Poutanen T, Pihkala JI. Cardiac troponin I in congenital heart defects with pressure or volume overload. *Scand Cardiovasc J.* 2013 Jun;47(3):154–9.
85. Correale M, Nunno L, Ieva R, Rinaldi M, Maffei G, Magaldi R, et al. Troponin in newborns and pediatric patients. *Cardiovasc Hematol Agents Med Chem.* 2009 Oct;7(4):270–8.
86. Trevisanuto D, Pitton M, Altinier S, Zaninotto M, Plebani M, Zanardo V. Cardiac troponin I, cardiac troponin T and creatine kinase MB concentrations in umbilical cord blood of healthy term neonates. *Acta Paediatr.* 2003 Dec;92(12):1463–7.
87. Sugimoto M, Ota K, Kajihama A, Nakau K, Manabe H, Kajino H. Volume overload and pressure overload due to left-to-right shunt-induced myocardial injury. - Evaluation using a highly sensitive cardiac Troponin-I assay in children with congenital heart disease-. *Circ J.* 2011;75(9):2213–9.
88. Bottio T, Vida V, Padalino M, Gerosa G, Stellin G. Early and long-term prognostic value of Troponin-I after cardiac surgery in newborns and children. *Eur J Cardiothorac Surg.* 2006 Aug;30(2):250–5.
89. Mondal T, Ryan PM, Gupta K, Radovanovic G, Pugh E, Chan AKC, et al. Cord-blood high-sensitivity troponin-I reference interval and association with early neonatal outcomes. *Am J Perinatol.* 2022 Oct;29(14):1548–54.
90. Türker G, Babaoğlu K, Gökalp AS, Sarper N, Zengin E, Arisoy AE. Cord blood cardiac troponin I as an early predictor of short-term outcome in perinatal hypoxia. *Biol*

Neonate. 2004;86(2):131–7.

91. Alexandre SM, D'Almeida V, Guinsburg R, Nakamura MU, Tufik S, Moron A. Cord blood cardiac troponin I, fetal Doppler velocimetry, and acid base status at birth. *Int J Gynaecol Obstet.* 2008 Feb;100(2):136–40.
92. McAuliffe F, Mears K, Fleming S, Grimes H, Morrison JJ. Fetal cardiac troponin I in relation to intrapartum events and umbilical artery pH. *Am J Perinatol.* 2004 Apr;21(3):147–52.
93. Ren LL, Li XJ, Duan TT, Li ZH, Yang JZ, Zhang YM, et al. Transforming growth factor- β signaling: From tissue fibrosis to therapeutic opportunities. *Chem Biol Interact.* 2023 Jan 5;369:110289.
94. Goumans MJ, Liu Z, ten Dijke P. TGF-beta signaling in vascular biology and dysfunction. *Cell Res.* 2009 Jan;19(1):116–27.
95. Dobaczewski M, Chen W, Frangogiannis NG. Transforming growth factor (TGF)- β signaling in cardiac remodeling. *J Mol Cell Cardiol.* 2011 Oct;51(4):600–6.
96. Swartz MF, Morrow D, Atallah-Yunes N, Cholette JM, Gensini F, Kavey RE, et al. Hypertensive changes within the aortic arch of infants and children with isolated coarctation. *Ann Thorac Surg.* 2013 Jul;96(1):190–5.
97. Guerri-Guttenberg RA, Castilla R, Francos GC, Müller A, Ambrosio G, Milei J. Transforming growth factor β 1 and coronary intimal hyperplasia in pediatric patients with congenital heart disease. *Can J Cardiol.* 2013 Jul;29(7):849–57.
98. Cheung YF, Chow PC, So EKF, Chan KW. Circulating transforming growth factor- β and aortic dilation in patients with repaired congenital heart disease. *Sci Rep.* 2019 Jan 17;9(1):162.
99. Seki M, Kurishima C, Saiki H, Masutani S, Arakawa H, Tamura M, et al. Progressive aortic dilation and aortic stiffness in children with repaired tetralogy of Fallot. *Heart Vessels.* 2014 Jan;29(1):83–7.
100. Doetschman T, Barnett JV, Runyan RB, Camenisch TD, Heimark RL, Granzier HL, et al. Transforming growth factor beta signaling in adult cardiovascular diseases and repair. *Cell Tissue Res.* 2012 Jan;347(1):203–23.
101. Briana DD, Liosi S, Gourgiotis D, Boutsikou M, Marmarinos A, Baka S, et al. Fetal concentrations of the growth factors TGF- α and TGF- β 1 in relation to normal and restricted fetal growth at term. *Cytokine.* 2012 Oct;60(1):157–61.

102. Wilson RL, Yuan V, Courtney JA, Tipler A, Cnota JF, Jones HN. Analysis of commonly expressed genes between first trimester fetal heart and placenta cell types in the context of congenital heart disease. *Sci Rep*. 2022 Jun 24;12(1):10756.
103. Albalawi A, Brancusi F, Askin F, Ehsanipoor R, Jiangxia W, Burd I, et al. Placental characteristics of fetuses with congenital heart disease. *J Ultrasound Med*. 2017 May;36(5):965-972.
104. Burton GJ, Jauniaux E. Development of the Human Placenta and Fetal Heart: Synergic or Independent? *Front Physiol* 2018 Apr 12;9:373.
105. Snoep MC, Alias M, van der Meeren LE, Jongbloed MRM, DeRuiter MC, Haak MC. Placenta morphology and biomarkers in pregnancies with congenital heart disease - A systematic review. *Placenta*. 2021 Sep 1;112:189–96.
106. Alias M, Snoep MC, van Geloven N, Haak MC. Birthweight and isolated congenital heart defects - A systematic review and meta-analysis. *BJOG*. 2022 Oct;129(11):1805–16.
107. Accornero F, van Berlo JH, Benard MJ, Lorenz JN, Carmeliet P, Molkentin JD. Placental growth factor regulates cardiac adaptation and hypertrophy through a paracrine mechanism. *Circ Res*. 2011 Jul 22;109(3):272–80.
108. Nakamura T, Funayama H, Kubo N, Yasu T, Kawakami M, Momomura S ichi, et al. Elevation of plasma placental growth factor in the patients with ischemic cardiomyopathy. *Int J Cardiol*. 2009 Jan 9;131(2):186–91.
109. Iwama H, Uemura S, Naya N, Imagawa K ichi, Takemoto Y, Asai O, et al. Cardiac expression of placental growth factor predicts the improvement of chronic phase left ventricular function in patients with acute myocardial infarction. *J Am Coll Cardiol*. 2006 Apr 18;47(8):1559–67.
110. Ikeda T, Sun L, Tsuruoka N, Ishigaki Y, Yoshitomi Y, Yoshitake Y, et al. Hypoxia down-regulates sFlt-1 (sVEGFR-1) expression in human microvascular endothelial cells by a mechanism involving mRNA alternative processing. *Biochem J*. 2011 Jun 1;436(2):399–407.
111. Draker N, Torry DS, Torry RJ. Placenta growth factor and sFlt-1 as biomarkers in ischemic heart disease and heart failure: a review. *Biomark Med*. 2019 Jun;13(9):785–99.
112. Sugimoto M, Oka H, Kajihama A, Nakau K, Kuwata S, Kurishima C, et al. Ratio

- between fms-like tyrosine kinase 1 and placental growth factor in children with congenital heart disease. *Pediatr Cardiol*. 2015 Mar;*36*(3):591–9.
113. Llurba E, Sánchez O, Ferrer Q, Nicolaides KH, Ruíz A, Domínguez C, et al. Maternal and foetal angiogenic imbalance in congenital heart defects. *Eur Heart J*. 2014 Mar;*35*(11):701–7.
 114. Lesieur E, Zaffran S, Chaoui R, Quarello E. Prenatal screening and diagnosis of pulmonary artery anomalies. *Ultrasound Obstet Gynecol*. 2023 Apr;*61*(4):445–57.
 115. Roman KS, Fouron JC, Nii M, Smallhorn JF, Chaturvedi R, Jaeggi ET. Determinants of outcome in fetal pulmonary valve stenosis or atresia with intact ventricular septum. *Am J Cardiol*. 2007 Mar 1;*99*(5):699–703.
 116. Gardiner HM, Belmar C, Tulzer G, Barlow A, Pasquini L, Carvalho JS, et al. Morphologic and functional predictors of eventual circulation in the fetus with pulmonary atresia or critical pulmonary stenosis with intact septum. *J Am Coll Cardiol*. 2008 Apr 1;*51*(13):1299–308.
 117. Shivaram P, Van den Eynde J, Barnes BT, Danford DA, Cedars A, Kutty S. Fetal echocardiographic predictors of postnatal surgical strategies in critical pulmonary stenosis or atresia with intact ventricular septum: a meta-analysis. *Fetal Diagn Ther*. 2022;*49*(5–6):225–34.
 118. Wang Q, Wu YR, Jiao XT, Wu PF, Zhao LQ, Chen S, et al. Fetal pulmonary valve stenosis or atresia with intact ventricular septum: Predictors of need for neonatal intervention. *Prenat Diagn*. 2018 Mar;*38*(4):273–9.
 119. Lowenthal A, Lemley B, Kipps AK, Brook MM, Moon-Grady AJ. Prenatal tricuspid valve size as a predictor of postnatal outcome in patients with severe pulmonary stenosis or pulmonary atresia with intact ventricular septum. *Fetal Diagn Ther*. 2014;*35*(2):101–7.
 120. Kawazu Y, Inamura N, Kayatani F. Prediction of therapeutic strategy and outcome for antenatally diagnosed pulmonary atresia/stenosis with intact ventricular septum. *Circ J*. 2008 Sep;*72*(9):1471–5.
 121. Wolter A, Markert N, Wolter JS, Kurkevych A, Degenhardt J, Ritgen J, et al. Natural history of pulmonary atresia with intact ventricular septum (PAIVS) and critical pulmonary stenosis (CPS) and prediction of outcome. *Arch Gynecol Obstet*. 2021 Jul;*304*(1):81–90.

122. Jatavan P, Tongprasert F, Srisupundit K, Luewan S, Traisrisilp K, Tongsong T. Quantitative cardiac assessment in fetal tetralogy of fallot. *J Ultrasound Med*. 2016 Jul;35(7):1481–8.
123. DeVore GR, Afshar Y, Harake D, Satou G, Sklansky M. Speckle-tracking analysis in fetuses with tetralogy of fallot: evaluation of right and left ventricular contractility and left ventricular function. *J Ultrasound Med*. 2022 Dec;41(12):2955–64.
124. Taketazu M, Sugimoto M, Saiki H, Ishido H, Masutani S, Senzaki H. Developmental changes in aortic mechanical properties in normal fetuses and fetuses with cardiovascular disease. *Pediatr Neonatol*. 2017 Jun;58(3):245–50.
125. Niwa K, Siu SC, Webb GD, Gatzoulis MA. Progressive aortic root dilatation in adults late after repair of tetralogy of Fallot. *Circulation*. 2002 Sep 10;106(11):1374–8.
126. Rosenthal GL, Wilson PD, Permutt T, Boughman JA, Ferencz C. Birth weight and cardiovascular malformations: a population-based study. The Baltimore-Washington Infant Study. *Am J Epidemiol*. 1991 Jun 15;133(12):1273–81.
127. Qureshi AM, Caldarone CA, Romano JC, Chai PJ, Mascio CE, Glatz AC, et al. Comparison of management strategies for neonates with symptomatic tetralogy of Fallot and weight <2.5 kg. *J Thorac Cardiovasc Surg*. 2022 Jan;163(1):192-207.e3.
128. Park S, Won HS, Kim R, Kim M, Yu JJ, Park CS, et al. Fetal cardiac parameters for predicting postnatal operation type of fetuses with tetralogy of Fallot. *Cardiovasc Ultrasound*. 2022 Feb 21;20(1):4.
129. Escribano D, Herraiz I, Granados M, Arbues J, Mendoza A, Galindo A. Tetralogy of Fallot: prediction of outcome in the mid-second trimester of pregnancy. *Prenat Diagn*. 2011 Dec;31(12):1126–33.
130. Zhang B, Wu P, Zhao L, Lu Y, Bai K, Sun K, et al. Predictive value of fetal echocardiographic parameters in surgical strategy for Tetralogy of Fallot. *Echocardiography*. 2023 Mar;40(3):244-251.
131. Buca D, Winberg P, Rizzo G, Khalil A, Liberati M, Makatsariya A, et al. Prenatal risk factors for urgent atrial septostomy at birth in fetuses with transposition of the great arteries: a systematic review and meta-analysis. *J Matern Fetal Neonatal Med*. 2022 Feb;35(3):598–606.
132. Crispi F, Sepulveda-swatson E, Cruz-lemeni M. Feasibility and reproducibility of a

- standard protocol for 2d speckle tracking and tissue doppler-based strain and strain rate analysis of the fetal heart. *Fetal Diagn Ther.* 2012;32:96–108.
133. Enzensberger C, Achterberg F, Degenhardt J, Wolter A, Graupner O, Herrmann J, et al. Feasibility and reproducibility of two-dimensional wall motion tracking (WMT) in fetal echocardiography study population. *Ultrasound Int Open.* 2017 Feb;3(1):E26–E33.
 134. Voigt JU, Pedrizzetti G, Lysyansky P, Marwick TH, Houle H, Baumann R, et al. Definitions for a common standard for 2D speckle tracking echocardiography : consensus document of the EACVI / ASE / Industry Task Force to standardize deformation imaging. *J Am Soc Echocardiogr.* 2015 Feb;28(2):183-93.
 135. Ta-shma A, Perles Z, Gavri S, Golender J. Analysis of segmental and global function of the fetal heart using novel automatic functional imaging. *J Am Soc Echocardiogr.* 2008 Feb;21(2):146–50.
 136. Younoszai AK, Saudek DE, Emery SP, Thomas JD. Evaluation of myocardial mechanics in the fetus by velocity vector imaging. *J Am Soc of Echocardiogr.* 2008;21(5):470–4.
 137. Belghiti H, Brette S, Lafitte S, Reant P, Picard F, Serri K, et al. Automated function imaging : a new operator-independent strain method for assessing left ventricular function. *Arch Cardiovasc Dis.* 2008 Mar;101(3):163–9.
 138. Barker PCA, Houle H, Li JS, Miller S, Herlong JR, Camitta MGW. Global longitudinal cardiac strain and strain rate for assessment of fetal cardiac function : novel experience with velocity vector imaging. *Echocardiography.* 2009 Jan;26(1):28-36.
 139. Maskatia SA, Pignatelli RH, Ayres NA, Altman CA, Sangi-haghpeykar H, Lee W. Longitudinal changes and interobserver variability of systolic myocardial deformation values in a prospective cohort of healthy fetuses across gestation and after delivery. *J Am Soc Echocardiogr.* 2016 Apr;29(4):341–9.
 140. Devore GR, Klas B, Satou G, Sklansky M. Longitudinal annular systolic displacement compared to global strain in normal fetal hearts and those with cardiac abnormalities. *J Ultrasound Med.* 2018;37(5):1156–71.
 141. van Oostrum NHM, de Vet CM, van der Woude DAA, Kemps HMC, Oei SG, van Laar JOEH. Fetal strain and strain rate during pregnancy measured with speckle tracking echocardiography : A systematic review. *Eur J Obstet Gynecol Reprod Biol.* 2020

Jul;250:178–87.

142. Huntley ES, Hernandez-Andrade E, Soto E, Devore G, Sibai BM. Novel speckle tracking analysis showed excellent reproducibility for size and shape of the fetal heart and good reproducibility for strain and fractional shortening. *Fetal Diagn Ther.* 2021;(48):541–50.
143. Hata T, Koyanagi A, Yamanishi T, Bouno S, Takayoshi R. A 24-segment fractional shortening of the fetal heart using Fetal HQ. *J Perinat Med.* 2021;49(3):371–6.
144. Hata T, Koyanagi A, Yamanishi T, Bouno S, Ahmed M, Aboellail M, et al. Evaluation of 24-segment sphericity index of fetal heart using Fetal HQ. *J Matern Fetal Neonatal Med.* 2020 Dec;35(23):4573-4579.
145. Luo Y, Xiao F, Long C, Kuang H, Jiang M. Evaluation of the sphericity index of the fetal heart during middle and late pregnancy using fetalHQ. *J Mater Fetal Neonatal Med.* 2022Dec;35(25): 8006-80011.
146. Dodaro MG, Montaguti E, Balducci A, Perolo A, Angeli E, Lenzi J, et al. Fetal speckle-tracking echocardiography: a comparison between two-dimensional and electronic spatio-temporal image correlation (e- STIC) technique two-dimensional and electronic spatio-temporal image correlation. *J Mater Fetal Neonatal Med.* 2022 Dec;35(25):6090-6096.
147. Devore GR, Klas B, Satou G, Sklansky M. 24-segment sphericity index: a new technique to evaluate fetal cardiac diastolic shape. *Ultrasound Obstet Gynecol.* 2018 May;51(5):650–658.
148. Devore GR, Klas B, Satou G, Sklansky M. Twenty-four segment transverse ventricular fractional shortening. *J Ultrasound Med.* 2018 May;37(5):1129–1141.
149. Guirado L, Crispi F, Soveral I, Valenzuela-alcaraz B, Rodriguez-López M, García-Otero L, et al. Nomograms of fetal right ventricular fractional area change by 2d echocardiography. *Fetal Diagn Ther.* 2020;47(5):399–410.
150. Semmler J, Day TG, Georgiopoulos G, Garcia-gonzalez C, Aguilera J, Vigneswaran T V, et al. Fetal speckle-tracking: impact of angle of insonation and frame rate on global longitudinal strain. *J Am Soc Echocardiogr.* 2020;33(9):1141–6.
151. Devore GR, Satou G, Sklansky M. Comparing the non-quiver and quiver techniques for identification of the endocardial borders used for speckle-tracking analysis of the ventricles of the fetal heart. *J Ultrasound Med.* 2020 Sep;40(9):1955–1961.

152. Gozar L, Iancu M, Gozar H, Sglimbea A, Cerghit Paler A, Gabor-Miklosi D, et al. Assessment of biventricular myocardial function with 2-dimensional strain and conventional echocardiographic parameters: a comparative analysis in healthy infants and patients with severe and critical pulmonary stenosis. *J Pers Med*. 2022 Jan 6;12(1):57.
153. Germanakis I. Assessment of fetal myocardial deformation using speckle tracking techniques. *Fetal Diagn Ther*. 2012;32(1):39–46.
154. Mahfouz RA, Moustafa TM, Gouda M, Gad M. Longitudinal function and ventricular dyssynchrony are restored in children with pulmonary stenosis after percutaneous balloon pulmonary valvuloplasty. *Int J Cardiovasc Imaging*. 2017 Apr;33(4):533–8.
155. Hui W, Slorach C, Dragulescu A, Mertens L, Bijmens B, Friedberg MK. Mechanisms of right ventricular electromechanical dyssynchrony and mechanical inefficiency in children after repair of tetralogy of Fallot. *Circ Cardiovasc Imaging*. 2014 Jul;7(4):610–8.
156. Li SJ, Yu HK, Wong SJ, Cheung YF. Right and left ventricular mechanics and interaction late after balloon valvoplasty for pulmonary stenosis. *Eur Heart J Cardiovasc Imaging*. 2014 Sep;15(9):1020–8.
157. Di Angelantonio E, Chowdhury R, Sarwar N, Ray KK, Gobin R, Saleheen D, et al. B-type natriuretic peptides and cardiovascular risk: systematic review and meta-analysis of 40 prospective studies. *Circulation*. 2009 Dec 1;120(22):2177–87.
158. Wiputra H, Chen CK, Talbi E, Lim GL, Soomar SM, Biswas A, et al. Human fetal hearts with tetralogy of Fallot have altered fluid dynamics and forces. *Am J Physiol Heart Circ Physiol*. 2018 Dec 1;315(6):H1649–59.
159. Groenendijk BCW, Hierck BP, Gittenberger-De Groot AC, Poelmann RE. Development-related changes in the expression of shear stress responsive genes KLF-2, ET-1, and NOS-3 in the developing cardiovascular system of chicken embryos. *Dev Dyn*. 2004 May;230(1):57–68.
160. Sun L, van Amerom JFP, Marini D, Portnoy S, Lee FT, Saini BS, et al. MRI characterization of hemodynamic patterns of human fetuses with cyanotic congenital heart disease. *Ultrasound Obstet Gynecol*. 2021 Dec;58(6):824–36.
161. El-Hamamsy I, Yacoub MH. Cellular and molecular mechanisms of thoracic aortic

- aneurysms. *Nat Rev Cardiol*. 2009 Dec;6(12):771–86.
162. Franken R, den Hartog AW, de Waard V, Engele L, Radonic T, Lutter R, et al. Circulating transforming growth factor- β as a prognostic biomarker in Marfan syndrome. *Int J Cardiol*. 2013 Oct 3;168(3):2441–6.
163. Ghanchi A, Rahshenas M, Bonnet D, Derridj N, LeLong N, Salomon LJ, et al. Prevalence of growth restriction at birth for newborns with congenital heart defects: a population-based prospective cohort study EPICARD. *Front Pediatr*. 2021 May 28;9:676994.
164. Escobar-Diaz MC, Pérez-Cruz M, Arráez M, Cascant-Vilaplana MM, Albiach-Delgado A, Kuligowski J, et al. Brain oxygen perfusion and oxidative stress biomarkers in fetuses with congenital heart disease—a retrospective, case-control pilot study. *Antioxidants (Basel)*. 2022 Jan 31;11(2):299.
165. Keelan J, Pasumarti N, Crook S, Decost G, Wang Y, Crystal MA, et al. Right ventricular strain in patients with ductal-dependent tetralogy of Fallot. *J Am Soc Echocardiogr*. 2023 Jun;36(6):654–65.
166. Willruth AM, Geipel A, Berg C, Fimmers R, Gembruch U. Assessment of fetal global and regional ventricular function in congenital heart disease using a novel feature tracking technique. *Ultraschall Med*. 2012 Jun;33(3):251–7.
167. Sanchez-Quintana D, Anderson RH, Ho SY. Ventricular myoarchitecture in tetralogy of Fallot. *Heart*. 1996 Sep;76(3):280–6.
168. Rodenbarger A, Thorsson T, Stiver C, Jantzen D, Chevenon M, Yu S, et al. Third trimester predictors of interventional timing and accuracy of fetal anticipatory guidance in tetralogy of Fallot: A multi-center study. *Prenat Diagn*. 2020 Jun;40(7):870–7.
169. Friedman K, Balasubramanian S, Tworetzky W. Midgestation fetal pulmonary annulus size is predictive of outcome in tetralogy of Fallot. *Congenit Heart Dis*. 2014;9(3):187–93.
170. Arya B, Levasseur SM, Woldu K, Glickstein JS, Andrews HF, Williams IA. Fetal echocardiographic measurements and the need for neonatal surgical intervention in Tetralogy of Fallot. *Pediatr Cardiol*. 2014 Jun;35(5):810–6.
171. Wolter A, Gebert M, Enzensberger C, Kawecki A, Stessig R, Degenhardt J, et al. Outcome and Associated Findings in Individuals with Pre- and Postnatal Diagnosis

of Tetralogy of Fallot (TOF) and Prediction of Early Postnatal Intervention. *Ultraschall Med.* 2020 Oct;41(5):504–13.

172. Quartermain MD, Glatz AC, Goldberg DJ, Cohen MS, Elias MD, Tian Z, et al. Pulmonary outflow tract obstruction in fetuses with complex congenital heart disease: predicting the need for neonatal intervention. *Ultrasound Obstet Gynecol.* 2013 Jan;41(1):47–53.
173. Ruiz A, Ferrer Q, Sánchez O, Ribera I, Arévalo S, Alomar O, et al. Placenta-related complications in women carrying a foetus with congenital heart disease. *J Matern Fetal Neonatal Med.* 2016 Oct;29(20):3271–5.